Novel mechanisms of resistance to EGFR inhibitory drugs in non-small cell lung cancer

Catherine Cowell

University College London

and

Cancer Research UK London Research Institute

PhD Supervisor: Professor Julian Downward

A thesis submitted for the degree of

Doctor of Philosophy

University College London

September 2012

Declaration

I Catherine Frances Cowell confirm that the work presented in this thesis is my own. Where information has been derived from other sources, I confirm that this has been indicated in the thesis.

Abstract

EGFR activating mutations are present in 10-40% of non-small cell lung cancer. Such mutations render tumour cells sensitive to EGFR tyrosine kinase inhibitors (EGFR TKIs), with responses of up to 80% in populations selected for the presence of an activating mutation. Unfortunately, almost all patients develop resistance after about a year. Clinically described mechanisms of resistance include the presence of a secondary mutation (T790M) in *EGFR* which prevents EGFR TKIs binding to the EGF receptor, and amplification *MET* which permits survival signalling via the ERBB3 receptor. However in 30% of cases, the mechanism of acquired resistance to EGFR TKIs is still unknown. My aim was to carry out a genome-wide siRNA screen to identify novel mechanisms of resistance to EGFR TKIs. I identified two genes that have not been implicated in EGFR TKI resistance previously, *NF1* and *DEPTOR*, which are negative regulators of RAS and mTOR respectively. Depletion of NF1 or DEPTOR leads to increased resistance to EGFR TKIs via upregulation of MAPK signalling by direct and indirect mechanisms.

Acknowledgements

The work presented here would have not been possible without the help of many people. Firstly, I would like to thank my supervisor, Julian Downward, for giving me the opportunity to work in his lab, and for his support and direction.

I would like to thank all the members of the Signal Transduction Laboratory – Clare, Elza, Esther, Elena, Ralph, Nadia, Miriam, Miguel, Georgios, Pat, Dave, Britta, and Madhu, for all their helpful advice and for making the lab an enjoyable place to work. I would particularly like to thank Elza, for her guidance and contribution to the project.

Further I would like to thank my thesis committee Almut Schulze and Peter Parker for their advice and assistance. Also, thanks to the staff of the excellent research services including the Equipment Park and FACS Laboratory, and especially Mike, Ming, Becky and Rachael in the High-throughput Laboratory.

Outside the lab, many people made the last four years an amazing period of my life full of friendship. Special thanks go to Amy, Sara, Lisa, Nicola, and Victoria, as well as the amazing Whitby Road girls and my friends from Billericay who have made many special dispensations for me whilst studying for my PhD.

Above all, I have to thank my incredible parents and my wonderful sister Laura. I really could not have done this without their love and encouragement.

Table of Contents

Abstract 3
Acknowledgements 4
Table of Contents 5
Table of figures 8
List of tables 12
Abbreviations 13
Chapter 1. Introduction 15
1.1 Cancer 15
1.2 Non-small Cell Lung Cancer 16
1.3 EGFR signalling 18
1.4 EGFR signalling in NSCLC 20
1.5 RAS signalling 22
1.5.1 RAS family proteins 22
1.5.2 RAS function 23
1.5.3 RAS activation in response to EGFR stimulation 24
1.6 RAF/MEK/ERK 25
1.6.1 RAF/MEK/ERK activation in cancer 26
1.7 PI3K signalling 27
1.7.1 PI3K/AKT signalling in cancer 28
1.7.2 mTOR signalling 29
1.7.3 mTOR signalling in cancer 34
1.8 Mechanisms of resistance to EGFR TKIs in *EGFR*-mutant NSCLC 34
1.8.1 Primary resistance to EGFR TKIs 34
1.8.2 The T790M mutation 35
1.8.3 Other secondary *EGFR* mutations that confer resistance to EGFR TKIs 37
1.8.4 Amplification of *MET* 37
1.8.5 Histological transformation to SCLC 38
1.8.6 Activation of PI3K/AKT signalling by somatic mutations in *PIK3CA* and *PTEN* 39
1.8.7 Epithelial-Mesenchymal Transition 40
1.8.8 Alterations in IGFR signalling 40
1.8.9 NF Kappa B signalling 41
1.8.10 *CRKL* amplification 42
1.8.11 Activation of AXL kinase 42
1.8.12 Alternative mechanisms of resistance 42
1.8.13 Outline of subsequent chapters 43
Chapter 2. Materials & Methods 44
2.1 Materials 44
2.1.1 Drugs 44
2.1.2 Antibodies 44
2.1.3 Buffers and solutions 46
2.1.4 siRNA oligonucleotides 47
2.1.5 ShRNA constructs 51
2.2 Methods 52
2.2.1 Mammalian cell culture 52

2.2.2 Screening 53
2.2.3 RNAi follow up experiments 56
2.2.4 Quantitative Real Time PCR 58
2.2.5 Protein analysis 59
2.2.6 Statistical analysis 62
Chapter 3. Identifying determinants of resistance to erlotinib treatment – a genome-wide screen 63
3.1 Introduction 63
3.2 RNAi technology 63
3.3 Genome-wide screen set up 64
3.3.1 siRNA library 64
3.3.2 Choice of cell line 64
3.3.3 Screen read-out 64
3.3.4 Erlotinib treatment 66
3.3.5 Transfection reagent and conditions 68
3.3.6 384-well plate format 71
3.3.7 Control siRNAs 74
3.3.8 Screen Protocol 75
3.4 Analysis of genome-wide screen data 76
3.4.1 Normalisation 76
3.4.2 Correlation of replicates and performance of siRNA controls 81
3.4.3 Residual Z score – difference between control and drug-treated conditions 82
3.5 Repeat of genome-wide screen 84
3.6 Deconvolution screen 85
3.7 Discussion 87
Chapter 4. NF1 loss increases resistance of NSCLC to EGFR TKI treatment. 91
4.1 Introduction 91
4.2 Reduction of NF1 expression renders lung cancer cells less sensitive to EGFR-TKI treatment 93
4.3 NF1 silencing leads to MAPK pathway activation in the presence of erlotinib 97
4.4 Combination treatment of EGFR-TKIs and MEK inhibitors is effective against NF1-depleted cells 107
4.5 Discussion 113
Chapter 5. DEPTOR loss increases resistance of non-small cell lung cancer (NSCLC) to EGFR tyrosine kinase inhibitors (TKIs) by feedback upregulation of EGFR. 121
5.1 DEPTOR structure and function 121
5.2 DEPTOR expression and mTOR signalling in cancer 121
5.3 Reduction in DEPTOR expression increases resistance of NSCLC cells to erlotinib treatment 123
5.4 DEPTOR silencing does not increase resistance of PC9 cells to other chemotherapeutic drugs 129
5.5 DEPTOR silencing increases EGFR protein levels and AKT, ERK1/2 and mTORC2 activation. 132
5.6 DEPTOR silencing increases the abundance of EGFR protein. 137

5.7 Inhibition of mTOR or MEK restores sensitivity of siDEPTOR cells to erlotinib 142
5.8 Discussion 153
Chapter 6. Discussion 163
6.1 Targeted therapeutics 163
6.2 Resistance – primary or acquired? 164
6.3 Common themes of resistance mechanisms 165
6.3.1 Reactivation of the targeted pathway 165
6.3.2 Activation of alternative signalling pathways 167
6.3.3 Histological transformation 168
6.4 Tumour heterogeneity as a challenge to targeted therapeutics 169
6.4.1 Evolutionary dynamics and implications for therapy 169
6.4.2 Tumour heterogeneity – not so heterogenous after all? 171
6.5 Tumour microenvironment in drug resistance 172
6.6 The future of targeted therapeutics 173
6.6.1 Combination therapies 173
6.6.2 Combinations of targeted therapies – targeting the same pathway or different pathways? 174
6.6.3 Multi-target therapeutic agents 175
6.6.4 Novel approaches to modelling resistance 176
6.7 Concluding remarks 178
Chapter 7. Appendix 181
Reference List 183

Table of figures

Figure 1.1. Hallmarks of Cancer. 16
Figure 1.1.2. Common mutations in NSCLC. 18
Figure 1.1.3. Key EGFR-activated signalling pathways 20
Figure 1.1.4. Ras activation. 24
Figure 1.1.5. PI3K-AKT signalling. 28
Figure 1.1.6. Components of mTORC1 and 2. 30
Figure 1.1.7. Overview of mTOR signalling. 32
Figure 1.1.8. MET-mediated acquired resistance to EGFR-TKIs. 38
Figure 1.1.9. Mechanisms of acquired resistance to EGFR-TKIs in NSCLC. 43
Figure 3.1. Test of methods to use as a read-out of cell survival. 66
Figure 3.2. PC9 cells are exquisitely sensitive to inhibition by erlotinib. 67
Figure 3.3. Test for optimal duration of erlotinib treatment. 68
Figure 3.4. Transfection reagent test for gene-silencing and toxicity. 71
Figure 3.5. Transfection conditions for a 384-well plate format. 74
Figure 3.6. Screen set-up. 76
Figure 3.7. Effect of plate normalisation. 79
Figure 3.8. Effect of position normalisation. 81
Figure 3.9. Correlation of replicates. 82
Figure 3.10. Residual difference method. 84
Figure 4.1. Nf1 expression is reduced in a murine model of erlotinib-resistant NSCLC (unpublished data provided by Katerina Politi).. 92
Figure 4.2. NF1 protein and mRNA levels are efficiently reduced by shRNA constructs targeting NF1. 93
Figure 4.3. NF1 silencing increases resistance to erlotinib. 94
Figure 4.4. NF1 loss increases resistance to erlotinib in longer term assays. 95
Figure 4.5. NF1 loss increases resistance of PC9 cells to gefitinib treatment. 96
Figure 4.6. NF1 silencing does not increase resistance to other chemotherapeutic drugs. 97
Figure 4.7. RNAi-mediated NF1 silencing increases RAS activation. 98
Figure 4.8. NF1 loss leads to sustained activation of ERK1/2 in the presence of erlotinib. 99

Figure 4.9. NF1 loss leads to sustained phosphorylation of ERK in erlotinib-treated conditions in other NSCLC cell lines. 100
Figure 4.10. NF1 loss increases resistance of other NSCLC cell lines to erlotinib in long term survival assays. 101
Figure 4.11. Expression of an shRNA resistant NF1-GRD and silencing of endogenous NF1 by shRNA. 102
Figure 4.12. NF1-GRD expression prevents increased resistance to erlotinib in shNF1 cells. 103
Figure 4.13. Expression of the NF1 GRD restores signalling of shNF1 cells. 104
Figure 4.14. Expression of myristoylated AKT and MEK-DD constructs in PC9 cells. 105
Figure 4.15. PC9 cells expressing activated forms of AKT or MEK have increased resistance to erlotinib treatment. 106
Figure 4.16. Active AKT and MEK increase resistance of PC9 cells to erlotinib treatment. 106
Figure 4.17. MEK-DD expressing cells are sensitive to a combination of erlotinib and a MEK inhibitor. 107
Figure 4.18. Combination treatment of erlotinib and a MEK inhibitor is effective against NF1-depleted cells. 108
Figure 4.19. Combined erlotinib and MEK inhibitor treatment abolishes phosphorylation of ERK1/2 in shNF1 cells. 109
Figure 4.20. Combination treatment of erlotinib and an AKT inhibitor is not effective in NF1-depleted cells. 110
Figure 4.21. PC9-ER cells are not sensitive to a combination of erlotinib and a MEK inhibitor. 111
Figure 4.22. PC9-ER cells retain phosphorylated ERK1/2 in the presence of combined erlotinib and MEK inhibitor treatment. 112
Figure 4.23. PC9-ER cells are not sensitive to a combination of erlotinib and an AKT inhibitor. 113
Figure 4.24. NF1 loss activates RAS-MAPK signalling. 116
Figure 5.1. The deconvoluted SMARTpool targeting DEPTOR efficiently reduces DEPTOR mRNA levels. 124
Figure 5.2. The deconvoluted SMARTpool targeting DEPTOR efficiently reduced DEPTOR protein levels. 124

Figure 5.3. DEPTOR silencing increases resistance of PC9 cells to erlotinib treatment. 125
Figure 5.4. shRNAs targeting DEPTOR efficiently reduce DEPTOR expression at the mRNA and protein level. 126
Figure 5.5. Silencing of DEPTOR increases resistance of PC9 cells to erlotinib treatment in long term cell survival assays. 127
Figure 5.6. Efficiency of DEPTOR silencing in HCC4006 cells. 128
Figure 5.7. shRNA targeting DEPTOR increases resistance of HCC4006 cells to erlotinib treatment. 129
Figure 5.8. DEPTOR depletion increases resistance of PC9 cells to gefitinib. 130
Figure 5.9. DEPTOR silencing does not effect responses to other chemotherapeutic drugs. 131
Figure 5.10. DEPTOR silencing activates AKT, ERK1/2 and mTORC2 signalling. 134
Figure 5.11. shRNA targeting DEPTOR increases EGFR, AKT, ERK1/2 and mTORC2 signalling. 135
Figure 5.12. Depletion of DEPTOR increases activation of ERK1/2 and mTORC2 in HCC4006 cells. 136
Figure 5.13. DEPTOR silencing increases the abundance of EGFR protein compared to Sc control cells 137
Figure 5.14. DEPTOR silencing by siRNA and shRNA increases EGFR mRNA levels. 138
Figure 5.15. DEPTOR depletion does not affect abundance of other key receptor tyrosine kinases. 139
Figure 5.16. DEPTOR-depleted cells have increased levels of EGFR and EGFR-mediated signalling. 140
Figure 5.17. DEPTOR-depleted cells have slightly higher levels of active RAS than control cells. 141
Figure 5.18. EGFR abundance is not affected by active MEK or AKT 142
Figure 5.19. Combination treatment of erlotinib and a MEK inhibitor restores sensitivity of siDEPTOR cells to erlotinib to that of Sc control cells. 144
Figure 5.20. Combination treatment of erlotinib and MEK inhibitor restores sensitivity of siDEPTOR cells to erlotinib by abolishing activation of ERK1/2. 145

Figure 5.21. Combination treatment of erlotinib and an AKT inhibitor partially resensitises DEPTOR-depleted cells to erlotinib treatment. 146
Figure 5.22. Combined erlotinib and AKT inhibition partially resensitises DEPTOR-depleted cells to erlotinib treatment. 147
Figure 5.23. Combined treatment of erlotinib and an mTOR kinase inhibitor restores sensitivity of siDEPTOR cells to erlotinib to that of Sc control cells. 148
Figure 5.24. Combined erlotinib and mTOR kinase inhibitor treatment restores sensitivity to erlotinib. 149
Figure 5.25. Combination treatment of erlotinib and temsirolimus does not restore sensitivity of siDEPTOR cells to Sc control levels. 150
Figure 5.26. Temsirolimus treatment effectively inhibits rpS6 phosphorylation, but does not resensitise cells to erlotinib treament. 151
Figure 5.27. RICTOR and RAPTOR are both essential for survival of DEPTOR-depleted cells in the presence of erlotinib. 152
Figure 5.28. Proposed mechanism - DEPTOR loss leads to upregulation of EGFR levels and MAPK pathway signalling. 159

List of tables

Table 3.1. Transfection reagents and conditions tested for use in PC9 cells. 70
Table 3.2. Genes that upon RNAi-mediated silencing affected cell survival in response to erlotinib treatment 86

Abbreviations

AKT	v-akt murine thymoma viral oncogene homolog 1
ATP	Adenosine triphosphate
BSA	Bovine serum albumin
DAPI	4'6-Diamidino-2-phenylindole
DEPTOR	DEP domain containing mTOR interacting protein
DMSO	Dimethyl sulfoxide
DNA	Deoxyribonucleic acid
DTT	Dithiothreitol
ECL	Enhanced chemiluminescence
EGF	Epidermal growth factor
EGFR	Epidermal growth factor receptor
EMT	Epithelial-mesenchymal transition
ERK	Extracellular signal-regulated kinase
FACS	Fluorescence activated cell sorting
FBS	Foetal bovine serum
g	Gram
GAP	GTPase activating protein
GDP	Guanosine diphosphate
GEF	Guanosine exchange factor
GFP	Green fluorescent protein
GRB2	Growth factor receptor-bound protein 2
GRD	GAP-related domain
GST	Glutathione S-transferase
GTP	Guanosine triphosphate
h/hrs	Hour/hours
HBSS	Hank's balanced salt solution
l	Litre
LDS	Lithium dodecyl sulphate
m	Milli
MAPK	Mitogen-activated protein kinase
MEK	MAPK/ERK kinase
MES	2-(N-Morpholino)ethanesulfonic acid
MET	Met proto-oncogene tyrosine kinase

mRNA	Messenger RNA
miRNA	Micro RNA
mTOR	Mammalian target of rapamycin
n	Nanomolar
NDRG1	N-myc downstream regulated 1
NF1	Neurofibromin 1
nm	Nanometer
NSCLC	Non-small cell lung cancer
p	Pico
PBS	Phosphate buffered saline
PCR	Polymerase chain reaction
PI3K	Phosphoinositide-3-kinase
PTEN	Phosphatase and tensin homolog
RAS	Rat sarcoma
RBD	Ras binding domain
RHEB	Ras homolog enriched in brain
RNA	Ribonucleic acid
RNAi	RNA interference
rpm	Revolutions per minute
RPMI	Roswell park memorial institute medium
RTK	Receptor tyrosine kinase
S6	Ribosomal protein S6
S6K	p70 S6 kinase
SC	Scrambled (non-targeting control)
SGK1	Serum/glucocorticoid regulated kinase 1
shRNA	Short hairpin RNA
siRNA	Small interfering RNA
SDS-PAGE	Sodium dodecyl sulphate polyacrylamide gel electrophoresis
SOS	Son of sevenless
TBS	Tris buffered saline
TCA	Trichloroacetic acid
TKI	Tyrosine kinase inhibitor
V	Volts
µ	Micro

Chapter 1. Introduction

1.1 Cancer

Cancer is a term that covers over two hundred different diseases defined by the uncontrolled proliferation of cells. Cancer cells undergo cell division without the proper regulation present in normal cells, leading to the formation of tumours. Cancer cells have acquired properties that normal cells do not have as a result of mutations in their DNA. These mutations can arise as a result of a variety of causes, for example, exposure to various substances e.g. tobacco, radiation, or some viruses. The transformation of a normal cell to a cancer cell is multi-step process (Foulds, 1954). Early in vitro experiments showed that cells require at least two genetic aberrations before they are fully transformed (Hahn et al., 1999; Land et al., 1983), and research into cancer susceptibility syndromes seemed to support this hypothesis. Knudson proposed the 'two hit' model on the basis of dominant inheritance of cancer in retinoblastoma patients, where statistical analysis suggested patients that inherited one mutation in *RB1* (retinoblamstoma) required one more mutational event to develop cancer (Knudson, 1971). Two mutations appear to be the minimum for tumourigenesis, and more mutations are thought to be necessary in non-inheritable cancers (Berger et al., 2011).

Weinberg and Hanahan suggested a list of properties cancer cells must have acquired to successfully develop into malignant disease in their seminal paper, 'Hallmarks of Cancer' which they re-evaluated in 2011(Hanahan and Weinberg, 2011)(Fig.1.1).

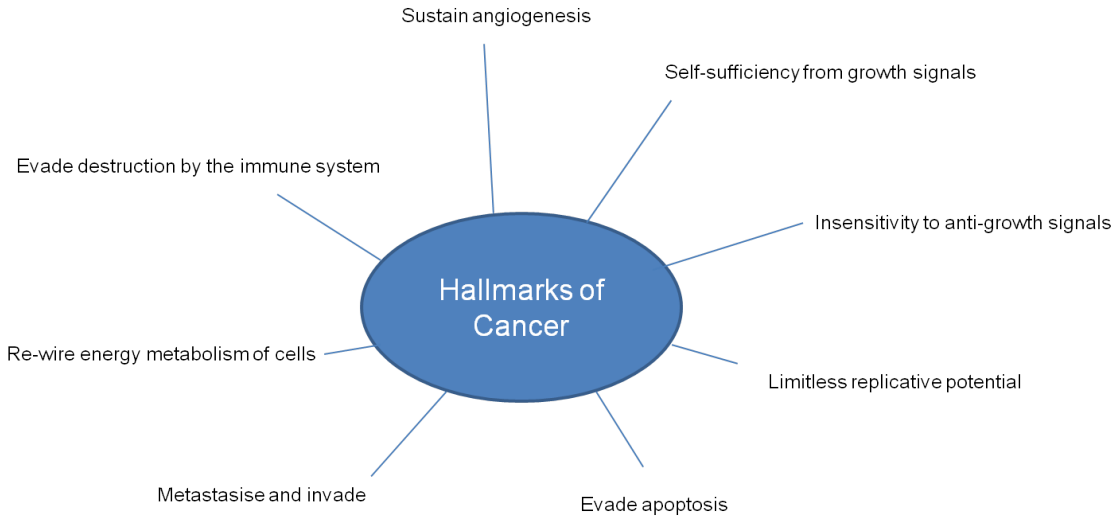

Figure 1.1. Hallmarks of Cancer.
Properties cancer cells must acquire in order to develop into malignant disease.

These properties include self-sufficiency from growth signals, insensitivity to anti-growth signals, and the ability to evade apoptosis. Mutations that confer these abilities to tumour cells and drive carcinogenesis can be broadly divided into two groups, those that affect tumour suppressors and those that affect oncogenes. Tumour suppressors are proteins whose action provides a block to tumour formation. Mutations in the genes encoding these proteins cause their loss of function, and remove their blockade to cancer formation. The most well-known tumour suppressor is p53. p53 acts as a tumour suppressor in a variety of ways, for example inducing cell cycle arrest in response to DNA damage to allow cells to repair it, and inducing apoptosis if the damage is irreparable (Vousden and Lu, 2002). On the other hand oncogenes promote cancer formation. These tend to be genes that in normal cells promote growth and survival, but in cancer have undergone mutations that activate them to abnormally high levels. Examples of oncogenes that will be discussed in greater detail are *KRAS* and *EGFR*.

1.2 Non-small Cell Lung Cancer

Lung cancer is the biggest cause of cancer deaths claiming over one million lives a year worldwide. The most prevalent form of lung cancer is non-small cell lung cancer (NSCLC), comprising 80% of all lung cancer cases. NSCLC can be histologically subdivided into squamous-cell carcinoma, large-cell carcinoma, and adenocarcinoma, with adenocarcinoma accounting for 50% of cases (Pao and

Girard, 2011). In recent years several genes have been identified which are frequently mutated in NSCLC, leading to the development of rationale driven targeted therapies. The most common genetic alterations are mutations in *KRAS*, *EGFR*, and the occurrence of *EML4-ALK* gene fusions, all of which appear to be mutually exclusive (Kim et al., 2011). *KRAS* mutations are mostly associated with smokers, whereas *EML4-ALK* gene fusions and *EGFR* mutations are more common in never-smokers. Also *EGFR* mutations are more common in women and patients of Asian origin. Several other potential driver mutations have been identified in NSCLC at lower frequencies, including *HER2*, *BRAF*, *AKT1*, *MAP2K1* and *PI3KCA* and translocations in *RET* and *ROS* (Fig.1.2.) (Pao and Hutchinson, 2012) (Heist and Engelman, 2012), providing attractive new therapeutic opportunities. However, the major problem with all targeted therapies is the ability of cancer cells to mutate and adapt to adverse conditions, leading to development of drug resistance and disease progression. Such examples of drug resistance have been identified in *EGFR*-mutant and *EML-ALK* expressing NSCLC targeted with EGFR and ALK inhibitors respectively (Choi et al., 2010; Pao et al., 2005a). The remainder of this body of work will focus on the use of EGFR tyrosine kinase inhibitors in *EGFR*-mutant NSCLC and arising mechanisms of resistance.

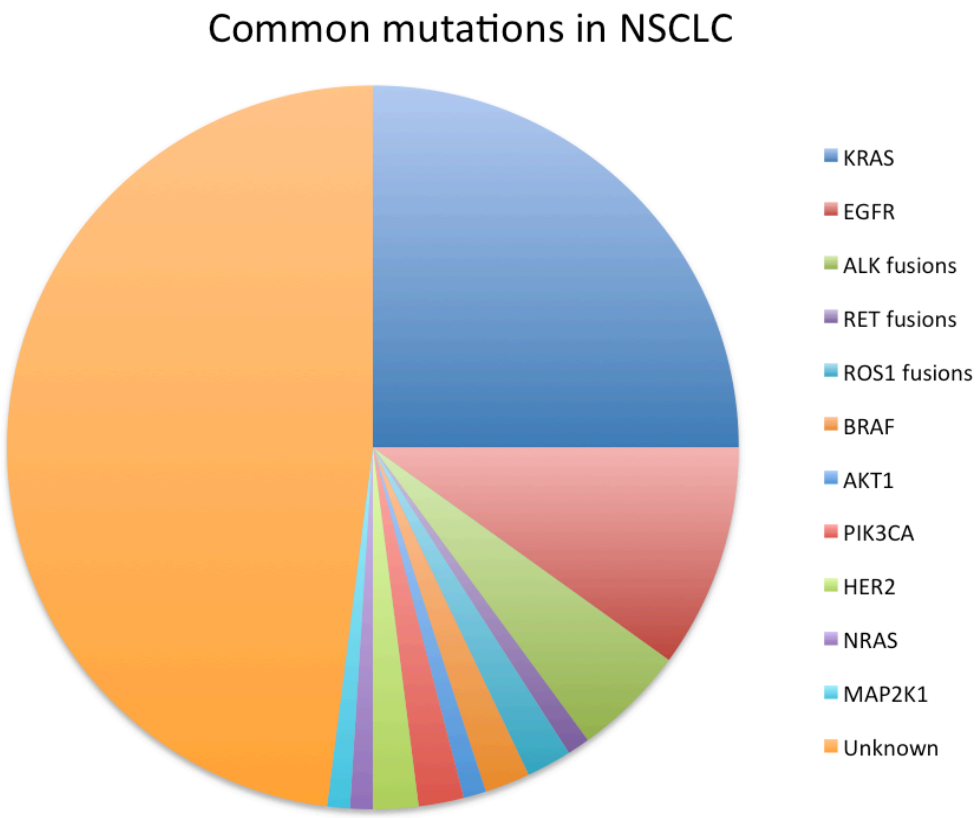

Figure 1.1.2. Common mutations in NSCLC.

Pie chart showing identified driver mutations in NSCLC representing the percentage of cases in which they have been identified. *TP53* and *LKB1* are not shown as they significantly overlap with mutations indicated. The data represented is from Pao and Hutchinson, 2012 and Heist and Engelman 2012.

1.3 EGFR signalling

The role of EGFR in cancer was first indicated by the discovery that *EGFR* is the cellular homolog of the avian erythrocytosis virus (*AEV*) oncogene (Downward et al., 1984). AEV is a c-term truncated version of EGFR, with additional mutations in the intracellular domain rendering it constitutively activated. This finding suggested that *EGFR* is a proto-oncogene, present in normal cells that when aberrantly activated functions as an oncogene to drive tumourigenesis (Downward et al., 1984). Subsequently, constitutively active EGFR signalling has been found in a range of human neoplasms including glioma, colorectal carcinoma and non-small cell lung cancer (Salomon et al., 1995). The human epidermal growth factor receptor family (ERBB/Her) consists of four related receptors EGFR (HER1, ERBB1), HER2 (ERBB2) (King et al., 1985; Schechter et al., 1985), HER3

(ERBB3) (Kraus et al., 1989; Plowman et al., 1990) and HER4 (ERBB4) (Plowman et al., 1993). When EGFR ligands bind to the extracellular domain of the receptors they induce either heterodimerisation or homodimerisation of receptors and activation of intracellular tyrosine kinase activity. The exact method of activation varies substantially between family members. EGFR and ERBB4 kinase activity are both activated by ligand binding. On the other hand ERBB2 is not known to bind any ligand with high affinity and is thought to function mainly as a binding partner for other ERBB family members (Klapper et al., 1999). Instead, ERBB2 is the preferred dimerization partner of all ErbB family receptors (Graus-Porta et al., 1997) and ERBB heterodimers containing ERBB2 are strong inducers of downstream signalling (Graus-Porta et al., 1995). Conversely, ERBB3 can only activate signalling when heterodimerised with other ERBB receptors as it lacks intracellular kinase activity (Kim et al., 1998).

In the case of EGFR, ligand binding induces a conformational change in the receptor allowing the formation of receptor dimers. EGFR has six ligands: EGF, amphiregulin, TGF-α, heparin-binding growth factor, epiregulin and betacellulin (Salomon et al., 1995). Autophosphorylation of the intracellular tyrosine kinase domain creates phosphotyrosine residues that act as SH2 binding sites for adaptor proteins, such as GRB2 (Lowenstein et al., 1992) and SHC (Pelicci et al., 1992), and other SH2-domain containing signalling proteins, such as PLC gamma, SRC and STATs (Marmor et al., 2004). Recruitment of adaptor proteins is vital for activation of RAS-MAPK and PI3K-AKT signalling pathways that will be discussed in more detail in later sections. Briefly, RAS is activated via GRB2/SOS, and PI3K via GRB2/GAB1 to potentiate downstream signalling. Fig.1.3. shows recruitment of various signalling molecules to EGFR and the downstream pathways they activate.

EGFR signalling is terminated by ubiquitination and recruitment to clathrin coated pits at the membrane. Activated receptors are then internalised via endocytosis to early endosomes, and subsequently either recycled to the plasma membrane or sorted to the lysosome for degradation (Madshus and Stang, 2009). It is thought that EGFR is still able to signal in the cytoplasm from endosomes, and that may be important in sustained MAPK and AKT activation. However, recent research in dynamin-depleted cells, where EGFR endocytosis is inhibited, showed similar

stimulation of MAPK, indicating that the majority of signal activation occurs at the plasma membrane (Sousa et al., 2012).

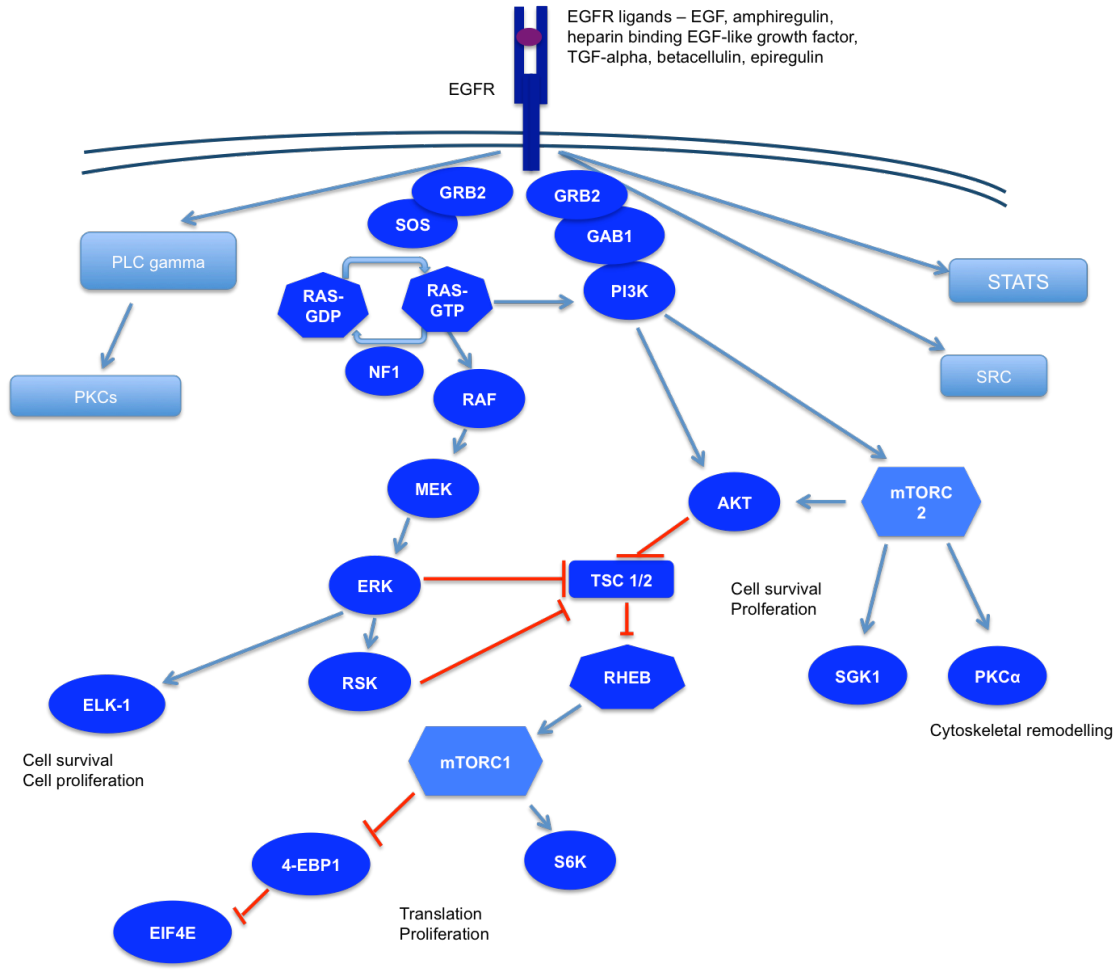

Figure 1.1.3. Key EGFR-activated signalling pathways

Outline of major signalling pathways activated by EGFR. Activation of EGFR by ligands leads to autophosphorylation of the receptor and recruitment of adaptor molecules such as GRB2, and signalling molecules such as PLC gamma, SRC and STATs. GRB2/SOS binds to and activates RAS resulting in activation of downstream MAPK, whilst recruitment of GAB1 to GRB2 activates PI3K signalling.

1.4 EGFR signalling in NSCLC

EGFR signalling is hyper-activated in a large subset of NSCLC, via mutation, gene amplification, and overexpression of EGFR and its ligands, leading to the dependence of these tumours on EGFR signalling for survival. *EGFR* mutations have been reported in 10-40% of NSCLC, the majority of which are deletions of between 2 and 15 nucleotides in exon 19 or point mutation of L858R in exon 21

(Lynch et al., 2004; Paez et al., 2004). Both of these common mutations affect the kinase domain of the receptor, leading to ligand-independent EGFR signalling. The other known *EGFR* activating mutations also occur within exons 18-21 in the kinase domain (Gazdar, 2009). Missense mutations of glycine 719 to serine, alanine or cysteine, and V765A and T783A, account for 4% and 1% of activating *EGFR* mutations respectively (Sharma et al., 2007), and additional in-frame duplications and insertions exist in exon 20 (Sharma et al., 2007). Presence of these activating *EGFR* mutations was demonstrated to confer sensitivity to EGFR inhibitory drugs, and drove the use of EGFR tyrosine kinase inhibitors (EGFR-TKIs), such as erlotinib and gefitinib, in selected populations in NSCLC (Lynch et al., 2004; Paez et al., 2004).

Initially EGFR tyrosine kinase inhibitors were used in unselected populations of non-small cell lung cancer patients refractory to chemotherapy, under the rationale that EGFR is expressed or overexpressed in NSCLC (Fujino et al., 1996). In phase II clinical trials, using gefinitib as a monotherapy, between 12.3 and 18.7% of patients exhibited a partial clinical response (Fukuoka et al., 2003; Kris et al., 2003). A clinical response is defined by Response Evaluation Criteria In Solid Tumors (RECIST) as a 30% reduction in tumour size.(Therasse et al., 2000). At the phase III clinical trial stage erlotinib treatment prolonged survival by a median of 2 months, which was deemed clinically meaningful (Shepherd et al., 2005). Upon selection for activating *EGFR* mutations, the proportion of patients benefiting from treatment increases dramatically. Approximately 70% of patients with activating *EGFR* mutations exhibit a clinical response to EGFR tyrosine kinase inhibitors, as found in several clinical trials (Maemondo et al., 2010; Mitsudomi et al., 2010; Mok et al., 2009). In these cases EGFR-TKI treatment increases progression free survival by between 3 and 5 months, compared to standard chemotherapy. These trials were carried out in Asian populations, however similar results have recently been reported in a European phase III clinical trial comparing erlotinib treatment with standard chemotherapy. In this instance 64% of patients responded to the EGFR-TKI, and erlotinib treatment lead to superior progression free survival (9.7 months versus 5.2 months)(Rosell et al., 2012).

EGFR amplification has also been identified in approximately 9% of NSCLC, where high gene copy number correlates to poor prognosis (Hirsch et al., 2003). There is some evidence that patients with no *EGFR* mutation but *EGFR* gene amplification can benefit from EGFR TKI therapy (Cappuzzo et al., 2005; Helfrich et al., 2006). Overexpression of EGFR is present in 40-80% of NSCLC patients and is generally associated with poor prognosis, however it is less strongly associated with response to EGFR-TKIs than *EGFR* copy number, or the presence of activating mutations (Hirsch et al., 2009). It has also been suggested that high expression of other ERBB family members (ERBB2 and ERBB3) and EGFR ligands (amphiregulin and epiregulin) can confer sensitivity to EGFR-TKIs, however this is less well established (Fujimoto et al., 2005). Ultimately the vast majority of patients with *EGFR* activating mutations are responsive to EGFR-TKIs, as well as a minor population of wildtype *EGFR* patients, who may have upregulated EGFR signalling via other mechanisms. Unfortunately, after a year or so of treatment with TKIs almost all patients who initially show a clinical response develop resistance and exhibit tumour progression.

1.5 RAS signalling

1.5.1 RAS family proteins

As mentioned previously, one of the major effectors of EGFR signalling is RAS. The RAS superfamily consists of over 150 different proteins, which can be subdivided into 5 major groups, RAS, RHO, RAB, RAN and ARF (Wennerberg et al., 2005). The RAS subfamily in humans contains 39 proteins encoded by 36 genes. Of the RAS subfamily the most studied members are H-RAS, K-RAS and N-RAS due to their extensive roles in cancer, as they are mutated in around 20% of human tumours (Downward, 2009). The cellular homologues of viral *H-RAS* and *K-RAS* were first identified in the rat genome in 1981 (DeFeo et al., 1981). Subsequently mutant alleles of *K-RAS* and *H-RAS* were identified in a variety of human cancer cell lines (Der et al., 1982) and human tumours (Santos et al., 1984).

1.5.2 RAS function

RAS is essential for growth and survival signals in response to extracellular stimuli. RAS is a GTPase, which means it hydrolyses GTP to GDP, and through this activity functions as a molecular switch. When RAS is bound to GTP it is in an active signalling state and can activate downstream effectors. Hydrolysis of GTP then converts RAS back to its inactive form, switching off RAS signalling (Fig.1.4). The function of RAS as a GTPase was discovered by three groups by comparing normal and oncogenic alleles of RAS, which differed by a single amino acid (at position 12, 13 and 61) (Gibbs et al., 1984; McGrath et al., 1984) (Sweet et al., 1984). It was determined that these mutations decrease the ability of RAS to hydrolyse GTP, therefore lock it in a constitutively active state.

The ratio of RAS-GTP to RAS-GDP is regulated by RAS GEFs (Guanine nucleotide Exchange Factors) and GAPs (GTPase Activating Proteins). GTP hydrolysis by RAS proteins alone occurs at a level too low to be physiologically important, instead GTPase activity is stimulated by the interaction with GEFs. RAS GEFs, such as SOS bind to RAS and cause conformational changes resulting in a 10,000-fold increase in the rate of release of GDP from RAS, which is replaced by the more abundant GTP, activating RAS (Karnoub and Weinberg, 2008). RAS GAPs, such as p120 (Trahey and McCormick, 1987) and NF1 (Martin et al., 1990) inactivate RAS by catalysing the hydrolysis rate of GTP to GDP by approximately 100,000 fold returning RAS to an inactive state (Gideon et al., 1992).

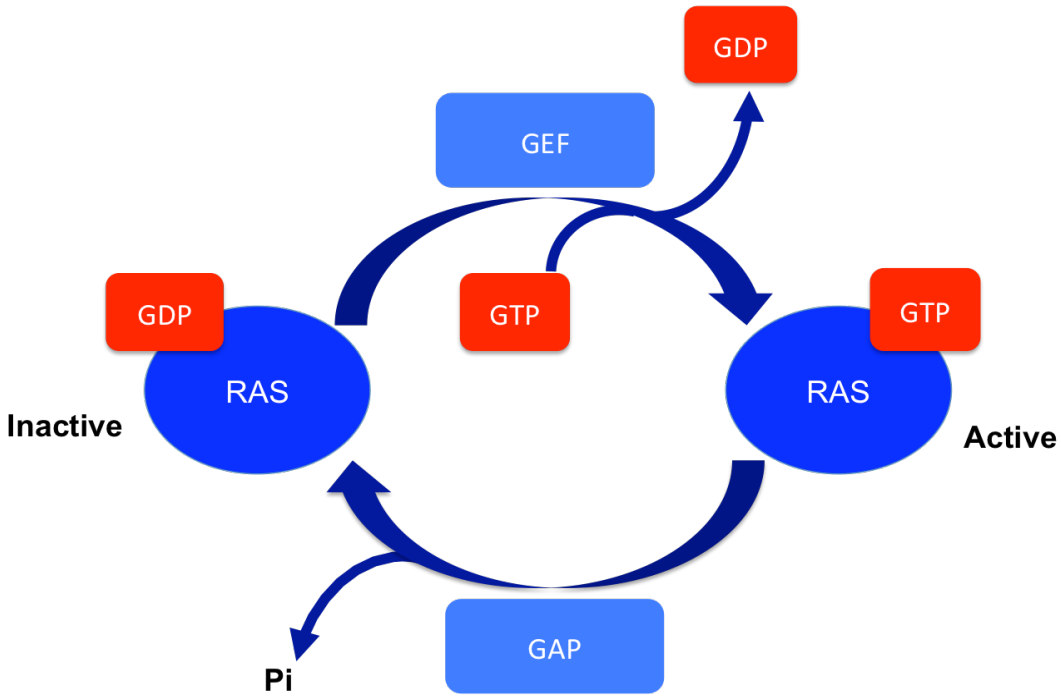

Figure 1.1.4. Ras activation.

RAS is active when bound to GTP, GEFs activate RAS by increasing the rate at which GDP is released from RAS and replaced with GTP. GAPs inactivate RAS by catalysing the hydrolysis of GTP to GDP and Pi (inorganic phosphate, orthophosphate).

1.5.3 RAS activation in response to EGFR stimulation

In 1993 it was discovered that RAS is activated in response to EGFR signalling (Buday and Downward, 1993). Downstream of EGFR activation, adaptor molecules GRB2 and SOS are recruited in a pre-complexed form to SH2 binding sites of the intracellular kinase domain of EGFR (Rozakis-Adcock et al., 1993). This brings SOS into close proximity with RAS, for which it acts as a GEF, thereby activating RAS (Bonfini et al., 1992). RAS-GTP can then activate a number of effectors, including RAF, PI3K, RALGDS, Tiam, RASSF1 and PLCε (Rajalingam et al., 2007). The RAF/MEK/ERK and PI3K signalling pathways are the RAS effector pathways most prominently involved in cancer, particularly in drug resistance, therefore these will be discussed in more detail.

1.6 RAF/MEK/ERK

Upon activation RAS directly binds to the N-terminus of RAF (Moodie et al., 1993; Vojtek et al., 1993; Warne et al., 1993). There are 3 isoforms of RAF in humans, RAF-1 (C-RAF), B-RAF, and A-RAF, which are structurally conserved in invertebrates and mammals (Wellbrock et al., 2004). All isoforms are activated by RAS, however the mechanism of activation differs. RAF-1 and A-RAF require RAS binding and phosphorylation by SRC for activation, whereas B-RAF only requires RAS for activation (Marais et al., 1997). Key sites for RAF-1 activation are S338 and Y341. Tyrosine phosphorylation at Y341 is mediated by SRC, however the kinase responsible for S338 phosphorylation is less clear. Three other phosphorylation sites and several other proteins such as 14-3-3, p21-activated kinase (PAK), and calcium/calmodulin-dependent kinase II (CaMKII) have been implicated in RAF-1 activation (Salzano et al., 2012; Wellbrock et al., 2004).

Binding of RAF to RAS results in the recruitment of RAF to the plasma membrane (Marais et al., 1995) where it can then phosphorylate and activate extracellular signal regulated kinase (ERK) kinase (MEK) (Dent et al., 1992). The two isoforms of MEK (MEK1 and MEK2) are activated by RAF phosphorylating them at two serine residues within their activation domain (S217 and S221 in MEK1) (Zheng and Guan, 1994). The activation of MEK is enhanced by scaffold proteins such as kinase suppressor of RAS (KSR), which recruits MEK to the membrane and presents it to RAF (Brown and Sacks, 2009). KSR was first identified in C-elegans as a positive regulator of MAPK signalling (Kornfeld et al., 1995), then later found to bind Raf-1, MEK1/2 and ERK1/2 suggesting it's role as a scaffold (Morrison, 2001). Activated MEK then phosphorylates ERK1/2, linking RAS and ERK1/2 signalling. RAS was originally discovered to positively regulate ERK1/2 signalling in 1992 (Leevers and Marshall, 1992), before knowledge of the RAS-RAF-MEK-ERK1/2 signalling cascade had been fully established.

ERK1/2 proteins when activated can either form homodimers and activate a number of cytosolic proteins or translocate to the nucleus in monomeric form to phosphorylate transcription factors, such as the ETS family of transcription factors including ELK1 (Casar et al., 2008). Phosphorylation of ELK1 increases its DNA

binding and transactivation ability. ELK1 in cooperation with serum response factor (SRF) binds to serum response elements (SRE) in promoters to activate transcription of genes such as c-FOS to promote proliferation (Yordy and Muise-Helmericks, 2000). ERK1 and 2 activate the transcription of a number of genes important in cell survival and cell cycle progression, for example MYC (Chuang and Ng, 1994) and Cyclin D1 (Weber et al., 1997). Cytosolic targets of ERK1/2 include the BH3-only pro-apopotic protein BIM_{EL} (Ley et al., 2003). ERK1/2 phosphorylate BIM_{EL}, which targets BIM_{EL} for degradation by the proteasome and inhibits apoptosis. ERK1/2 also phosphorylates FOXO3a, promoting its translocation from the nucleus to the cytoplasm, and targeting it for further ubiquitination by MDM2 and proteasomal degradation (Yang et al., 2008).

1.6.1 RAF/MEK/ERK activation in cancer

The RAF/MEK/ERK pathway is frequently dysregulated in cancer, not just at the level of activation by oncogenic *RAS* or upstream receptors. ERK1/2 is dysregulated in approximately 30% of all cancers, demonstrating its pivotal role in cancer cell signalling. *BRAF* is frequently mutated in melanoma, thyroid cancer, colorectal cancer and ovarian cancers leading to hyperactivation of ERK1/2 in these tumours (Wellbrock et al., 2004). *MEK1* and *MEK2* mutations are not commonly observed in human cancers, however a mutated form of *MEK1* was recently identified in NSCLC (Pao and Girard, 2011). Other mechanisms of ERK1/2 activation include repression of negative regulators of the MAPK pathway such as SPROUTY2 (Frank et al., 2009) and NF1 (Mendes-Pereira et al., 2011). As previously mentioned NF1 is a RAS GAP, therefore it negatively regulates RAS activity (Basu et al., 1992). Mutations in *NF1* are the genetic basis for neurofibromatosis type 1, a hereditary disease characterised by increased formation of benign and malignant tumours of neural crest origin. NF1 functions as a tumour suppressor and *NF1* genetic inactivation has been reported in a number of tumour types including sporadically occurring gliomas, ovarian cancer, adult acute myelogenous leukaemia and lung adenocarcinomas (The Cancer Genome Atlas Research Network, 2008; The Cancer Genome Atlas Research Network, 2011; Ding et al., 2008; Parkin et al., 2010). Ding et al. reported that 13/188 lung tumours had *NF1* mutations indicating that mutations in *NF1* may have a role in NSCLC.

1.7 PI3K signalling

The other major RAS effector pathway most commonly aberrantly activated in cancer is the PI3K/AKT pathway (Castellano and Downward, 2011). PI3K converts phosphatidylinositol (4,5)-bisphosphate (PIP_2) to phosphatidylinositol (3,4,5)-trisphosphate (PIP_3), which in turn recruits AKT to the plasma membrane via its pleckstrin homology domain where it is activated. PI3K is a heterodimeric protein consisting of a regulatory and catalytic subunit. The PI3K family is subdivided into class I, II and III members, of which class I can be further separated into A and B members. Classification separates family members by the regulatory and catalytic subunits they contain (Vanhaesebroeck et al., 2010). The most common isoform implicated in cancer is a class IA PI3K (and will be the isoform referred to hereon in) and consists of a p110α catalytic subunit bound to a p85 regulatory subunit (Zhao and Vogt, 2008). RAS can bind directly to p110α, where it is thought to induce conformational changes to enhance activity (Pacold et al., 2000). PI3K can also be activated by EGFR signalling independently of RAS, via GRB2. As previously stated GRB2 can bind SH2 sites on EGFR, and can then recruit GAB1, a scaffold protein which binds to p85 (Pawson, 2004). The p85 subunit of PI3K is recruited directly to pYXXM motifs within the intracellular domain of RTKs such as ErbB3, created upon ligand activation, but p85 is not thought to bind to EGFR directly (Olayioye et al., 2000). The production of PIP_3 by PI3K also leads to the recruitment of PDK1 (3-phosphoinositide dependent protein kinase-1) to the plasma membrane, where in close proximity it can phosphorylate AKT at Thr308 (Currie et al., 1999). AKT is then fully activated by further phosphorylation at Ser473 by mTORC2 (Hresko and Mueckler, 2005; Sarbassov et al., 2005).

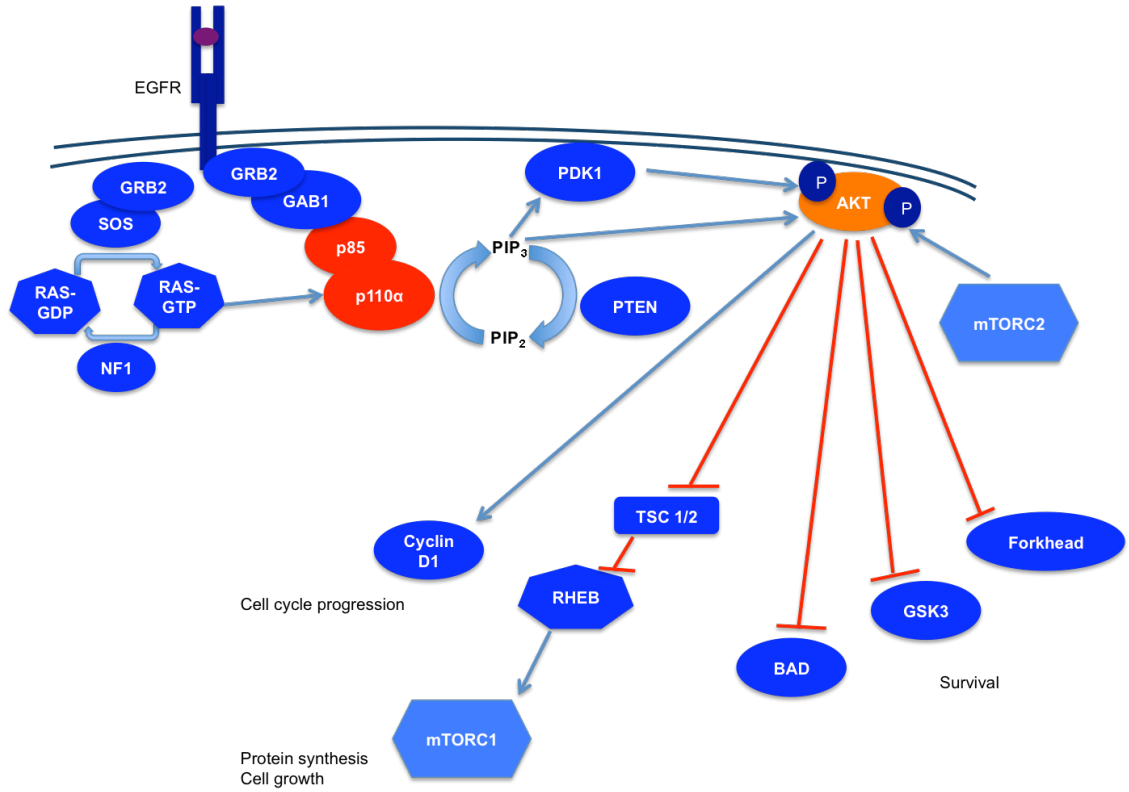

Figure 1.1.5. PI3K-AKT signalling.

PI3K activation downstream of EGFR. Activated PI3K produces PIP_3 which recruits AKT and PDK to the plasma membrane. PDK then phosphorylates AKT, which is then fully activated by phosphorylation by mTORC2. AKT substrates include forkhead transcription factors, GSK3 and BAD, which it inhibits to prevent apoptosis. AKT activates cyclin D1 and mTORC1 to promote proliferation, and protein synthesis.

1.7.1 PI3K/AKT signalling in cancer

PI3K/AKT signalling is dysregulated in a variety of tumour types at multiple points in the pathway, from amplification and activation of receptors at the cell membrane downwards. The most common mechanisms of aberrant activation occur though activating mutations in *PIK3CA*, the gene encoding the catalytic PI3K subunit p110α, and loss of PTEN (phosphatase and tensin homolog), a negative regulator of PI3K/AKT signalling (Yuan and Cantley, 2008).

PIK3CA is mutated in approximately 30% of human cancers, including those of the breast, colon, endometrium and prostate (Zhao and Vogt, 2008). 80% of mutations are one of three 'hotspot' mutations that lead to increased lipid kinase activity (Vogt et al., 2007). PTEN is a dual protein and lipid phosphatase whose lipid

phosphatase activity counteracts the function of PI3K. PTEN desphosphorylates PIP_3 , and therefore attenuates recruitment and activation of AKT at the plasma membrane (Cantley and Neel, 1999). Loss of PTEN leads to an accumulation of PIP_3 and unrestrained activation of downstream signalling. *PTEN* germline mutations result in PTEN hamartoma tumour syndrome (PHTS) that is characterised by benign growths and high susceptibility to developing cancers of the breast, endometrium and thyroid (Hollander et al., 2011). *PTEN* is also mutated or deleted in a range of sporadically occurring tumours, for example loss of heterozygosity at 10q23 (which includes *PTEN*) is present in approximately 40% of sporadic breast tumours (Singh et al., 1998). Additionally levels of PTEN can be downregulated by promoter methylation, microRNAs, and loss of the *PTEN* pseudogene, and activity can be affected by posttranslational modifications such as ubiquitination and acetylation (Carracedo et al., 2011). Also, PI3K signalling can be aberrantly activated by mutations in the p85 regulatory subunit of PI3K. Inactivating mutations in *PIK3R1* and *PIK3R2* are relatively rare in common cancers, but are mutated at a high frequency in endometrial cancer (Cheung et al., 2011b).

Downstream of PI3K, amplifications of *AKT* isoforms have been found in pancreatic, ovarian and head and neck cancers (Engelman et al., 2006). An activating somatic mutation has also been discovered in *AKT1* in breast, colorectal, ovarian and endometrial cancers (Carpten et al., 2007; Shoji et al., 2009). This mutation (E17K) in the pleckstrin homology domain constitutively tethers AKT to the plasma membrane, activating signalling.

1.7.2 mTOR signalling

One of the major pathways downstream of AKT activation is the mTOR (mechanistic target of rapamycin) signalling pathway. mTOR signalling is a highly complex pathway subject to much crosstalk and feedback inhibition. mTOR is a serine/threonine kinase of the phosphatidylinositol kinase related protein family (Menon and Manning, 2008). mTOR kinase exists in two distinct macromolecular complexes in humans (mTORC1 and mTORC2)(Fig 1.1.6). Both complexes contain mTOR, mLST8 (mammalian Lethal with SEC13 protein 8), DEPTOR (DEP domain-containing mTOR interacting protein), and scaffold proteins TTI1 (TEL2

interacting protein 1) and TEL2 (telomere maintance 2) (Kaizuka et al., 2010). mTORC1 also contains RAPTOR (Regulatory associated protein of mTOR), and PRAS40 (40 kDa Pro-rich Akt substrate). mTORC2 includes RICTOR (Rapamycin insensitive companion of mTOR), mSIN1 (mammalian Stress-activated protein kinase-interacting protein 1) and PROTOR (protein observed with RICTOR) (Laplante and Sabatini, 2012). Due to the presence of these different non-core components mTORC1 and 2 are functionally distinct, and subject to differences in regulation. For example mTORC1 is sensitive to inhibition with rapamycin whereas mTORC2 is substantially less sensitive, as rapamycin forms a complex with FKBP12 which binds to and inhibits mTORC1 only (Sarbassov et al., 2004).

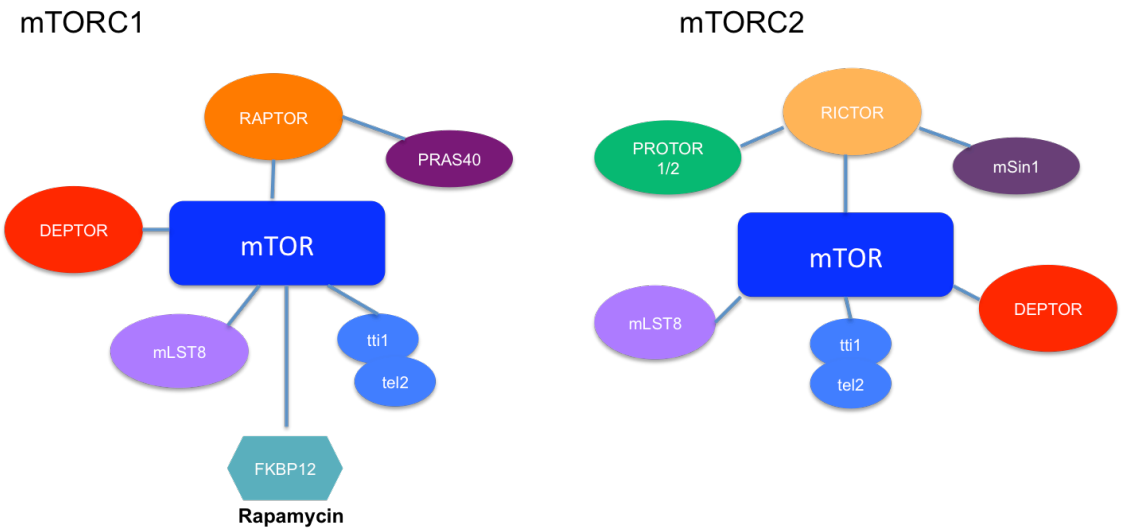

Figure 1.1.6. Components of mTORC1 and 2.
mTOR complex 1 and 2 differ by non-core components, as shown here (adapted from Laplante and Sabatini, 2012).

mTORC1 and 2 are activated by different upstream pathways. As is a recurrent theme in mTOR signalling much more is known about the activation of mTORC1 than mTORC2. mTORC1 incorporates signals from multiple intracellular and extracellular inputs including amino acids, energy status, growth factors, stress and oxygen levels (Zoncu et al., 2011). The majority of these inputs converge at the level of TSC1/2 (tuberous sclerosis 1/2) heterodimer, which acts as a GTPase activating protein for Rheb (Ras homolog enriched in brain). Rheb in its active GTP-bound form binds to and activates mTORC1, therefore TSC1/2 negatively regulates mTORC1 activity by speeding up the conversion of Rheb-GTP to Rheb-

GDP (Inoki et al., 2003a). Several pathways act on TSC1/2 as demonstrated in Fig 1.1.7. TSC1/2 activity is inhibited by AKT, ERK and RSK phosphorylation, and further enhanced by phosphorylation by AMPK (Inoki et al., 2002) (Ma et al., 2005) (Roux et al., 2004) (Inoki et al., 2003b). Additionally mTORC1 activity is regulated independently of TSC1/2 by AKT via inhibition of PRAS40 (an mTORC1 inhibitor). Upon activation of insulin signalling PRAS40 is phosphorylated by AKT, after which it ceases to bind mTOR, and is instead sequestered by 14-3-3 proteins, allowing activation of mTORC1 signalling (Vander Haar et al., 2007). Also, AMPK can directly phosphorylate RAPTOR causing allosteric inhibition of mTORC1 in a low energy state (Inoki et al., 2003b). Amino acids are essential for the activation of mTORC1 by all inputs, for translocation from the cytoplasm to the lysosomal surface via interaction with Rag GTPases. This is thought to bring mTORC1 into proximity with Rheb, which is localised in endomembranes (Sancak et al., 2010).

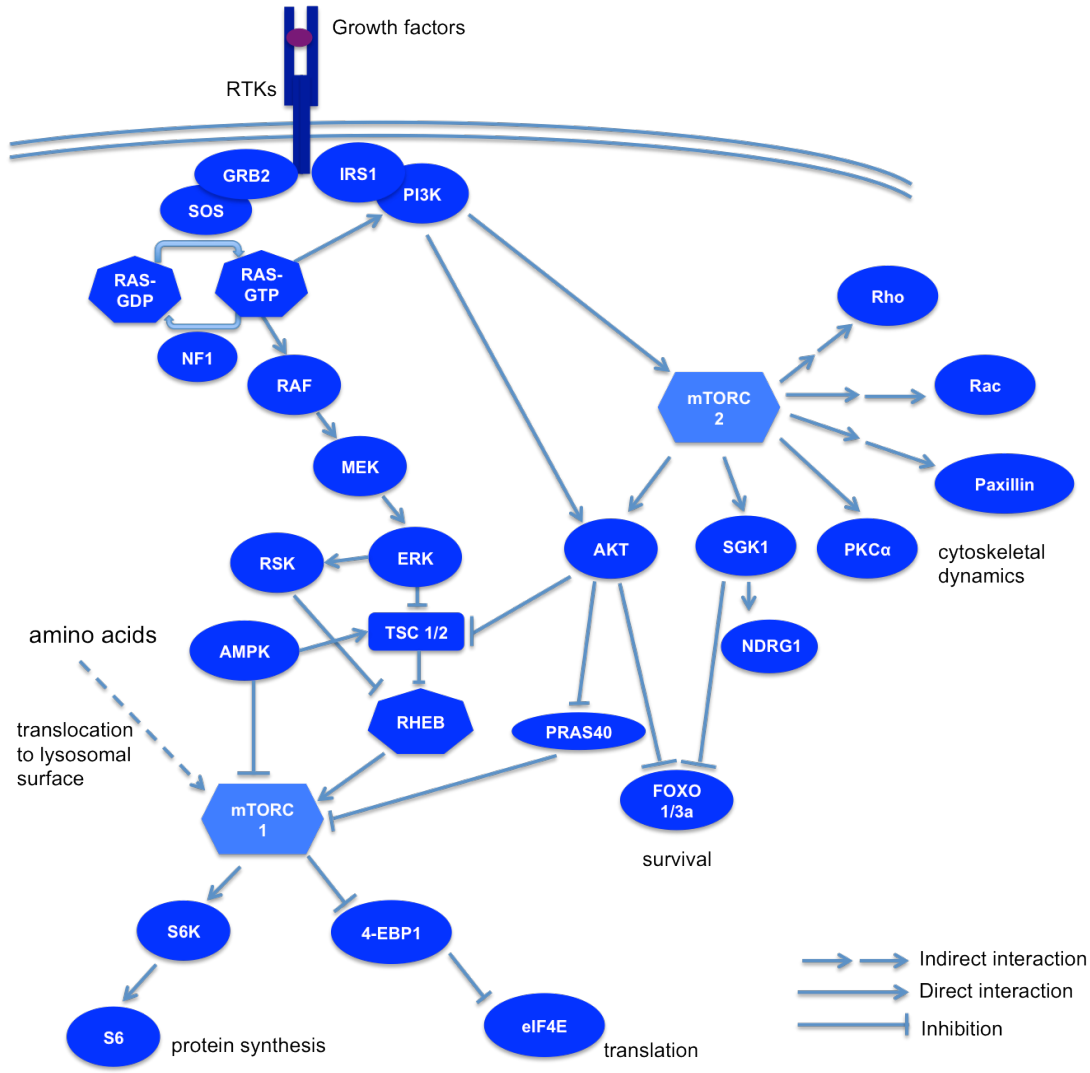

Figure 1.1.7. Overview of mTOR signalling.

mTORC1 is activated in response to growth factor signalling through RAS-MAPK, PI3K-AKT, as well as amino acids which facilitate translocation to the lysosomal surface. mTORC1 is inhibited by hypoxia and stress signalling through AMPK. Key substrates of mTORC1 are S6K and 4EBP1 resulting in increased translation. mTORC2 is activated through growth factors via PI3K, to stimulate AGC kinases AKT, SGK1 and PKCα, to promote cell survival and cytoskeletal reorganisation.

On the other hand, the mechanism of mTORC2 activation is not well defined. It is not activated by Rheb, and appears to be stimulated by growth factors via PI3K, although the exact mechanism is still unclear. More recently a role for ribosomes in mTORC2 activation has been postulated as mTORC2-ribosome association is stimulated by PI3K signalling, and seemingly required for mTORC2 activation (Zinzalla et al., 2011).

mTORC1 is involved in the activation of a variety of cellular processes, the most well studied being protein synthesis. Key mTORC1 effectors in this process are S6K and 4-EBP1 (Ma and Blenis, 2009). mTORC1 phosphorylates and activates S6K, which has important functions in regulating translation initiation factors and ribosomal biogenesis. For example, S6K1 phosphorylates eIF4B that promotes recruitment of eIF4B to the pre-initiation complex, where it enhances eIF4A function (Holz et al., 2005). eIF4A is required to unwind structured mRNAs to allow ribosome binding and translation. Additionally S6K1 enhances eIF4A function by inhibiting the negative regulator of eIF4A, PDCD4 (Dorrello et al., 2006). mTORC1 phosphorylates 4-EBP1 to relieve its repression of eIF4E, also important in translation. 4-EBP1 phosphorylation promotes disassociation from eIF4E, which can then bind eIF4G and is recruited to the 5' end of an mRNA, to promote cap-dependent translation (Ma and Blenis, 2009).

Downstream of mTORC2 activation, relatively few targets have been well described. Confirmed downstream substrates of mTORC2 are the AGC kinases AKT, SGK1 and PKC alpha. After many years of searching mTORC2 was identified as the second AKT kinase, phosphorylating AKT on Ser473 which is required for full activation (Hresko and Mueckler, 2005) (Sarbassov et al., 2005). mTORC2 activates SGK1 which in conjunction with AKT, negatively regulates FOXO1/3a to prevent apoptosis (Garcia-Martinez and Alessi, 2008). FOXO induces the expression of pro-apoptotic factors such as Fas-L and the BH3-only protein BIM_{EL} (Fu and Tindall, 2008). AKT and SGK1 can also phosphorylate BAD, which leads to its sequestration by 14-3-3 proteins in the cytoplasm, and blocks its pro-apoptotic function (Datta et al., 1997). mTORC2 regulates the cell cytoskeleton through activation of PKC alpha, rho, rac and paxillin (Jacinto et al., 2004; Sarbassov et al., 2004).

mTOR activity is negatively regulated by interaction with a number of other proteins. TSC1/2 and PRAS40 only affect the activity of mTORC1, whilst DEPTOR equally inhibits both complexes (Peterson et al., 2009). DEPTOR binds to both mTOR complexes as the endogenous protein can be immunoprecipitated with antibodies against mTOR, RICTOR and RAPTOR from HeLa cell lysates. DEPTOR inhibits mTOR signalling, however the mechanism by which this occurs is not well defined.

DEPTOR loss leads to increased activation of mTORC substrates S6K, AKT and SGK in full serum conditions (Peterson et al., 2009).

1.7.3 mTOR signalling in cancer

mTORC signalling is aberrantly activated in a wide range of tumours, as the previously described PI3K/AKT and MAPK pathways which are frequently activated in cancer both feed into this pathway. Aside from this, mTORC signalling is also upregulated by mutations in *LKB1* and *TSC1* and *TSC2*. LKB1 is an important upstream activator of AMPK, which inhibits mTORC1 in nutrient deprived conditions. LKB1 loss therefore leads to loss of AMPK activation and subsequent downregulation of TSC2 activity. *LKB1* has been described as one of the most frequently mutated genes in lung adenocarcinoma (Ding et al., 2008). Either by mutation or homozygous deletion *LKB1* is thought to be inactivated in approximately 40% of NSCLC (Gill et al., 2011). Mutations in *TSC1/2* result in Tuberous Sclerosis Complex, a tumour susceptibility syndrome characterised by benign tumours in multiple organs as a consequence of constitutively active mTORC1 signalling. Occasionally, such tumours progress to malignant tumours, most commonly in the kidney or pancreas (Inoki and Guan, 2009). Additionally mTORC2 is hyperactivated in glioma compared to normal brain through overexpression of RICTOR (Masri et al., 2007).

1.8 Mechanisms of resistance to EGFR TKIs in *EGFR*-mutant NSCLC

1.8.1 Primary resistance to EGFR TKIs

In populations of patients in which the presence of activating *EGFR*-mutations has not been selected for, treatment with EGFR TKIs provides little advantage to the patient. In unselected trials response rate ranges from 10–55%, whereas in patients selected for *EGFR* activating mutations response rates are substantially higher at 70-75% (Pircher et al., 2010). In addition to lack of response in wild type *EGFR* patients, it has been suggested *KRAS* mutations cause primary resistance to EGFR TKIs in NSCLC, analogous to the situation in colorectal cancer (Dempke and Heinemann, 2010). *KRAS* mutations are associated with poor outcome in

response to EGFR TKIs (Bonanno et al., 2010). However, it also appears that *EGFR* and *KRAS* mutations are mutually exclusive in NSCLC, therefore patients with mutated *KRAS* would most likely express wildtype *EGFR*, and consequently be unlikely to respond to EGFR-TKIs (Pao et al., 2005b). *EML4-ALK* chromosomal rearrangements have also been linked to lack of response to EGFR-TKIs, however yet again *EML4-ALK* expressing tumours generally have wildtype *EGFR* (Shaw et al., 2009).

It also appears that some *EGFR* mutations although they cause constitutive activation of EGFR signalling, and are able to transform NIH-3T3 cells, do not render cells sensitive to EGFR tyrosine kinase inhibitors (Greulich et al., 2005). Lung adenocarcinoma patients with insertion mutations in exon 20 of *EGFR* are not sensitive to erlotinib or gefitinib, although they are sensitive to irreversible EGFR inhibitors.

1.8.2 The T790M mutation

As aforementioned, the occurrence of resistance to EGFR TKI is a major problem in their efficacy to treat lung cancer. Several mechanisms of acquired resistance have been suggested, however few have been validated in a clinical setting. The most common causes of resistance occurring in patients are a secondary mutation in the EGFR kinase domain (T790M) and the amplification of *MET*, encoding the receptor for HGF (Engelman et al., 2007; Pao et al., 2005a).

A secondary T790M mutation in the EGFR kinase domain is the most frequently found mechanism of acquired resistance, occurring in approximately 60% of resistant cases (Pao et al., 2005a). This 'gate-keeper' mutation reduces the ability of EGFR TKIs to bind in the ATP cleft, analogous to the T315I mutation conferring resistance to the BCR-ABL inhibitor imatinib (Gorre et al., 2001). It is also thought that T790M mutation mediates resistance by increasing the affinity of EGFR for ATP (Yun et al., 2008). EGFR TKIs must compete with ATP, the natural substrate of EGFR to bind in the ATP binding pocket. *EGFR* activating mutations sensitise EGFR to inhibition by TKIs as they reduce its affinity for ATP, allowing TKIs opportunity to bind. The T790M mutation restores the affinity of mutant EGFR to wildtype levels, thereby reducing the effect of TKIs (Yun et al., 2008).

There is some evidence that T790M when occurring in cis with activating *EGFR* mutations, enhances EGFR signalling and increases oncogenic capacity of cells (Godin-Heymann et al., 2008). However counter-intuitively, patients with acquired resistance to EGFR TKIs and the T790M mutation have been shown to have longer progression-free survival and tend to develop metastases later than patients without the mutation when maintained on EGFR TKI treatment (Oxnard et al., 2011b). This indicates T790M mutation may not enhance the tumourigenic capacity of cells beyond conferring resistance to EGFR TKIs. It has been argued that the T790M mutation may actually slow growth of tumour cells, therefore it does not provide any growth advantage in the absence of the selection pressure provided by EGFR TKIs (Chmielecki et al., 2011). Chmielecki et al. derived PC9 and HCC827 cells resistant to erlotinib or an irreversible EGFR inhibitor, which they found to contain the T790M allele. The growth rate of T790M-containing cells was significantly slower than that of the TKI-sensitive non-T790M cells, and the T790M mutation was lost from the cell population over time in the absence of an EGFR TKI (Chmielecki et al., 2011). This indicates that in the absence of drug selection the T790M provides no proliferative advantage to tumour cells, and could possibly explain how patients who have become resistant to erlotinib, may re-respond to treatment after a 'drug holiday' (Becker et al., 2011; Oxnard et al., 2011a). However it is important to note that H3225 cells generated in the same manner retained T790M in the absence of EGFR TKIs, and it did not affect the growth rate, indicating it is likely to be highly context dependent (Chmielecki et al., 2011). Therefore whether T790M in cis with activating *EGFR* mutations increases oncogenic capacity beyond EGFR-TKI resistance is still under debate.

Another question surrounding T790M mediated resistance, is how it arises? Is it a de novo mutation, or is it present at a low level in tumours and selected for during drug treatment? With the development of increasingly sensitive techniques it seems that T790M drug resistant clones are present at low frequencies in tumours pre-treatment, and that they are selected for during TKI treatment due to their survival advantage (Maheswaran et al., 2008) (Oh et al., 2011).

1.8.3 Other secondary *EGFR* mutations that confer resistance to EGFR TKIs

T790M is the secondary *EGFR* mutation overwhelmingly associated with EGFR TKI resistance, however it is possible other *EGFR* mutations may also play a role. D761Y mutations have been found in rare cases in NSCLC patients that have $EGFR^{L858R}$ activating mutations but are refractory to EGFR TKI treatment (Balak et al., 2006; Tokumo et al., 2006). In one patient who initially responded to gefitinib the $EGFR^{D761Y}$ mutation was found in a brain metastasis shortly after disease progression (Balak et al., 2006). In a separate case study the D761Y mutation was found in the primary tumour and liver metastasis of a patient unresponsive to gefitinib (Tokumo et al., 2006). 293T cells transfected with an L858R D761Y mutant *EGFR* cDNA were modestly more resistant to gefitinib treatment than the L858R mutant alone, indicating the mutation increases resistance to EGFR TKIs. However the increase in resistance was small compared to that conferred by the T790M mutation (Balak et al., 2006).

1.8.4 Amplification of *MET*

Aside from the T790M mutation, amplification of the *MET* gene encoding the MET tyrosine kinase receptor is the most prevalent mechanism, found in 5-15% of resistant cases (Arcila et al., 2011; Sequist et al., 2011). *MET* amplification provides an alternative route to maintain AKT signalling, necessary for survival, in erlotinib-treated cells. In *MET* amplified cells MET heterodimerises with ERBB3, leading to the recruitment of p85, and through this mechanism PI3K-AKT signalling is retained in the presence of EGFR TKIs (Engelman et al., 2007).

As with the T790M mutation, recent studies suggest *MET* amplification is also present at low levels within a tumour cell population, and preferentially selected for during drug treatment. Turke and colleagues detected *MET* amplification in 6% HCC827 cells examined (Turke et al., 2010). Turke et al. also linked expression of MET receptor ligand HGF to the emergence of *MET* amplification in HCC827 cells. They found that co-treatment of HCC827 cells with gefitinib and HGF, lead to a significant increase in gefitinib resistance, and that cells remained resistant after HGF withdrawal due to a 3 to 4 fold amplification of *MET*. This is presumably because cells expressing amplified levels of *MET* have a selective advantage in the

presence of high levels of HGF. Interestingly, it appears that whilst accelerating selection of *MET* amplified clones, HGF also causes a transient increase in resistance by a distinct signalling mechanism. HGF treatment renders NSCLC cells transiently resistant to EGFR TKIs by promoting the association of GAB1 and the p85 subunit of PI3K, thus activating AKT. However in contrast to *MET* amplified cells, this mechanism is independent of ERBB3 (Yano et al., 2008) (Fig.1.8).

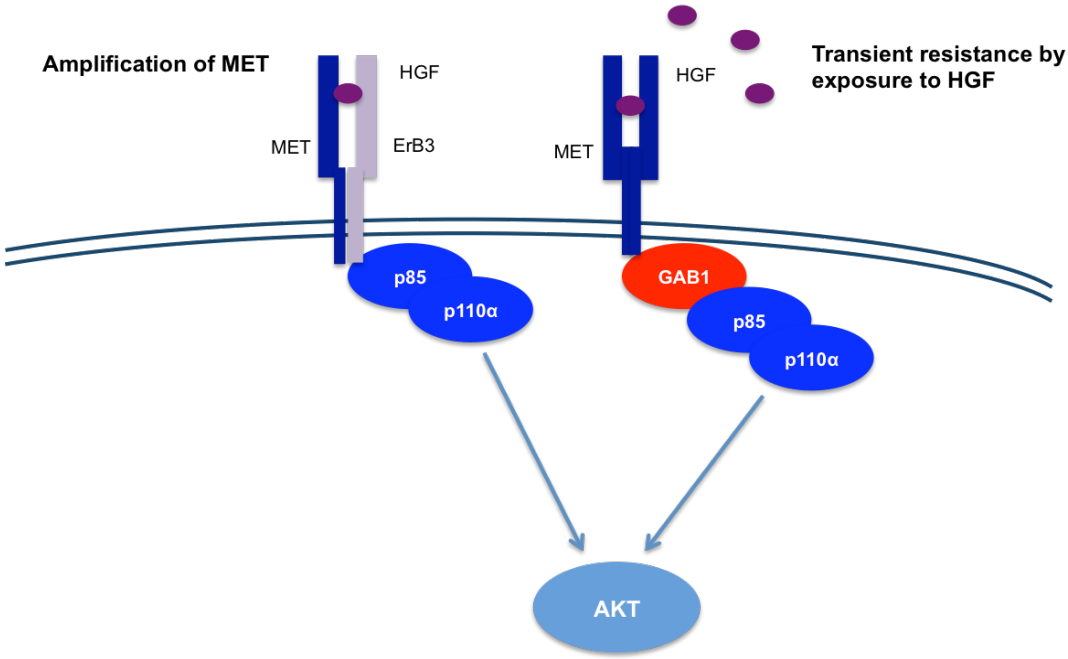

Figure 1.1.8. MET-mediated acquired resistance to EGFR-TKIs.
Amplification of *MET* leads to increased PI3K-AKT activation via heterodimerisation with ERBB3. *MET* amplification is hastened by exposure to HGF, however HGF also mediates transient resistance by increasing PI3K-AKT signalling via GAB1 independently of ERBB3.

1.8.5 Histological transformation to SCLC

Recently Sequist and colleagues published a study detailing the histological and genetic alterations of 37 patients with drug-resistant NSCLC with *EGFR* mutations (Sequist et al., 2011). In this study they identified the previously known T790M mutation and *MET* amplification as well as some novel mechanisms of resistance. The most surprising finding was the histological transition of 5 patients' tumours from NSCLC to SCLC, and their subsequent sensitisation to standard SCLC treatments. Another rebiopsy study also revealed this phenomenon, albeit at a lower frequency. Arcila and colleagues found 2% of patients exhibited SCLC morphology in resistant tumours, where NSCLC had been observed before treatment, a substantially lower percentage than the 14% identified by Sequist et

al.(Arcila et al., 2011). Detection of EGFR-TKI refractory SCLC after an initial diagnosis of *EGFR*-mutant adenocarcinoma is rare but had been reported prior to the new studies. Zakowski describes one patient with adenocarcinoma who had a partial response to erlotinib treatment, but after disease progression was found to have SCLC, however this patient did not respond to etoposide, a common treatment for SCLC (Zakowski et al., 2006).

1.8.6 Activation of PI3K/AKT signalling by somatic mutations in *PIK3CA* and *PTEN*

Other mechanisms of resistance observed by Sequist and colleagues included an acquired *PIK3CA* mutation, with resistance presumably arising from increased PI3K signalling. Other groups have observed *PIK3CA* mutations in approximately 4% of NSCLC, which is correlated to poor outcome for patients treated with EGFR TKIs (Ludovini et al., 2011). In this study time to progression between wildtype and mutant *PIKCA3* patients was 30.2 months compared to 9.9 months respectively. They identified one patient with an *EGFR* and a *PIKC3A* mutation, who experienced an extremely short (4 months) response to erlotinib suggesting *PI3KCA* mutations may attenuate response to TKI treatment. *PIK3CA* mutations have been linked to poor response to other ERBB family (HER2) inhibitors trastuzumab and lapatinib in HER2-positive breast cancer indicating they may cause resistance to ERBB family targeted therapies (Wang et al., 2011).

Loss of PTEN, again activating PI3K signalling has also been suggested as a mechanism for resistance to EGFR TKIs in NSCLC. Sos and colleagues identified homozygous loss of *PTEN* as the reason for erlotinib resistance in the *EGFR*-mutant NSCLC cell line H1650 (Sos et al., 2009). As a result of *PTEN* loss H1650 cells retained high levels of phosphorylated AKT despite inhibition of EGFR by erlotinib. This effect could be reversed by reconstitution of PTEN expression in these cells. They also described that silencing of PTEN in PC9 cells lead to increased phosphorylation of ERK and EGFR in erlotinib-treated conditions compared to PTEN expressing cells, possibly through upregulation of EGFR ligand expression by ERK. Additionally, PTEN instability has been described to cause resistance to gefitinib in a cetuximab resistant subline of *EGFR*-mutant NSCLC

HCC827 cells, whereas parental HCC827 cells are sensitive to EGFR TKIs (Kim et al., 2010a). PTEN loss is relatively common in NSCLC (approximately 35%), however a causative link to EGFR-TKI resistance in patients is yet to be clinically established (O'Byrne et al., 2011).

1.8.7 Epithelial-Mesenchymal Transition

Sequist and colleagues additionally found 2 cases of epithelial-to-mesenchymal transition (EMT) (Sequist et al., 2011). EMT is a phenotypic transformation of epithelial cells to a more mesenchymal phenotype. Presence of EMT is often demonstrated by loss of epithelial markers such as E-cadherin and cytokeratins, and gain of mesenchymal markers such as vimentin and N-cadherin (Thiery, 2002). EMT has been proposed as a mechanism of resistance to EGFR inhibitors in a number of studies in vitro (Buck et al., 2007; Thomson et al., 2005; Thomson et al., 2008). Thomson et al. suggest EMT confers resistance by causing a switch in kinase pathway activation. They find EGFR, ERBB2 and ERBB3 phosphorylation is attenuated in mesenchymal-like cells, and expression of EGFR family ligands is decreased (Thomson et al., 2005; Thomson et al., 2008). Conversely PDGFR, FGFR and TGFβ receptor expression increased in cells stimulated to undergo EMT by TGFβ overexpression (Thomson et al., 2008). However it is important to note these studies were carried out in wild-type *EGFR* cell lines, potentially limiting their relevance to the clinical situation.

Sequist et al provides clinical evidence for EMT as a mechanism of acquired resistance in *EGFR*-mutant NSCLC (Sequist et al., 2011). This discovery is supported by another study where Chung and colleagues found HCC827 cells generated to be resistant to irreversible EGFR inhibitor CL-387,785 showed the hallmarks of EMT such as loss of E-cadherin and increased vimentin expression (Chung et al., 2010).

1.8.8 Alterations in IGFR signalling

Other potential mechanisms of resistance discovered link to alterations in IGFR signalling. It has been described that loss of IGF binding proteins can cause resistance to EGFR TKIs by activating the IGF1 receptor (Guix et al., 2008). In

gefitinib resistant A431 cells IGFR1 activation lead to constitutive association of IRS-1 with PI3K, and subsequent phosphorylation of AKT, even in the presence of EGFR TKIs. IRS-1 and PI3K are not found to be associated in parental A431 cells, which are sensitive to EGFR inhibition, indicating this interaction is an adaptation acquired by resistant cells (Guix et al., 2008).

IGFR1 signalling was also found to be essential for the emergence of drug tolerant PC9 NSCLC cells (Sharma et al., 2010). Sharma and colleagues noticed that whenever they acutely treated PC9 cells with EGFR TKIs, there was always a small population of cells still surviving after 9 days treatment. Upon further investigation they found these cells arise de novo from the population and are transiently resistant to drug treatment due to epigenetic mechanisms. Drug tolerant cells express higher levels of KDM5A, a histone demethylase, and also increased levels of IGFBP3 that leads to elevated IGFR1 phosphorylation. Co-treatment of PC9 cells with EGFR TKI and an IGF1R inhibitor prevents the emergence of drug tolerant cells. Elevated IGF1R signalling and KMD5A expression appear to be linked and necessary for acquisition of transient drug tolerance (Sharma et al., 2010).

1.8.9 NF Kappa B signalling

Another suggested mechanism of resistance to erlotinib in NSCLC is via activation of the NF Kappa B signalling pathway (Bivona et al., 2011). NF Kappa B signalling has previously been implicated in lung tumourigenesis in a KRAS-driven p53 null background. Bivona and colleagues found that RNAi mediated silencing of FAS and other components of the NF Kappa B pathway such as RELA and c-FLIP enhances sensitivity of NSCLC cells to erlotinib treatment (Bivona et al., 2011). Additionally they found IkB expression correlated with survival in a cohort of 52 *EGFR*-mutant lung cancer patients who had been treated with EGFR TKIs. Low expression of IkB, indicating high NF Kappa B activation, correlated with poorer progression-free survival. This effect seemed specific to EGFR TKI treatment, as IkB expression was not predictive of outcome in patients receiving chemotherapy and surgery.

1.8.10 *CRKL* amplification

One of the most recently proposed mechanisms of resistance to EGFR-TKIs is the amplification of *CRKL* (Cheung et al., 2011a). CRKL is an adaptor protein containing an SH2 domain and two SH3 domains, allowing binding to other important signalling proteins such as GAB1, SOS and p85 (Birge et al., 2009; Feller, 2001). *CRKL* is amplified in a subset of primary lung adenocarcinomas and NSCLC cell lines (Kim et al., 2010b). Cheung and colleagues found *CRKL* amplification in samples from a patient with acquired resistance to EGFR-TKIs, where there was no evidence of *CRKL* amplification prior to EGFR-TKI treatment. *CRKL* amplification is thought to mediate resistance by activation of MAPK signalling via increased recruitment of SOS to the plasma membrane, and enhanced PI3K-AKT signalling via p85 (Cheung et al., 2011a).

1.8.11 Activation of AXL kinase

A novel mechanism of resistance established this year is the activation of the receptor tyrosine kinase AXL (Zhang et al., 2012). Zhang and colleagues found AXL expression and activation was increased in erlotinib resistant HCC827 cells and resistant tumour xenografts. AXL upregulation seems to increase resistance at least in part by activating the PI3K-AKT and MAPK pathways. Additionally AXL ligand GAS6 expression was increased in erlotinib resistant cell lines and some erlotinib resistant tumours, indicating overexpression of AXL or increased activation by GAS6 can drive resistance (Zhang et al., 2012). Also Zhang et al. found increased expression of vimentin in some erlotinib resistant tumours with AXL upregulation, which is suggestive of EMT, however a direct link between AXL expression and EMT is yet to be established.

1.8.12 Alternative mechanisms of resistance

Current clinically validated mechanisms of resistance; $EGFR^{T790M}$ mutation, *MET* amplification and SCLC transformation account for 70% of EGFR TKI resistant NSCLC cases (Fig.1.9) (Oxnard et al., 2011a; Sequist et al., 2011). Taking in to account all mechanisms, cause of resistance is still unknown in 25-30% of cases. Therefore the aim of my project was to determine novel mechanisms of resistance to EGFR TKIs.

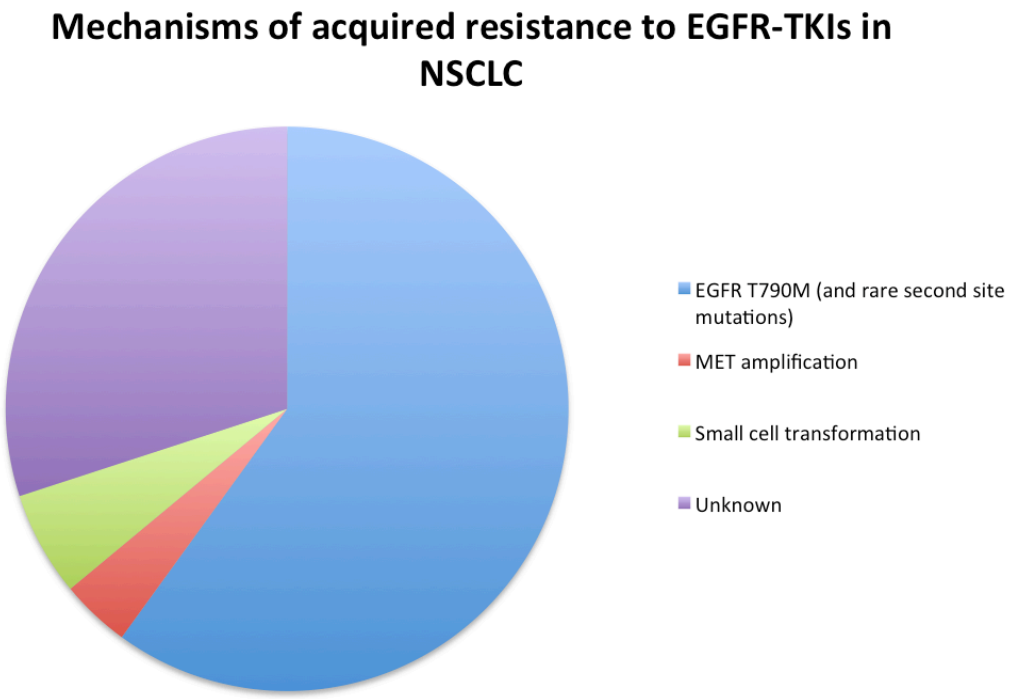

Figure 1.1.9. Mechanisms of acquired resistance to EGFR-TKIs in NSCLC.
Frequency of acquired resistance to EGFR-TKIs. PIK3CA mutations and EMT are included in unknown, as they have been found in small subsets of patients and currently the prevalence is unclear. Adapted from Sequist et al., 2011.

1.8.13 Outline of subsequent chapters

The first results chapter of this thesis describes a genome-wide siRNA screen we carried out in order to identify novel genes involved in the response to EGFR-TKIs in *EGFR*-mutant NSCLC. The aim of the screen was to identify new therapeutic targets that could be targeted to improve the efficacy of erlotinib, or alternatively identify potential biomarkers of resistance. The remaining results chapters describe two genes that we identified in the screen (*DEPTOR* and *NF1* respectively). Depletion of these genes by RNAi increases resistance of *EGFR*-mutant NSCLC to erlotinib treatment. Mechanisms of resistance caused by loss of these genes are described, as well as potential combination therapies for patients in which function of these genes is lost.

Chapter 2. Materials & Methods

2.1 Materials

2.1.1 Drugs

All drugs were solubilised in DMSO or H_20 according to manufacturer's instructions and stored at -20°C.

AKT inhibitors

MK2206 (Acitve Biochem)

mTOR allosteric inhibitors

Temsirolimus (LC Laboratories)

mTOR kinase inhibitors

AZD8055 (ChemieTek)

EGFR inhibitors

Erlotinib (Enzo Life Sciences)

Gefitinib (Enzo Life Sciences)

MEK inhibitors

AZD6244 (Axon MedChem)

Taxane and platinum-based therapeutric drugs

Docetaxel (Sigma)

Cisplatin (Sigma)

2.1.2 Antibodies

Antibodies were used at the dilutions indicated in PBS supplemented with 0.1% Tween-20 and 3% BSA. Antibodies were stored at -20°C or 4°C according to manufacturer's instructions.

α-Tubulin

Mouse monoclonal (Sigma), 1:1000 dilution

Phospho-p44/42 MAPK (ERK1/2) (Thr202/Tyr204)

Rabbit polyclonal (Cell Signalling), 1:1000 dilution

p44/42 MAPK (ERK1/2)

Rabbit polyclonal (Cell Signalling), 1:1000 dilution

Phospho-AKT (Ser473)

Rabbit polyclonal (Cell Signalling), 1:1000 dilution

AKT

Rabbit polyclonal (Cell Signalling), 1:1000 dilution

Phospho-EGF Receptor (Tyr1068)

Rabbit polyclonal (Cell Signalling), 1:1000 dilution

EGF Receptor

Rabbit polyclonal (Cell Signalling), 1:1000 dilution

EGF Receptor coupled to agarose beads

Goat IgG (Santa Cruz), 50 µl per immunoprecipitation

HER2

Rabbit polyclonal (Cell Signalling), 1:1000 dilution

HER3

Rabbit monoclonal (Cell Signalling), 1:1000 dilution

IGF-IR β

Rabbit polyclonal (Cell Signalling), 1:1000 dilution

MET

Mouse monoclonal (Cell Signalling), 1:1000 dilution

NF1

Rabbit polyclonal (Bethyl Laboratories), 1:1000 dilution

Phospho-S6 Ribosomal Protein (Ser235/236)

Rabbit polyclonal (Cell Signalling) 1:1000 dilution

S6 Ribosomal Protein

Rabbit monoclonal (Cell Signalling), 1:1000 dilution

Phospho-4-EBP1 (Thr37/46)

Rabbit polyclonal (Cell Signalling), 1:1000 dilution

4-EBP1

Rabbit polyclonal (Cell Signalling), 1:1000 dilution

DEPTOR

Rabbit polyclonal (Novus Biologicals), 1:500 dilution

Phospho-NDRG1 (Thr346)

Rabbit polyclonal (Cell Signalling), 1:1000 dilution

NDRG1

Rabbit polyclonal (Cell Signalling), 1:1000 dilution

2.1.3 Buffers and solutions

NuPAGE LDS Sample buffer and MES running buffer were purchased from Invitrogen. PBS, trypsin and versene were provided by CRUK Cell Services. Dried milk was from Marvel. All chemicals were from Sigma.

Commonly used buffers and solutions were:

Cell lysis buffer

20 mM Tris-HCl (pH 7.4)

137 mM NaCl

2 mM EDTA

10% glycerol

1% Triton X-100

Tris buffered saline (TBS)

137 mM NaCl

25 mM Tris-HCl (pH 7.4)

Triton X-100 lysis buffer

20 nM Tris-HCl (pH 7.4)

137 mM NaCl

2 mM EDTA

10% Glycerol

1% Triton X-100

Transfer buffer

25 mM Tris Base

250 mM glycine

20% methanol

Washing buffer (TBST)

TBS

0.1% Tween-20

Blocking solution

TBS

0.1% Tween-20

5% dried milk (Marvel)

2.1.4 siRNA oligonucleotides

The human genome wide siGENOME SMARTpool library was purchased from Dharmacon. Each SMARTpool contained 4 oligonucleotides of different sequences to target the gene of interest. Shown below is the sequence information of each of the 4 oligos of the 26 top hits from the genome-wide screen, which validated in the deconvolution analysis.

Top Hits

Target Gene	Locus ID	RefSeq	19mer sense sequence
ABBC8	6833	NM_000352	GGUCAACGCCAGCGAAUCA
ABBC8	6833	NM_000352	GGUCUACUAUCACAACAUC
ABBC8	6833	NM_000352	GGUACAAGAUGGUCAUUGA
ABBC8	6833	NM_000352	CAACAUUGCUUCCCUCUUC
BRD2	6046	NM_005104	UUAGAGAGCUUGAGCGCUA
BRD2	6046	NM_005104	GAUGAAGGCUCUGUGGAAA
BRD2	6046	NM_005104	GAAAAGAUAUUCCUACAGA
BRD2	6046	NM_005104	AGAAAGGGCUCAUCGCUUA
C10ORF76	79591	NM_024541	UAUCACAUAUGGCGACACA
C10ORF76	79591	NM_024541	CAGAAGAAGUGUCGGGUAC

C10ORF76	79591	NM_024541	UCAAAGAGCUGGUUCGAUC
C10ORF76	79591	NM_024541	GGUCAGCCUUGAUAAAUUU
C21ORF2	755	NM_004928	GAAGACAUAUGGCAAGUUU
C21ORF2	755	NM_004928	CGAAACAGCUGGAUUCAGA
C21ORF2	755	NM_004928	UCAACAGACUCACUAAAUA
C21ORF2	755	NM_004928	GGAAGAAGCUUGUACGUGA
CD72	971	NM_001782	GUUCACAGGUGUCGCGAUC
CD72	971	NM_001782	GACAAAGCCUCCUUCGCUA
CD72	971	NM_001782	ACACCAGGGUCUCGGAAUU
CD72	971	NM_001782	CAACGCGGGUCUCAGGUUU
CDX4	1046	NM_005193	AAUAAUGCCCACAGGGACA
CDX4	1046	NM_005193	GCGCAACAAUGGCCACAGU
CDX4	1046	NM_005193	CGACGCAGCCUUUGAAUGG
CDX4	1046	NM_005193	GGAUCUACCUGAAGUUAAG
COX4I1	1327	NM_001861	CCAAGUGGGACUACGAAAA
COX4I1	1327	NM_001861	CGAGUUGUAUCGCAUUAAG
COX4I1	1327	NM_001861	GCAGAAGCACUAUGUGUAC
COX4I1	1327	NM_001861	UGUACGAGCUCAUGAAAGU
DEPDC6	64798	NM_022783	GGACGAUUGUCAUGGAAGU
DEPDC6	64798	NM_022783	GAUCGUGUCUGCAGUGAGG
DEPDC6	64798	NM_022783	ACAGAGAGACGGCAAUUAA
DEPDC6	64798	NM_022783	GGACAGAGGCUAUAUGAAA
ECGF1	1890	NM_001953	GUAUCGUGGGUCAGAGUGA
ECGF1	1890	NM_001953	GGACGGAAUCCUAUAUGCA
ECGF1	1890	NM_001953	GCUGCAAGGUGCCAAUGAU
ECGF1	1890	NM_001953	CAGCCUCCAUUCUCAGUAA
IRAK4	51135	NM_016123	AAAGUUAGCUGAAUAUGGA
IRAK4	51135	NM_016123	GAACAGCUCACAAGUAUAU
IRAK4	51135	NM_016123	GUACAUACCUGGCUGGAUU
IRAK4	51135	NM_016123	GCACGAGUAUCUUUGUUUA
LOC388633	388633	NM_001010978	GUUCACAGGUGUCGCGAUC
LOC388633	388633	NM_001010978	GACAAAGCCUCCUUCGCUA
LOC388633	388633	NM_001010978	ACACCAGGGUCUCGGAAUU
LOC388633	388633	NM_001010978	CAACGCGGGUCUCAGGUUU

LPXN	9404	NM_004811	GGUACAAGUUCCAUCCUGA
LPXN	9404	NM_004811	GCGCAGCUCGUGUAUACUA
LPXN	9404	NM_004811	CUUCGGAGAUCCUUUCUAU
LPXN	9404	NM_004811	AGAGUUAGAUGCCUUAUUG
MEF2A	4205	NM_005587	CAACAGCUCUAACAAACUG
MEF2A	4205	NM_005587	GAAUGGAUUUGUAAACUCA
MEF2A	4205	NM_005587	CAAACCACAUUACAUAGAA
MEF2A	4205	NM_005587	GAGAAAGUUUGGAUUAAUG
MGC26818	127281	NM_152371	GAUGAUGUUUUCCUACUUU
MGC26818	127281	NM_152371	CUGUUAAGCUUCAUCAGUA
MGC26818	127281	NM_152371	GAACUGAGGAGACUCUUUG
MGC26818	127281	NM_152371	GGACAGGGAAGUCUUAUUU
NF1	4763	NM_000267	GGAAUAAGAUGGUAGAAUA
NF1	4763	NM_000267	GAUAGAAGCUACAGUAAUA
NF1	4763	NM_000267	CAACAAAGCUAAUCCUUAA
NF1	4763	NM_000267	CACCGAGUCUUACAUUUAA
PDXK	8566	NM_003681	GAGGAAGCCUUGCGGGUGA
PDXK	8566	NM_003681	ACUACGUGCUCACAGGUUA
PDXK	8566	NM_003681	UGACCGAAACUUGAUAUUU
PDXK	8566	NM_003681	GACCGAAACUUGAUAUUUU
PHF8	23133	NM_015107	GGACAUCUUUCGCGGUUUG
PHF8	23133	NM_015107	GGAGGGAACUUCUUACACA
PHF8	23133	NM_015107	CAGCAGACCUCUUCAGAUU
PHF8	23133	NM_015107	GAACCAAGAUAGCAAAGAA
PHKA1	5255	NM_002637	GGUCUGAUCAUACAAGUUA
PHKA1	5255	NM_002637	GAACAGACCUCUCCUACCU
PHKA1	5255	NM_002637	UCACUCAGCUGAUAGAUGA
PHKA1	5255	NM_002637	GCAAACAACCUGCGACUUA
POLE4	56655	NM_019896	ACGUGACGCUAGCGGGACA
POLE4	56655	NM_019896	AGAGGAGAGACUUGGAUAA
POLE4	56655	NM_019896	GAGUGAAGGCCUUGGUGAA
POLE4	56655	NM_019896	GGAAGGUACUUUAGAUUGA
PQLC1	80148	NM_025078	UCAAGAUGGUGCUCAUGUG
PQLC1	80148	NM_025078	GGAGCAGCUUCUCGGACUA

PQLC1	80148	NM_025078	GCAGAGCGCCAUCAUGAUC
PQLC1	80148	NM_025078	UCACCUACCUGUCCAUUGA
SDC2	6383	NM_002998	GGUCAGAUGCACUCGGAAC
SDC2	6383	NM_002998	AGGUCCUGGUGUACAAUAA
SDC2	6383	NM_002998	CUACUGACUUUCCCGGUAA
SDC2	6383	NM_002998	GGAAUGAGAAGCUAAAGAA
SGPP2	130367	NM_152386	ACUGGAAUAUUGACCCUUA
SGPP2	130367	NM_152386	CAUCUGCGCUACAACCUUU
SGPP2	130367	NM_152386	AGAAGUACGUCGUGAAGAA
SGPP2	130367	NM_152386	UGAAGUGCCUUACAAGUUU
SLC4A8	9498	NM_004858	GGACACUCAUUCAGAGGUA
SLC4A8	9498	NM_004858	CAAAUGCUGUGUCUUAUAG
SLC4A8	9498	NM_004858	UCACUAAGCACUCGUGUUA
SLC4A8	9498	NM_004858	GAACCAAGAUGAAUAGCAA
WDFY1	57590	NM_020830	UCGAGGCGCUUUCAGGUAA
WDFY1	57590	NM_020830	GCAAAGGAUUCGGAAACUU
WDFY1	57590	NM_020830	UAGACAAACUGAAUGGAUU
WDFY1	57590	NM_020830	GAACGCACUAUUACAGUUA
ZC3HDC6	376940	NM_198581	CAAACAGCGUGGUCAAGUA
ZC3HDC6	376940	NM_198581	CAAGAAAGGCCACUACGAA
ZC3HDC6	376940	NM_198581	GGAAUUCUGUCUUCACAAG
ZC3HDC6	376940	NM_198581	CAAAGCAGCUGUACUUCUC
ZNF291	49855	NM_020843	GAACAUCGAUCGCAACAUC
ZNF291	49855	NM_020843	UGAGAGAGGAUGAUUCUUA
ZNF291	49855	NM_020843	CAGCAAGUCUGAAGUUGAA
ZNF291	49855	NM_020843	CCAUGAACAUCGAUCGCAA

Controls

Target Gene	Locus ID	RefSeq	19mer sense sequence
PLK1	5430	NM_005030	CAACCAAAGUCGAAUAUGA
PLK1	5430	NM_005030	CAAGAAGAAUGAAUACAGU
PLK1	5430	NM_005030	GAAGAUGUCCAUGGAAAUA
PLK1	5430	NM_005030	CAACACGCCUCAUCCUCUA
UBB	7314	NM_018955	GCCGUACUCUUUCUGACUA

UBB	7314	NM_018955	GUAUGCAGAUCUUCGUGAA
UBB	7314	NM_018955	GACCAUCACUCUGGAGGUG
UBB	7314	NM_018955	UCGAAAAUGUGAAGGCCAA
BIRC5	332	NM_001168	CAACGGAUUUGGUCGUAUU
BIRC5	332	NM_001168	CAACGGAUUUGGUCGUAUU
BIRC5	332	NM_001168	CAACGGAUUUGGUCGUAUU
BIRC5	332	NM_001168	GUCAACGGAUUUGGUCGUA

Also used as controls were:
siGENOME RISC-Free Control siRNA
siGENOME Non-Targeting siRNA Pool #2
ON-TARGET Non-Targeting pool
(All purchased from Dharmacon)

2.1.5 ShRNA constructs

Open Biosystems

The following shRNA constucts were purchased from Open Biosystems as target sets of varying numbers of constructs. Listed below are the mature sense sequences of each hairpin used. These constructs were based on the pGIPZ lentiviral vector backbone.

NF1 (Target set for NM_000267)

shNF1 #1	V2LHS_ 189526	CAGATACACCTGTCAGCAA
shNF1#2	V2LHS_76027	CTGGCAGTTTCAAACGTAA

Non-silencing GIPZ lentiviral shRNAmir negative control viral particles (RHS4348) were used to generate shSC control cells.

Addgene

The following constructs were purchased from Addgene. Shown below are the sequences of the hairpins expressed from these constructs.

Addgene plasmid 1864 - Scrambled shRNA (Sarbassov et al., 2005).

5'- CCTAAGGTTAAGTCGCCCTCGCTCGAGCGAGGGCGACTTAACCTTAGG

Addgene plasmid 21335 - DEPTOR shRNA 1 (Peterson et al., 2009).

5'-
CCGGGCCATGACAATCGGAAATCTACTCGAGTAGATTTCCGATTGTCATGGCT
TTTTG

Addgene plasmid 21336 - DEPTOR shRNA 2 (Peterson et al., 2009)

5'-
CCGGGCAAGGAAGACATTCACGATTCTCGAGAATCGTGAATGTCTTCCTTGCT
TTTTG

2.2 Methods

2.2.1 Mammalian cell culture

2.2.1.1 Cell lines and culture conditions

HCC827, H1650, H3255, HCC2935 and HCC4006 cells were obtained from ATCC (American Type Culture Collection). PC9 cells and Phoenix-ampho cells were provided by Cancer Research UK Cell Services. HEK293T cells were obtained from Thermo Scientific Open Biosystems. With the exception of the packaging cell lines, all cells were cultured as monolayers in RPMI (Roswell Park Memorial Institute) media supplemented with 10% foetal bovine serum (FBS), and antibiotics penicillin (0.006g/l) and streptomycin (0.1g/l). Cells were kept in incubators at 37°C and 5% CO_2 atmosphere and were split at 1:10 every 2-3 days when they had become confluent. HEK293T and Phoenix-ampho cell lines were cultured in DMEM (Dulbecco's Modified Eagle Medium) with the aforementioned supplements, and kept in incubators at 37°C and 5% CO_2 atmosphere. To split the cells, the media was removed, the cells were washed once in PBS and then a 1:3 tryspin/versene mixture was added to detach cells. Once cells had detached the trypsin was

neutralised with fresh media. Cells were counted using a cell counter (Countess, Invitrogen), and replated.

For storage cells were trypsinised and centrifuged at for 4 mins at 1200 rpm, and resuspended in freezing media (RPMI media containing 10% FBS and 10% DMSO). Cell were aliquoted into 1.5 ml cryogenic vials and frozen in isopropanol freezing tanks at -80°C for 24 hours before being transferred to liquid nitrogen for long term storage.

PC9-ER (erlotinib resistant) cells were generated previously by growing PC9 cells in media containing 1μM erlotinib. Surviving clones were picked and cultured in the presence of 1μM erlotinib for 3 months, and thereafter without erlotinib.

2.2.2 Screening

2.2.2.1 Genome-wide screen

The genome-wide screen was conducted in both erlotinib-treated and untreated conditions in two independent experiments. In each screen every siRNA was transfected in triplicate for treated and untreated conditions. The Dharmacon siGENOME SMARTpool siRNA library containing 21121 siRNA pools was aliquoted into sets of 201 384-well plates by the High Throughput Screening Facility and stored at -20°C. On the first day of each screen, we transfected one batch of 201 plates in the morning and one in the afternoon, for the control and drug treated plates respectively. Firstly, the library was thawed for 20 mins and the plates were centrifuged at 1500 rpm for 1 min. Then 2.5 µl/ well of the control siRNAs were added per well to the first four columns of each plate which had been left empty for this purpose. Risc Free and ON TARGET-non-targeting were used as negative controls to normalise for the stress of transfection without gene silencing. BIRC5, PLK1 and UBB were included as killing controls, which cause a significant amount of cell death.

Next, 3 µl diluted Dharmafect 2 (Dharmacon) (0.025 µl/µl) was added per well using the WellMate dispenser to give a final amount of 0.075 µl Dharmafect 2 per

well. Plates were then incubated at room temperature for 15 mins, before the WellMate was again used to dispense 80 µl per well PC9 cell suspension (6.25 × 10^3 cell/ml) resulting in a final cell number of 500 cells per well. After 48 hours, media was removed from the cells using a plate washer and 80 µl of fresh RPMI was added either with or without 30 nM erlotinib using the WellMate. As a control for the drug treatment 2 columns of the control siRNAs were left untreated in the erlotinib-treated plates. After an additional 72 hours media was removed with a plate washer and 90 µl ice-cold 80% EthOH was added with the WellMate. Plates were then stored at -20°C and subsequently stained in batches. For the staining each plate was washed 3 times with PBS using a plate washer, then 20 µl/well DAPI (diluted in PBS 1:10,000) was added using WellMate. Plates were incubated at room temperature in the dark for 1 hour before plates were washed once with PBS. Plates were sealed and stored at 4°C in PBS for scanning. Plates were scanned using an Acumen Explorer microplate cytometer (TTP LabTech) to quantify the number of cells in each well.

The subsequent deconvolution screen was also carried out using the same method as described here, however the plate layouts were adapted so that untreated and erlotinib-treated wells for each siRNA were in the same plate. Additonally, siGENOME non-targeting siRNA pool #2 was included as a negative control.

2.2.2.2 Data analysis of genome-wide screen

The raw value recorded for each sample was cell number. Each screening plate was normalised using a robust Z score calculation:

$$x_{ki}^{z} = \frac{x_{ki} - median_i}{MAD_i}$$

The median value of all samples on plate *i* is represented by $median_i$ and is subtracted from the raw value of well *k* represented by x_{ki}. Each well is then divided by the median absolute deviation (MAD) of all sample wells on that plate (MAD_i) to provide the normalised Z score shown as x_{ki}^{z}. In order to account for positional and edge effects a smoothed Z score was also calculated. This was based on the median and MAD calculated when comparing the distribution of Z

scores of a well position across all plates within the screen. Here $median_{ks}$ is the median Z score of a single well position (*k*) in all plates in the screen. MAD_{ks} is the MAD calculated from all samples at position (*k*) across all plates of the screen.

$$Smoothed\ \ Z\ score = \frac{x_{ki}^{z} - \ median_{ks}}{MAD_{ks}}$$

In order to identify differences between drug and control screens, the smoothed Z score from the drug screen was plotted against the smoothed Z score from the control screen for each replicate (nine comparisons in total). The residual difference for each data point was then calculated as the perpendicular distance between the data point and the line of best fit (as calculated by linear regression). Negative residual differences represent those genes where the viability score within the drug screen is lower than would be expected based on the control viability, whereas positive scores indicate genes with viability within the drug screen that is higher than expected based on the control viability. Data analysis was carried out by the High-throughput laboratory. Z scores were calculated using the software package CellHTS2 (Boutros et al., 2006) and residual Z scores were calculated using R programming language and software.

2.2.2.3 Data analysis of deconvolution screen

In the deconvolution screen we measured the Sensitivity Index (SI) of each siRNA. The SI is an index used to determine whether an siRNA oligo antagonises or sensitises cells to drug treatment. The SI for each siRNA was calculated by subtracting the observed combined effect of drug and siRNA from the expected total viability effect (Swanton et al., 2007).

$$SI = \frac{Rc}{Cc} * \frac{Cd}{Cc} - \frac{Rd}{Cc}$$

Rc/Cc represents the viability effect of the siRNA without drug compared to the SC control (siGENOME non-targeting siRNA pool #2). The effect of drug treatment on

SC control transfected cells is represented by Cd/Cc. Therefore the expected combined effect of the siRNA and drug on viability is Rc/Cc*Cd/Cc. From this the observed combined effect on viability (Rd/Cc) can be substracted. Positive SI values indicate a sensitising effect of the siRNA, whereas negative SI values indicate an antagonistic effect of the siRNA to drug treatment. For our final hit selection we used the cut-off SI value of ≥ 0.10 for sensitising siRNAs and ≤ -0.15 for desensitising siRNAs, which is the same as the criteria employed by Swanton et al (Swanton et al., 2007). SI values shown are the median of 3 replicates.

2.2.3 RNAi follow up experiments

2.2.3.1 siRNA transfections

In 96 well experiments in the screen follow up siRNA transfections were carried out as follows. Reverse transfections were performed using 0.1 µl Dharmafect 2 transfection reagent per well and a final concentration of 37.5 nM siRNA. For transfection of PC9 cells 1000 cells per well were seeded. Firstly, siRNA was diluted to 375 nM in HBSS (Hanks' Balanced Salt Solution), and Dharmafect 2 was diluted to 0.01µl/µl in Optimem media. The siRNA and transfection reagent dilutions were incubated separately at room temperature for 5 mins, before equal volumes of both mixtures were combined and left for 15 mins to allow complexes to form. 20 µl of this mix was plated per well, before 80 µl of cell suspension (12,500 cells/ml) in RPMI was added. To assess gene silencing by Real Time-QPCR cells were lysed 48 hours after transfection. In cell survival assays, cells were exposed to drug for 72 hours, which commenced 48 hours after transfection. For protein analysis, transfections were scaled up to 6 well plate format. Reverse transfections were performed using 1 µl Dharmafect 2 transfection reagent per well and a final concentration of 37.5 nM siRNA. For transfection of 100,000 cells per well were seeded. siRNA was diluted to 375 nM in HBSS, and Dharmafect 2 was diluted to 0.01µl/µl in Optimem media, which were incubated and combined as described previously. 200 µl of this mix was plated per well, before the addition of 800 µl cell suspension (125,000 cells/ml). In experiments where drug treatments were performed drug treatments were commenced 48 hours after transfection. In experiments involving co-transfection of two siRNAs, each sRNA was used at a final concentration of 25 nM.

2.2.3.2 Generation of stable cell lines

To generate shRNA expressing cells 293T cells were infected with the lentiviral shRNAmir construct in combination with the packaging plasmids pCMV-VSVg (Addgene plasmid #8454) and pCMV-Δ8.2 (Addgene plasmid #8455) using Lipofectamine 2000 (Invitrogen). Viral supernatants were collected after 48 and 72 hours, concentrated by ultracentrifugation, and added to the culture medium of NSCLC cells in the presence of polybrene (8μg/ml). Cells with successful lentiviral integration were selected by puromycin (1.5μg/ml). shRNAmir constructs which included an EGFP expression cassette (pGIPZ constructs) were subsequently sorted by FACS (Fluorescence Activated Cell Sorting) to obtain the top 25% EGFP expressing cells which enriched the population for high expression of the lentiviral shRNAmir construct.

MEK-DD and myr-AKT expressing cells were generated by retroviral transfection of PC9-EcoR cells. PC9-EcoR cells expressing the murine ecotropic receptor had been generated previously. Briefly, Phoenix cells were transfected with MEK-DD (Addgene #15268) and myr-AKT1 (Addgene #15294) retroviral constructs using Effectene transfection reagent (Qiagen) to produce viral supernatants. Viral supernatants were filtered then added to the media of PC9-EcoR cells in the presence of polybrene (8μg/ml). Cells with successful lentiviral integration were selected by puromycin (1.5μg/ml).

For the studies re-expressing NF1-GRD, PC9 cells were transfected using Lipofectamine 2000. The full-length NF1 construct was kindly provided by Dr. D. Lowy (Johnson et al., 1994). The NF1-GRD expression construct was generated by subcloning of this region into pcDNA3.1 expression vector. pcDNA3.1 was transfected into PC9 cells to generate empty vector (ev) control cells. Transfected cells were selected for the presence of the expression construct by G418 Sulphate (Geneticin) (1 μg/ml).

2.2.3.3 Cell survival assays

For siRNA experiments, cells were transfected as described above and drug treatment commenced 48 hours after transfection. In experiments where cells

stably expressing shRNA were used drug treatment was started 24 hours after plating (2000 cells/well) in 96 well plates. Cell viability was measured after an additional 72hr using the CellTiter-Blue assay (Promega). This assay is based on the ability of living cells to convert a redox dye (resazurin) into a fluorescent end product (resorufin). 5 µl CellTiter-Blue reagent was added to each well, and plates were incubated at 37°C for 1.5 hours before fluorescence was read on a plate reader (EnVision, Perkin Elmer), excitation was achieved at 560 nm and fluorescence was read at 590 nm. Values were normalised to the untreated control wells. Graphical representations of these data were produced using GraphPad Prism version 5, and were used to calculate the effect on $IC_{50.}$ IC_{50} is the concentration of drug needed to give half the maximal biological response, therefore the higher the IC_{50} the more resistant cells are to a drug. Alternatively, SF_{50} (survival fraction 50) is used as a measure of cell viability in response to drug treatment. SF_{50} is the concentration of drug at which 50% of cells are surviving compared to the untreated control (Turner et al., 2010), which was also calculated using GraphPad Prism version 5.

2.2.3.4 Colony formation assays

Single cell suspensions were seeded into 24-well plates (200 cells/well) and cultured in the indicated concentration of erlotinib. The media was replaced every 2-3 days to ensure the drug remained active. At the point that untreated cells reached confluency, cells were fixed with 10% TCA, washed and stained with Sulphorhodamine B as described by V Vichai and K Kirtikara (Vichai and Kirtikara, 2006). The protein-bound dye is dissolved in 10 mM Tris base solution for OD determination at 530 nm using a microplate reader, and normalised to the untreated control wells.

2.2.4 Quantitative Real Time PCR

Total RNA was isolated from cells using RNeasy Mini Kit (Qiagen). For Real-Time RT-PCR assays analysing levels of NF1 and EGFR assays were performed with QuantiTect SYBR Green RT-PCR Kit (Qiagen), using 7500 Fast Real-Time-PCR system (Applied Biosystems) according to manufacturer's instructions. Thermocycling conditions were: reverse transcription at 50°C for 30min, first

denaturation at 95°C for 15 min followed by 40 cycles of denaturation at 94°C for 15 s, annealing at 55°C for 30s and extension at 72°C for 30 s. Fluorescence data collection was performed during the extension phase of the cycle. A dissociation curve was produced after each run to verify that only one product has been amplified. All primers were QuantiTect Primers obtained from Qiagen, with the exception of NF1-GRD primers that were as described previously (Holzel et al., 2010). Relative mRNA levels were analysed using the comparative C_T method (Livak and Schmittgen, 2001) and normalised to the housekeeping gene GAPDH.

For analysis of DEPTOR mRNA levels RNA was isolated using the RNeasy Mini Kit, and performed using the Taqman RNA-to-C_T 1 Step Kit (Applied Biosystems) according to manufacturer's instructions. Thermocycling conditions were: reverse transcription at 48°C for 15 min, first denaturation at 95°C for 10 min followed by 40 cycles of denaturation at 94°C for 15 s, annealing and extension at 60°C for 1 min. Fluorescence data collection was performed during the anneal/extension phase of the cycle. cDNA was amplified using Taqman Gene Expression Assays for DEPTOR and GAPDH. Relative mRNA levels were analysed using the comparative C_T method (Livak and Schmittgen, 2001) and normalised to the housekeeping gene GAPDH as before.

2.2.5 Protein analysis

2.2.5.1 Lysis of cells

Cells were washed with ice-cold PBS, then lysed on ice with Triton X-100 lysis buffer (20 mM Tris-HCl (pH 7.4), 137 mM NaCl, 2 mM EDTA, 10% glycerol, I% Triton X-100) supplemented with 1% Protease Inhibitor Cocktail set III (Calbiochem) and 1% Phosphatase Inhibitor Cocktail set III (Calbiochem). Lysates were vortexed and incubated on ice for 20 mins, then centrifuged at 14000 rpm at 4°C for 20 mins. After determining the protein concentration, the appropriate volume of 4x NuPAGE LDS sample buffer (Invitrogen) containing 250 mM DTT was added to supernatant, lysates were boiled for 5 mins at 95°C, and briefly centrifuged. Alternatively cells were lysed directly in 1x NuPAGE LDS sample buffer with DTT, then sonicated before boiling and centrifugation.

2.2.5.2 Determination of protein concentration

Protein concentration of cell lysates was determined using Bio-Rad Protein Assay based on the Bradford dye-binding assay (Bradford, 1976). It is a colorimetric assay based on the colour change of Coomassie Brilliant Blue G-250 in response to binding to basic and aromatic amino acids. BSA standards from 0 to 10 mg/ml protein were made by dilution in lysis buffer. 1 µl of BSA standard or protein lysate was plated in duplicate in a 96 well plate with 200 µl protein assay solution and incubated for 5 mins. The plate was read on a plate reader at 595 nm, and the BSA standard values used to construct a standard curve and determine the protein concentration of the cell lysates.

2.2.5.3 SDS PAGE

Cell lysates were resolved by SDS-PAGE (sodium dodecyl sulphate polyacrylamide gel electrophoresis) on NuPAGE 4-12% Bis-Tris gradient gels in MES buffer (Invitrogen). A full-range pre-stained molecular weight marker (Full Range Rainbow Marker, GE Healthcare) was also run on each gel to check proteins detected were of the correct molecular weight. Gels were run at 120 V for 2 hours.

2.2.5.4 Western blotting

After gel electrophoresis, proteins were transferred to Immobilon PVDF(polyvinylidene fluoridine) membranes (Millipore) in transfer buffer (25 mM Tris Base, 250 mM glycine, 20% methanol). The transfer was carried out in a wet transfer chamber for 1.5 hrs at 100 V at 4°C.

2.2.5.5 Detection of immobilised proteins

Membranes were blocked in 5% milk in TBS for 1 hour whilst gently shaking. Primary antibodies were diluted in PBS containing 0.1% Tween-20 and 3% BSA, and incubated with the membranes overnight at 4°C. Membranes were washed 3 times with TBST for 10 mins, then incubated for 1 hour with the appropriate secondary antibody diluted 1 in 5000 in TBS containing 1% milk. Membranes were again washed 3 times with TBST for 10 mins. Proteins were visualised by enhanced chemoluminesence using Amersham ECL western blotting detection reagents (GE Healthcare). Equal volumes of reagents 1 and 2 were mixed, applied

to the membrane and incubated for 1 minute. Enhanced chemoluminescence visualises a peroxidase-catalysed reaction, therefore detects the peroxidase labelled secondary antibodies, which are bound via the specific primary antibodies to the target proteins on the membrane. The membranes were exposed to X-ray film (FujiFilm) in a hypercassette to visualise the reaction.

2.2.5.6 Ras activation assay

Ras-GTP levels were detected using a Ras activation assay, following the manufacturer's instructions (Pierce Biotechnology). Cells were cultured in the presence or absence of 30 nM erlotinib for 1hr, then washed with ice-cold TBS and lysed with Lysis/Binding/Wash buffer (25mM Tris-HCl pH 7.2, 150mM NaCl, 5mM $MgCl_2$, 1% NP-40, 5% glycerol) supplemented with 1% Protease Inhibitor Cocktail set III and 1% Phosphatase Inhibitor Cocktail set III. The lysates were then vortexed and centrifuged at 14000 rpm at 4°C for 15 mins. At this point some supernatant (total cell lysate) was reserved from each sample to use as loading controls. The remaining supernatant was added to spin cups containing glutathione-coupled beads and GST-tagged Raf1-RBD (80 µg), and incubated with gentle shaking for 1 hr. Ras-GTP is immunoprecipitated from cell lysates by the GST-tagged Raf1-RBD, which is in turn immobilised on the glutathione resin. After incubation beads are washed with Lysis/Binding/Wash buffer and collected by centrifugation (6000 g, at 4°C for 30 secs) 3 times. Active Ras is eluted with 50 µl of 2x SDS Sample Buffer (1.5mL, contains 125mM Tris-HCl pH 6.8, 2% glycerol, 4% SDS (w/v), 0.05% bromophenol blue, 5% β-mercaptoethanol), and boiled for 5 mins 95°C. Ras pull-down assays were resolved by SDS-PAGE alongside total cell lysates as loading controls.

2.2.5.7 EGFR Immunoprecipitation

Cells were cultured in the presence or absence of 30 nM erlotinib for 1hr, then washed with ice-cold PBS, and lysed on ice with RIPA buffer (1% Triton X-100, 10 mM Tris-HCl (pH 8.0), 150 mM NaCl, 1% aprotinin, 250 µM PMSF, 1 mM NaF, 100 µM sodium orthovanadate). Lysates were centrifuged at 14000 rpm at 4°C for 10 mins, and the supernatant was carefully removed. Protein concentration was

determined by Bradford and equalised in all samples. At this point some total lysate was reserved from each sample to use as loading controls. The remaining equalised lysates were incubated with shaking, with 50 µl of EGFR-goat IgG coupled to agarose beads (Santa Cruz) for 2 hrs at 4°C. The beads were washed two times with Buffer A (0.2% Triton X-100, 10 mM Tris-HCl (pH 8.0), 150 mM NaCl, 2 mM EDTA), by 30 secs vortexing, and centrifuged at 5000 rpm at 4°C for 30 secs to collect the beads, then the supernatant was removed. This was repeated with one wash with Buffer B (0.2% Triton X-100, 10 mM Tris-HCl (pH 8.0), 500 mM NaCl, 2 mM EDTA). The bound proteins were eluted in 30 µl of 2x LDS buffer containing DTT, lysates were boiled for 5 mins at 95°C, and briefly centrifuged. Lysates were resolved by SDS-PAGE as described previously.

2.2.6 Statistical analysis

Data are presented as mean values. For RT-QPCR error bars represent standard deviation of triplicate samples. For long term and short term cell survival assays, statistics were calculated using GraphPad Prism 5 software and error bars represent standard error of the mean. All experiments were performed at least three times and a representative experiment is depicted.

Chapter 3. Identifying determinants of resistance to erlotinib treatment – a genome-wide screen

3.1 Introduction

In order to identify novel mechanisms of resistance to EGFR tyrosine kinase inhibitors we carried out a genome-wide siRNA screen in PC9 cells. PC9 cells are a NSCLC cell line carrying an activating *EGFR* mutation (exon 19 deletion E746-A750), which renders them exquisitely sensitive to EGFR TKI treatment (McDermott et al., 2007). We carried out a genome-wide screen in the presence and absence of erlotinib to determine which genes upon silencing have a sensitising or desensitising effect on the cells to drug treatment. We hoped our results might inform how to best treat erlotinib resistant patients, for example if loss of a gene sensitises cells to erlotinib it could potentially be a therapeutic target. On the other hand if loss of a gene makes cells more resistant it could be screened for in resistant patients, and the signalling pathway it influences could be targeted in combination with erlotinib if such drugs are available.

3.2 RNAi technology

RNA inference (RNAi) is an incredibly useful tool in biological research as it allows you to block the expression of a gene, and observe the effect that has on cells. This permits you to probe the functions of specific genes. RNAi-mediated silencing takes advantage of a cell's degradation of double-stranded RNA, which functions as a defence against RNA-based viruses. RNAi was identified in C.elegans where injection of dsRNA caused silencing of endogenous genes with sequences complementary to the dsRNA (Fire et al., 1998). The genome-wide screen we conducted employed the use of synthetic small interfering RNAs (siRNAs). siRNA molecules are 20-25 nuclotide long double-stranded RNA fragments, with a 3' 2nt overhang and a 5' phosphate group. Natural siRNAs are produced by the processing of long dsRNAs by the RNAse enzyme DICER. siRNAs were first identified in plants (Hamilton and Baulcombe, 1999) and it was shown subsequently that synthetic siRNAs could be used to silence gene expression in mammalian cells (Elbashir et al., 2001). One strand of the siRNA molecule becomes incorporated into the RISC (RNA-induced silencing complex) by

association with the Argonaut family of proteins. The strand that is incorporated is determined by the thermostability of the 5' end. The strand whose 5'end is at the least stable end of the dsRNA is incorporated into RISC and is called the guide strand (Schwarz et al., 2003). Once the siRNA duplex has been unwound by helicases, and the guide strand incorporated into RISC, the endonuclease component of RISC cleaves mRNA complementary to the siRNA sequence (Sontheimer, 2005).

3.3 Genome-wide screen set up

3.3.1 siRNA library

We used the Dharmacon siRNA library which consists of 4 subsets: G Protein Coupled Receptor set (516 genes), Protein Kinase set (779 genes), Human Druggable set (6,022 genes) and the Human Genome set (13,858 genes), which together totals 21,175 genes. Each gene is targeted by a SMARTpool consisting of 4 different siRNA oligos targeting different sequences in the mRNA transcript. The rationale behind pooling of siRNAs is to keep the concentration of individual siRNAs low, to limit non-specific effects, whilst maintaining a high enough overall siRNA concentration for effective gene silencing.

3.3.2 Choice of cell line

PC9 cells were used for the screen as they are a well-studied NSCLC cell line, carrying a defined *EGFR* mutation (DelE746A750) that makes them extremely sensitive to erlotinib treatment (McDermott et al., 2007). Other advantages of this cell line are that it is fast growing, so we were easily able to culture enough cells necessary for genome-wide experiments, and PC9 cells are relatively easy to transfect. Additionally they have an epithelial phenotype, forming classical cobblestone colonies. This makes them easy to scan on automated plate-readers, unlike some other cell types, which form clusters making individual cells difficult to distinguish.

3.3.3 Screen read-out

The desired read-out of the screen was cell survival. A measurement of cell survival can be obtained either by counting cell number, or by using measuring metabolic activity. We tested four different methods of determining survival to

ascertain which would give the most accurate, and reproducible reading. Methods tested based on cell number were staining with crystal violet, and DAPI staining. Crystal violet is a protein-binding dye, with can be measured using colorimetry (absoption read at 568 nm), to quantify cell number. DAPI is a fluorescent DNA-binding dye, which we used to count cell nuclei. Metabolic assays were CellTiter-Blue and CellTiter-Glo, which quantify the reducing capacity and ATP-content of cells respectively. Fig.3.1 shows the comparison of all four methods used to determine survival of PC9 cells over a dose response curve of erlotinib. DAPI, crystal violet and CellTiter-Glo all gave similar results, suggesting any of these methods would be appropriate to use for the screen. We decided not to use CellTiter-Glo, as it is used on live cells, and it would not be possible to scan all plates of the screen within the limited timescale in which an accurate reading could be obtained. We could have divided the screen into separate batches however this would have introduced additional variation in transfection efficiency. We decided to use DAPI staining as it measures absolute cell number, and leaves the cells intact allowing us to stain them subsequently with an antibody, if desired.

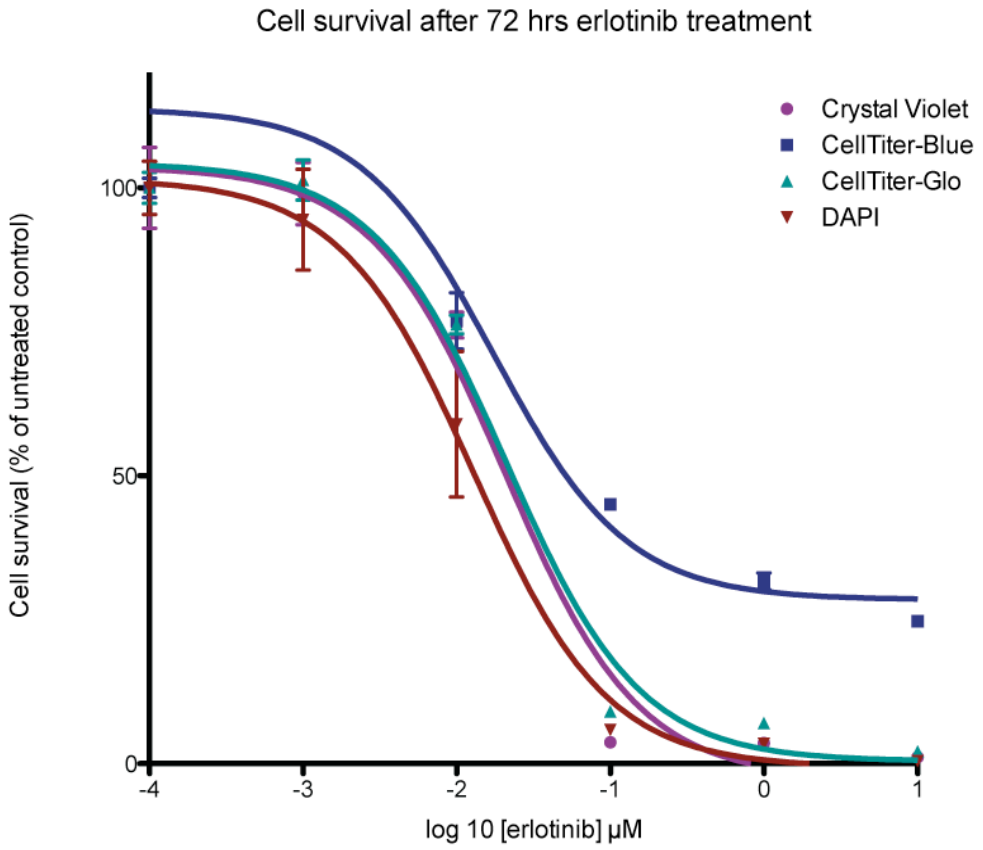

Figure 3.1. Test of methods to use as a read-out of cell survival.

PC9 cells were treated with the indicated concentrations of erlotinib for 72 hours before cell survival was determined using four different methods, CellTiter-Blue, CellTiter-Glo, crystal violet and DAPI staining.

3.3.4 Erlotinib treatment

In the screen we wanted to compare cell survival in untreated and erlotinib-treated conditions. The concentration of erlotinib used was 30 nM as this concentration results in 40% cell survival after 72 hours of erlotinib treatment (Fig 3.2). This level of survival allowed us to look both for genes that 'sensitised' or 'desensitised' cells to erlotinib treatment.

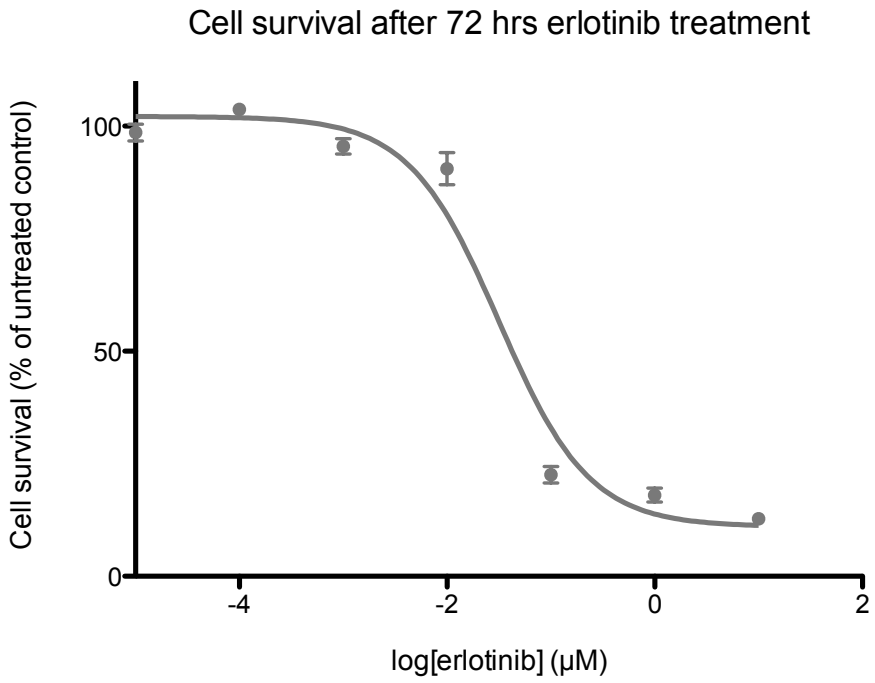

Figure 3.2. PC9 cells are exquisitely sensitive to inhibition by erlotinib.
PC9 cells were treated with the indicated control of erlotinib for 72 hours. Cell survival was measured using the Cell Titer Blue Assay. Cell survival is expressed as a percentage of untreated controls.

We chose 72 hours of drug treatment, as this duration is commonly used in cell survival assays (Engelman et al., 2007) and was the maximum length of time we were able to treat cells whilst ensuring there was still sufficient gene silencing. We waited 48 hours after transfection to treat the cells with erlotinib to ensure effective silencing at the protein level. The duration of effective silencing by siRNA is between 5-7 days, therefore treating the cells for 72 hours, allowed us to finish the assay within 5 days of transfection. Also when we tested different durations of drug treatment, we found that 72 hours provided the greatest difference in cell survival between untreated controls and the maximum erlotinib dose used. Therefore we chose this time point as this would hopefully make siRNAs that have an effect on cell survival easier to distinguish from the majority of siRNAs with no effect (Fig 3.3)

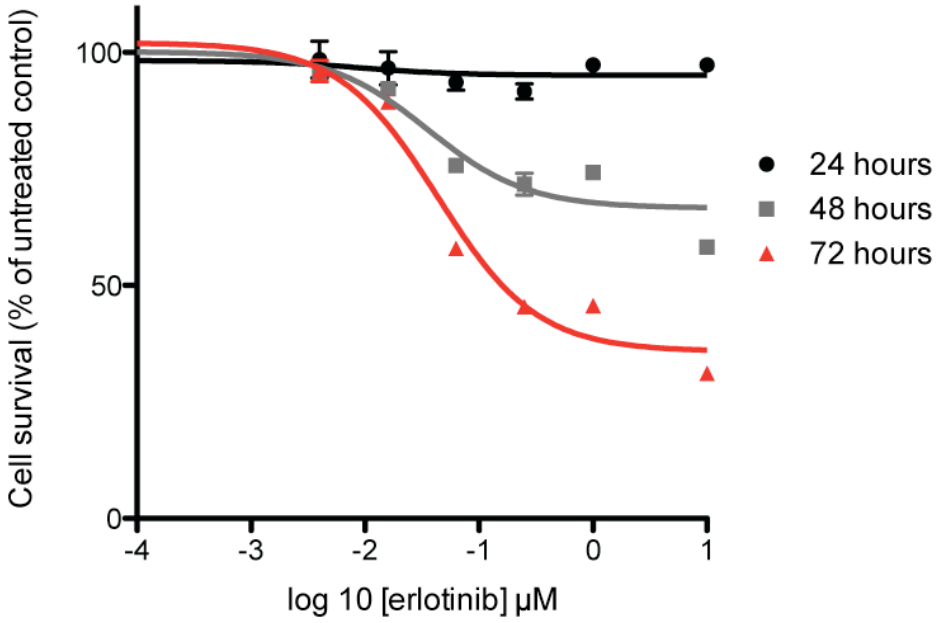

Figure 3.3. Test for optimal duration of erlotinib treatment.

PC9 cells were treated with the indicated concentrations of erlotinib for 24, 48 or 72 hours. The maximal response, as measured by CellTiter-Blue was observed at 72 hours.

3.3.5 Transfection reagent and conditions

Next, it was necessary to determine the most efficient and least toxic transfection reagent to transfect the siRNA library into PC9 cells. The High-throughput lab had tested previously various concentrations of siRNA to find the lowest concentration of siRNA oligonucleotides to use that achieved maximum gene silencing. Additionally low concentrations of siRNA are desirable to prevent the occurrence of off-target effects (effects not dependent on silencing of the intended target gene), which are explained further in the discussion. We used a final total concentration of 37.5 nM siRNA in all experiments as it was the concentration found to achieve the most efficient gene silencing. Twenty-two transfection reagents were tested at different concentrations for their ability to transfect PC9 cells with siRNA targeting *LMNA* the gene encoding Lamin A/C (Table 3.1). At this time we intended to perform the screen in a 96-well plate format, therefore these conditions were tested in a 96-well plate format.

	1	2	3	4	5	6
A	Oligofectamine, 0.1 µl	Oligofectamine, 0.3 µl	TransIT-siQuest, 0.1 µl	TransIT-siQuest, 0.3 µl	silenAmine, 0.1 µl	silenAmine, 0.3 µl
B	INTERFERin, 0.1µl	INTERFERin, 0.3µl	Lipofectamine RNAiMAX, 0.	Lipofectamine RNAiMAX, 0.	CodeBreaker, 0.1µl	CodeBreaker, 0.3 µl
C	DharmaFect1, 0.1µl	DharmaFect1, 0.3µl	Lullaby, 0.1 µl	Lullaby, 0.3 µl	RiboJuice, 0.1 µl	RiboJuice, 0.3 µl
D	DharmaFect2, 0.1µl	DharmaFect2, 0.3µl	TransIT-TKO, 0.1 µl	TransIT-TKO, 0.3 µl	HiPerFect, 0.1 µl	HiPerFect, 0.3 µl
E	DharmaFect3, 0.1µl	DharmaFect3, 0.3µl	GeneSilencer, 0.1 µl	GeneSilencer, 0.3 µl	N-TER Nanoparticle, 0.1 µl	N-TER Nanoparticle, 0.3 µl
F	DharmaFect4, 0.1µl	DharmaFect4, 0.3µl	SilenNFX, 0.1 µl	SilenNFX, 0.3 µl	siIMPORTER, 0.1 µl	siIMPORTER, 0.3 µl
G	Lipofectamine 2000, 0.1 µl	Lipofectamine 2000, 0.3 µl	GeneEraser, 0.1 µl	GeneEraser, 0.3 µl	Metafectene, 0.1 µl	Metafectene, 0.3 µl
H	DreamFect Gold, 0.1 µl	DreamFect Gold, 0.3 µl	TransPass R1, 0.1 µl	TransPass R1, 0.3 µl	siRNA only	siRNA only

Table 3.1. Transfection reagents and conditions tested for use in PC9 cells.
Twenty-two transfection reagents were tested at two concentrations to determine optimum transfection conditions for PC9 cells.

Silencing efficiency was determined by measuring Lamin A/C protein levels by immunofluorescence using the Acumen Explorer microplate cytometer. We excluded the possibility of using any reagent or condition that caused a dramatic decrease in cell viability compared to control transfected cells, as this indicated a high level of toxicity. As the intended screen read-out was cell survival, we wished to limit any additional cell death that was due to the stress of transfection and not specifically a consequence of gene silencing or drug treatment. The Dharmafect transfection reagents (C1, D1, E1 and F1) (Fig 3.4) caused the most efficient gene silencing, with the smallest reduction in cell viability compared to siRNA only/no transfection reagent control (H5 and H6)(Fig 3.4). We decided to use Dharmafect 2 for the screen, however all Dharmafect reagents performed similarly and any of the four would have been suitable.

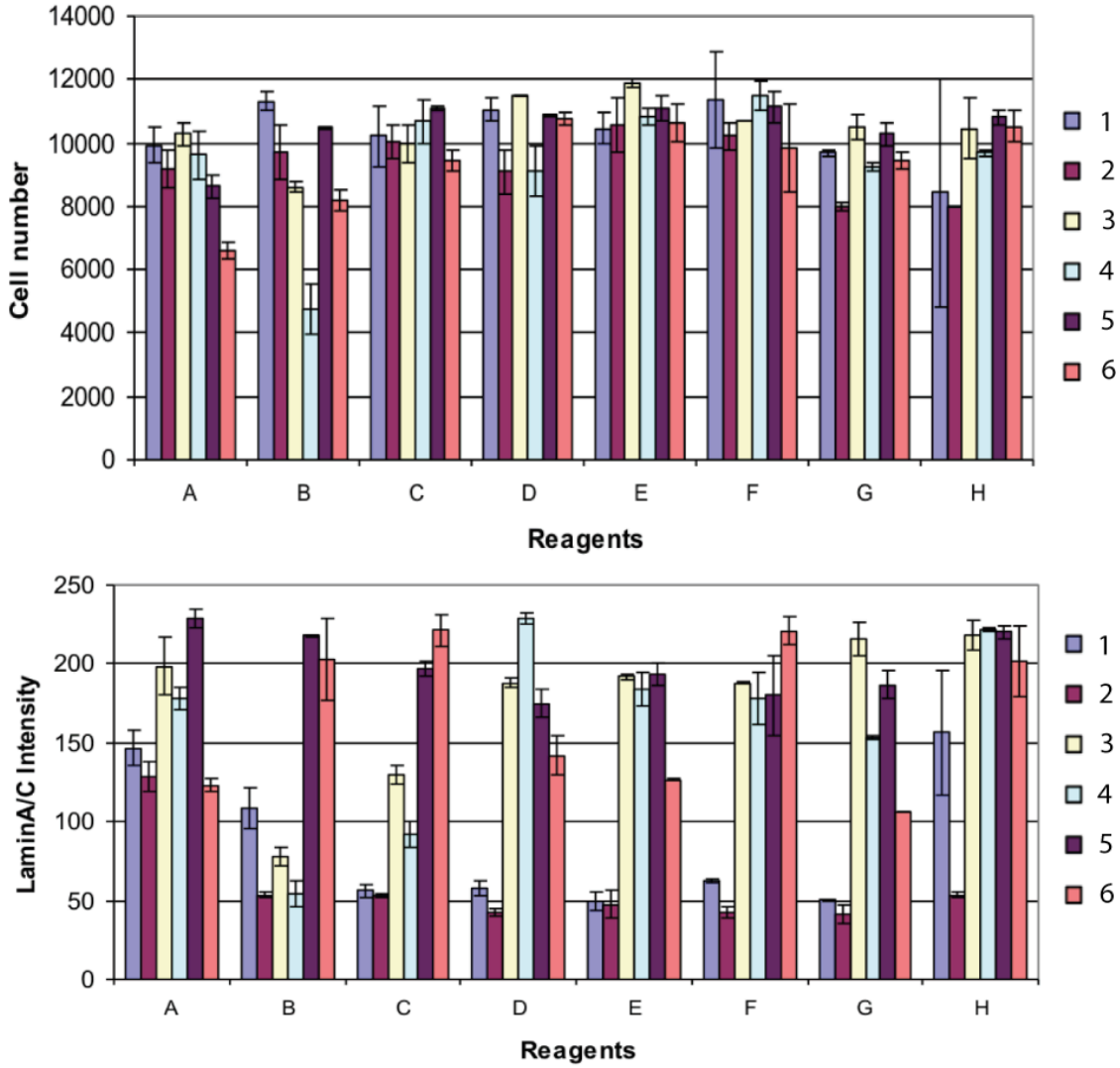

Figure 3.4. Transfection reagent test for gene-silencing and toxicity.

PC9 cells were transfected using the conditions listed in Table 1. Cell number (DAPI) and Lamin A/C were quantified by immunofluorescence using the Acumen Explorer microplate cytometer.

3.3.6 384-well plate format

During optimisation of the screening conditions, we decided to move from a 96-well plate format to a 384-well plate format. The primary reason for this alteration was to make the screen more cost-effective. Genome-wide screens are extremely expensive experiments, one of the most costly aspects of which is the plastic ware. We carried out two genome-wide screens, in untreated and erlotinib-treated conditions, and by using 384-well plates the number of plates used was reduced to 402 plates in total. Consequently, reducing the well size reduces the amount of

siRNA, transfection reagent, cells and all other reagents needed thereby also reducing cost. Additionally, changing the format greatly increased the speed at which we were able to conduct the screen. This allowed us to transfect the entire control screen in triplicate in the morning, and the entire drug treated screen in triplicate in the afternoon of the same day. This meant all cells used were expanded from the same batch and were of identical passage number, also reducing variation.

However, changing well size required further optimisation of the cell number and volume of transfection reagent needed. Additionally we tested RISC-free and PLK1 siRNA transfection in the presence and absence of erlotinib to ensure these controls behaved as expected in erlotinib-treated conditions. We wanted to ensure there was not an interaction between the act of transfection and erlotinib treatment, i.e. that the stress of transfection, not specific gene-silencing sensitised cells to drug treatment. As anticipated, RISC-free transfected cells had substantially reduced cell survival in erlotinib-treated conditions compared to untreated wells (Fig. 3.5). On the other hand PLK1 and TOP2A silencing resulted in low levels of cell survival in both untreated and erlotinib-treated conditions (Fig 3.5). These results indicated both drug treatment and gene silencing were effective in our chosen conditions.

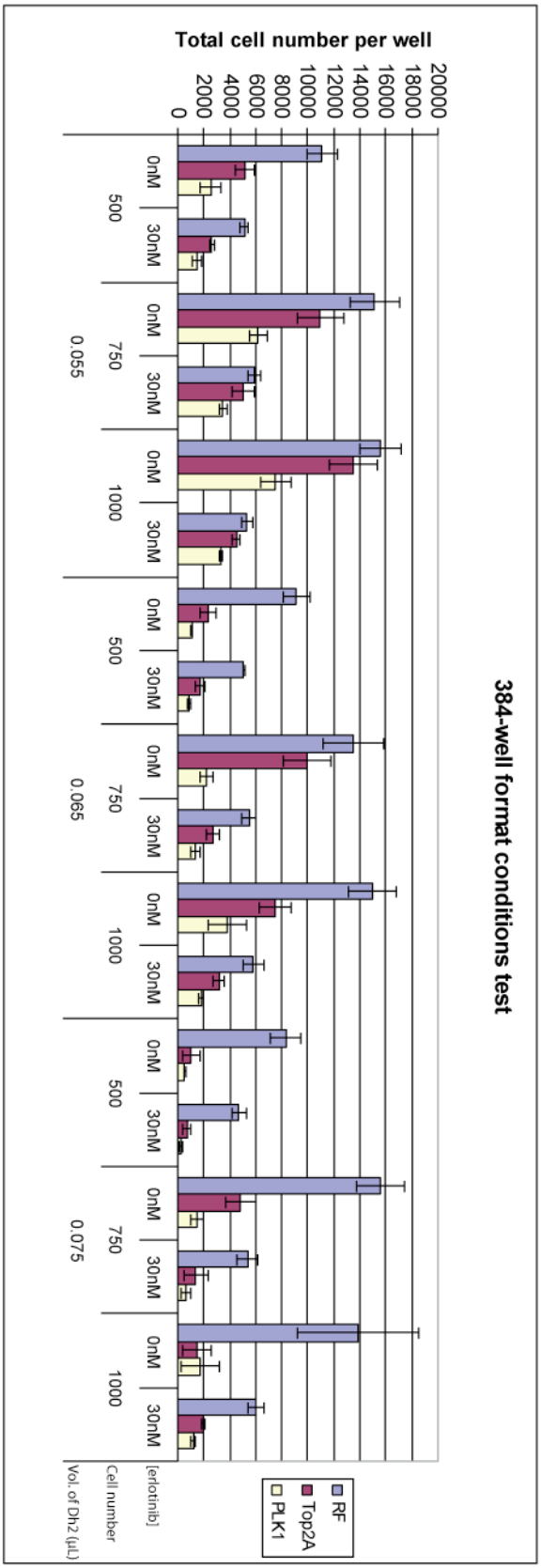
384-well format conditions test
Total cell number per well
20000
18000
16000
14000
12000
10000
8000
6000
4000
2000
0
RF
Top2A
PLK1
[erlotinib]
Cell number
Vol. of Dh2 (µL)
0nM
30nM
500
750
1000
0.055
0.065
0.075

Figure 3.5. Transfection conditions for a 384-well plate format.

PC9 were plated at the different starting cell numbers indicated, and transfected with either RISC-free (RF), DNA topoisomerase 2α (Top2A) or PLK1, using the three difference volumes of Dharmafect 2 (Dh2) shown. 48 hours after transfection, cells were either left untreated, or treated with 30 nM erlotinib for 72 hours.

3.3.7 Control siRNAs

In the screen we used several control siRNAs in each plate, in order to confirm the transfection had been successful across all plates of the screen. The performance of controls in the screen will be described in more detail later in this chapter. To control for the stress of transfection, RISC-free siRNA was used. RISC-free siRNA oligonucleotides are modified so they are not processed by RISC, therefore any change in cell survival in RISC-free transfected cells reflects the stress of transfection, and not engagement of the siRNA machinery or gene silencing. Also used as a negative control was OT-NT (On-Target Non-Targeting siRNA). OT-NT is designed to minimally target any known gene expressed in humans, therefore should only reflect effects on cell viability caused by transfection stress. OT-NT can be incorporated into RISC, however it is designed not to be complementary to known mRNAs so should not result in gene silencing.

Additionally we used several killing controls to confirm efficiency of transfection and gene silencing. Killing controls used were BIRC5, UBB, PLK1. *BIRC5* encodes for the protein survivin, which belongs to the Inhibitor of Apoptosis (IAP) family. Survivin inhibits apoptosis, and is thought to function by directly binding to active forms of caspase-3 and -7 to block their activity (Tamm et al., 1998). *UBB* encodes for ubiquitin, a 76-amino acid protein which can be conjugated to the ε-amino group of lysine residues. This conjugation, termed ubiquitination is a post-translational modification found to be essential in many cellular processes, such as proteasomal degradation of proteins, receptor endocytosis, DNA damage repair and DNA replication (Wagner et al., 2011). Therefore, due to the involvement of ubiquitin in many processes, silencing of UBB strongly induces apoptosis. The final killing control used was siRNA targeting PLK1. PLK1 is a mitotic kinase that plays key roles in multiple points during mitotic progression, the silencing of which causes apoptosis in multiple cancer cell lines (Liu and Erikson, 2003).

3.3.8 Screen Protocol

On day 1 of the experiment PC9 cells were plated at 500 cells per well and reverse transfected with 37.5 nM siRNA using 0.075 μl Dharmafect 2 transfection reagent per well. 48 hours after transfection the media was replaced with fresh media either with or without 30 nM erlotinib. 72 hours after treatment cells were fixed, washed and stained with DAPI. The read-out of the screen was cell number. This was quantified by counting the nuclei of DAPI stained cells using the Acumen Explorer microplate cytometer. See Fig 3.6 for a schematic of the screen set up. A more detailed account of the screen method is given in Materials and Methods.

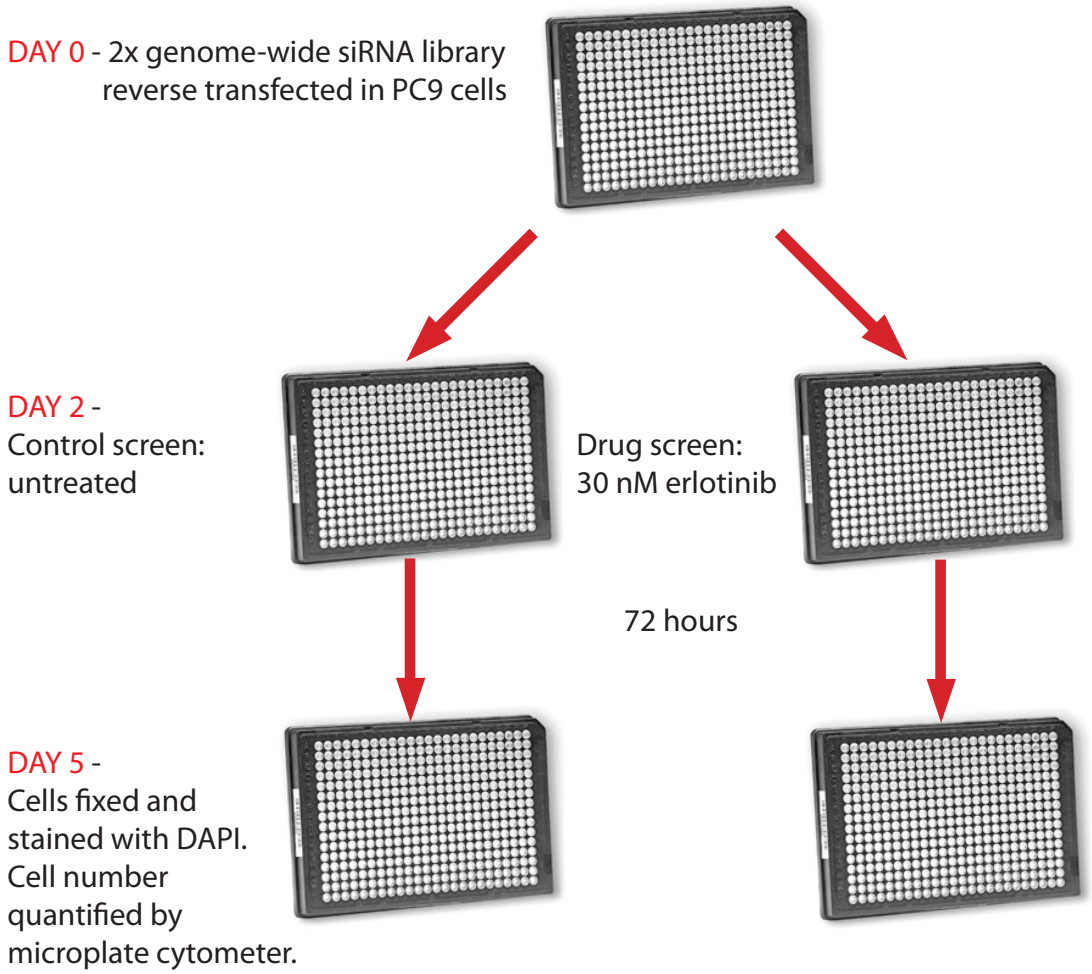

Figure 3.6. Screen set-up.

Schematic of screen. PC9 cells were transfected with the genome-wide siRNA to use in either the control or drug screen. After 48 hours the media was replaced with either 30 nM erlotinib on one set of plates, or normal media on the other set 72 hours after drug treatment cells were fixed and stained with DAPI. The screen read-out was cell numer, as quantified on the Acumen Explorer microplate cytometer.

3.4 Analysis of genome-wide screen data

3.4.1 Normalisation

The initial statistic we used to score our siRNAs was the Z score, which is the number of standard deviations by which the result differs from the mean of the

entire data set. During the analysis of a large-scale experiment it is necessary to perform normalisation steps in order to make data points comparable across the whole data set. There are many factors that can introduce variability into a large-scale experiment. Variability was reduced where possible by automating various steps, such as cell plating, dispensing of media and all liquid reagents, however some variability is unavoidable. The largest source of variability in screening is plate-to-plate variation, meaning the same samples can give rise to different scores on different plates. To correct for plate-to-plate variation each screening plate was normalised using a robust Z score calculation. This method is based on the distribution of values rather than controls and is described in the materials and methods chapter. Briefly, the median value of samples on each plate was subtracted from each well, and then each well was divided by the median absolute deviation (MAD) of all sample wells on that plate. Figure 3.7 shows the raw cell number values across all the plates of the screen, followed by the data after plate normalisation has been performed. Plate normalisation creates a more uniform distribution of siRNAs that do not have a significant impact on cell viability. Also represented in the plots are the negative controls OT-NT and RISC-free, and the killing controls PLK1 and UBB.

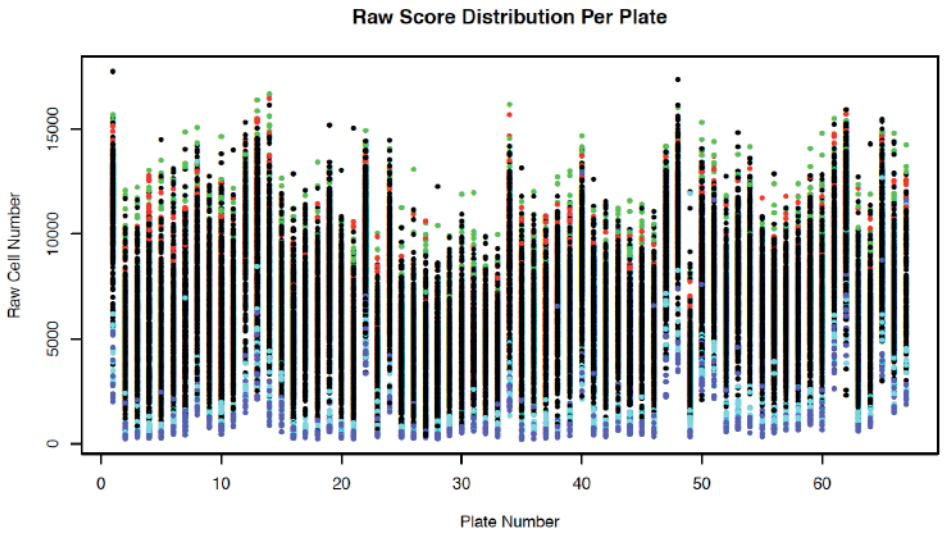
Raw Score Distribution Per Plate
Raw Cell Number
0
5000
10000
15000
0
10
20
30
40
50
60
Plate Number

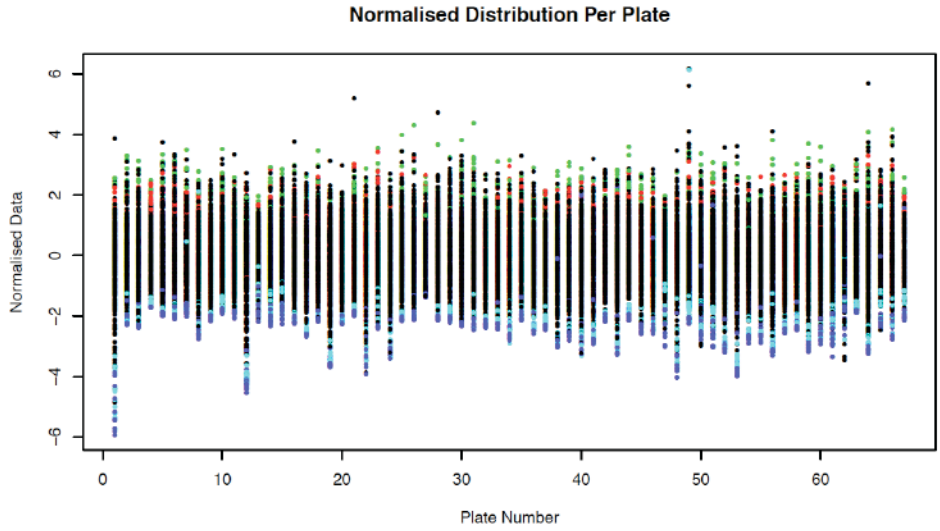
Normalised Distribution Per Plate
Normalised Data
−6
−4
−2
0
2
4
6
0
10
20
30
40
50
60
Plate Number


Sample
OT−NT
risc−free
ubb
plk1

Figure 3.7. Effect of plate normalisation.

Scatter plots showing raw values and values after plate normalisation. A. the raw cell number of all samples is plotted for each plate of the screen. B. Normalised Z score of all samples are plotted for each plate to demonstrate effect of plate normalisation. Negative and killing siRNA controls are reperesented as colour-coded in the key.

Within a single plate there is also variation between wells due to slight differences in temperature and evaporation. As evaporation is higher in the outer wells, cells in these positions tend to behave slightly differently from cells in central wells of the plate. Typically such effects produce repetitive patterns therefore it is possible to distinguish them from real differences, which are a result of biological effects of treatment, and correct for them in the analysis. In order to account for positional and edge effects a smoothed Z score was also calculated, as described in the materials and methods. This was based on the median and MAD calculated when comparing the distribution of Z scores at each well position across all plates within the screen. The median Z score of a well position in all plates in the screen is subtracted from the previously calculated Z score. This is then divided by the MAD, which is calculated from all samples at this well position in all plates. Figure 3.8 shows a scatterplot of the raw cell number for each well position divided by the plate median, followed by the data after smoothing, which normalises for positional effects. This step has less of an impact than plate normalisation, however clearly makes it easier to distinguish between the bulk of sample siRNAs with no effect on viability and the killing controls.

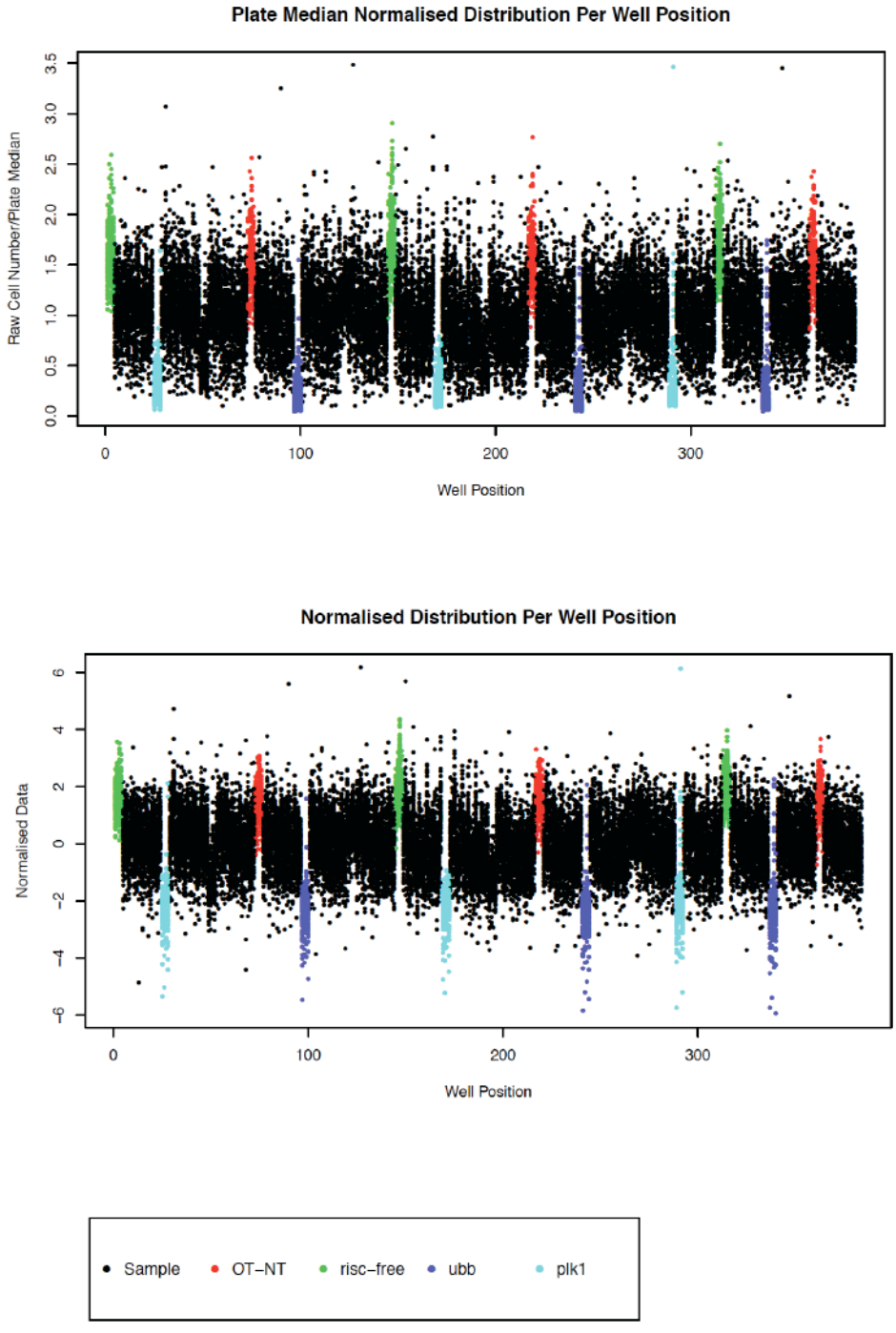
Plate Median Normalised Distribution Per Well Position
Raw Cell Number/Plate Median
0.0
0.5
1.0
1.5
2.0
2.5
3.0
3.5
0
100
200
300
Well Position
Normalised Distribution Per Well Position
Normalised Data
−6
−4
−2
0
2
4
6
0
100
200
300
Well Position
Sample
OT−NT
risc−free
ubb
plk1

Figure 3.8. Effect of position normalisation.

A. Scatterplot showing raw cell number/plate median for each well position per plate. B. Scatterplot showing normalised distribution per well position to demonstrate the effect of position normalisation.

3.4.2 Correlation of replicates and performance of siRNA controls

Another way to ascertain the amount of variability within the screen is to examine the similarity of the replicates. By plotting one replicate against another one can see there is a good correlation between the replicates in the screen, the example shown in Fig, 3.9 is the correlation between replicates 1 and 3. In this scatterplot it is also possible to see the performance of the controls in the screen. The killing controls PLK1 and UBB generally have a negative Z score indicating that the siRNA had the intended negative impact on cell survival. On the scatterplot they are clustered together at the left hand side of the plot and are distinguishable from the bulk of siRNAs, indicating they performed as effective killing controls. The negative controls OT-NT and RISC-free on the other hand tended to have positive Z scores and cluster towards the right hand side of the plot. Ideally these controls should have appeared more centrally in the distribution of the population (ie. Z score =0), as they are designed to demonstrate the stress of transfection without gene-silencing, therefore should not have an impact on cell viability. However they appear skewed towards having a positive effect on cell survival. One possibility for this is that as RISC-free does not engage the RNAi machinery, therefore in comparison to all other siRNAs that do, RISC-free transfected cells are under less stress and are more viable. OT-NT is designed to engage the RISC-free machinery without causing gene silencing, but it is possible it does not do this as efficiently as siRNAs targeted against human transcripts.

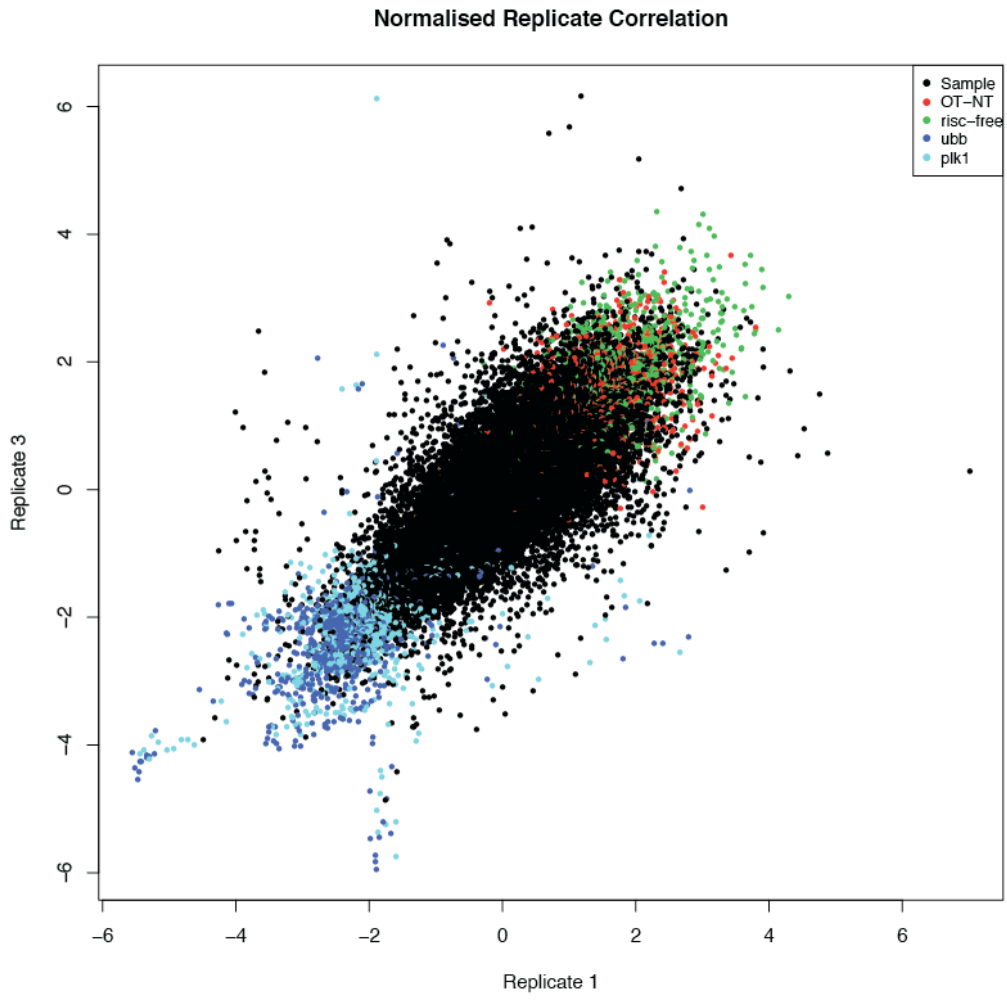

Figure 3.9. Correlation of replicates.

Scatterplot of normalised Z scores for replicates 1 and 3 of the control screen to demonstrate correlation of replicates. Negative and killing controls are represented as colour-coded in the key.

3.4.3 Residual Z score – difference between control and drug-treated conditions

As previously stated the Z score is the number of standard deviations away from the mean of the population that a data point lies. At this stage we had calculated the Z scores for each siRNA pool in the control screen and the drug screen. The information we really wanted to know was which siRNAs had the most different effects on survival in the drug screen than would be expected from the control screen. One would predict these siRNAs targeted genes that in some way

antagonised or enhanced the effect of erlotinib treatment. In order to identify differences between drug and control screens, the smoothed Z score from the drug screen was plotted against the smoothed Z score from the control screen for each replicate (nine comparisons in total) to obtain a residual Z score (Fig 3.10). The residual difference for each data point was calculated as the perpendicular distance between the data point and the line of best fit (as calculated by linear regression). The regression line is indicated in red. Negative residual differences represent those genes where the viability score within the drug screen is lower than would be expected based on the control viability, whereas positive scores indicate genes with viability within the drug screen that is higher than expected based on the control viability. All nine residual Z scores are given in Appendix 1. The median of the 9 residual Z scores was used to evaluate the performance of each siRNA pool in the screen (highlighted in yellow in Appendix 1).

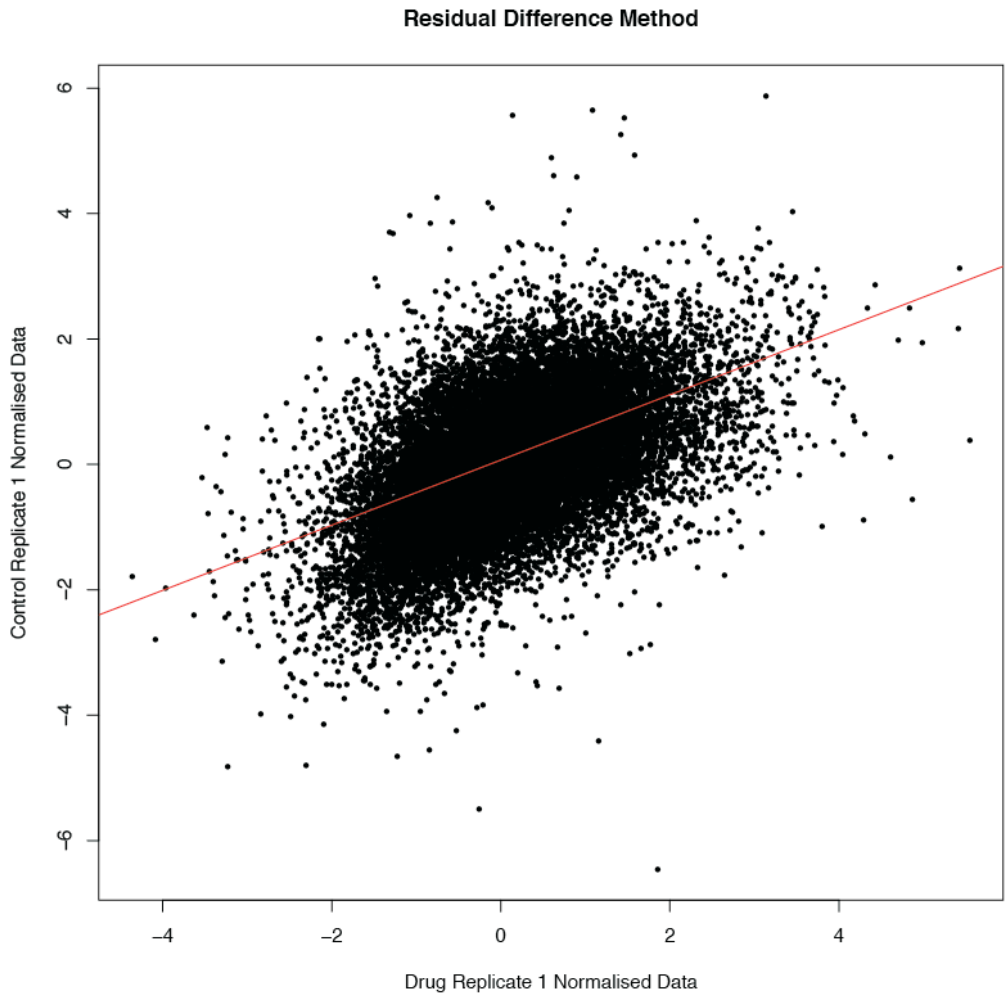

Figure 3.10. Residual difference method.

Scatterplot demonstrating the residual difference method. Normalised Z scores of each control and drug replicate were plotted against each other, and a line of best fit calculated by linear regression (shown in red). The residual Z score is calculated by measuring the perpendicular distance of each data point to the line of best fit, to give a positive or negative value.

3.5 Repeat of genome-wide screen

We repeated the genome-wide screen using the same conditions to test the reproducibility of the screen. The screen was normalised and analysed in the same way as the first screen, and the residual Z scores are provided in Appendix 1. As is clear in Appendix 1, the Z score values differ substantially between the two screens, however by ranking siRNAs in order of residual Z score we were able to analyse the overlap between the first and second screen. Residual Z scores were ranked by difference to 0 (i.e. the most positive or most negative scores were

ranked highest) to select for siRNAs that had the most substantially different effects in the drug and control screens. siRNA pools were selected that appeared in the top 2.5% of hits from the first screen, which gave us 528 siRNA pools. This corresponded to a residual Z score of greater than or equal to 1.7 or less than or equal to -1.7.126 of these siRNA pools were in the top 5% of hits in the second screen when ranked by residual Z score in the same way (Appendix 2). The percentages chosen were relatively arbitrary in that they gave us a reasonable number of siRNA pools to follow up in more detail. These 126 siRNA pools were taken forward to a deconvolution screen.

3.6 Deconvolution screen

In order to determine the effects on erlotinib sensitivity were the result of gene silencing, rather than off-target effects we carried out a deconvolution screen (Echeverri et al., 2006). In the genome-wide screen, each gene was targeted by a SMARTpool, consisting of 4 individual siRNA oligos targeting different regions of the nucleotide sequence. In the deconvolution screen each oligo is assessed individually for the effect it has on erlotinib sensitivity. The deconvolution screen was also carried out in 384-well plate format, using the same method as used for the genome-wide screen. As siRNAs in the deconvolution screen had already been selected for having an effect on cell survival it was no longer possible to normalise the data based on background plate medians. Instead, we calculated a Sensitivity Index (SI) for each siRNA oligo, which is a measure of the synergistic or antagonistic effect of an siRNA on drug treatment (SI = si control/sc control * sc drug/sc control – si drug/ sc control) (Swanton et al., 2007). This equation allows the calculation of the individual effect of the drug (sc drug/sc control) and the siRNA (siRNA control/sc control), and then lets you calculate whether the expected combined effect of the siRNA and drug on cell viability is different to the observed combined effect (siRNA drug/sc control). Positive SI values indicate a sensitising effect of the siRNA, whereas negative SI values indicate an antagonistic effect of the siRNA to drug treatment. The control siRNA we used to normalise the data was non-targeting scrambled control pool #2. We did not use RISC-free siRNA, as we did in the genome-wide screens as RISC-free controls appeared skewed towards enhancing cell survival instead of having no effect (Fig 3.10). SI scores of each

siRNA are shown in Appendix 3. For our final hit selection we used the cut-off SI value of ≥ 0.10 for sensitising siRNAs and ≤ -0.15 for desensitising siRNAs, which is the same as the criteria employed by Swanton et al (Swanton et al., 2007). 26 siRNA pools confirmed a reproducible phenotype with at least two out of four of their individual deconvoluted siRNAs meeting the above criteria (Table 3.2).

RefSeq ID	Gene Name	siRNA 1	siRNA 2	siRNA 3	siRNA 4
NM_000352	ABCC8	0.09	0.11	0.36	0.14
NM_001113182	BRD2	-0.25	-0.17	-0.10	-0.05
NM_024541	C10orf76	-0.04	-0.33	-0.33	-0.10
NM_004928	C21orf2	-0.24	-0.21	-0.22	0.06
NM_001782	CD72	-0.28	-0.11	-0.08	-0.21
NM_005193	CDX4	0.04	-0.14	-0.25	-0.18
NM_001861	COX4I1	-0.40	-0.10	-0.32	-0.11
NM_022783	DEPDC6	0.02	-0.26	-0.07	-0.22
NM_001953	ECGF1	-0.16	-0.22	-0.23	-0.03
NM_016123	IRAK4	-0.09	-0.05	-0.39	-0.46
NM_001010978	LOC38863	-0.03	-0.19	-0.21	0.00
NM_004811	LPXN	-0.33	-0.07	-0.22	-0.20
NM_005587	MEF2A	-0.30	-0.14	-0.38	-0.31
NM_152371	MGC26818	-0.25	-0.11	-0.02	0.02
NM_000267	NF1	-0.23	-0.07	-0.18	-0.11
NM_003681	PDXK	-0.13	-0.22	-0.58	-0.28
NM_015107	PHF8	-0.23	-0.37	-0.18	-0.25
NM_002637	PHKA1	-0.11	0.00	-0.30	-0.07
NM_019896	POLE4	-0.15	-0.20	-0.13	-0.09
NM_025078	PQLC1	-0.04	-0.16	-0.32	-0.05
NM_002998	SDC2	-0.02	-0.22	-0.14	-0.20
NM_152386	SGPP2	-0.26	-0.15	-0.02	-0.05
NM_004858	SLC4A8	0.15	-0.07	0.16	-0.01
NM_020830	WDFY1	-0.16	-0.08	-0.20	-0.15
NM_198581	ZC3HDC6	-0.11	-0.30	-0.20	-0.15
NM_020843	ZNF291	-0.25	-0.01	-0.34	-0.26

Sensitivity Index

Sensitising
- ≥ 0.10 - 0.15
- ≥ 0.15 - 0.2
- ≥ 0.20 - 0.30
- ≥ 0.30

Desensitising
- ≤ -0.15--0.2
- ≤ -0.2 --0.3
- ≤ -0.3 --0.4
- ≤ -0.4

Table 3.2. Genes that upon RNAi-mediated silencing affected cell survival in response to erlotinib treatment

List of genes for which 2 out of 4 oligos met our hit criteria (SI value of ≥ 0.10 for sensitising siRNAs and ≤ -0.15 for desensitising siRNAs). The value given for each oligo is the Sensitivity Index (SI) explained in the text. The strength of the effect is indicated by the colour coding in the key. No colour indicates the siRNA had no effect on drug response.

3.7 Discussion

In the final hit selection were 26 genes that had a reproducible effect on cell viability in the presence of erlotinib (Table 3.2). Silencing of only two of the genes, *ABCC8* (ATP-binding cassette sub-family C member 8) and *SLC4A8* (solute carrier 4 sodium bicarbonate cotransporter member 8) resulted in increased sensitivity to erlotinib treatment. It appears that our screen set-up preferentially aided the identification of genes that increase resistance to erlotinib treatment upon silencing. This may be because PC9 cells are already exquisitely sensitive to erlotinib treatment therefore it is difficult to make them more sensitive to erlotinib. It seems that most siRNAs that decreased cell viability in the presence of erlotinib treatment also had an effect in the control screen, therefore the effect is not specific to erlotinib-induced cell death. The genes targeted by these siRNAs could still yield interesting results, as silencing of these genes decreases the viability of a NSCLC cell line, however further work would be needed to confirm the specificity of the effects on cell viability. If silencing of these genes also affects the viability of non-cancerous cells in the same way, then targeting of these gene products would be likely to cause high levels of toxicity in patients. We were more interested in genes that specifically affected response to erlotinib, therefore did not include more general killing siRNA pools in our follow-up.

In our screen we used the siGENOME SMARTpool library as it contained 4 different oligos to target each gene. Using multiple siRNAs is necessary as siRNAs targeting the same gene can have variable effects of phenotype. This was highlighted in a study by Collinet et al. (Collinet et al., 2010) where they used two different siRNA libraries and one endoribonuclease-prepared siRNA to target each transcript of a set of genes involved in endocytosis. They found that siRNAs from the same and different siRNA libraries can have inconsistent phenotypic effects. There are many reasons for such differences, one of which is that not all siRNAs can silence their target gene with the same efficiency, possibility due to differences in thermostability or sequence complementarity between the siRNA oligo and target transcript. Also, for some genes it seems to be there is a threshold of gene silencing required to have a biological effect, i.e. that a phenotype is only seen when the level of gene silencing is 90% or greater. Therefore although all siRNA

pools may silence gene expression to some degree, only a couple may reach the level of silencing required to produce a phenotype.

As mentioned previously, siRNA can have off-target effects, which are not caused by specific silencing of the intended target gene. Off-target effects are caused by silencing of genes other than the intended target due to similarities in nucleotide sequence. Complete complementarity between the siRNA and target nucleotide sequence is not necessary, and it is thought that 14 or even fewer base pairings are necessary for RISC-mediated cleavage of mRNA (Jackson et al., 2003). Additionally, siRNAs can cause off-target effects at the level of protein expression without affecting mRNA levels, as they can mimic the function of endogenous microRNAs (miRNAs). miRNAs are small RNA molecules which inhibit gene expression at a post-transciptional level, by binding to complementary sequences in the 3'UTR of mRNA and inhibiting their translation (Bartel, 2009). It is for these reasons that we carried out a repeat screen and a deconvolution screen. It is clear that at multiple stages of the process, siRNAs did not validate as 128 genes from the genome-wide screens were whittled down to 26 genes in the final hit list when we applied criteria as defined by Swanton et al. (Swanton et al., 2007). Due to the fact that at least 2 of 4 siRNAs produced the same phenotypic effect in the deconvolution screen we are fairly confident that the genes in our hit list are not subject to off-target effects.

Other potential issues are that some gene perturbations may indirectly effect drug sensitivity, rather than directly making an individual cell more resistant to erlotinib treatment. For example, from experimental observations, it seems that more confluent cells are more resistant to erlotinib treatment, probably as increased cell-cell contacts leads to increased pro-survival signalling. Therefore genes that increase proliferation will most probably increase resistance to erlotinib. Such effects were identified in a study by Snijder et al. where they found the position of a cell in the centre or at the edge of a colony significantly affected the susceptibility of cells to viral infection (Snijder et al., 2009). Hopefully, employing the use of a residual Z score would remove most of the siRNA pools which contribute to drug response by affecting proliferation. Any effects on cell growth should be identified

in the control screen, thereby reducing the residual Z score and preventing their evaluation as a hit.

Another consideration was the length of the assay. We used siRNA in order to target gene transcripts, which as described earlier imposed limits on the timescale of the experiment. One concern is that silencing of genes that cause increased cell survival in erlotinib-treated conditions in short term assays do not necessarily have the same effect in the long term. This may indicate they are less likely to be mechanisms of resistance in vivo, as they are not well tolerated by cells for more than a few days. We did obtain hits from the screen that validate in longer term (10 day) experiments and are described in chapters 4 and 5, however this is not the case for all genes. One example of a gene that did not validate in long term experients is *PHF8* (PHD finger protein 8), a histone demethylase with activity towards H3K9me1/2 (Qi et al., 2010). In the screen *PHF8* siRNA appears to cause increased resistance to erlotinib, however long term experiments using shRNA targeting *PHF8* failed to confirm this result. Lui et al. suggest that PHF8 is essential in cell cycle progression, and it is possible that silencing of *PHF8* prevents cancer cell proliferation. Erlotinib is thought to exert a growth inhibitory effect mostly in the G1/S transition of the cell cycle (Ling et al., 2007) therefore, it is possible short term silencing of *PHF8* reduces erlotinib-mediated cell death as it renders cells quiescent. A quiescent phenotype has been associated with increased drug tolerance and is a mechanism of transient drug resistance (Sharma et al., 2010). However, in this example longterm silencing of *PHF8* by shRNA induced p16 expression and substantially reduced proliferation of PC9 cells which still have intact p16 and Rb expression (Arifin et al., 2010).

Additionally of note, it has recently been published that loss of *PDXK* encoding Pyridoxal Kinase can increase resistance of NSCLC to cisplatin (Galluzzi et al., 2012). PDXK generates the bioactive form of vitamin B6 which exacerbates cisplatin-induced cell death. Galluzzi and colleagues found that addition of the vitamin B6 precursor Pyridoxine sensitised NSCLC to a variety of stress conditions including hypoxia, nutrient depletion, ionizing irradiation and respiratory chain inhibition in a PDXK-dependent manner which suggests it is involved in general stress responses. Although this study links PDXK to resistance to a different class

of therapeutics, it indicates PDXK plays a role in cell death in response to multiple stress conditions which could potentially extend to treatment with EGFR TKIs. Galluzzi et al. found low PDXK expression was associated with decreased disease-free and overall survival of NSCLC patients regardless of whether they received adjuvant chemotherapy (Galluzzi et al., 2012). Although this is a general association with survival, not specific to EGFR TKI response, it is encouraging that our screen uncovered a gene that has been associated with a prognostic value in patients.

Of the other 22 genes identified, there are a few genes, which immediately caught our attention, notably *NF1* (Neurofibromin 1) and *DEPDC6/DEPTOR* (DEP domain containing 6), as they both encode for negative regulators of pathways activated downstream of EGFR. NF1 is a RAS GTPase activating protein, negatively regulating the function of RAS (Basu et al., 1992), and DEPDC6 is a negative regulator of mTOR (Peterson et al., 2009). Both of these genes were followed up in more detail and will be discussed in chapters 4 and 5

Chapter 4. NF1 loss increases resistance of NSCLC to EGFR TKI treatment.

4.1 Introduction

One of the genes identified in the screen as causing increased resistance to erlotinib upon gene silencing is *NF1* (Neurofibromin 1). As previously mentioned in the introduction NF1 is a RAS GTPase activating protein that negatively regulates RAS function by stimulating the hydrolysis of RAS-GTP to RAS-GDP (Basu et al., 1992). Recently NF1 has gained attention as a tumour suppressor, whose loss can lead to resistance to drug treatment in a number of different settings. An shRNA screen in a neuroblastoma cell line identified that NF1 loss causes increased resistance to retinoic acid (Holzel et al., 2010). In this tumour type loss of NF1 activates RAS-MEK signalling which in turn represses ZNF423, a transcriptional co-activator of retinoic acid receptors, reducing responsiveness to retinoic acid therapy. Also, loss of NF1 expression has been identified as a determinant of resistance to tamoxifen treatment in estrogen receptor positive breast cancer, most likely via activation of classical RAS family proteins (HRAS, KRAS and NRAS) as well as the related RRAS2, leading to downstream activation of ERK (Mendes-Pereira et al., 2011). In an shRNA screen against tumour suppressor genes in A549 lung cancer cells, loss of NF1 increased paclitaxel resistance (Ji et al., 2007). These data indicate NF1 downregulation can cause resistance to multiple classes of drugs including microtubule stabilising agents as well as targeted therapies.

Additional support for the role of NF1 in erlotinib resistance came from murine models of EGFR-driven NSCLC. Politi and colleagues generated mouse models where expression of an active mutant *EGFR* can be induced in type II pneumocytes by doxycycline treatment. Expression of an L858R mutant or exon 19 deletion mutant (L747-S752), leads to formation of lung tumours that are dependent on the expression of the mutant *EGFR* allele and respond to EGFR TKIs (Politi et al., 2006). Further, Politi generated mice with erlotinib resistant tumours, by treating mice with multiple on-off cycles of erlotinib until they were no longer responsive to drug treatment (Politi et al., 2010). In resistant tumours they

detected the *EGFR*^{T790M} mutation, and *Met* amplifiation, however in half of all resistant tumours, non-overlapping with these common mechanisms they detected a reduction in Nf1 mRNA expression as quantified by qRT-PCR (Figure 4.1). This indicates NF1 loss may be involved in erlotinib resistance in clinically relevant models of NSCLC.

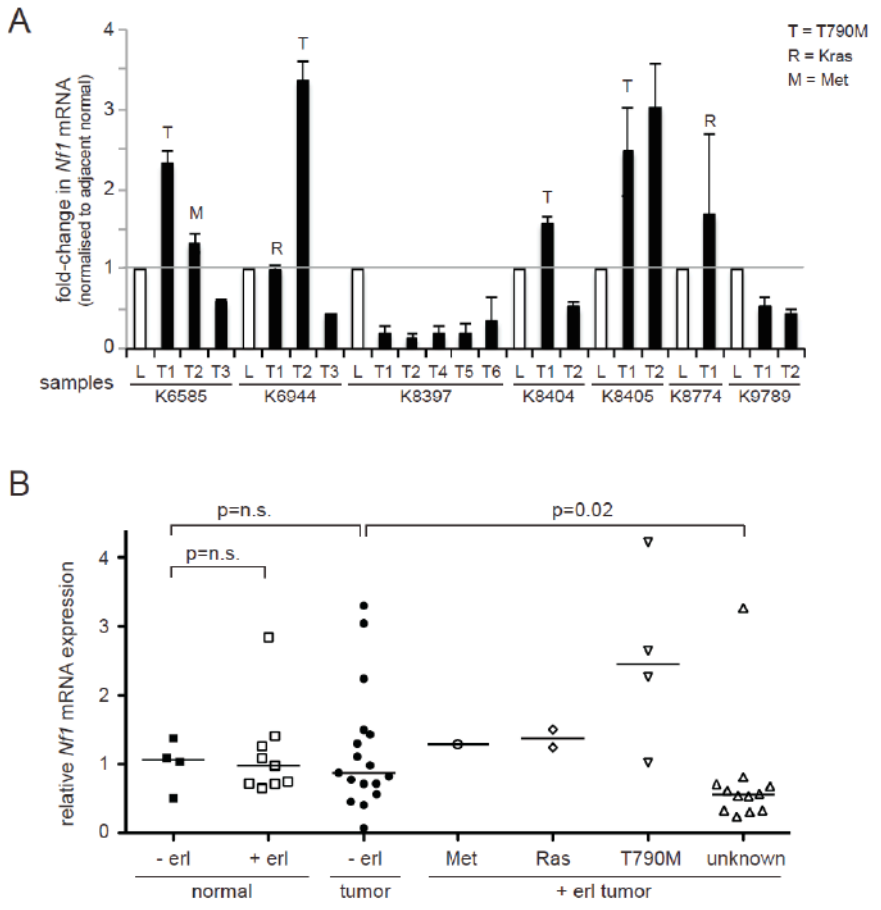

Figure 4.1. Nf1 expression is reduced in a murine model of erlotinib-resistant NSCLC (unpublished data provided by Katerina Politi)..

A. Nf1 mRNA was quantified by RT-QPCR and normalised to lung epithelial marker Surfactant Protein C. Nf1 mRNA levels for each tumour are shown relative to expression in normal adjacent lung tissue in each mouse. On the X-axis L=normal lung, T=tumour and the numbers correspond to the mouse from which the samples were taken. Where known mechanisms of resistance (*EGFR*^{T790M}, *Kras* mutation, or *Met* amplification) were found they are indicated on the graph.
B. Nf1 expression levels of untreated (-erl; erlotinib sensitive) and erlotinib-treated (+erl; erlotinib resistant) tumours and adjacent normal lung from EGFR mutant mice are plotted. Erlotinib-resistant tumours are subdivided according to

known secondary lesions present in the tumours as indicated. P-values were determined by Mann-Whitney U-test.

4.2 Reduction of NF1 expression renders lung cancer cells less sensitive to EGFR-TKI treatment

In order to validate the role of NF1 in erlotinib resistance further we generated PC9 cells stably expressing two individual shRNAs targeting different, non-overlapping regions of the NF1 coding sequence. Both shRNAs efficiently decreased NF1 expression at the protein and mRNA level, with shRNA #2 giving the most efficient silencing compared to scrambled control cells expressing a non-targeting shRNA (shSC) (Fig.4.2).

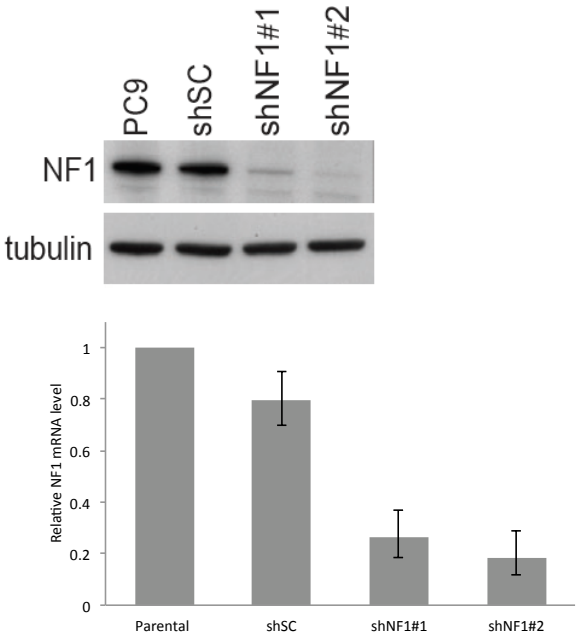

Figure 4.2. NF1 protein and mRNA levels are efficiently reduced by shRNA constructs targeting NF1.

PC9 cells were left uninfected or infected with a non-targeting shRNA (shSC) or shRNAs targeting NF1 (shNF1#1 and shNF1#2). NF1 protein and mRNA levels were measured by western blotting and qRT-PCR respectively.

In 72 hour survival assays both NF1 shRNA constructs increased resistance of PC9 cells to erlotinib treatment compared to shSC controls, with a 14-fold increase in IC_{50} for shNF1#1 and 21-fold for shNF1#2 (Fig 4.3).

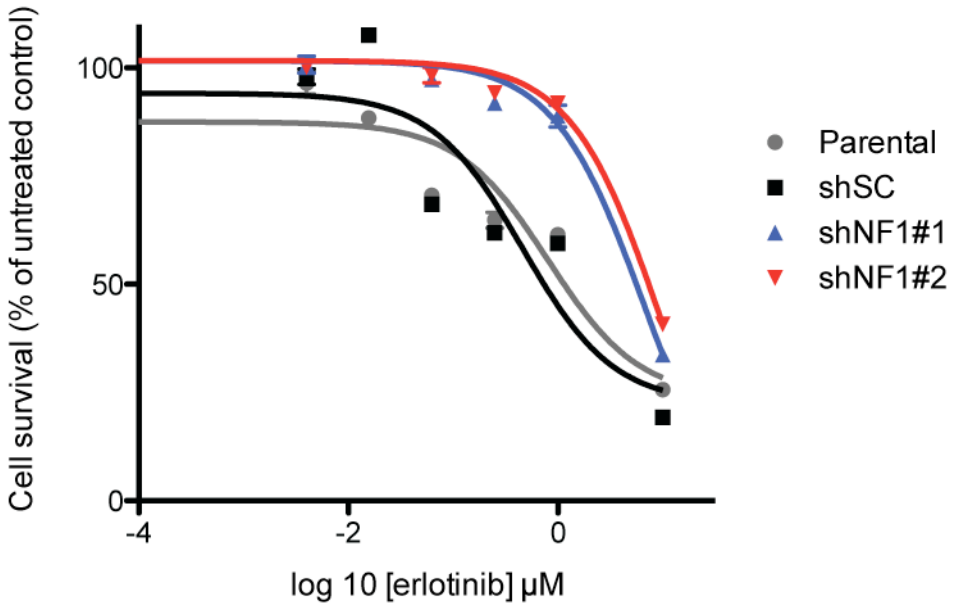

Figure 4.3. NF1 silencing increases resistance to erlotinib.

PC9 cells were left uninfected or infected with a non-targeting shRNA (shSC) or shRNAs targeting NF1 (shNF1#1 and shNF1#2). Cells were treated with the indicated concentrations of erlotinib for 72 hours, and cell survival was measured using the CellTiter-Blue assay.

To look at the effects of NF1 silencing in the longer term, we carried out colony formation assays, where cells were plated at low density and treated with erlotinib for 10 days. NF1 silencing substantially increased cell survival in these assays compared to shSC expressing cells (fig 4.4).

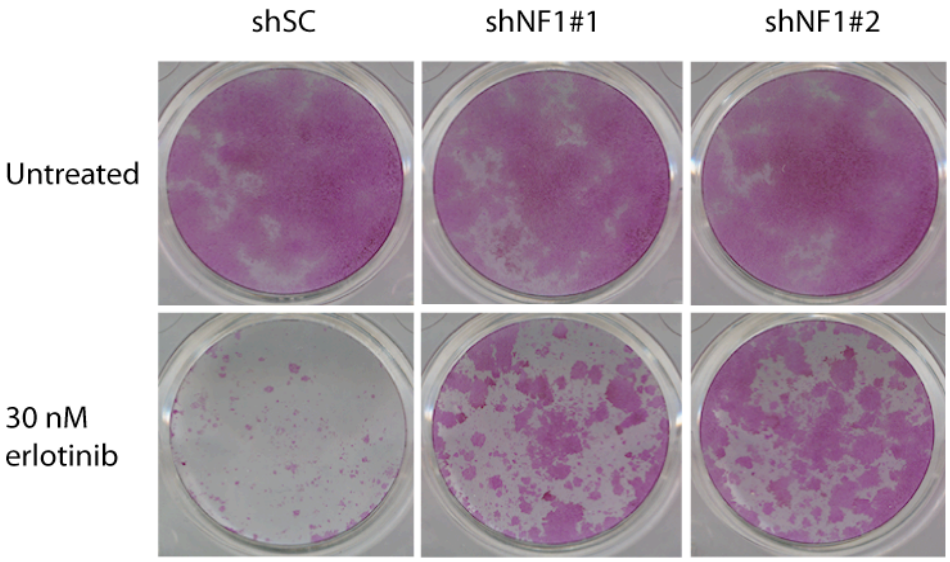

Figure 4.4. NF1 loss increases resistance to erlotinib in longer term assays.
PC9 cells were infected with non-targeting control shRNA (shSC), or shRNAs targeting NF1 (shNF1#1 and #2). Cells were grown in untreated or erlotinib-treated conditions for 10 days and then fixed and stained with Sulphorhodamine B.

In order to determine whether the effect of NF1 silencing is specific to EGFR-TKIs or whether it has a more general effect, increasing resistance to a broader range of drugs, we carried out 72 hour survival assays with other therapeutic drugs. NF1 silencing increased resistance to another EGFR-TKI (gefitinib) (Fig 4.5), however it had no effect on chemotherapeutic agents cisplatin or docetaxel, which function through DNA-crosslinking and microtubule stabilisation respectively (Fig 4.6).

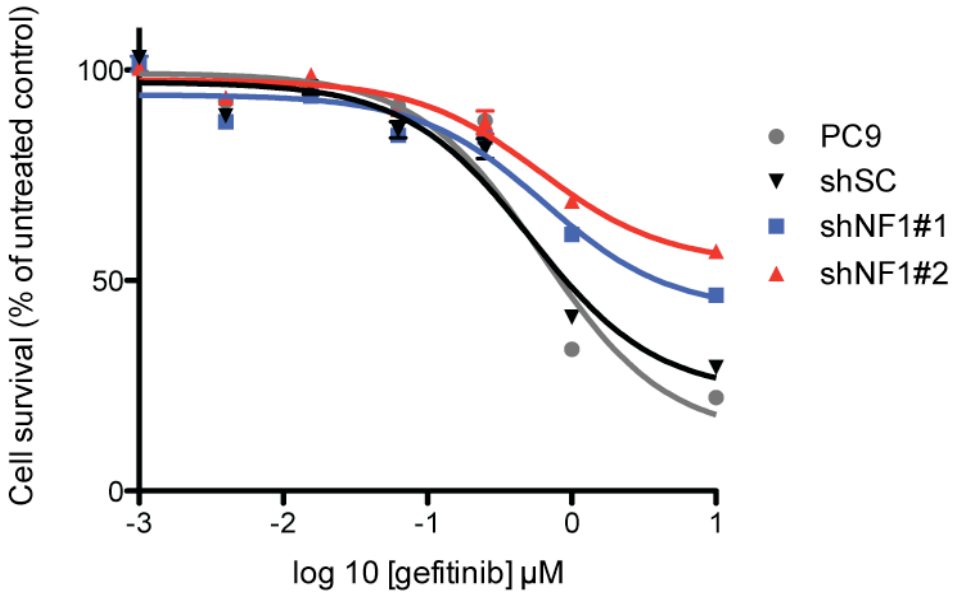

Figure 4.5. NF1 loss increases resistance of PC9 cells to gefitinib treatment. PC9 cells were left uninfected or infected with a non-targeting shRNA (shSC) or shRNAs targeting NF1 (shNF1#1 and shNF1#2). Cells were treated with the indicated concentrations of gefitinib for 72 hours and cell survival was measured using the CellTiter-Blue assay.

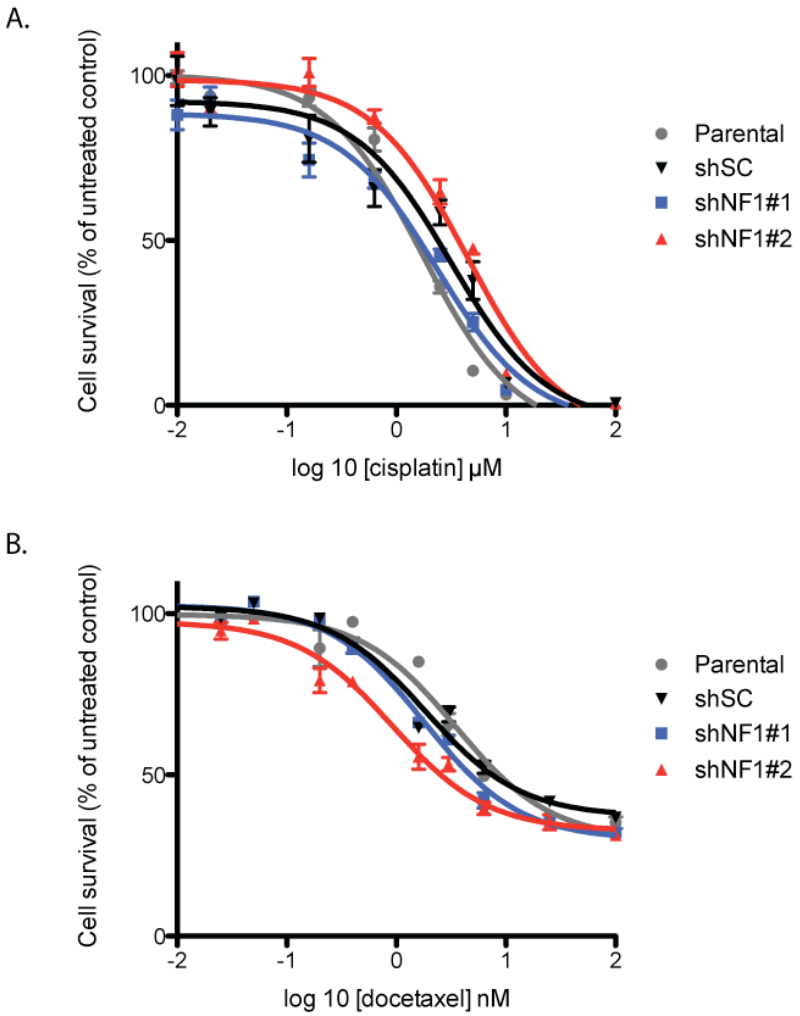

Figure 4.6. NF1 silencing does not increase resistance to other chemotherapeutic drugs.

PC9 cells were infected with a non-targeting shRNA (shSC) or shRNAs targeting NF1 (shNF1#1 and shNF1#2). Cells were treated with the indicated concentrations of (A) cisplatin or (B) docetaxel for 72 hours, and cell survival was measured using the CellTiter-Blue assay.

4.3 NF1 silencing leads to MAPK pathway activation in the presence of erlotinib

In order to determine whether NF1 silencing increases resistance to erlotinib via activation of RAS signalling, we assessed the levels of active RAS-GTP in shSC and shNF1 cells in the presence and absence of erlotinib. In experiments where only one shRNA targeting NF1 was used shNF1 refers to shNF1#2, as this short

hairpin RNA provided the most efficient silencing. Both shNF1 and shSC cells showed a dramatic decrease in RAS-GTP levels upon erlotinib treatment, however shNF1 cells retain more RAS-GTP in the presence of erlotinib (Fig 4.7).

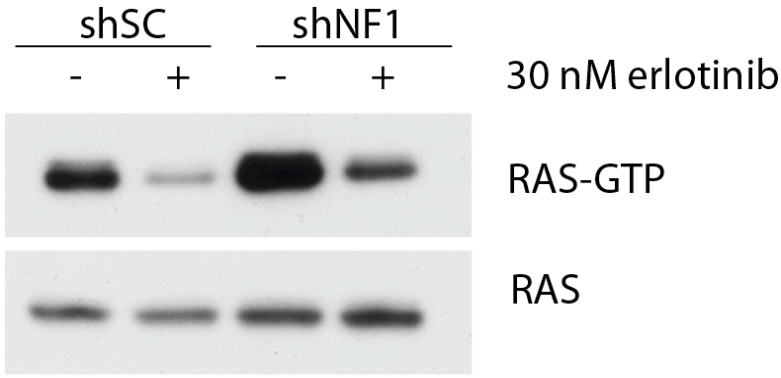

Figure 4.7. RNAi-mediated NF1 silencing increases RAS activation.
PC9 cells were infected with a non-targeting shRNA (shSC) or shRNA targeting NF1. Cells were treated with or without erlotinib for 1 hr before lysis, and RAS-GTP was immunoprecipated from lysates with GST-Raf1-Ras Binding Domain, as described in the materials and methods. Total RAS protein from total lysates is shown as loading control.

Downstream of RAS the two main signalling pathways are the MAPK pathway and PI3K pathway. To determine the effect of NF1 silencing on these signalling pathways we examined the phosphorylation status of downstream signalling proteins. Erlotinib treatment results in significantly decreased phosphorylation of EGFR, ERK1/2, and caused a less pronounced decrease in phosphorylation of AKT. shNF1-expressing cells however retain some phosphorylated ERK1/2 in the presence of erlotinib, whereas phosphorylated ERK1/2 is completely abolished in shSC-expressing and parental PC9 cells (Fig.4.8).

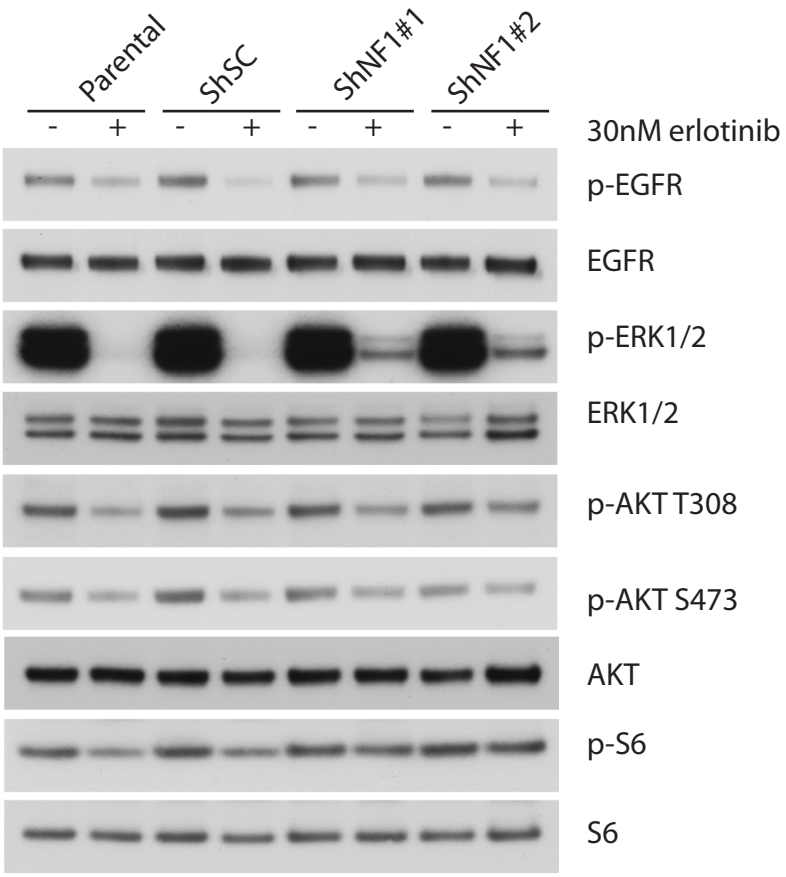

Figure 4.8. NF1 loss leads to sustained activation of ERK1/2 in the presence of erlotinib.

PC9 cells were uninfected (parental), or infected with non-targeting shRNA construct (shSC), or shRNAs targeting NF1 (shNF1#1 and shNF1#2). Cells were treated with or without 30 nM erlotinib for one hour prior to lysis for immunoblotting against indicated proteins.

To confirm that NF1 silencing leads to sustained phosphorylation of ERK1/2 upon erlotinib treatment in other EGFR-mutant NSCLC cell lines, and that it is not a PC9 cell line specific effect, H3255 and HCC4006 cells were infected with control shRNA (shSC) and shRNA targeting shNF1. NF1 silencing caused both cell lines to retain more phosphorylated ERK1/2 in erlotinib-treated conditions compared to control (shSC) cells (Fig 4.9). Silencing of NF1 also increased resistance of both cell lines to long term (10 day) erlotinib treatment (Fig 4.10), indicating NF1 loss can mediate resistance to erlotinib in multiple NSCLC cell lines.

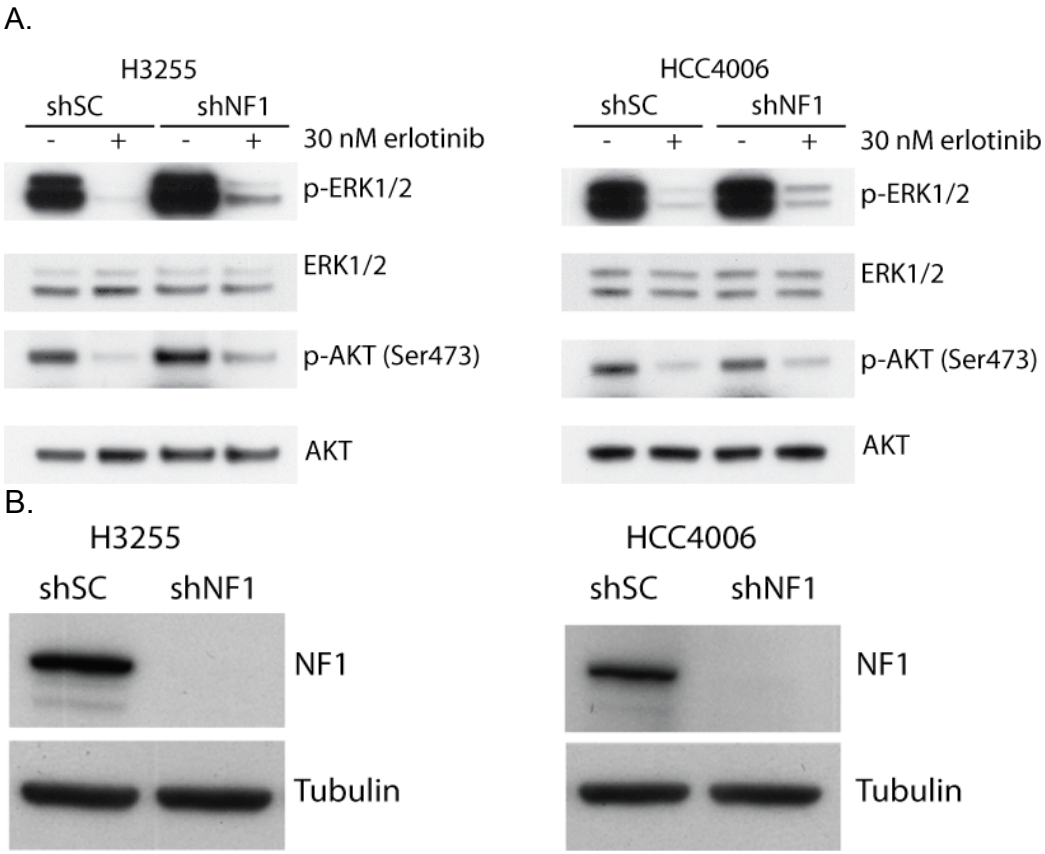

Figure 4.9. NF1 loss leads to sustained phosphorylation of ERK in erlotinib-treated conditions in other NSCLC cell lines.

H3255 and HCC4006 cells were infected with non-targeting shRNA construct (shSC), or shRNA targeting NF1 (shNF1). A. Cells were treated with or without 30 nM erlotinib for one hour prior to lysis for immunoblotting against indicated proteins. B. Cells were lysed for immunoblotting to confirm RNAi-mediated silencing of NF1.

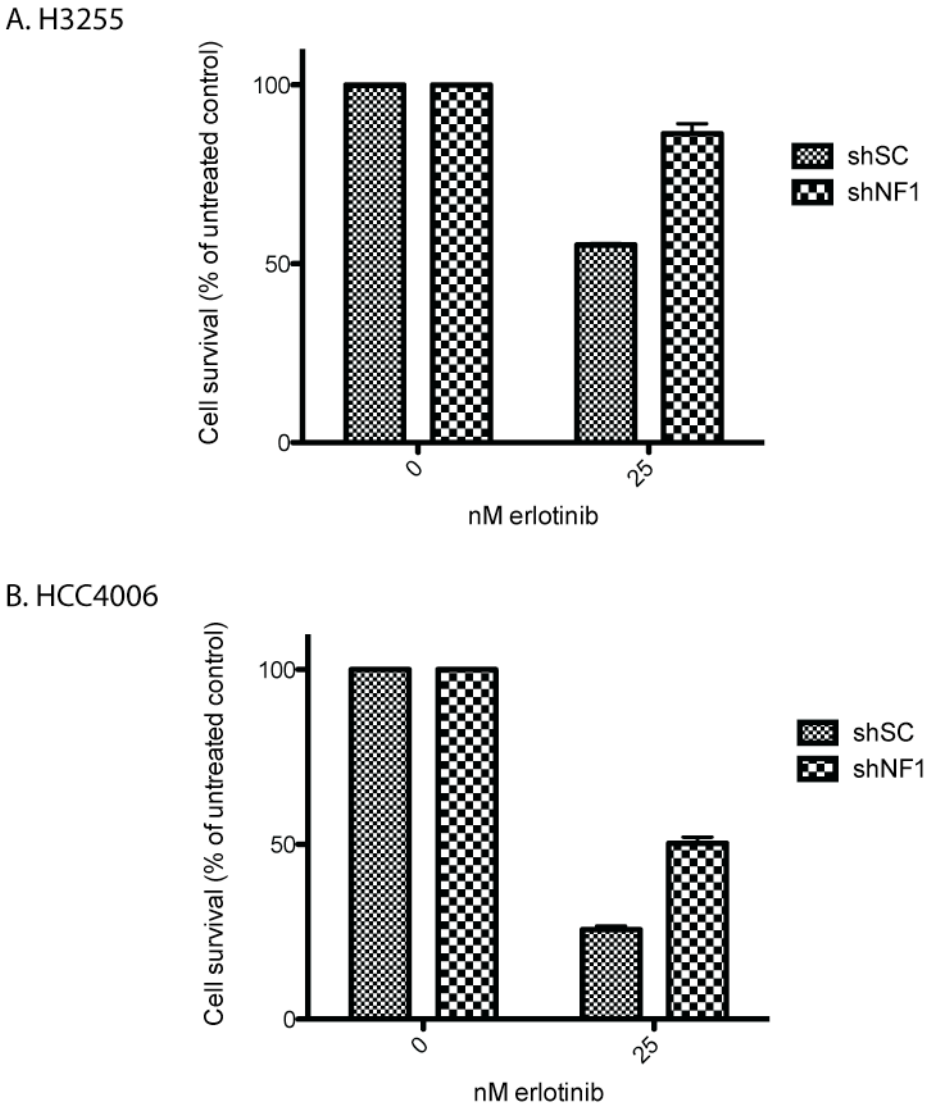

Figure 4.10. NF1 loss increases resistance of other NSCLC cell lines to erlotinib in long term survival assays.

H3255 and HCC4006 cells were infected with non-targeting shRNA construct (shSC), or shRNA targeting NF1 (shNF1). Cells were grown in untreated or erlotinib-treated conditions for 10 days and then fixed and stained with Sulphorhodamine B.

To confirm that NF1 silencing increases resistance to erlotinib by enhancing RAS signalling, we overexpressed the NF1-GRD (Gap Related Domain) in PC9 cells before silencing endogenous NF1 with shRNAs, which do not target the GRD (Fig.4.11).

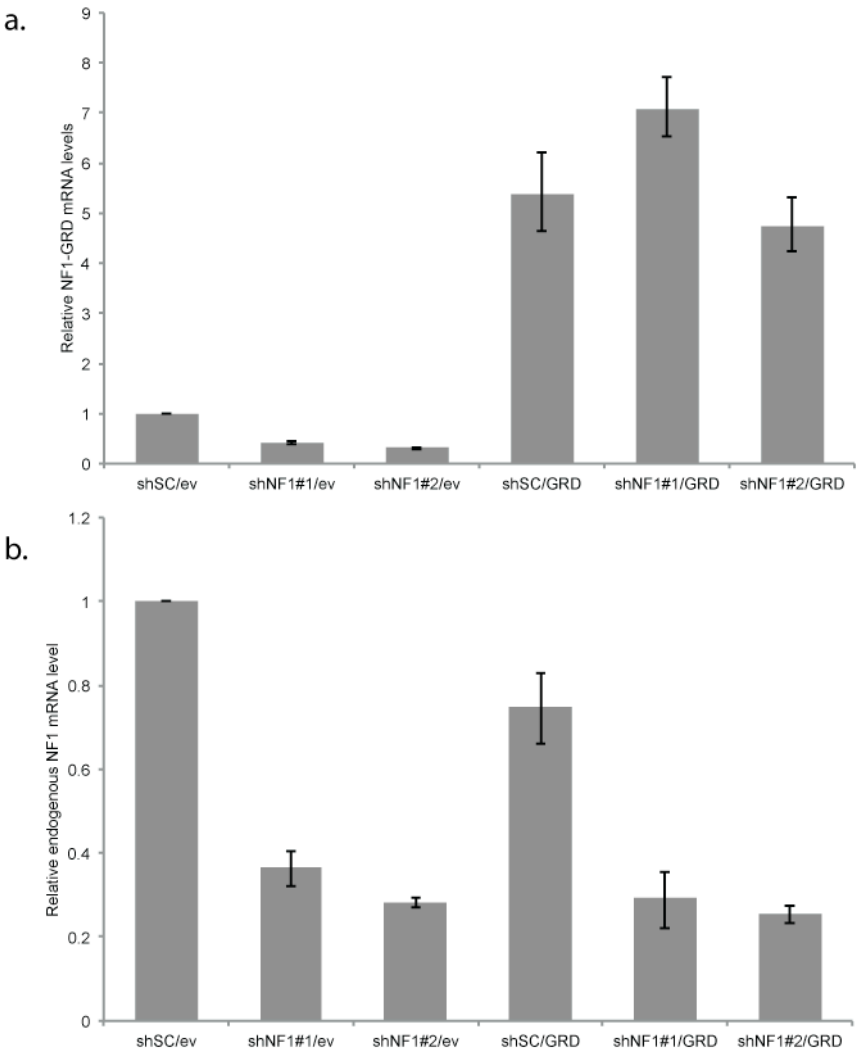

Figure 4.11. Expression of an shRNA resistant NF1-GRD and silencing of endogenous NF1 by shRNA.

PC9 cells were transfected with either the NF1-GRD (GRD) or empty vector (ev) and then infected with control shRNA (shSC) or shRNA targeting NF1. a) NF1-GRD mRNA levels detected by qRT-PCR with primers that recognise the NF1-GRD (endogenous and transfected). b) NF1 mRNA levels detected by qRT-PCR using primers that detect endogenous NF1, but not the transfected GRD.

We postulated that if the cells still had RAS GAP activity of NF1 conferred by the GRD, they would not become more resistant to erlotinib upon endogenous NF1 silencing. Indeed it appears that it is the loss of NF1 RAS GAP activity that causes the increase in resistance, as shNF1 cells expressing a control vector became more resistant to erlotinib treatment, whereas shNF1 cells expressing the NF1-GRD were substantially less resistant (Fig 4.12).

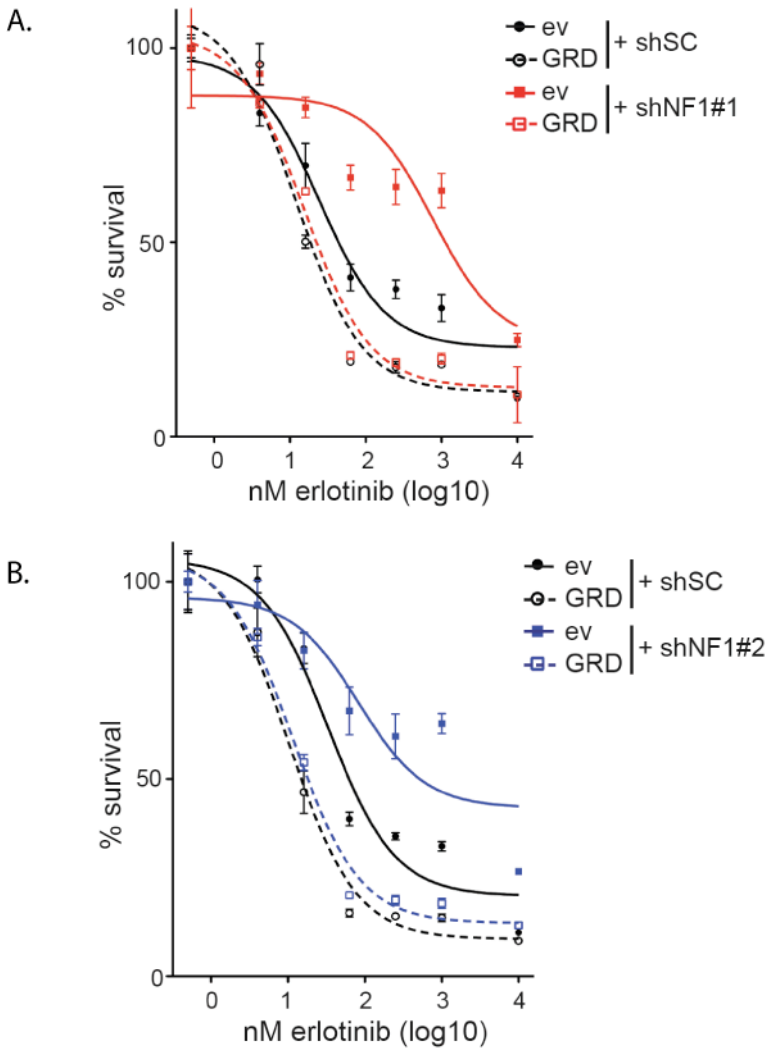

Figure 4.12. NF1-GRD expression prevents increased resistance to erlotinib in shNF1 cells.

PC9 cells were transfected with either the NF1-GRD (GRD) or empty vector (ev) and then infected with control shRNA (shSC) or shRNA targeting NF1 (A.shNF1#1 and B. shNF1#2). Cells were treated with the indicated concentrations of erlotinib for 72 hours and cell survival was measured using the CellTiter-Blue assay.

The effect on erlotinib resistance seen with expression of the NF1-GRD correlates to the effects on ERK1/2 phosphorylation. shNF1 cells expressing the empty vector retain phosphorylated ERK1/2 upon erlotinib treatment, whereas it is absent in shNF1 cells expressing the NF1-GRD (Fig 4.13).

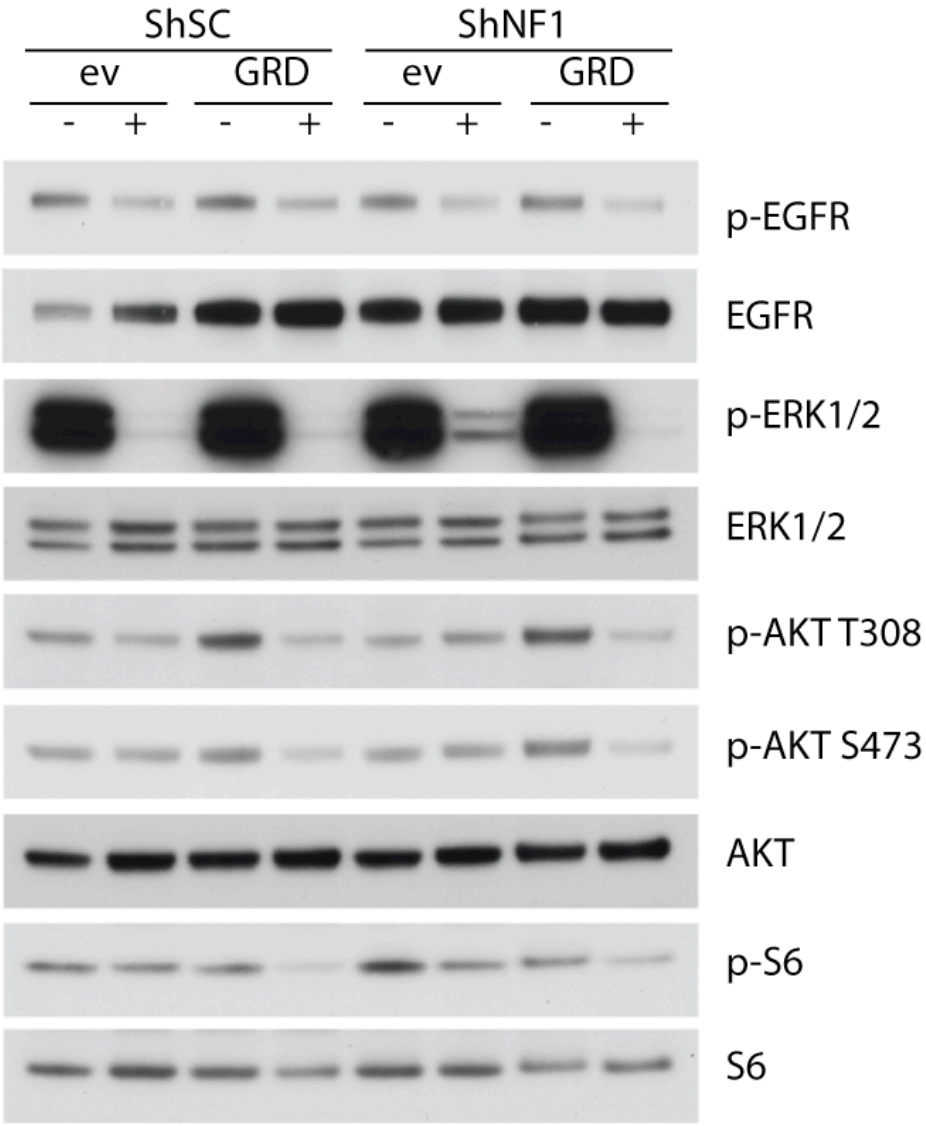

Figure 4.13. Expression of the NF1 GRD restores signalling of shNF1 cells.

PC9 cells expressing either an empty vector (ev) or NF1-GRD were infected with control shRNA (shSC) or shRNAs targeting NF1 (shNF1#1 and shNF1#2). Cells were left untreated or treated with erlotinib for 1 hr prior to lysis for immunoblotting against indicated proteins.

Our data thus far, pointed to the maintenance of ERK1/2 phosphorylation in shNF1 cells in erlotinib-treated conditions as the cause of increased resistance. This was supported by further work when we transfected PC9 cells with a myristoylated AKT, or MEK-DD construct. Myristoylated AKT is constitutively active as it is tethered to the plasma membrane. In the MEK-DD construct, serine has been substituted with negatively charged aspartate at residues 218 and 222 to mimic phosphorylation at these sites and constitutively activate the kinase. MEK-DD cells retained some phosphorylation of ERK1/2 in the presence of erlotinib and myrAKT had similar

levels of AKT phosphorylation in the presence and absence of erlotinib, indicating both constructs were expressed and the proteins activated (Fig 4.14). In 72 hour survival assays myr-AKT expressing cells were moderately more resistant to erlotinib treatment than control cells with a 2-fold increase in IC_{50}, whereas MEK-DD expressing cells were substantially more resistant with a 40-fold increase in IC_{50} (Fig 4.15). 10 day colony formation assays produced similar results. Myr-AKT cells were again moderately more resistant than control cells, whilst cell survival was dramatically increased in MEK-DD cells (Fig 4.16).

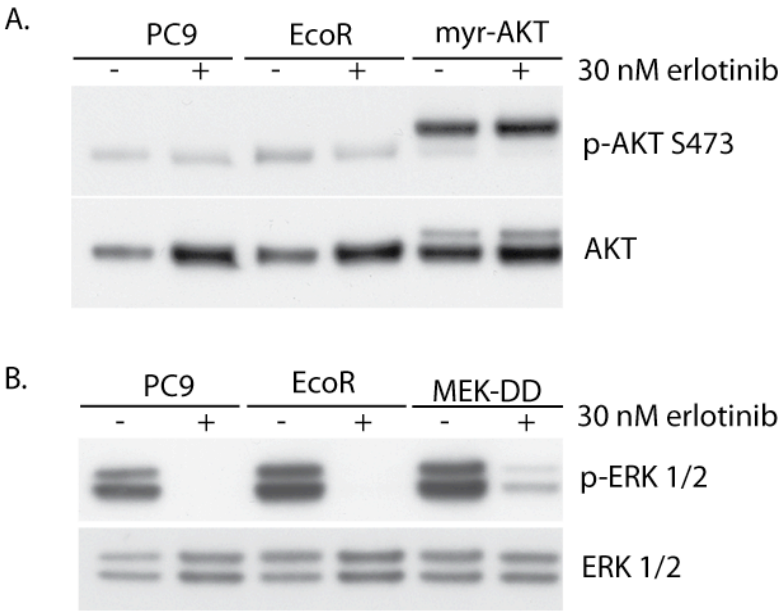

Figure 4.14. Expression of myristoylated AKT and MEK-DD constructs in PC9 cells.

PC9 cells expressing the murine ecotropic receptor (EcoR), were infected with retroviral myristoylated AKT and MEK-DD constructs. Cells were treated with erlotinib for 1 hr prior to lysis for immunoblotting. A. Expression of myristoylated AKT construct and constitutive activation in untreated and erlotinib-treated conditions. B. Activation of MEK-DD construct is shown by the sustained phosphorylation of ERK1/2 seen in MEK-DD cells upon erlotinib treatment.

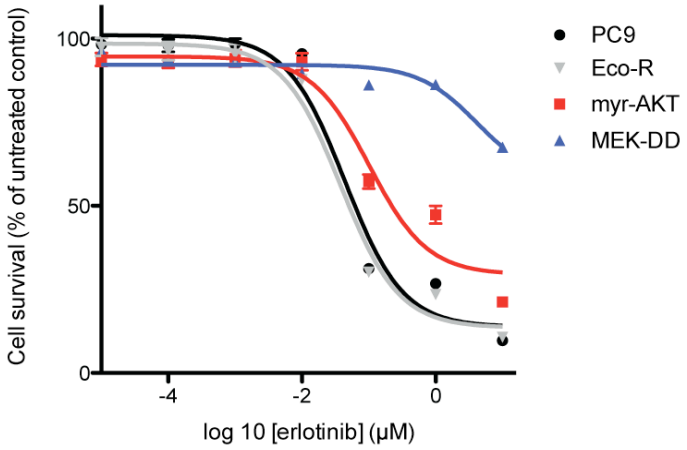

Figure 4.15. PC9 cells expressing activated forms of AKT or MEK have increased resistance to erlotinib treatment.

PC9 cells were left uninfected, infected with murine ecotropic receptor alone (Eco-R), or subsequently infected with myr-AKT or MEK-DD constructs. Cells were treated for 72 hours with indicated concentrations of erlotinib, and cell survival was measured using the CellTiter-Blue assay.

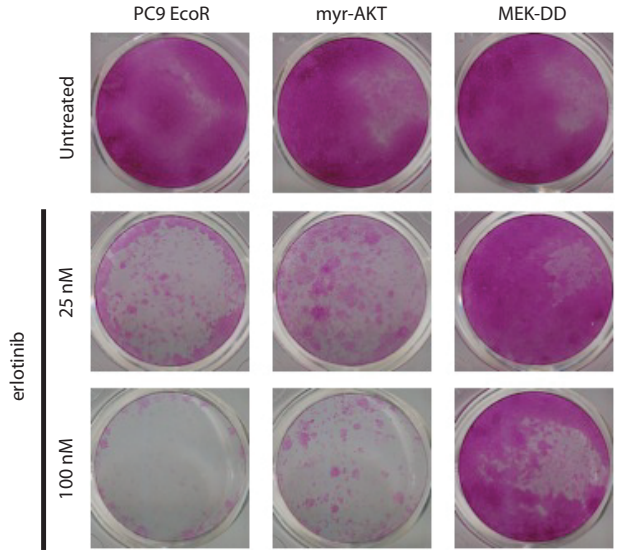

Figure 4.16. Active AKT and MEK increase resistance of PC9 cells to erlotinib treatment.

PC9 cells infected with the murine ecotropic receptor alone or expressing active forms of AKT (myr-AKT) and MEK (MEK-DD) were cultured in the presence of indicated concentrations of erlotinib for 10 days.

The increase in erlotinib resistance conferred by MEK-DD expression, could be prevented by combining erlotinib treatment with a MEK inhibitor AZD6244, indicating it is indeed the action of MEK which augments resistance to erlotinib in these cells (Fig 4.17).

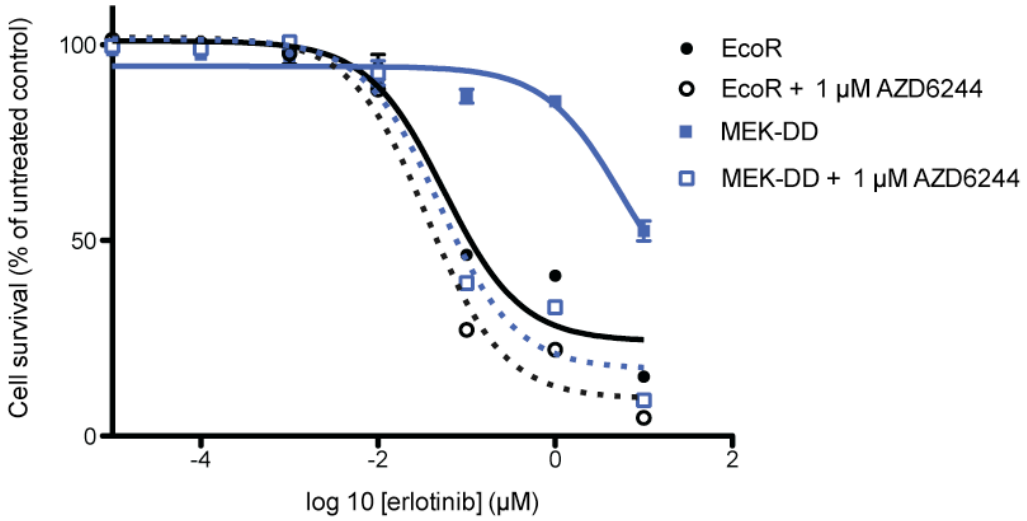

Figure 4.17. MEK-DD expressing cells are sensitive to a combination of erlotinib and a MEK inhibitor.

PC9 cells expressing the murine ecotropic receptor alone (EcoR) or expressing active MEK (MEK-DD) were treated with the indicated concentration of erlotinib, with (dotted line) or without (solid line) 1 μM AZD6244 for 72 hours.

4.4 Combination treatment of EGFR-TKIs and MEK inhibitors is effective against NF1-depleted cells

As shNF1 cells demonstrate higher levels of ERK phosphorylation than shSC cells in the presence of erlotinib, and expression of a constitutively active MEK variant dramatically increases resistance to erlotinib we postulated that inhibition of MEK may 'resensitise' shNF1 cells to erlotinib treatment. shSC expressing control cells are not sensitive to MEK inhibition alone and the combination treatment does not dramatically effect the IC_{50} (Fig 4.18). However as with the MEK-DD expressing cells, the combination of erlotinib treatment with MEK inhibitor AZD6244 restores the sensitivity of shNF1 cells to erlotinib treatment (Fig 4.18). In shNF1 cells EGFR inhibition or MEK inhibition alone is not sufficient to abolish phosphorylation of ERK1/2, however the combination of EGFR and MEK inhibition completely

eradicates phosphorylation of ERK1/2. Even when membranes are exposed for a long time no signal for phosphorylated ERK1/2 appears (Fig 4.19). This again supports the idea that NF1 loss increases resistance to erlotinib by maintaining a higher level of ERK1/2 phosphorylation in erlotinib-treated conditions.

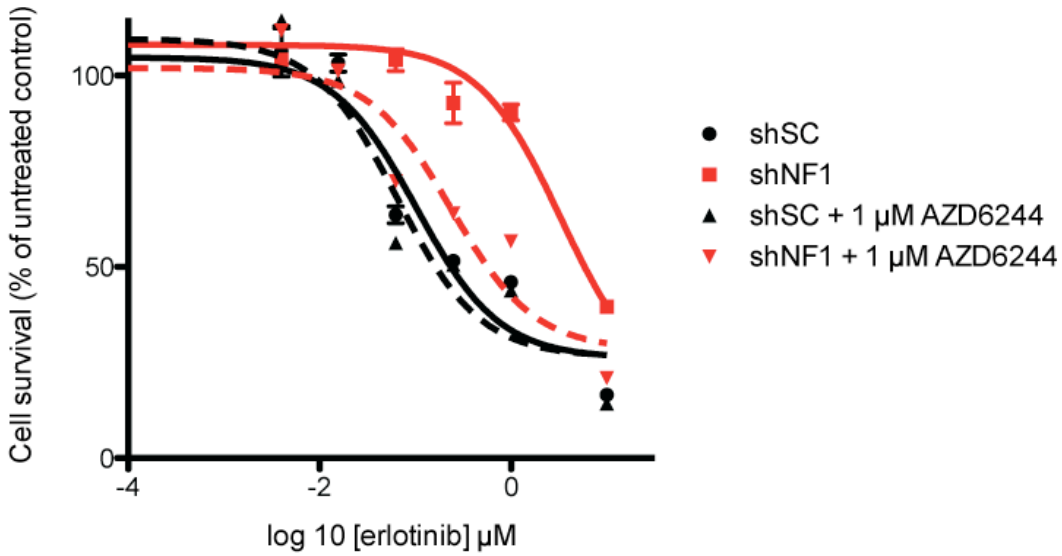

Figure 4.18. Combination treatment of erlotinib and a MEK inhibitor is effective against NF1-depleted cells.

PC9 cells stably infected with a non-targeting shRNA (shSC) or shRNA targeting NF1 (shNF1) were treated for 72 hours with the indicated concentrations of erlotinib, either alone or in combination with 1 µM AZD6244 (MEK inhibitor).

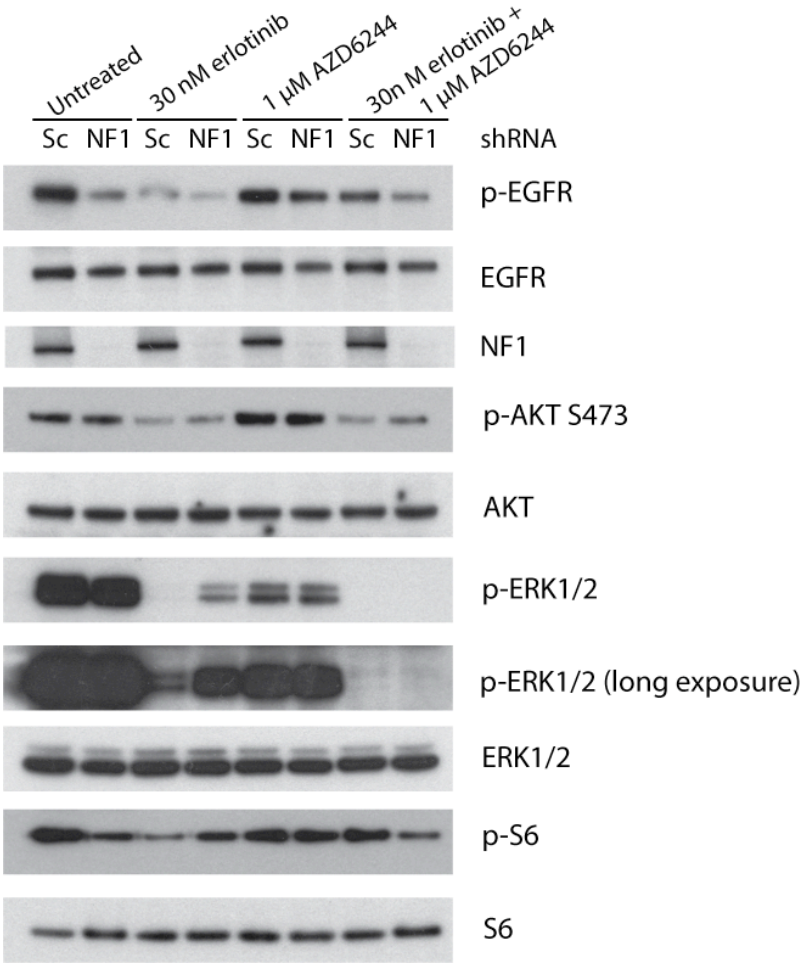

Figure 4.19. Combined erlotinib and MEK inhibitor treatment abolishes phosphorylation of ERK1/2 in shNF1 cells.

shSC and shNF1 expressing cells were treated with the indicated drugs for 1 hour prior to lysis for immunoblotting.

The same effect could not be produced by combination with an AKT inhibitor. Using a dose that inhibits AKT phosphorylation, without causing a substantial decrease in survival alone in the shSC cells, shNF1 cells could not be resensitised to erlotinib treatment (Fig 4.20).

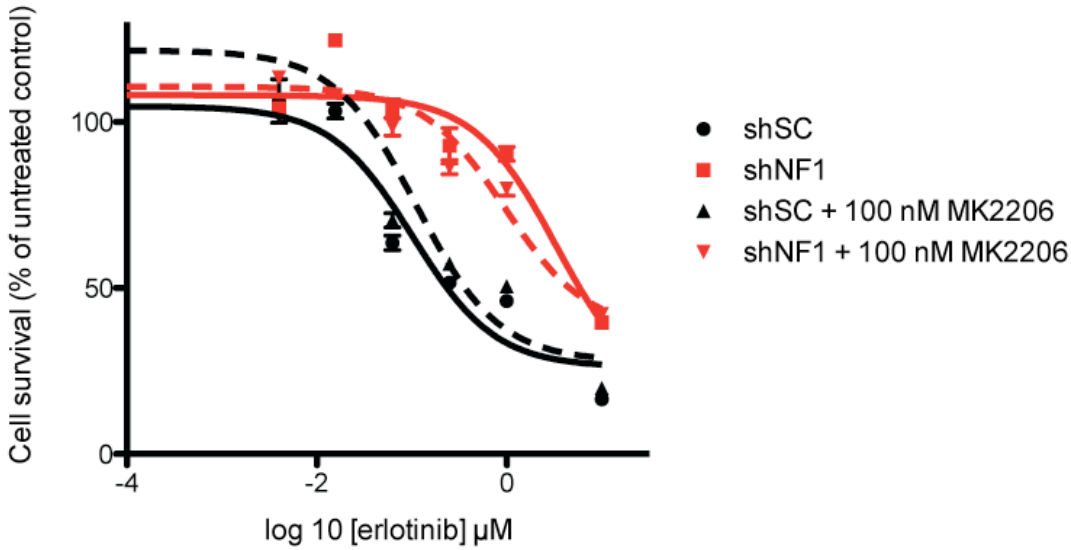

Figure 4.20. Combination treatment of erlotinib and an AKT inhibitor is not effective in NF1-depleted cells.

PC9 cells stably infected with a non-targeting shRNA (shSC) or shRNA targeting NF1 (shNF1) were treated for 72 hours with the indicated concentrations of erlotinib, either alone or in combination with 100 nM MK2206 (AKT inhibitor).

Interestingly PC9-ER cells (erlotinib resistant clones), generated by long term culturing in the presence of erlotinib are not sensitive to a combination of erlotinib and MEK inhibitor (Fig. 4.21).

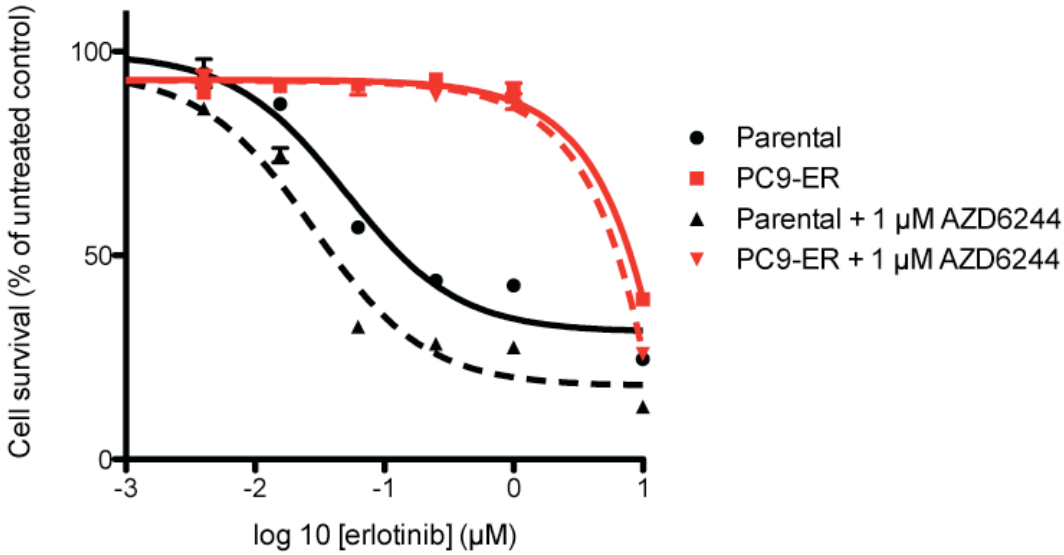

Figure 4.21. PC9-ER cells are not sensitive to a combination of erlotinib and a MEK inhibitor.

PC9 parental cells (Parental) or PC9 erlotinib resistant cells (PC9-ER) were treated with the indicated concentrations of erlotinib, either alone or in combination with a MEK inhibitor (AZD6244) for 72 hours. Cell survival was quantified using the CellTiter-Blue assay.

PC9-ER cells are extremely resistant to erlotinib. Previously, DNA sequencing revealed these cells contain the EGFR-T790M mutation, which is not detectable in the parental PC9 population. Analysis of signalling by immunoblotting reveals that PC9-ER cells retain a low level of phosphorylated ERK1/2 in the presence of the erlotinib and MEK inhibitor combination (Fig 4.22).

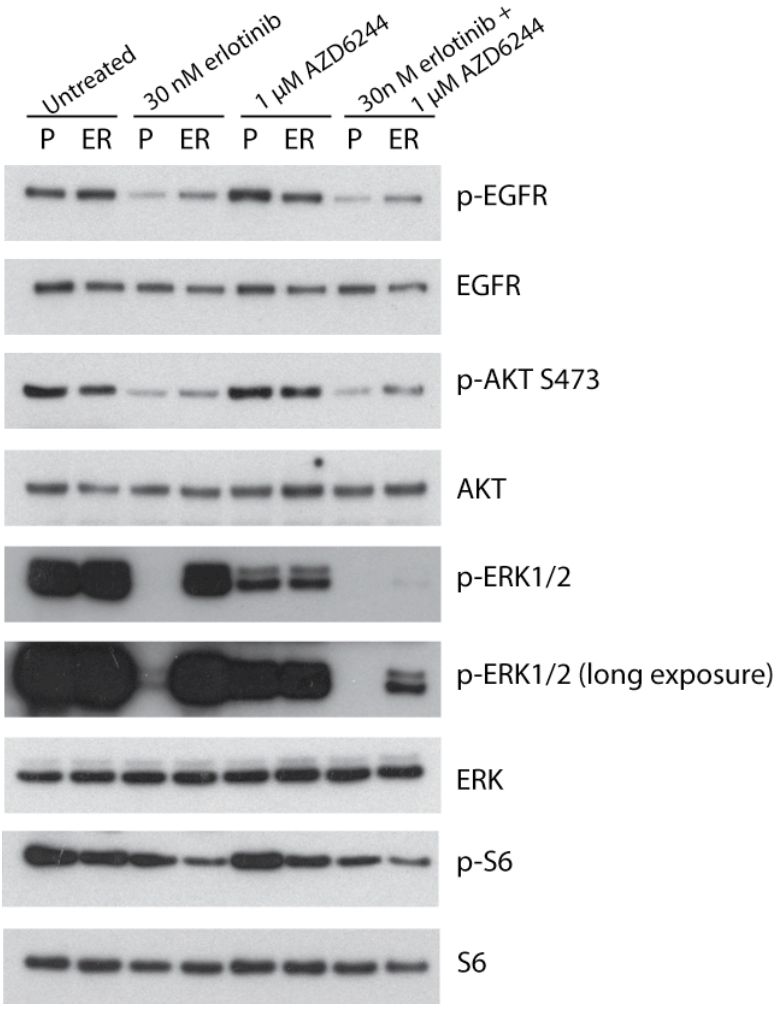

Figure 4.22. PC9-ER cells retain phosphorylated ERK1/2 in the presence of combined erlotinib and MEK inhibitor treatment.

PC9 parental and erlotinib resistant (PC9-ER) cells were treated with the indicated drug combinations for 1 hour prior to lysis for immunoblotting.

Additionally PC9-ER cells, like the shNF1 cells are not sensitive to the combination of erlotinib and an AKT inhibitor (Fig.4.23).

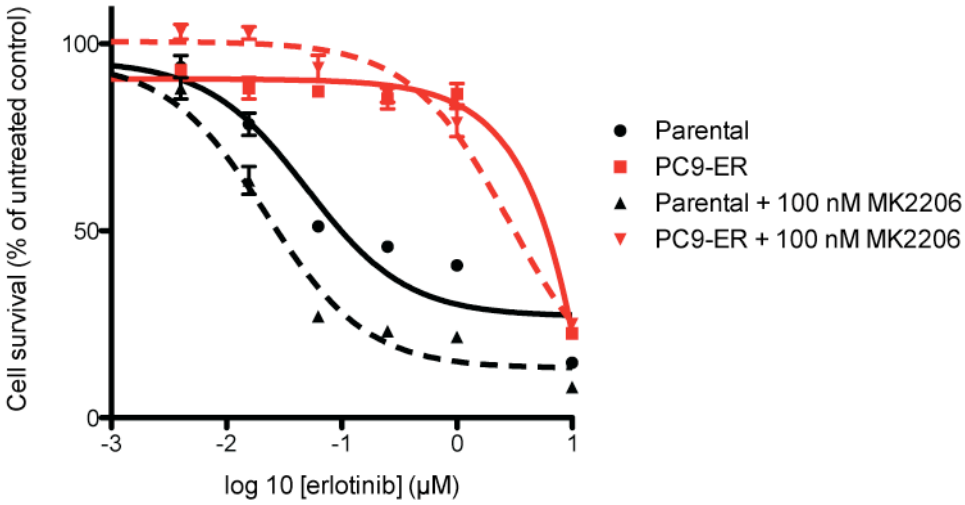

Figure 4.23. PC9-ER cells are not sensitive to a combination of erlotinib and an AKT inhibitor.

PC9 parental cells (Parental) or PC9 erlotinib resistant cells (PC9-ER) were treated with the indicated concentrations of erlotinib, either alone or in combination with an AKT inhibitor (MK2206) for 72 hours. Cell survival was quantified using the CellTiter-Blue assay

4.5 Discussion

In our genome-wide screen we identified *NF1* as a gene that increases resistance to erlotinib treatment upon RNAi- mediated silencing. We decided to follow up *NF1* as a hit, as it is a logical candidate due to its role as a negative regulator of RAS. Additional reasons for working further on *NF1* were that it is mutated in approximately 7% of lung adenocarcinomas, including a patient sample containing an *EGFR* activating mutation (Ding et al., 2008), and it was also identified as downregulated in erlotinib resistant tumours in a *EGFR*-mutant murine model of NSCLC (Figure 4.1). These data suggest NF1 loss of function may occur in vivo in NSCLC.

Since this project began NF1 loss has been identified in resistance to multiple targeted therapeutics, indicating it could be a common-node by which different cancer types re-activate signalling in response to targeted inhibition. Examples of this include increased resistance to retinoic acid in neuroblastoma (Holzel et al.,

2010), and resistance to tamoxifen in estrogen positive breast cancer (Mendes-Pereira et al., 2011). Aside from loss of NF1, other mutations that activate the MAPK pathway have been described to have comparable effects on resistance to EGFR inhibitory drugs. RAS activation by mutation had been described in primary resistance and more recently acquired resistance to EGFR inhibitors. *KRAS* mutation and amplification has been uncovered in colorectal cancer as a mechanism of acquired resistance to anti-EGFR antibodies cetuximab or panitumumab (Diaz et al., 2012; Misale et al., 2012). In lung cancer, an activating *NRAS* Q61K mutation was discovered in an erlotinib-resistant subline of erlotinib-sensitive 11-18 cells, which were generated by culturing cells in the presence of erlotinib for three to six months (Ohashi et al., 2012). In the same study, 1% of tumours sequenced from NSCLC with acquired resistance to erlotinib harboured a *BRAF* mutation. Together, these data suggest that mutations functioning to activate the MAPK pathway are common in acquired resistance to EGFR inhibitory drugs, and support our finding that NF1 loss contributes to resistance to erlotinib.

In keeping with the previous observations, we found activation of the MAPK pathway as the key determinant of resistance in NF1-depleted cells. The most striking difference we observed between shNF1 cells and shSC cells was a higher level of sustained ERK1/2 phosphorylation in shNF1 cells in the presence of erlotinib.(Figure 4.8). Phosphorylation of AKT did not dramatically differ between shSC and shNF1 cells, however erlotinib treatment does not inhibit AKT to the same extent as ERK, therefore any differences seen may be more difficult to detect (Figure 4.8). In colorectal cancer PI3K-AKT signalling seems to be activated predominantly by signalling from IGFR1 rather than EGFR (Corcoran et al., 2012b). Activation of PI3K-AKT downstream of other receptor tyrosine kinases could explain the rather minor inhibition of AKT by erlotinib in the NSCLC cells we used. The lack of increased phosphorylation of AKT in response to NF1 silencing also corresponds to data from *KRAS*-mutant colorectal cancer cell lines. Silencing of KRAS strongly reduces phosphorylation of ERK1/2 in these cells, but has little effect on activation of AKT, indicating RAS predominantly signals through the MAPK pathway in some contexts (Ebi et al., 2011).

Overexpression of constitutively active MEK and AKT confirmed the dominance of MAPK signalling in resistance to erlotinib treatment, as active MEK dramatically increased erlotinib resistance, whilst active AKT resulted in a much more modest increase in resistance (Figures 4.15 and 4.16). Due to the sustained ERK1/2 phosphorylation seen in shNF1 cells upon erlotinib treatment, as well as the effect of active MEK on resistance, we postulated combined erlotinib and MEK inhibitor treatment could be effective in resistant NF1-depleted cells. Indeed, the addition of a MEK inhibitor 'resensitised' shNF1 cells to erlotinib treatment, restoring their sensitivity to a similar level as shSC cells (Figure 4.18). An AKT inhibitor could not resensitise shNF1 cells to erlotinib, again indicating the increased resistance of shNF1 cells is not due to activation of AKT signalling (Figure 4.20). This is comparable to the situation observed in acquired resistance to EGFR inhibitors by *KRAS* mutation and amplification in colorectal cancer. Misale and colleagues found the combination of cetuximab and a MEK inhibitor effective against *KRAS* amplified or mutated resistant clones derived from sensitive parental cell lines. On the other hand cetuximab and a PI3K inhibitor was not effective (Misale et al., 2012).

Subsequently, by predominantly acting through MAPK signalling, loss of NF1 differs from the amplification of *MET* and the acquisition of a secondary mutation in *EGFR* in driving erlotinib resistance. Amplification of *MET*, observed in approximately 5% of patients is thought to predominantly drive activation of the PI3K-AKT pathway downstream of ERBB3, although additional activation of the MAPK pathway is observed (Engelman et al., 2007) The *EGFR*^{T790M} mutation, as it sustains activation of EGFR possibly activates additional pathways on top of the MAPK pathway, for example AKT or STAT signalling. Interestingly, we saw the combination of erlotinib and a MEK inhibitor was not effective in PC9 cells harbouring the *EGFR*^{T790M} mutation, suggesting additional signalling may contribute to resistance (Figure 4.21). Another explanation could be that T790M is simply a more potent inducer of MEK activity than NF1 loss, and we did not reach a combined dose of erlotinib and MEK inhibitor high enough to inhibit MEK signalling in these cells. There is clearly some residual ERK1/2 phosphorylation in PC9 erlotinib resistant cells after combined erlotinib and MEK inhibitor treatment (Figure 4.22) whereas it is completely abolished in shNF1 cells (Figure 4.19). However the

dose of MEK inhibitor used was already quite high (1 μM), therefore it is improbable that a combined dose that would inhibit ERK signalling in T790M-mutant tumours could be used *in vivo* without high toxicity and off-target effects. These results have substantial ramifications for the development of combination therapeutic regimes in EGFR-TKI resistant non-small cell lung cancer. Our data suggests an erlotinib and MEK inhibitor combination would be effective in some patients with erlotinib resistance, for example with NF1 loss of function or the activating mutations in the MAPK pathway described by others, but not in patients which have acquired the *EGFR*^{T790M} mutation.

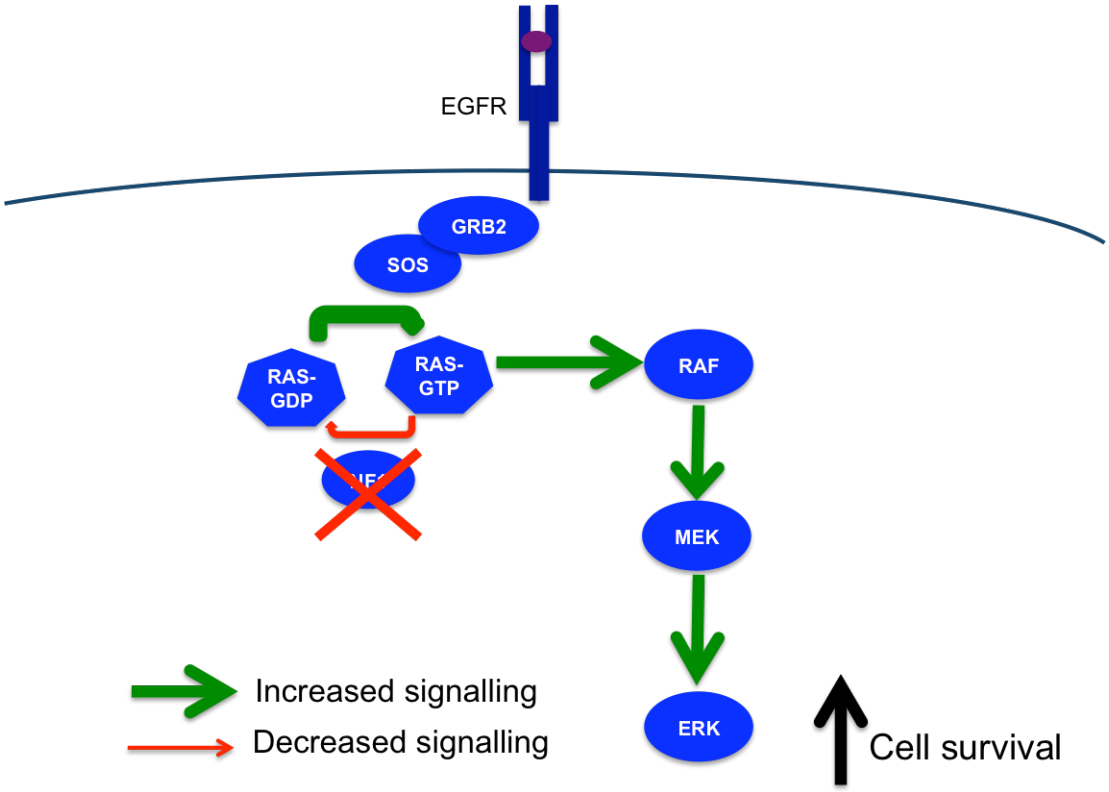

Figure 4.24. NF1 loss activates RAS-MAPK signalling.

NF1 loss increases levels of RAS-GTP in resistant cells, leading to higher activation of the MAPK pathway in the presence of erlotinib, and increased cell survival.

Additionally, it is possible NF1 loss contributes to erlotinib resistance via RAS-independent mechanisms. Shapira and colleagues noted that NF1-deficient mouse embryonic fibroblasts and malignant peripheral nerve sheath tumour cells were more resistant to apoptosis induced by treatment with staurosporine and UV

irradiation. This could not be reversed by inhibition of RAS, indicating a RAS-independent mechanism was involved (Shapira et al., 2007). However, our data strongly suggests NF1 loss contributes to erlotinib resistance via a RAS dependent mechanism as increased resistance to erlotinib upon endogenous NF1 silencing could be prevented by overexpression of the NF1-GRD (Figure 4.12). Other potential NF1-dependent RAS-independent mechanisms of increased resistance could be via Epithelial-Mesechymal Transition (EMT). As stated in the introduction EMT is a clinically validated mechanism of acquired resistance to EGFR-TKIs in NSCLC. NF1 loss contributes to EMT in neurofibromatosis type 1 (Arima et al., 2010), and in epicardial cells in development (Baek and Tallquist, 2012). However, when the expression of E-cadherin (epithelial marker) and vimentin (mesenchymal marker) was examined, there was no difference between shSC- and shNF1-expressing PC9 cells indicating EMT had not occurred in response to NF1 silencing.

Currently, we have validated our data in vitro, and it is supported by findings in a murine model of erlotinib resistant *EGFR*-mutant NSCLC (Katerina Politi, unpublished data). *NF1* mutations are common in a wide range of neoplasms and have been found in approximately 7% of NSCLC suggesting mutations in *NF1* could potentially yield non-functional protein products leading to acquired resistance to EGFR-TKIs *in vivo* (Ding et al., 2008). Unfortunately we have not been able to validate our findings in patients, due to a lack of access to clinical samples. In order to confirm the presence acquired *NF1* mutations, pre-treatment and post-treatment samples are required, and such patient data sets are difficult to obtain. Nf1 mRNA levels were decreased in erlotinib resistant tumours in the $EGFR^{L858R}$ murine model of NSCLC (Figure 4.1), however the mechanism by which this occurs is currently unknown. NF1 expression is regulated at multiple levels, therefore there are several potential routes by which NF1 function could be lost in resistant tumours. Aside from mutation possible mechanisms of downregulation include promoter methylation, proteasomal degradation, regulation by microRNA, alternative splicing and RNA editing (Andersen et al., 1993; Chai et al., 2010; Mancini et al., 1999; McGillicuddy et al., 2009; Skuse et al., 1996).

The NF1 promoter contains CpG dinucleotide rich regions, which are subject to methylation. In the promoter region is a methylation free CpG island, which if

methylated would affect binding of SP1 and CREB transcription factors, and could lead to NF1 silencing (Mancini et al., 1999). In order to see whether this is the case we asked our collaborator Dr. Marc Laydanyi to look at the methylation patterns of the NF1 promoter in EGFR mutant lung cancer patients who had developed resistance to EGFR TKIs. In the 4 matched pre-treatment and resistant samples of which there was enough DNA, bisulfite sequencing was performed. No hypermethylation of the NF1 promoter was found, and although the number of patient samples is limited and it is not possible to rule out methylation, this is in agreement with current literature, which suggests methylation of NF1 is not a common mechanism of NF1 inactivation (Harder et al., 2004; Luijten et al., 2000).

NF1 is ubiquitinated and degraded by the proteasome in response to growth factor stimulation in a number of cell lines, including schwann cells and fibroblasts. In these cell types Neurofibromin is rapidly degraded in response to stimulation, but then quickly restored to normal levels to attenuate RAS signalling (Cichowski et al., 2003). In a subset of glioblastoma cell lines proteasomal degradation of NF1 is aberrantly activated by hyperactivation of PKC alpha and this is essential for transformation and tumourigenesis (McGillicuddy et al., 2009). One potential way of NF1 degradation may be enhanced, would be the overexpression, or increased activation of components in the ubiquitination and proteasomal degradation pathway. Recently the E3 ubiquitin ligase RING component responsible for the transfer of ubiquitin from E2 to NF1, which targets NF1 for degradation has been identified as RNF7 (ring finger protein 7), also known as SAG/ROC2/RBX2 (Tan et al., 2011). Tan and colleagues discovered degradation of NF1 mediated by RNF7 was essential for vascular and neural development in mice. RNF7 resides on chromosome 3q which is frequently amplified in NSCLC (Balsara et al., 1997; Lu et al., 1999), and high RNF7/GAPDH expression is predictive of poorer patient survival in NSCLC (Sasaki et al., 2001). Therefore it is possible that overexpression of RNF7 as a result of gene amplification could increase NF1 degradation and subsequently increase resistance to erlotinib treatment.

NF1 protein expression can also be decreased by targeting by microRNAs (miRNAs). miRNAs are small RNA molecules which regulate gene expression at a post-transcriptional level. In recent years it has been shown that expression of

miRNAs is frequently altered in cancer, resulting in changes in protein expression. In the genetic disorder Neurofibromatosis type I microRNA 10b has been implicated in reducing the expression of NF1. Chai and colleagues found that NF1 malignant peripheral nerve sheath tumours (MPNST) had 20-30 fold higher levels of microRNA 10b than non-NF1 MPNSTs (Chai et al., 2010). In SK-ES1 cells, of neuroectodermal origin, high microRNA 10b expression correlated with low expression of NF1, and inhibition of microRNA 10b increased NF1 protein levels (Chai et al., 2010). However, transfection of an miR10b mimic into PC9 cells did not have a significant impact on NF1 expression or erlotinib resistance. There are multiple miRNA binding sites in the NF1 3'UTR, such as sites for miR103a/107, therefore it is possible that other miRNAs are involved in the regulation of NF1 expression (TargetScan: www.targetscan.org/vert_61/).

Also, NF1 activity can be affected by splicing. In humans there are two main isoforms of NF1, which differ in their RAS GTPase activity. Isoform I of NF1 contains an additional in-frame coding exon, exon 23a, which correlates to a 21 aa segment within the NF1 GRD. Isoform II does not contain this coding exon, and concordantly exhibits approximately 10-fold higher RAS GTPase activity (Andersen et al., 1993). It is possible that alterations in splicing regulation could cause changes in respective levels of the NF1 isoforms, resulting in more isoform I than isoform II. This would lead to an overall decrease in NF1 activity, and could be a potential mechanism for NF1 downregulation in erlotinib resistant tumours. In PC9 cells the vast majority of NF1 present was the less active isoform I, therefore a further increase in the proportion of isoform I is unlikely to have a significant impact on erlotinib resistance, however such a mechanism may occur *in vivo*.

A third isoform of NF1 lacking GTPase activity is generated by C-U editing of the NF1 RNA transcript. The NF1 transcript undergoes editing at nucleotide position 2914, which converts a cytidine to a uridine and generates a premature stop codon. This results in a truncated version of neurofibromin finishing in the amino terminus of the GAP related domain, therefore lacking GTPase activity (Skuse et al., 1996). Examples of such editing have been found in tumours from Neurofibromatosis type 1 patients (Cappione et al., 1997; Mukhopadhyay et al., 2002). C-U editing is carried out by the APOBEC family of cytidine deaminases. Recent publications

suggest the ABOPEC family may be involved in formation of mutational clusters in breast tumours (Nik-Zainal et al., 2012), therefore it is possible these ABOPECs have an active role in human cancer and could contribute additionally to tumourigenesis by editing of NF1 mRNA.

Currently, conclusive evidence for NF1 downregulation in erlotinib resistant NSCLC is lacking, and the mechanism of NF1 loss of function is unknown. Clearly, as previously stated here, this is a complicated problem to unravel, as there are multiple levels of regulation. Ultimately, we would like to analyse patient samples for differences in NF1 protein expression and for the presence of *NF1* mutations to confirm how this occurs in the real-life setting.

Chapter 5. DEPTOR loss increases resistance of non-small cell lung cancer (NSCLC) to EGFR tyrosine kinase inhibitors (TKIs) by feedback upregulation of EGFR.

5.1 DEPTOR structure and function

DEPTOR is a 48 KDa protein comprised of 2 N-terminal DEP domains and a C-terminal PDZ domain. It has been identified as a negative regulator of mTOR signalling. However, little is known about the exact mechanism by which DEPTOR inhibits mTOR function. It is known that endogenous DEPTOR interacts directly with mTOR via the PDZ domain of DEPTOR and the FAT domain of mTOR (Peterson et al., 2009). Loss of DEPTOR in HeLa cells leads to increased phosphorylation of downstream targets of mTOR signalling, predominantly S6K, AKT and SGK1 (Peterson et al., 2009). This mTOR signalling activation occurs via increased kinase activity of mTOR, as both mTORC1 and mTORC2 immunoprecipitated from DEPTOR-depleted cells displayed higher *in vitro* kinase activity (Peterson et al., 2009).

5.2 DEPTOR expression and mTOR signalling in cancer

DEPTOR expression is greatly varied in different cancer types. In some cancer types it is downregulated compared to normal tissue, while in other cancer types it is over-expressed (Peterson et al., 2009). Studies in different cell types suggest DEPTOR can act as an oncogene or a tumour suppressor by differentially affecting mTORC1 and mTORC2 through the action of various feedback loops. In multiple myeloma cells, DEPTOR overexpression is driven by overexpression of cMAF and MAFB transcription factors as a result of chromosomal translocations. In a subset of multiple myelomas, DEPTOR overexpression is essential for survival, as it asymmetrically inhibits mTOR signalling in this cell type (Peterson et al., 2009). Specifically, DEPTOR overexpression relieves the negative feedback of mTORC1 to IRS1. In this feedback loop inhibition of mTORC1 leads to inactivation of S6K and subsequently relieves repression of IRS1. This activation of IRS1 activates PI3K/AKT signalling (O'Reilly 2006). This is striking, since *in vitro* results suggest

DEPTOR should also inhibit mTORC2, but AKT remains phosphorylated at Ser473 with DEPTOR over-expression, indicating mTORC2 is still active (Peterson et al., 2009). Suppression of DEPTOR in multiple myeloma cell lines in which it is over-expressed induces apoptosis. By contrast, depletion of DEPTOR protects HeLa cells from serum deprivation induced apoptosis which indicates DEPTOR loss can have opposing effects on cell survival depending on the cell context (Peterson et al., 2009).

DEPTOR protein stability is tightly regulated by mTOR signalling. A set of papers recently described the mechanism by which DEPTOR is degraded by the proteasome in response to mTOR activation upon serum stimulation (Duan et al., 2011; Gao et al., 2011; Zhao et al., 2011). Gao and Duan both found that phosphorylation of DEPTOR by Casein Kinase I and mTOR creates a phosphodegron (phosphorylated amino acid sequence to which F box components of E3 ubiquitin ligases bind), targeting DEPTOR to the E3 ubiquitin ligase $SCF^{\beta TrCP}$ for ubiquitination and proteasomal degradation. Zhao and colleagues also found that DEPTOR was degraded via a $SCF^{\beta TrCP}$-dependent mechanism in response to growth factor stimulation. However they suggest that RSK1 and S6K1 are the kinases responsible for DEPTOR phosphorylation rather than mTOR and Casein Kinase I. mTOR signalling is activated in a variety of tumour types and often correlated with poor prognosis. In NSCLC patients showing phosphorylation of components of the mTOR signalling pathway (phosphorylation of mTOR, AKT and S6K) demonstrated a worse prognosis than those who scored negative for mTOR pathway activation (Liu et al., 2011). Also, activation of mTOR signalling via PTEN loss has been reported in H1650 cells, an EGFR-mutant NSCLC cell line. This loss of PTEN is believed to cause resistance to EGFR TKIs (Sos et al., 2009). Consequently, it is possible that DEPTOR protein levels are decreased in a subset of NSCLC with activated mTOR signalling, and that this reduction contributes to erlotinib resistance.

5.3 Reduction in DEPTOR expression increases resistance of NSCLC cells to erlotinib treatment.

DEPTOR was one of the candidates in our siRNA screen for erlotinib resistance, since DEPTOR silencing reduced sensitivity of PC9 cells to erlotinib treatment. As a negative regulator of mTOR, a downstream component of the EGFR signalling pathway, we first examined if DEPTOR loss would lead to increased mTOR signalling and whether this altered mTOR signalling could increase resistance to EGFR TKIs. Direct siRNA knockdown experiments demonstrated the Dharmacon SMARTpool, which efficiently reduces levels of DEPTOR mRNA (Figure 5.1) and protein (Figure 5.2), causes a reduction in erlotinib sensitivity over 72 hours (Figure 5.3). In deconvolution experiments, in which the siRNAs that comprise the SMARTpool were used individually, oligos 2 and 4 gave the most efficient silencing of DEPTOR at an mRNA level (Figure 5.1) and caused the largest increase in erlotinib resistance compared to non-targeting siRNA controls (Figure 5.3). Interestingly, these two siRNAs were the ones that initially validated in the larger screen. This suggests the effects seen on resistance are a consequence of DEPTOR silencing and are not off-target effects, as two independent siRNA produce the same biological effect.

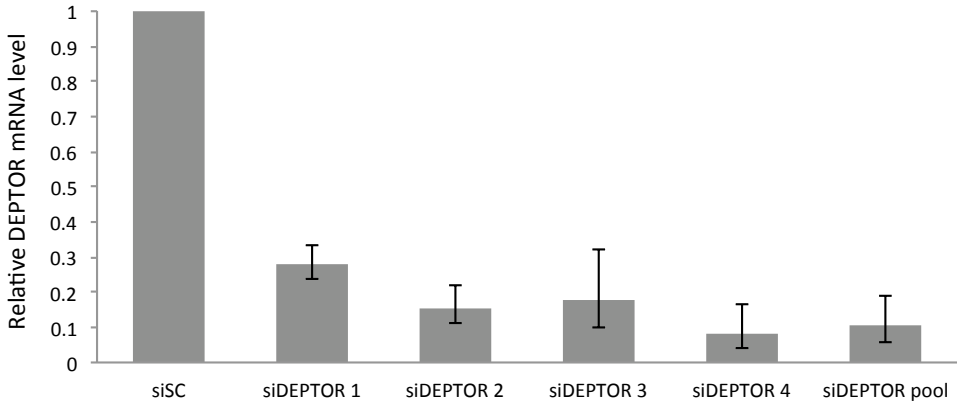

Figure 5.1. The deconvoluted SMARTpool targeting DEPTOR efficiently reduces DEPTOR mRNA levels.

DEPTOR mRNA levels were quantified by RT-QPCR 48 hours after transfection with either a non-targeting control (siSC), the individual siRNAs of the SMARTpool targeting DEPTOR, or the combined pool.

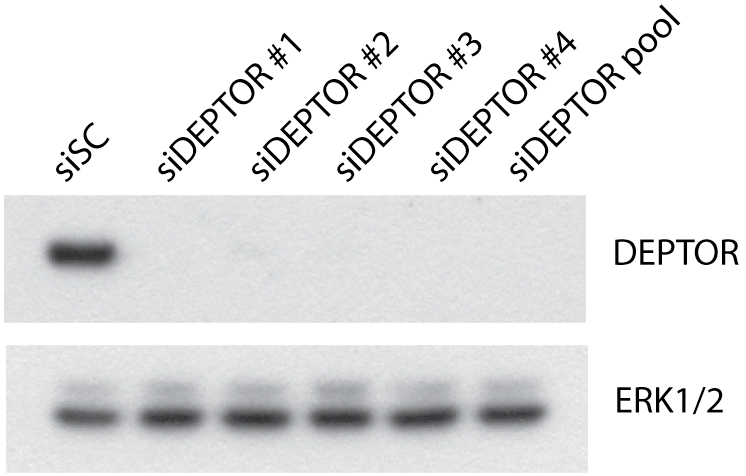

Figure 5.2. The deconvoluted SMARTpool targeting DEPTOR efficiently reduced DEPTOR protein levels.

PC9 cells were transfected with either a non-targeting control (siSC) or the individual or combined siRNAs of the SMARTpool targeting DEPTOR. Cells were lysed 48 hours after transfection and protein levels were quantified by immunoblotting. ERK1/2 is shown as a loading control.

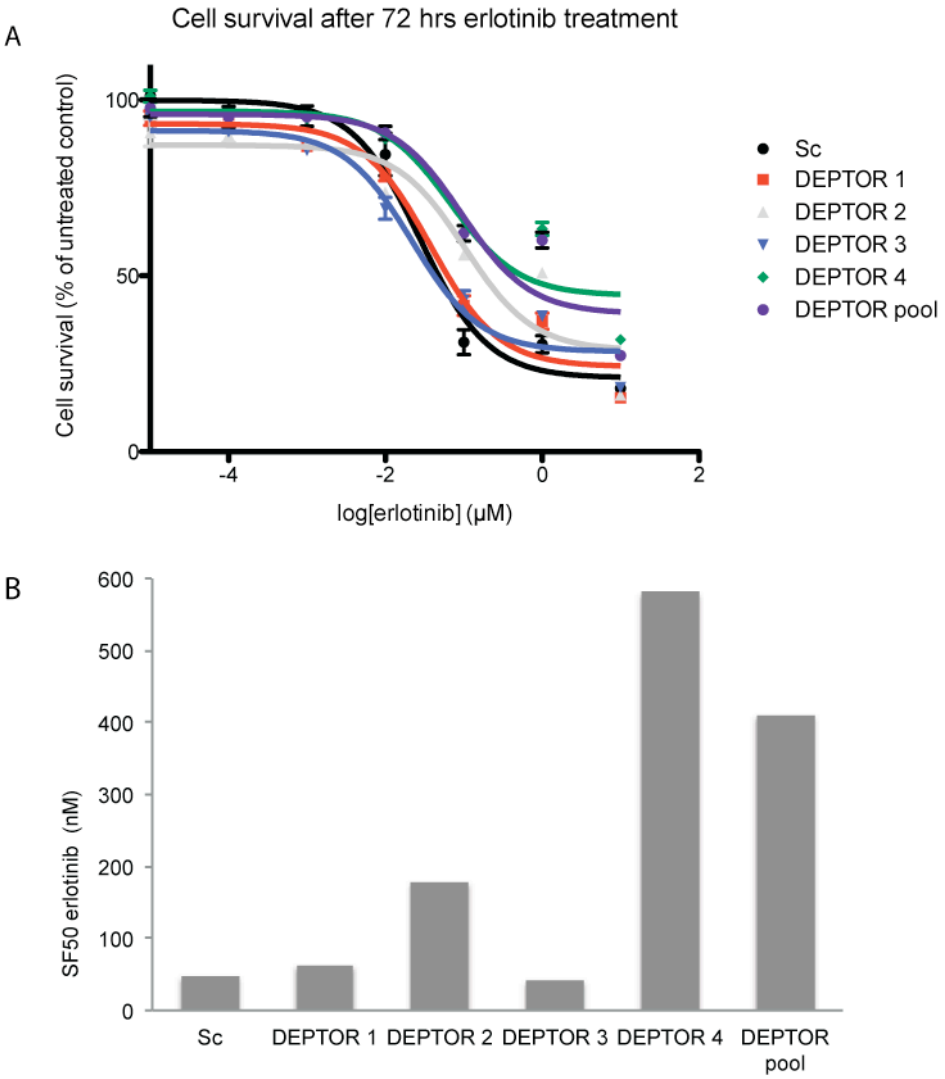

Figure 5.3. DEPTOR silencing increases resistance of PC9 cells to erlotinib treatment.

PC9 cells were transfected with the indicated siRNAs. 48 hours after transfection cells were treated with the indicated concentrations of erlotinib for 72 hours. Cell viability was measured using the Cell Titer Blue assay. A. Cell survival at each erlotinib dose plotted as a curve, results shown are triplicate samples from one representative experiment. B. Cell survival (the same data as in A) is shown as a Survival Fraction 50 (SF50), which is the concentration of erlotinib necessary to result in 50% cell survival compared to untreated controls.

To further validate these effects, and see if DEPTOR depletion could increase resistance to erlotinib in longer-term assays, we infected PC9 cells with two short hairpin RNA (shRNA) constructs targeting DEPTOR. Both constructs efficiently reduced DEPTOR mRNA and protein levels, compared to a control non-targeting shRNA (shSC) (Figure 5.4). To test whether DEPTOR-depletion could cause

increased resistance to erlotinib in the longer term we grew shSC and shDEPTOR cells in the presence of increasing doses of erlotinib for 10 days (Figure 5.5). Cells infected with either hairpin targeting DEPTOR were approximately twice as resistant as shSC cells to erlotinib treatment.

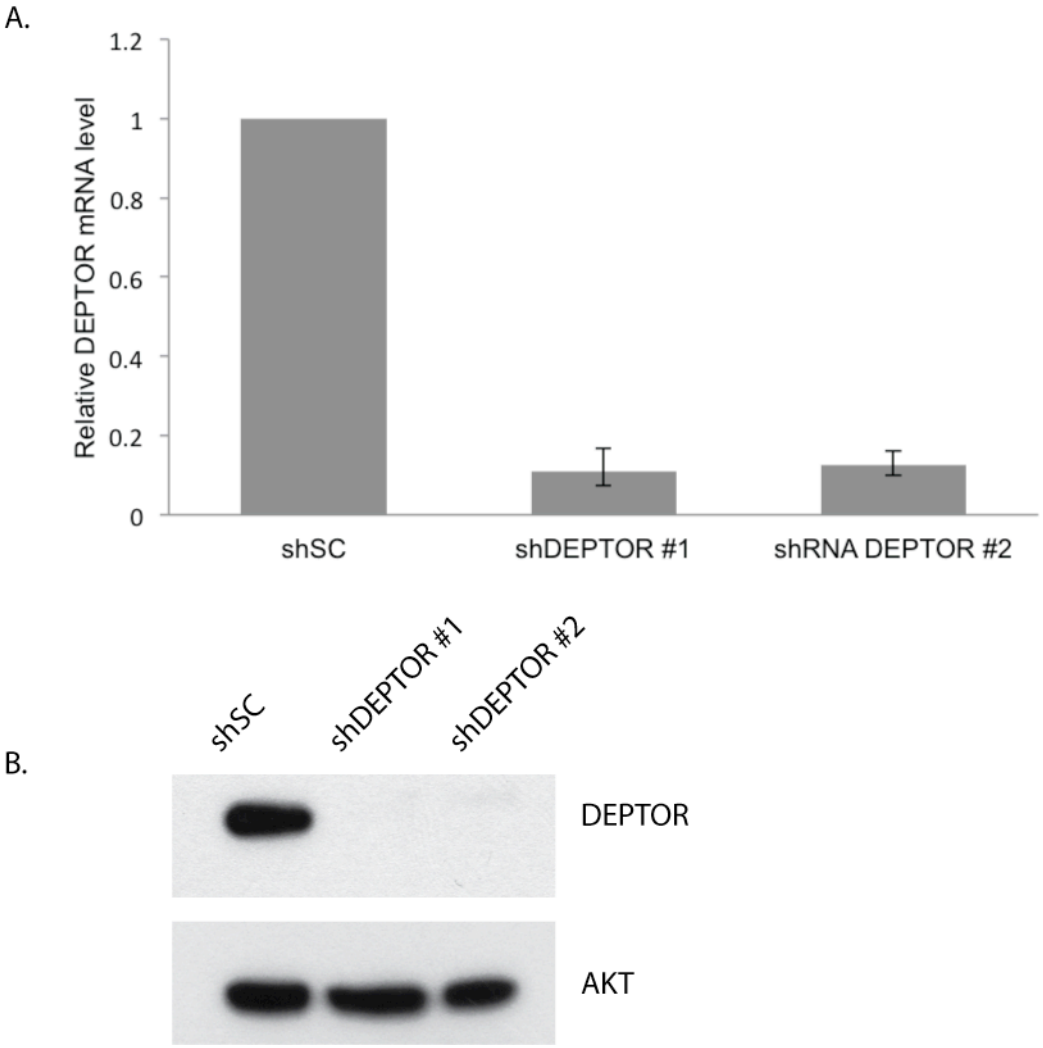

Figure 5.4. shRNAs targeting DEPTOR efficiently reduce DEPTOR expression at the mRNA and protein level.

PC9 cells were infected with either a control non-targeting shRNA (shSC), or shRNA constructs targeting DEPTOR (shDEPTOR #1 and shDEPTOR #2). A. mRNA levels were quantified by qRT-PCR. B. Protein levels were measured by immunoblotting, AKT is shown as a loading control.

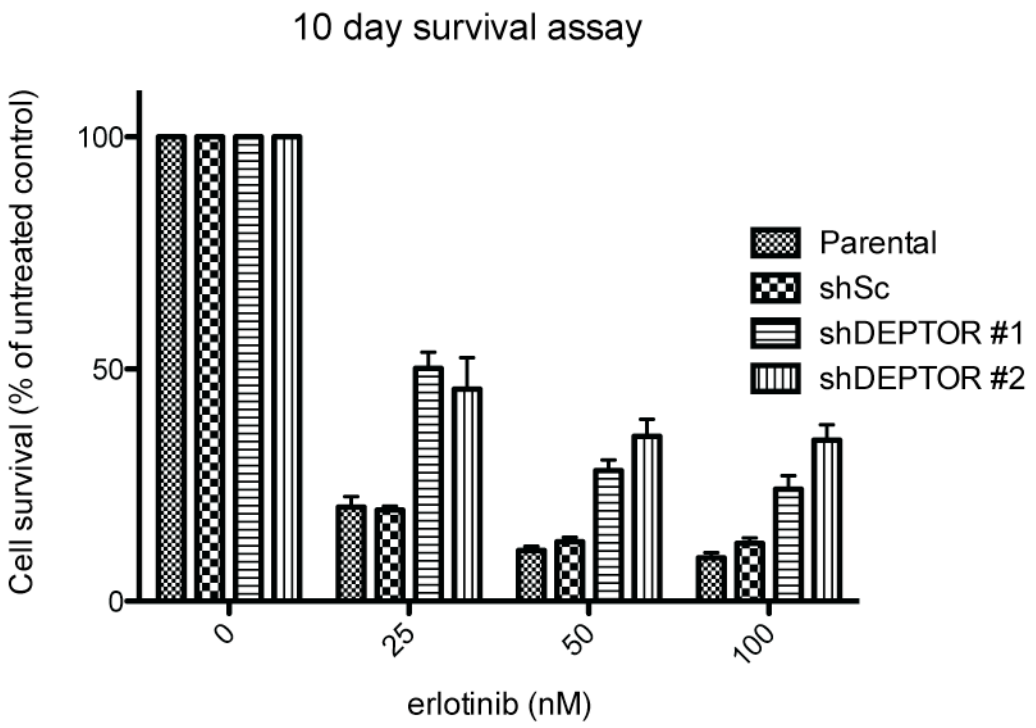

Figure 5.5. Silencing of DEPTOR increases resistance of PC9 cells to erlotinib treatment in long term cell survival assays.

PC9 cells were stably infected with either a non-targeting control shRNA construct or shRNA constructs targeting DEPTOR (shDEPTOR #1 and #2). Cells were grown in the presence of indicated concentrations of erlotinib for 10 days and then fixed and stained with Sulphorhodamine B.

To examine if this DEPTOR-mediated resistance was general to *EGFR*-mutant lung cancer cells, we also infected another *EGFR*-mutant NSCLC (HCC4006) with shSC and shDEPTOR constructs. shRNA targeting DEPTOR efficiently reduces DEPTOR mRNA and protein levels in HCC4006 cells (Figure 5.6). Longer-term cell survival assays showed similar results to those seen in PC9 cells. DEPTOR-depleted cells were again less sensitive to 25 nM erlotinib treatment, with an increase in overall cell survival from 26% to 43% (Figure 5.7). Although the differences in cell survival in long-term assays are relatively minimal, such modest reductions in drug response could over time result in a substantial increase in cell survival of shDEPTOR cells compared to control cells.

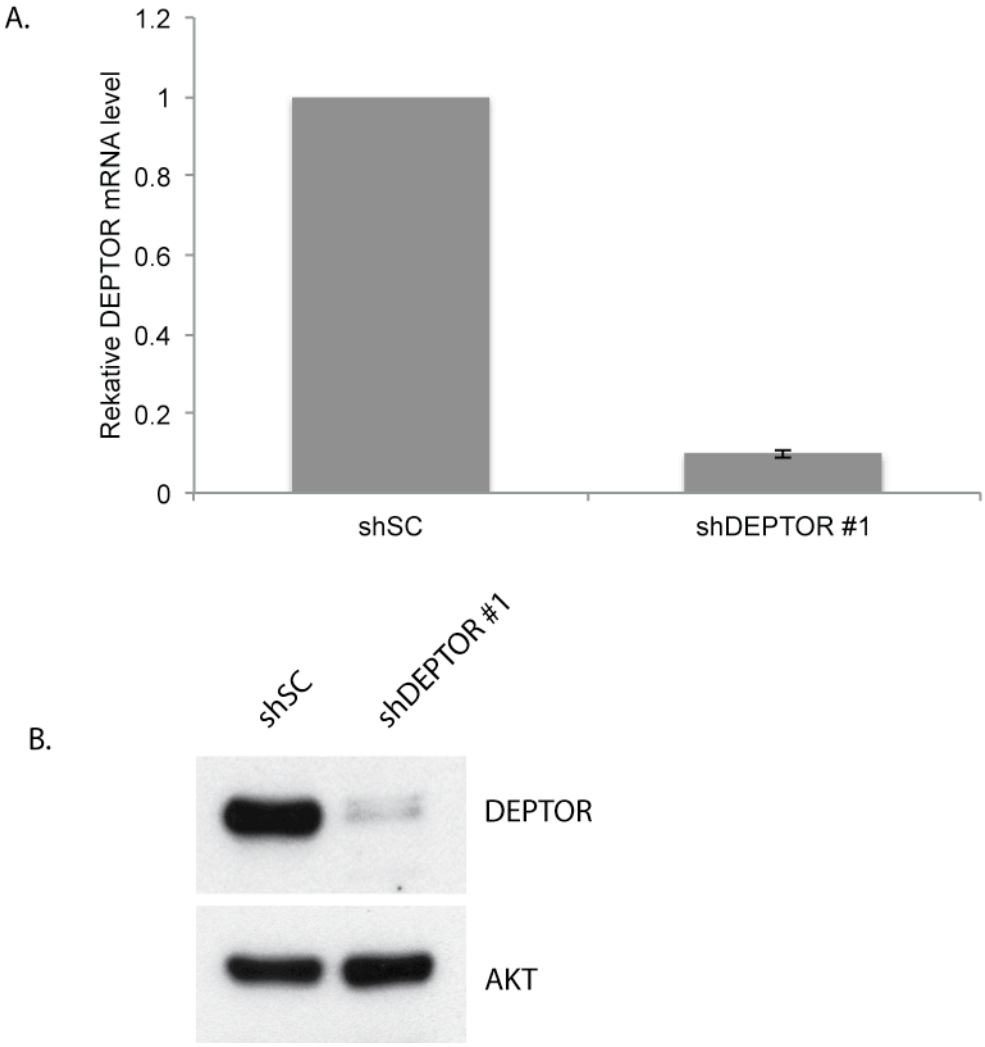

Figure 5.6. Efficiency of DEPTOR silencing in HCC4006 cells.

HCC4006 cells were infected with a non-targeting control shRNA construct (shSC) or shRNA construct targeting DEPTOR (shDEPTOR #1). A. mRNA levels were quantified by qRT-PCR. B. Protein levels were measured by immunoblotting, AKT is shown as a loading control.

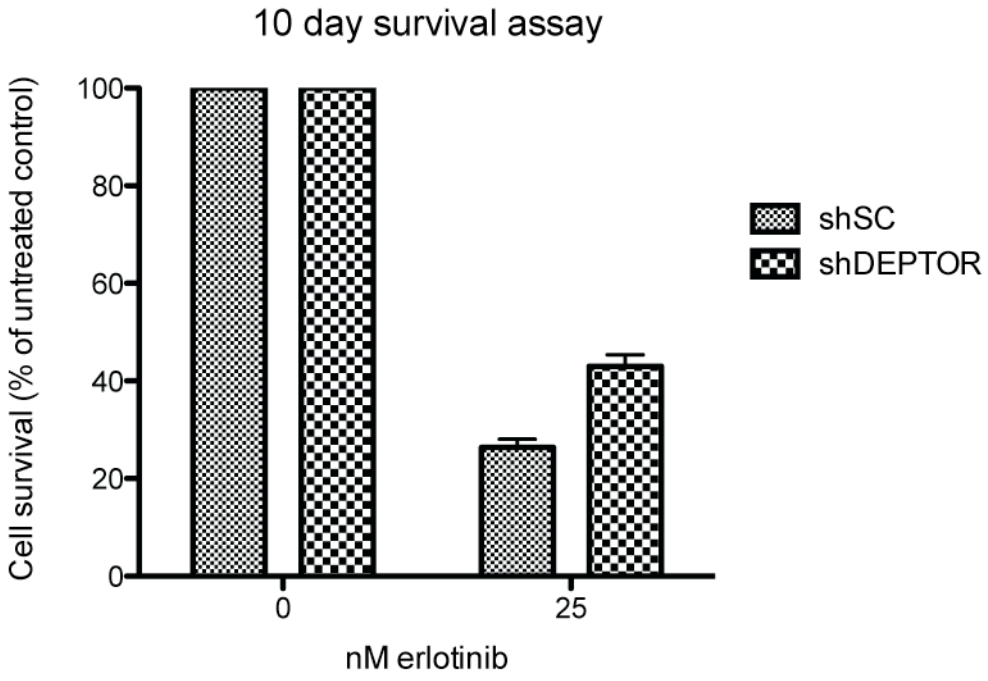

Figure 5.7. shRNA targeting DEPTOR increases resistance of HCC4006 cells to erlotinib treatment.

HCC4006 cells were infected with control shRNA (shSC) or shRNA targeting DEPTOR (shDEPTOR #1). Cells were grown in the presence of 25 nM erlotinib, or without drug for 10 days. Cells were fixed and stained with sulforhodamine B.

5.4 DEPTOR silencing does not increase resistance of PC9 cells to other chemotherapeutic drugs

To ascertain whether DEPTOR silencing causes a general increase in resistance to multiple classes of drugs, we tested whether DEPTOR silencing affected resistance to gefitinib (another EGFR-TKI) and two chemotherapeutic agents, cisplatin and docetaxel, which serve as standard of care in non-*EGFR*-mutant NSCLC. As seen in Figure 5.8, DEPTOR-depleted cells were substantially more resistant to gefitinib than control cells, similar to the effect seen with erlotinib. On the other hand, depletion of DEPTOR by siRNA had no effect on the resistance of PC9 cells to docetaxel or cisplatin (Figure 5.9). This suggests that DEPTOR loss specifically affects EGFR-TKI sensitivity without generally affecting the response to chemotherapeutics.

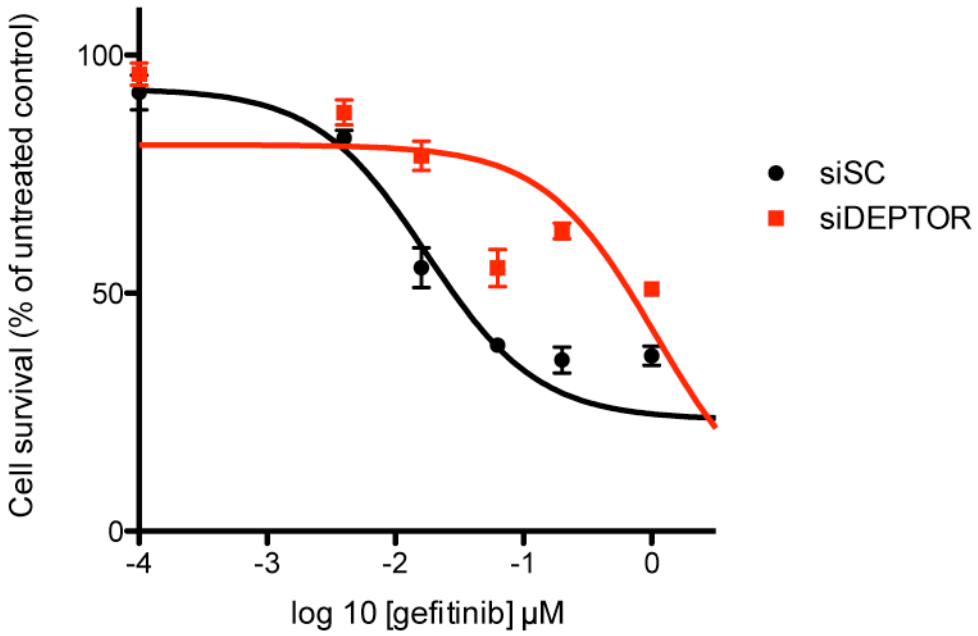

Figure 5.8. DEPTOR depletion increases resistance of PC9 cells to gefitinib.

PC9 cells were transfected with non-targeting siRNA (siSC) or siRNA targeting DEPTOR(siDEPTOR). 48 hours after transfection cells were treated with the indicated concentrations of gefitinib for 72 hours. Cell viability was measured using the CellTiter-Blue assay.

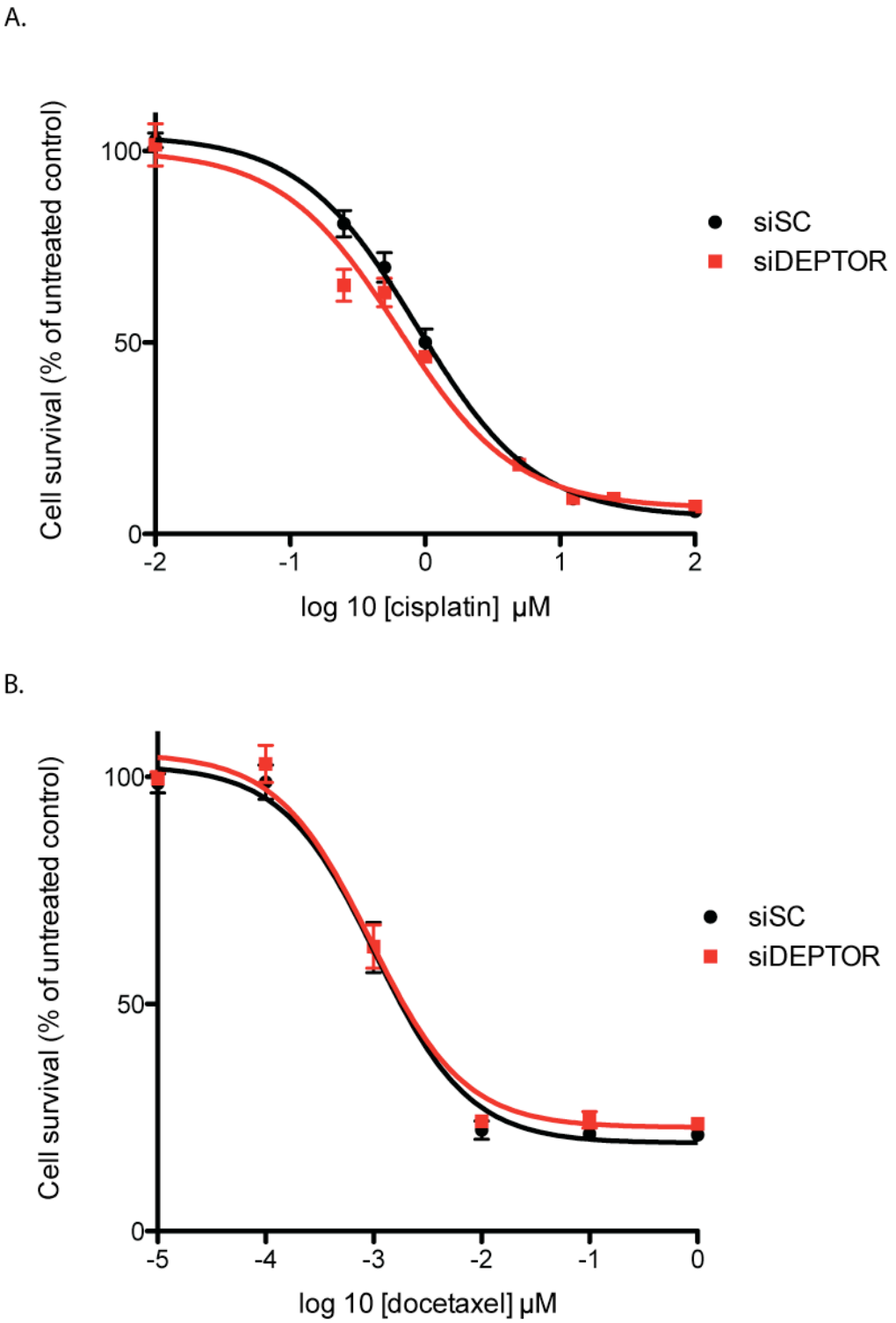

Figure 5.9. DEPTOR silencing does not effect responses to other chemotherapeutic drugs.

PC9 cells were transfected with siRNA targeting DEPTOR or a non-targeting control (SC). 48 hours after transfection, cells were treated with the indicated concentrations of A. cisplatin or B. docetaxel for 72 hours. Cell viability was measured using the CellTiter-Blue assay.

5.5 DEPTOR silencing increases EGFR protein levels and AKT, ERK1/2 and mTORC2 activation.

To elucidate the mechanism of decreased erlotinib sensitivity in DEPTOR-depleted cells, we assessed the total levels and phosphorylation states of several key components of the EGFR signalling pathway in siDEPTOR cells and siSC cells. We compared signalling in untreated and erlotinib-treated conditions. As expected, siDEPTOR cells had more active mTOR signalling, demonstrated by increased levels of AKT phosphorylation at Ser473 and increased phosphorylation (and protein levels) of SGK1 substrate NDRG1 (Figure 5.10). Unexpectedly, siDEPTOR cells showed a strong upregulation of EGFR protein levels, and maintain higher levels of phosphorylated EGFR than siSC cells after 1 hour of erlotinib treatment (Figure 5.10). This effect was also visible in PC9 cells stably expressing shRNA targeting DEPTOR (Figure 5.11A). As seen with DEPTOR siRNA, shDEPTOR cells had more phosphorylated ERK1/2 and NDRG1 than shSC control cells in the presence of erlotinib. Quantification of phosphorylated ERK1/2 indicated shDEPTOR cells have 3.7 times more phosphorylated ERK1/2 than shSC cells in untreated conditions and retain 60% more phosphorylated ERK1/2 than shSC cells upon erlotinib treatment (Figure 5.11B). These values are similar to those seen in siSC and siDEPTOR transfected cells (Figure 5.10B). Additionally similar effects on signalling (albeit at a lower magnitude) were observed in HCC4006 cells expressing shRNA targeting DEPTOR (Figure 5.12), indicating they were not cell line specific.

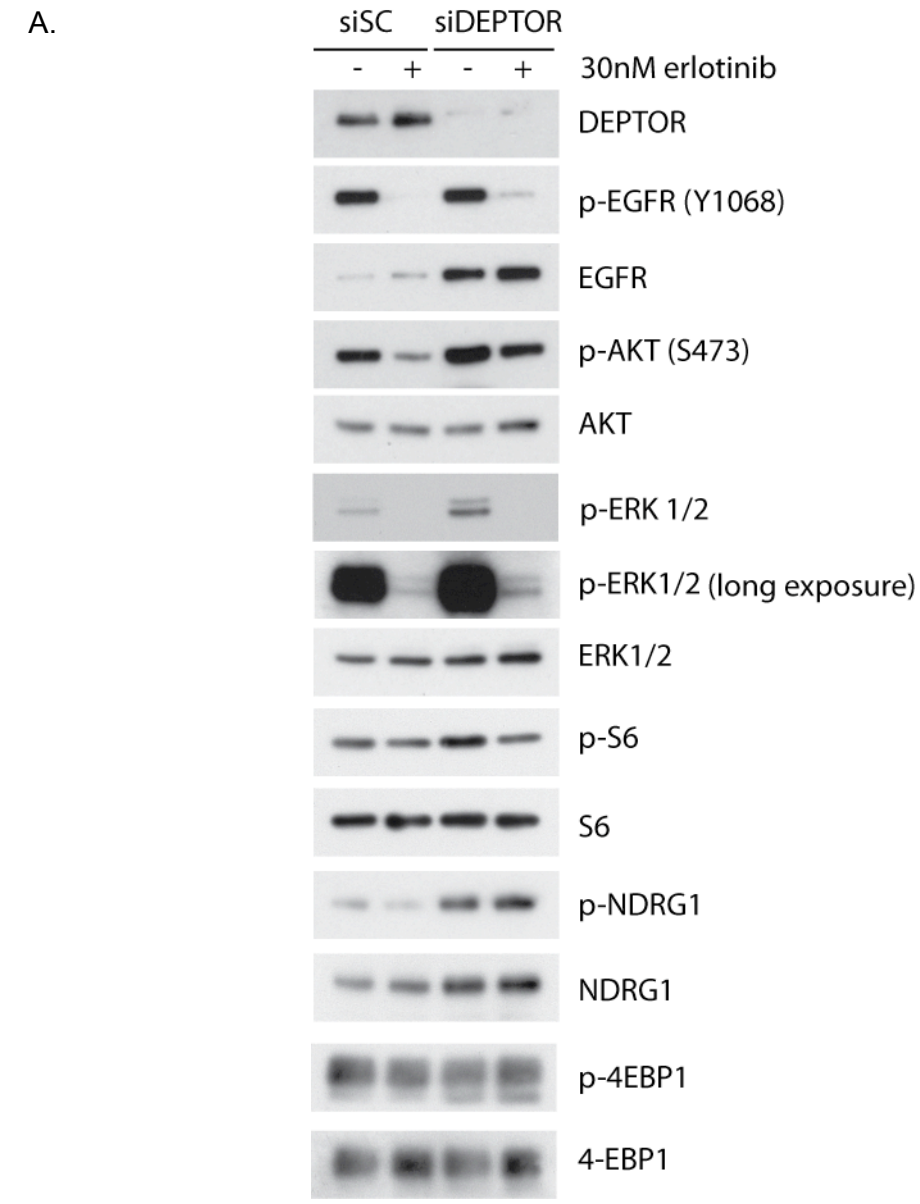
A.
siSC
siDEPTOR
- + - +
30nM erlotinib
DEPTOR
p-EGFR (Y1068)
EGFR
p-AKT (S473)
AKT
p-ERK 1/2
p-ERK1/2 (long exposure)
ERK1/2
p-S6
S6
p-NDRG1
NDRG1
p-4EBP1
4-EBP1

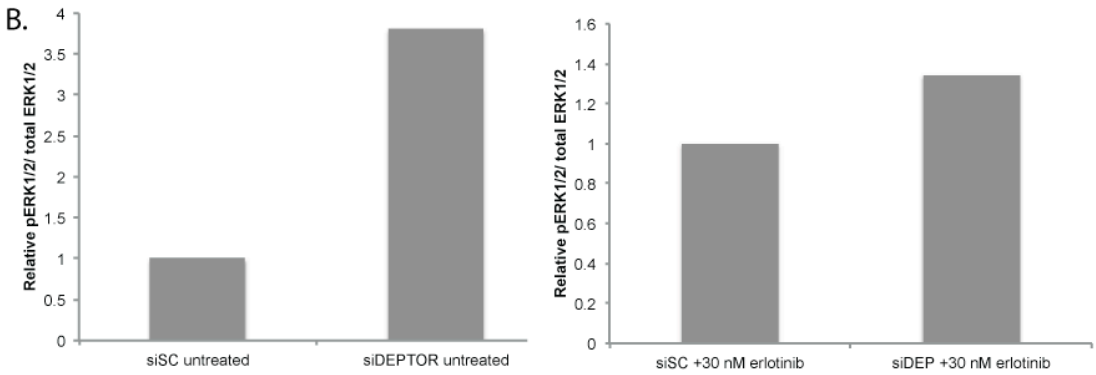
B.
Relative pERK1/2/ total ERK1/2
0
0.5
1
1.5
2
2.5
3
3.5
4
siSC untreated
siDEPTOR untreated
Relative pERK1/2/ total ERK1/2
0
0.2
0.4
0.6
0.8
1
1.2
1.4
1.6
siSC +30 nM erlotinib
siDEP +30 nM erlotinib

Figure 5.10. DEPTOR silencing activates AKT, ERK1/2 and mTORC2 signalling.

A. PC9 cells transfected with siSC (control siRNA), or siRNA targeting DEPTOR were treated with 30 nM erlotinib for 1 hr before lysis. Phosphorylation states of the proteins shown indicate AKT, ERK1/2 and mTORC2 (indicated by pNDRG1) are more active in siDEPTOR cells in the presence or absence of erlotinib. B. Levels of pERK1/2/ total ERK1/2 as shown in A were quantified using ImageJ. pERK1/2/ total ERK1/2 in the siDEPTOR transfected cells are presented relative to siSC transfected cells in untreated and erlotinib treated conditions.

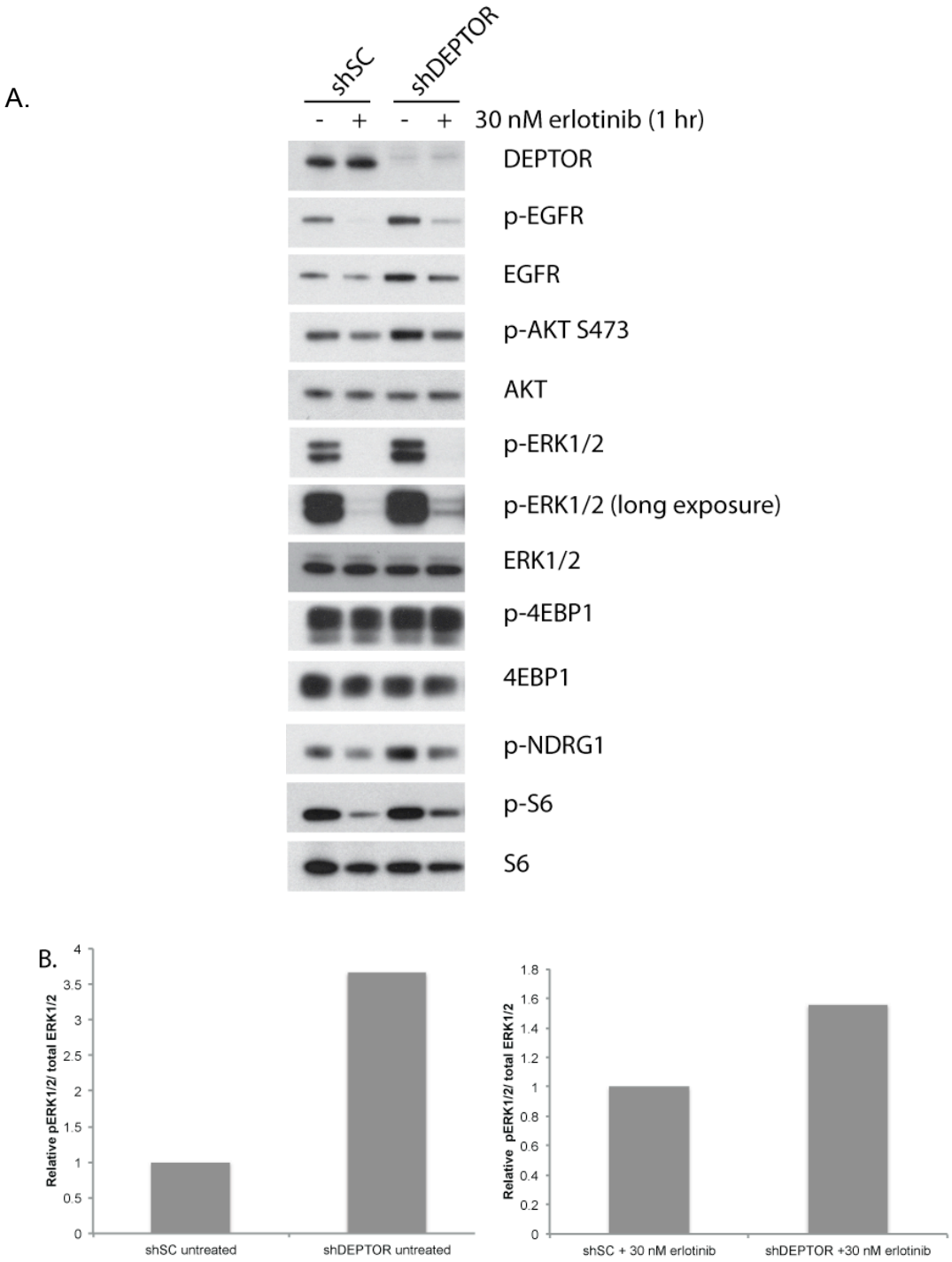

Figure 5.11. shRNA targeting DEPTOR increases EGFR, AKT, ERK1/2 and mTORC2 signalling.

A. PC9 cells expressing with shSC (control shRNA), or shRNA targeting DEPTOR were left untreated or treated with 30 nM erlotinib for 1 hr before lysis. Phosphorylation states of the proteins shown indicate AKT, ERK1/2 and mTORC2 (indicated by pNDRG1) are more active in shDEPTOR cells in the presence or absence of erlotinib. B. Levels of pERK1/2/ total ERK1/2 as shown in A were quantified using ImageJ. pERK1/2/ total ERK1/2 in the shDEPTOR

expressing cells are presented relative to shSC expressing cells in untreated and erlotinib treated conditions.

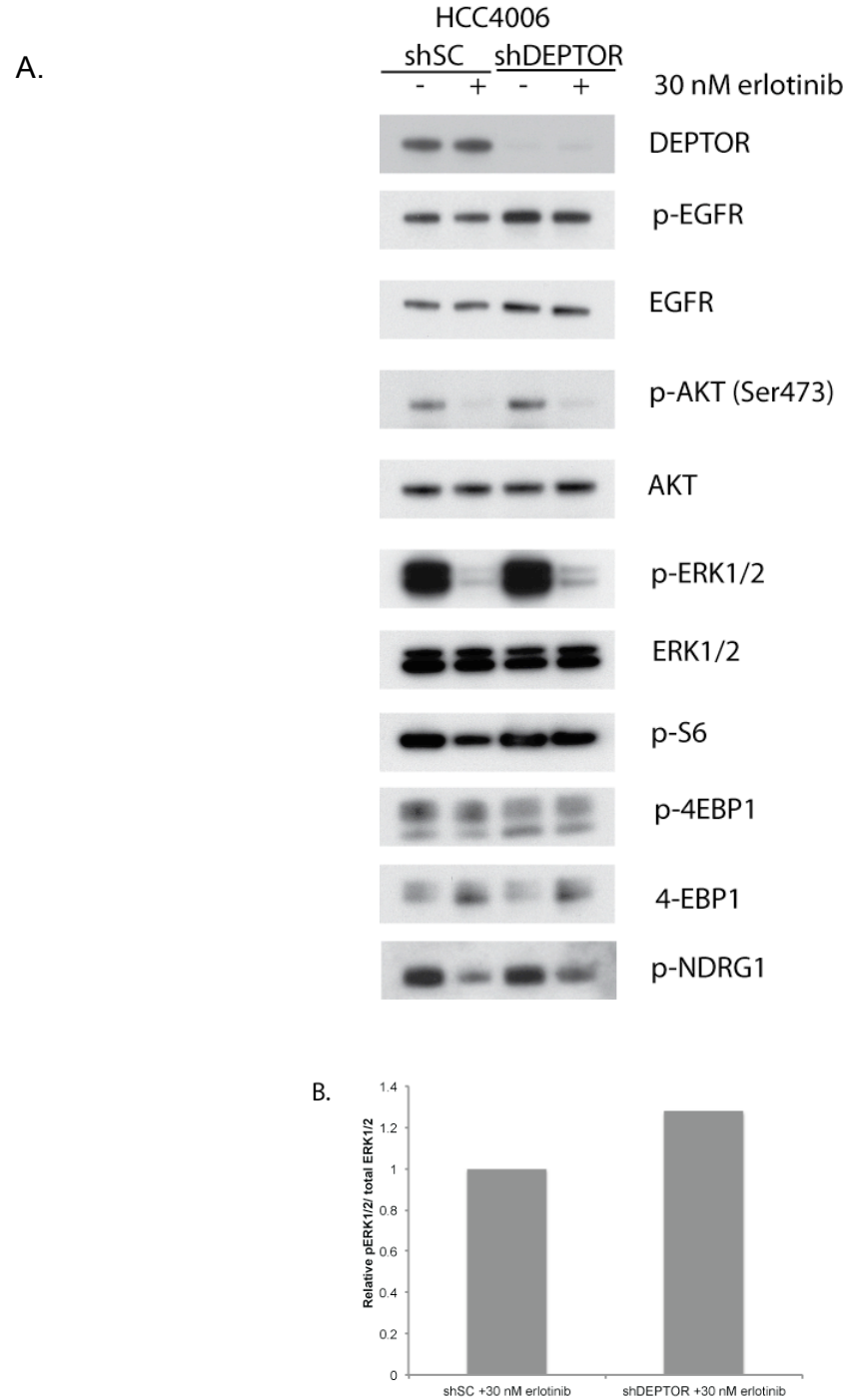

Figure 5.12. Depletion of DEPTOR increases activation of ERK1/2 and mTORC2 in HCC4006 cells.

A. PC9 cells expressing with shSC (control shRNA), or shRNA targeting DEPTOR were left untreated or treated with 30 nM erlotinib for 1 hr before lysis

for immunoblotting against the indicated proteins. B. Levels of pERK1/2/ total ERK1/2 as shown in A were quantified using ImageJ and levels of pERK1/2/ total ERK in shDEPTOR cells are presented relative to shSC cells in erlotinib treated conditions. Over-exposure of the blot meant that pERK1/2 /total ERK1/2 could not be accurately determined in untreated conditions.

5.6 DEPTOR silencing increases the abundance of EGFR protein.

Most surprisingly, DEPTOR-depleted cells have much higher EGFR protein levels than control cells (Figure 5.13). DEPTOR-depleted cells have augmented levels of MAPK and AKT signalling, as demonstrated by increased phosphorylation of ERK1/2 and AKT in untreated and erlotinib-treated conditions (Figure 5.11). We hypothesised that this increased downstream signalling, and consequently the decreased sensitivity of DEPTOR-depleted cells to erlotinib is a result of feedback upregulation of EGFR signalling.

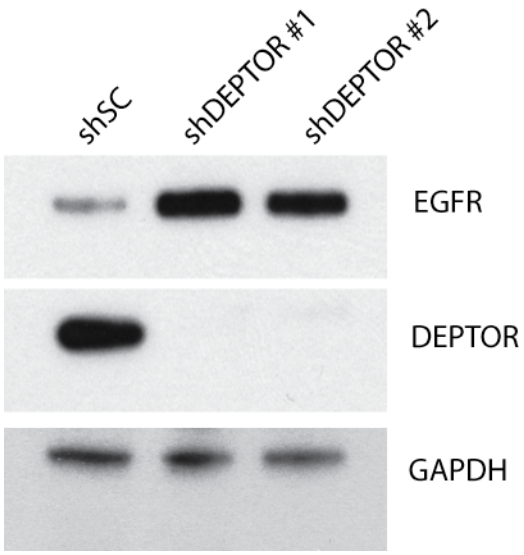

Figure 5.13. DEPTOR silencing increases the abundance of EGFR protein compared to Sc control cells

PC9 cells were infected with a non-targeting control shRNA (shSC) or one of two shRNAs targeting DEPTOR (shDEPTOR #1 and shDEPTOR #2).

To ascertain if the increase in EGFR protein levels was a result of increased levels of EGFR transcript, we analysed the mRNA levels of EGFR in DEPTOR-depleted cells relative to controls. siDEPTOR cells have approximately 1.7 fold more EGFR mRNA than control cells, whilst cells expressing shRNA against DEPTOR have

approximately 1.5 fold more EGFR mRNA than control cells (Figure 5.14). This indicates that loss of DEPTOR results in either increased transcription of EGFR mRNA or elevated stability of the EGFR transcript.

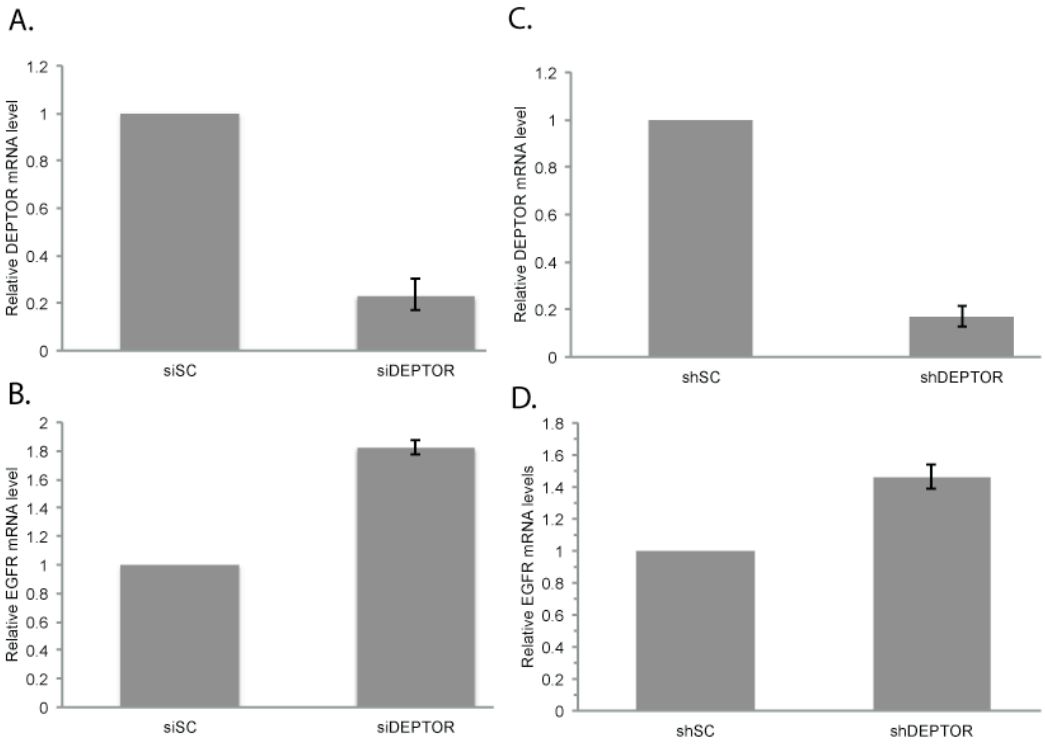

Figure 5.14. DEPTOR silencing by siRNA and shRNA increases EGFR mRNA levels.

A. DEPTOR expression is efficiently silenced by DEPTOR siRNA. B. DEPTOR silencing by siRNA leads to increased EGFR mRNA levels. C. DEPTOR silencing by shRNA (shDEPTOR #1) leads to increased EGFR mRNA levels (D).

Many reports have implicated the upregulation of alternative receptors in resistance to RTK-targeted therapies (Dua et al., 2010; Engelman et al., 2007). Therefore we checked the expression and activation of HER2, ERBB3, MET and IGFR1, as key receptors found to be involved in resistance to EGFR-targeted therapeutics. We found that there was no difference in expression or activation of these receptors indicating that it is not a general effect on RTKs, and that DEPTOR-loss specifically upregulates EGFR (Figure 5.15).

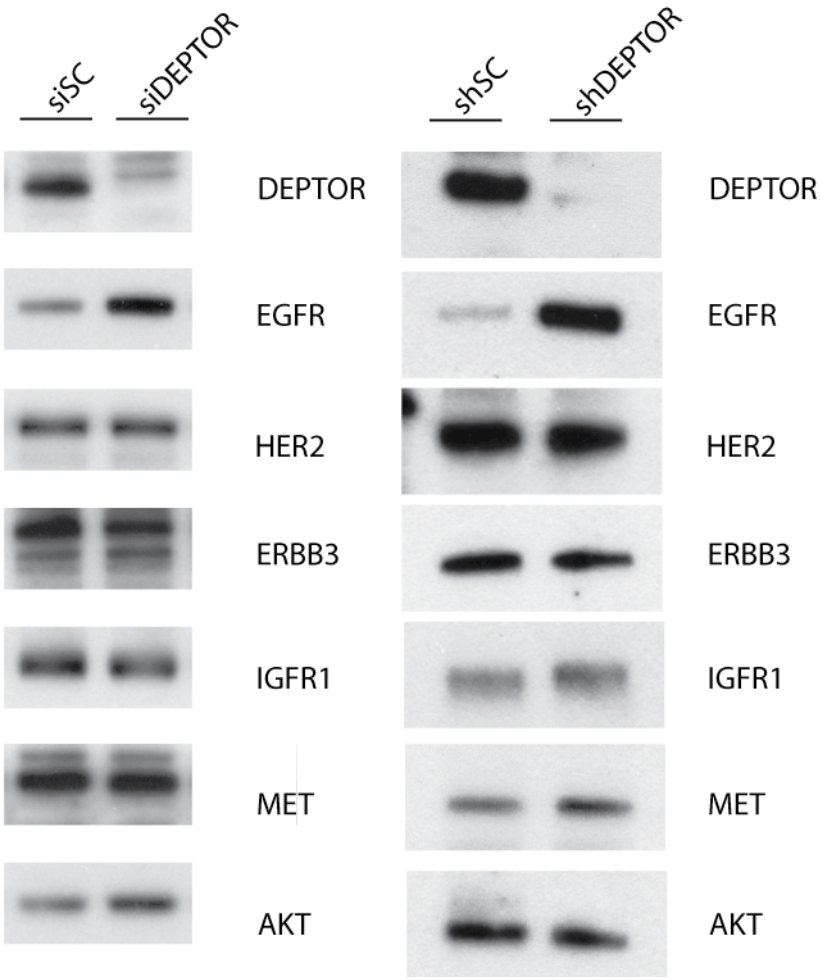

Figure 5.15. DEPTOR depletion does not affect abundance of other key receptor tyrosine kinases.

PC9 cells expressing shRNA targeting DEPTOR or a control non-targeting shRNA (shSC), were lysed, and cell lysates were immunoblotted for the indicated proteins.

To confirm that the increase in EGFR protein with DEPTOR loss correlates to increased downstream activity, we immunoprecipitated EGFR from shSC and shDEPTOR cells and assessed the binding of adaptor proteins that mediate signalling downstream of EGFR. In keeping with the increased EGFR protein levels in total lysates, more EGFR was immunoprecipitated from shDEPTOR cells than shSC cells. With this increase in EGFR, there was also an increase in GRB2 co-immunoprecipated with EGFR from shDEPTOR cells in the presence of erlotinib (Figure 5.16). This indicates the additional EGFR in DEPTOR-depleted cells is capable of downstream signalling, and results in higher total EGFR:GRB2 binding in shDEPTOR cells in the presence of erlotinib.

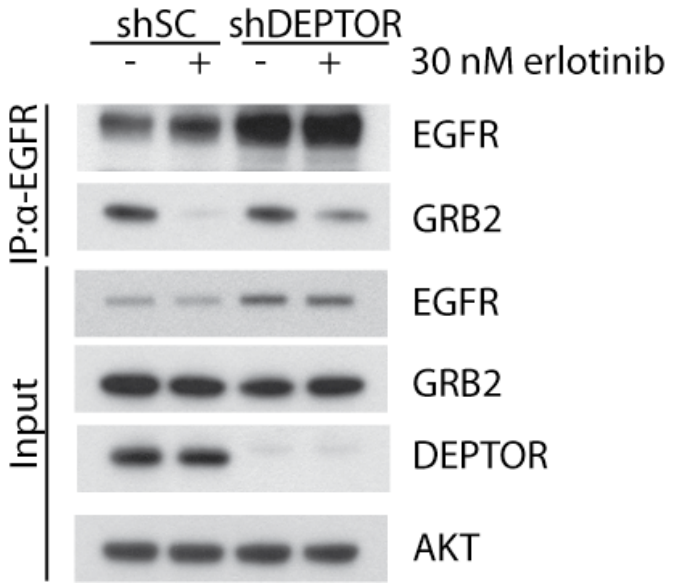

Figure 5.16. DEPTOR-depleted cells have increased levels of EGFR and EGFR-mediated signalling.

PC9 cells expressing shRNA targeting DEPTOR or a control non-targeting shRNA (shSC) were left untreated or treated for 1 hr with 30 nM erlotinib prior to lysis. EGFR was immunoprecipated from the cell lysates, and immunoprecipates were subjected to immunoblotting for EGFR and GRB2 (IP: α-EGFR). Total lysates are shown as loading controls.

SOS is one of the major binding partners of GRB2 downstream of EGFR, with which it normally binds to EGFR in a pre-complexed form. GRB2/SOS directly binds to RAS, where SOS acts as a Ras GEF, to enhance release of GDP from RAS and promote formation of active RAS-GTP. To confirm that shDEPTOR cells have more active RAS, RAS activity assays were performed. shDEPTOR cells had slightly higher levels of active RAS in erlotinib-treated conditions (Figure 5.17). While the difference between shSC and shDEPTOR cells is small, signalling pathways are capable of amplifying such modest effects downsteam enough to drive the decrease in sensitivity to erlotinib seen in shDEPTOR cells.

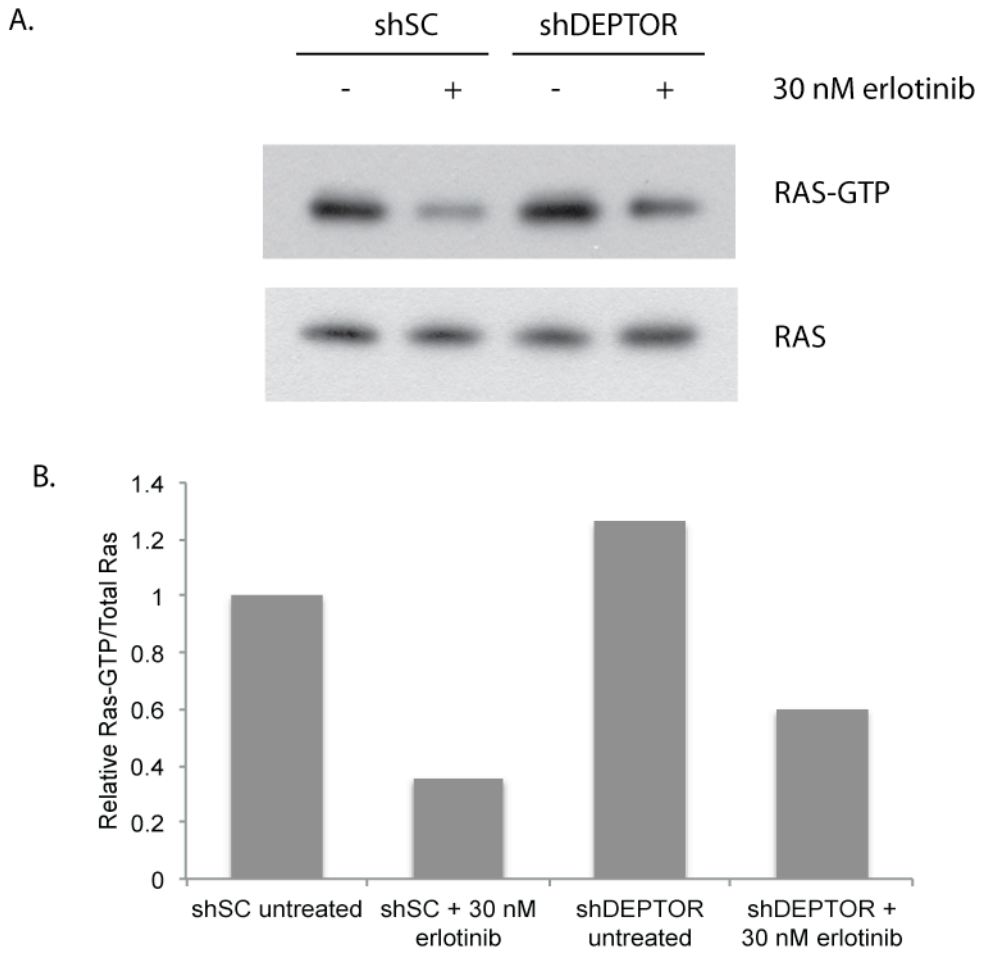

Figure 5.17. DEPTOR-depleted cells have slightly higher levels of active RAS than control cells.

PC9 cells expressing shRNA targeting DEPTOR or a control non-targeting shRNA (shSC) were left untreated or treated for 1 hr with 30 nM erlotinib prior to lysis. RAS-GTP was immunoprecipated from lysates with GST-Raf1-Ras Binding Domain, as described in the materials and methods. Total RAS protein from total lysates is shown as loading control. B. Levels of Ras-GTP/Total Ras were quantified using ImageJ and are presented relative to untreated shSC cells.

Taken together, the above results suggest that increased EGFR levels lead to augmented MAPK and AKT signalling. To test whether the upregulation of EGFR was simply a consequence of increased signalling through AKT and MEK we examined the levels of EGFR protein in PC9 cells overexpressing active forms of AKT and MEK, as described in chapter 4. There was no difference in EGFR expression between control cells (PC9 cells expressing the murine ecotropic receptor) and PC9 cells expressing active MEK or AKT (Figure 5.18). This

indicates that increased levels of EGFR protein are not simply an effect of increased downstream signalling flux.

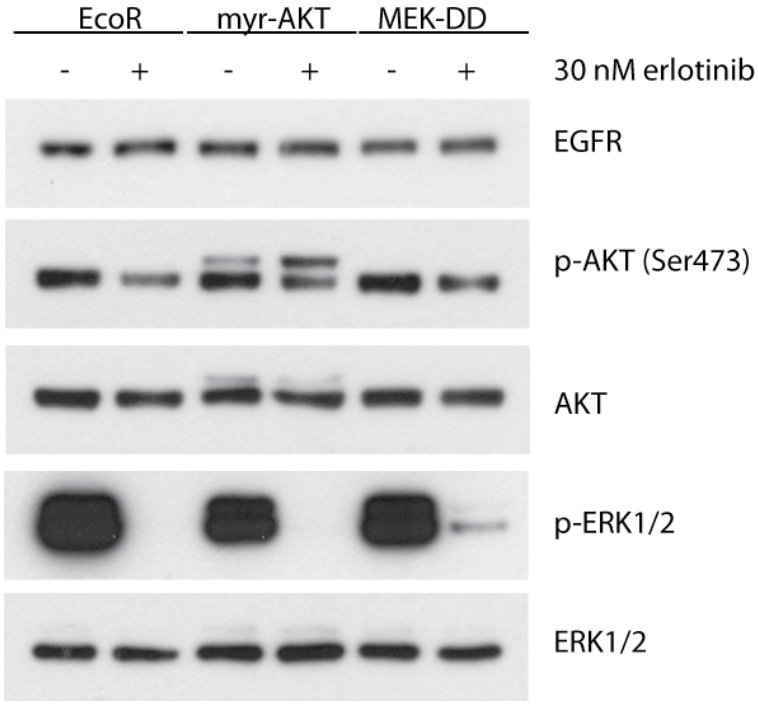

Figure 5.18. EGFR abundance is not affected by active MEK or AKT

PC9-EcoR cells were infected with retroviral MEK-DD and myr-AKT constructs. Cells were treated with erlotinib for 1 hr prior to lysis, to demonstrate activation of the MEK-DD construct.

5.7 Inhibition of mTOR or MEK restores sensitivity of siDEPTOR cells to erlotinib

To determine which effector pathways contribute to erlotinib resistance in DEPTOR-depleted cells, we treated siSC and siDEPTOR cells with various pathway inhibitors in combination with erlotinib. To examine downstream signalling, we employed a MEK inhibitor (AZD6244), an AKT inhibitor (MK2206), an allosteric mTOR inhibitor (temsirolimus) to inhibit mTORC1, and an mTOR kinase inhibitor (AZD8055) to inhibit both mTOR complexes. Each combination was examined over a 72-hour dose response (Figures 5.19-5.26). Only the mTOR kinase inhibitor and the MEK inhibitor effectively restore erlotinib sensitivity of siDEPTOR cells to that of the control cells (Figure 5.19 and Figure 5.23). Analysis of the signalling in siSC and siDEPTOR cells upon combined erlotinib and MEK inhibitor treatment

suggest this is due to a clear reduction in ERK phosphorylation (Figure 5.21). Additionally the combination leads to a further decrease in S6 phosphorylation than erlotinib treatment alone, however this is also seen with the mTOR allosteric inhibitor temsirolimus that does not restore erlotinib sensitivity of DEPTOR-depleted cells (Figure 5.25 and 5.26). The combination of erlotinib and an AKT inhibitor partially restores the sensitivity of siDEPTOR cells to erlotinib treatment, however this is not as effective as the erlotinib and MEK inhibitor combination (Figure 5.21). The combination of erlotinib and an AKT inhibitor decreases phosphorylation of AKT more than either drug alone, and also decreases activation of S6 (Figure 5.22). This is possibly as there is no additional inhibition of ERK, in fact phosphorylation of ERK is slightly higher with the combination treatment, rather than erlotinib alone (Figure 5.22).

The mTOR allosteric inhibitor did not resensitise DEPTOR-depleted cells to erlotinib. The difference in survival between DEPTOR-depleted cells and control cells was greater in the combination treatment of erlotinib and temsirolimus than with erlotinib alone. Immunoblotting suggests this is because only S6 phosphorylation is affected by temsirolimus treatment. There is no effect on phosphorylation of 4EBP1 indicating not all mTORC1 substrates are effectively targeted (Figure 5.26). There is a slight increase in phosphorylation of AKT upon temsirolimus treatment, which is likely to be a result of the feedback activation of AKT via IRS1 downstream of S6K inhibition (O'Reilly et al., 2006) and may account for the lack of effect on cell survival. On the other hand the combination of erlotinib and the mTOR kinase inhibitor restored the cell survival of the siDEPTOR cells to that of the control cells (Figure 5.23). Analysis of the activation of key signalling proteins suggests that the combination augments inhibition of AKT, S6 and decreases phosphorylation of 4EBP1 (Figure 5.24).

Taken together these results suggest that inhibition of ERK, or both mTOR complexes (or at least effective inhibition of mTORC1) in combination with erlotinib, can restore sensitivity of the siDEPTOR cells to erlotinib treatment.

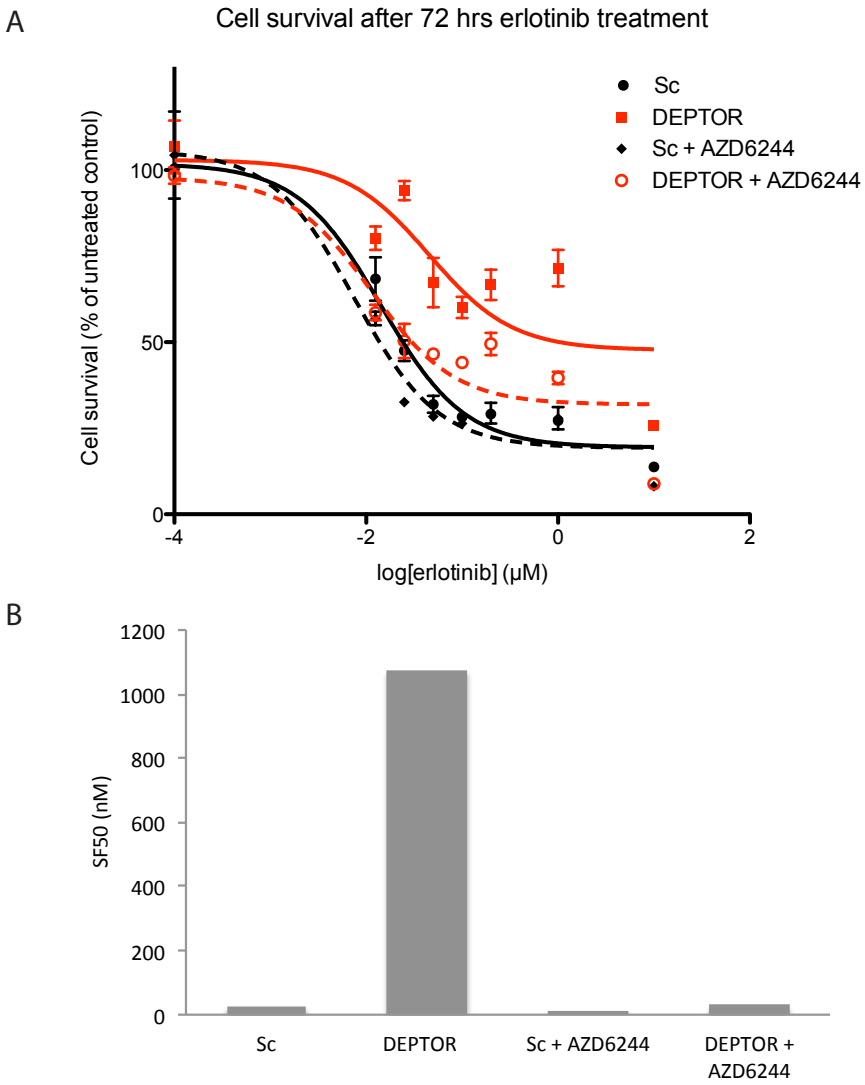

Figure 5.19. Combination treatment of erlotinib and a MEK inhibitor restores sensitivity of siDEPTOR cells to erlotinib to that of Sc control cells.

PC9 cells were transfected with siRNA targeting DEPTOR or a non-targeting control (SC). 48 hours after transfection, cells were treated with the indicated concentrations of erlotinib either with or without 1 μM AZD6244 for 72 hours. A. Cell survival at each erlotinib dose is plotted as a curve. Results shown are from triplicate samples from one representative experiment. B. Cell survival (the same data as in A) is shown as a Survival Fraction 50 (SF50).

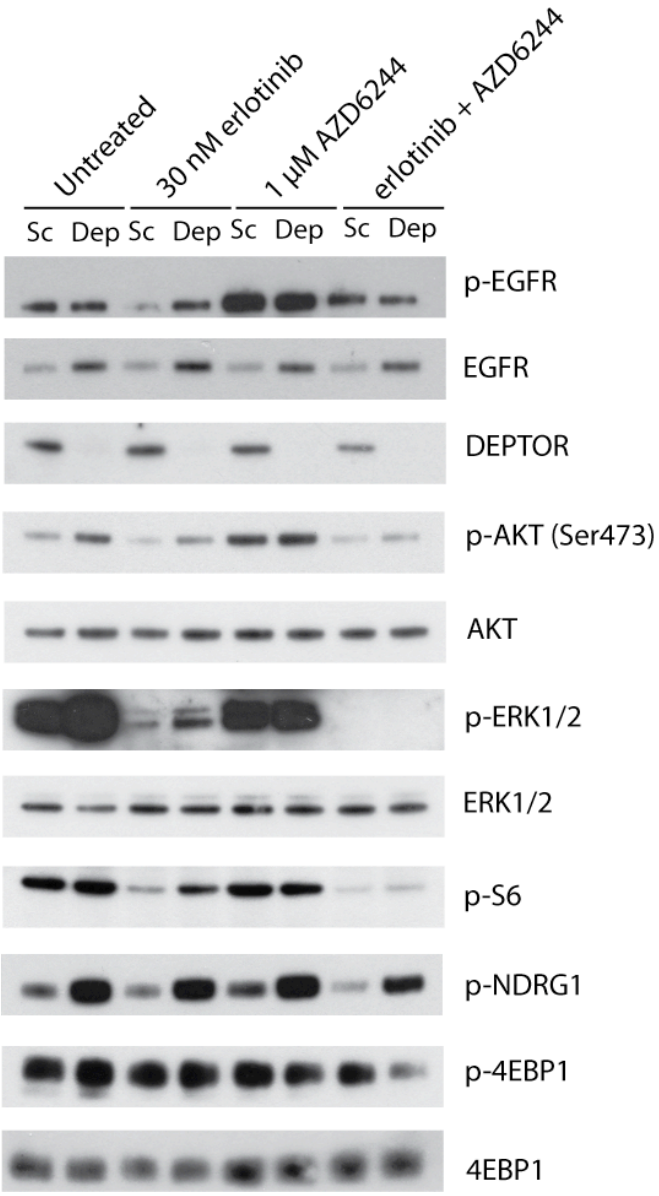

Figure 5.20. Combination treatment of erlotinib and MEK inhibitor restores sensitivity of siDEPTOR cells to erlotinib by abolishing activation of ERK1/2.

PC9 cells were transfected with siRNA targeting DEPTOR or a non-targeting control (SC). 48 hours after transfection, cells were treated with the indicated concentrations of erlotinib either with or without 1 μM AZD6244 for 4 hours prior to lysis for immunoblotting against the indicated proteins.

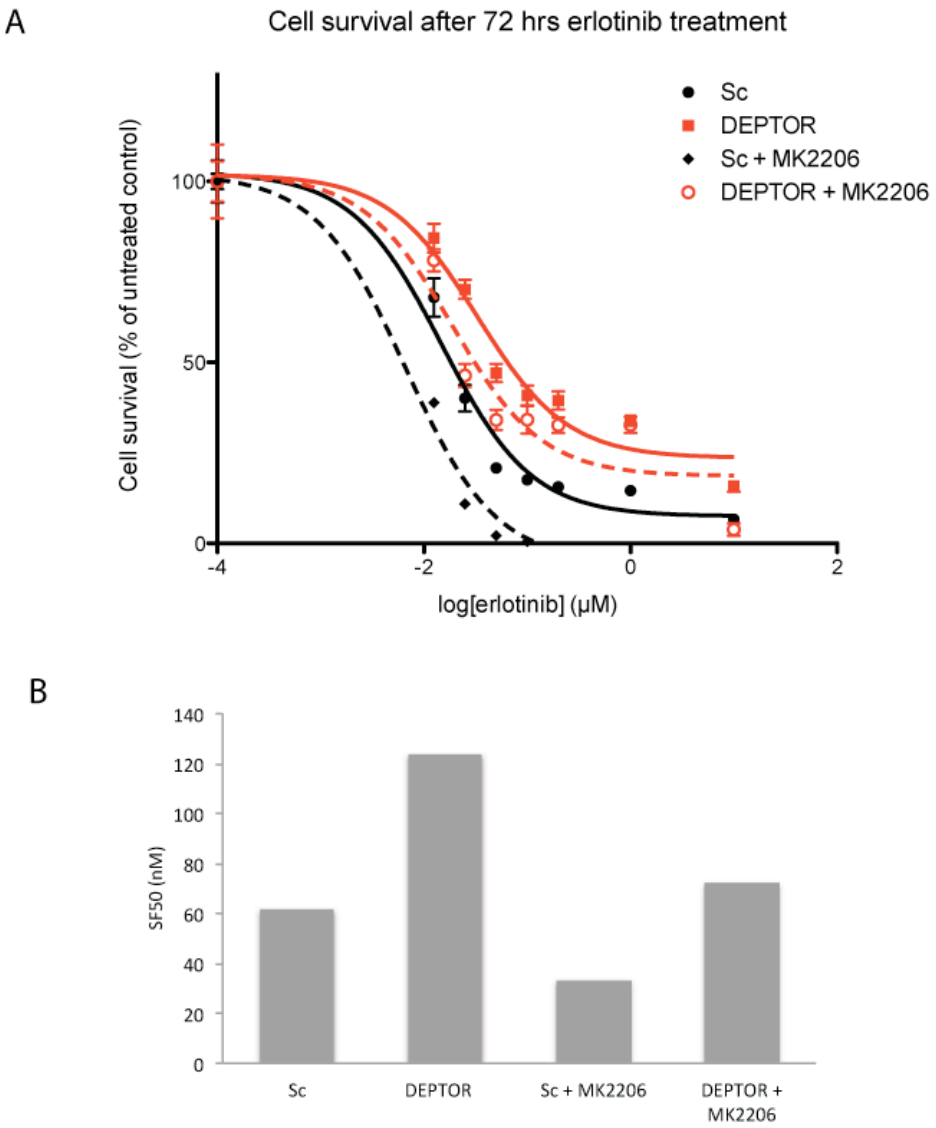

Figure 5.21. Combination treatment of erlotinib and an AKT inhibitor partially resensitises DEPTOR-depleted cells to erlotinib treatment.

PC9 cells were transfected with siRNA targeting DEPTOR or a non-targeting control (SC). 48 hours after transfection, cells were treated with the indicated concentrations of erlotinib either with or without 100 nM MK2206 for 72 hours. A. Cell survival at each erlotinib dose is plotted as a curve. Results shown are from triplicate samples from one representative experiment. B. Cell survival (the same data as in A) is shown as a Survival Fraction 50 (SF50.

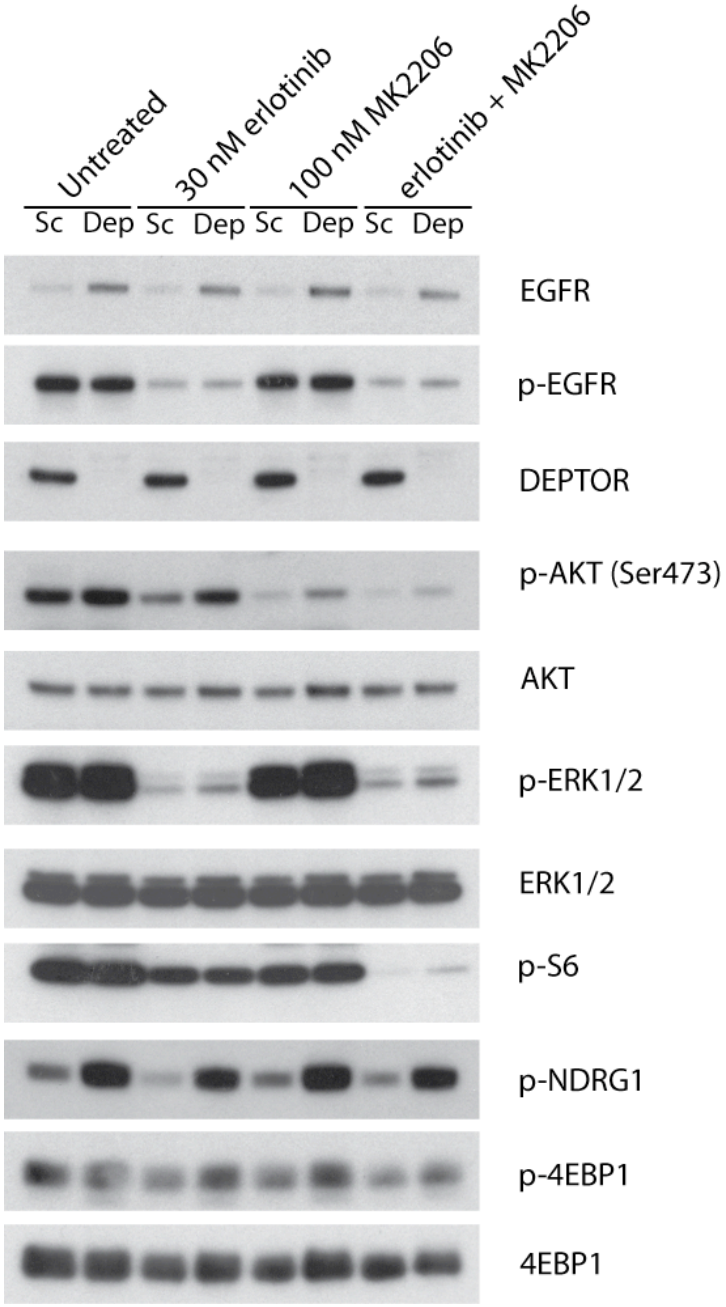

Figure 5.22. Combined erlotinib and AKT inhibition partially resensitises DEPTOR-depleted cells to erlotinib treatment.

PC9 cells were transfected with siRNA targeting DEPTOR or a non-targeting control (SC). 48 hours after transfection, cells were treated with the indicated concentrations of erlotinib and MK2206 (AKT inhibitor) for 4 hours prior to lysis for immunoblotting.

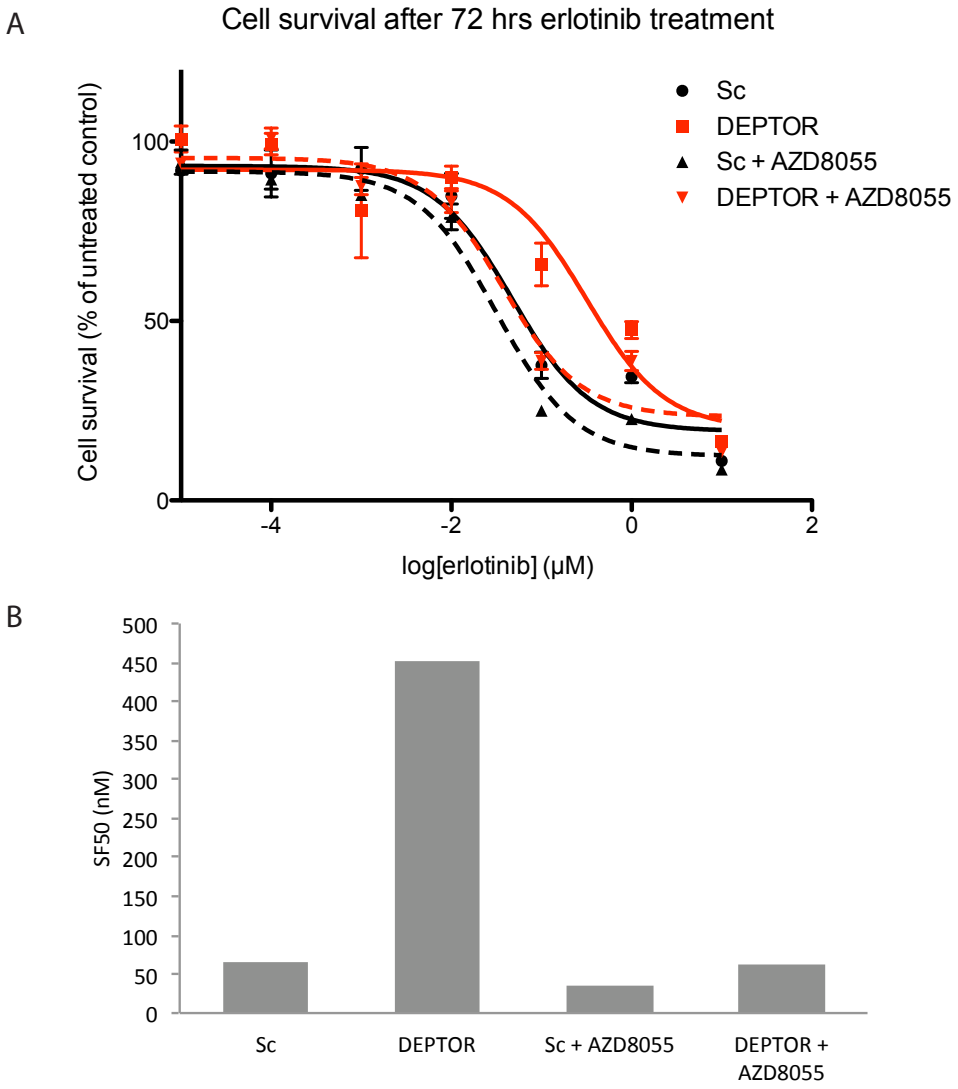

Figure 5.23. Combined treatment of erlotinib and an mTOR kinase inhibitor restores sensitivity of siDEPTOR cells to erlotinib to that of Sc control cells.

PC9 cells were transfected with siRNA targeting DEPTOR or a non-targeting control (SC). 48 hours after transfection, cells were treated with the indicated concentrations of erlotinib either with or without 25 nM AZD8055 for 72 hours. A. Cell survival at each erlotinib dose is plotted as a curve. Results shown are from triplicate samples from one representative experiment. B. Cell survival (the same data as in A) is shown as a Survival Fraction 50 (SF50).

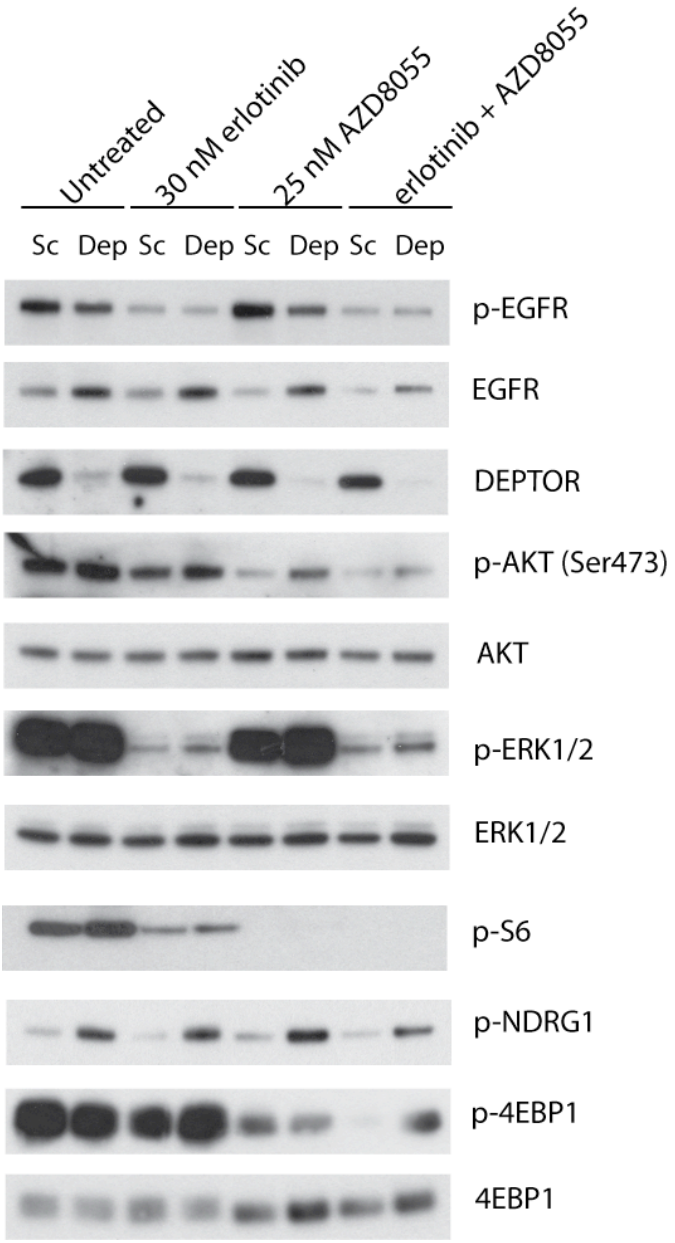

Figure 5.24. Combined erlotinib and mTOR kinase inhibitor treatment restores sensitivity to erlotinib.

PC9 cells were transfected with siRNA targeting DEPTOR or a non-targeting control (SC). 48 hours after transfection, cells were treated with the indicated concentrations of erlotinib either with or without 25 nM AZD8055 for 4 hours.

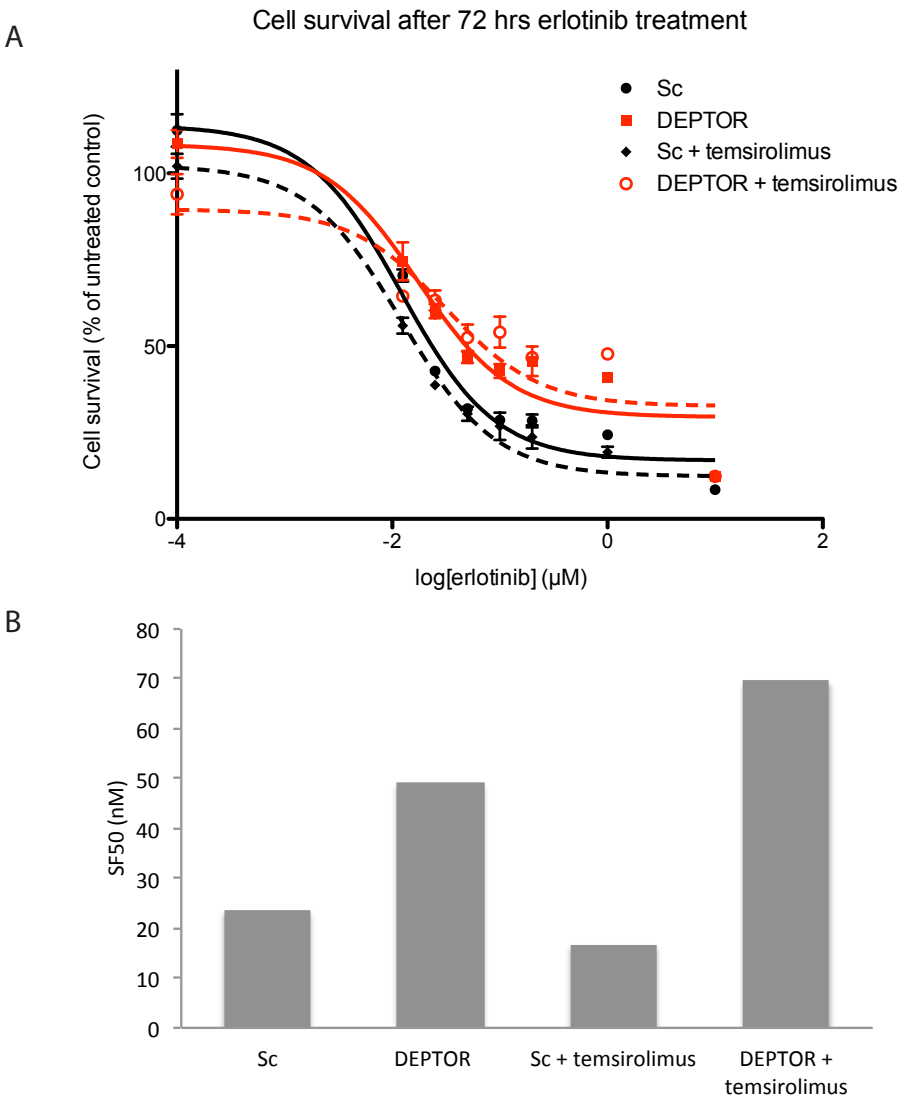

Figure 5.25. Combination treatment of erlotinib and temsirolimus does not restore sensitivity of siDEPTOR cells to Sc control levels.

PC9 cells were transfected with siRNA targeting DEPTOR or a non-targeting control (SC). 48 hours after transfection, cells were treated with the indicated concentrations of erlotinib either with or without 1 μM temsirolimus for 72 hours. A. Cell survival at each erlotinib dose is plotted as a curve. Results shown are from triplicate samples from one representative experiment. B. Cell survival (the same data as in A) is shown as a Survival Fraction 50 (SF50).

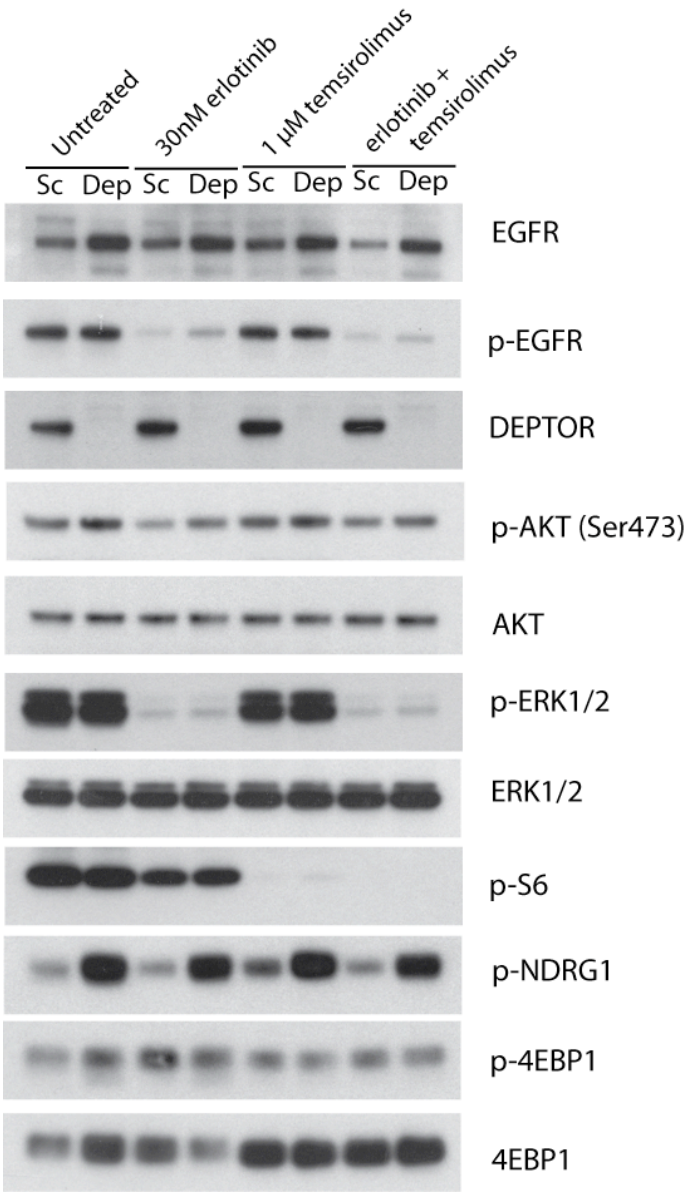

Figure 5.26. Temsirolimus treatment effectively inhibits rpS6 phosphorylation, but does not resensitise cells to erlotinib treament.

PC9 cells transfected with siSC or siDEPTOR were treated for 4 hours with the indicated drugs.

We were intrigued by the difference between the reversal of resistance with the mTOR kinase inhibitor compared with the minor effect of the rapamycin analogue. To further investigate the relative contributions of mTORC1 and mTORC2 to the decreased erlotinib sensitivity of DEPTOR-depleted cells, siRNAs targeting RAPTOR or RICTOR were used to specifically inhibit the function of mTORC1 (RAPTOR) and mTORC2 (RICTOR). Silencing of either RAPTOR or RICTOR substantially reduced the survival of DEPTOR-depleted cells, indicating that both

mTOR complexes are required for cell survival in DEPTOR-depleted cells (Figure 5.28).

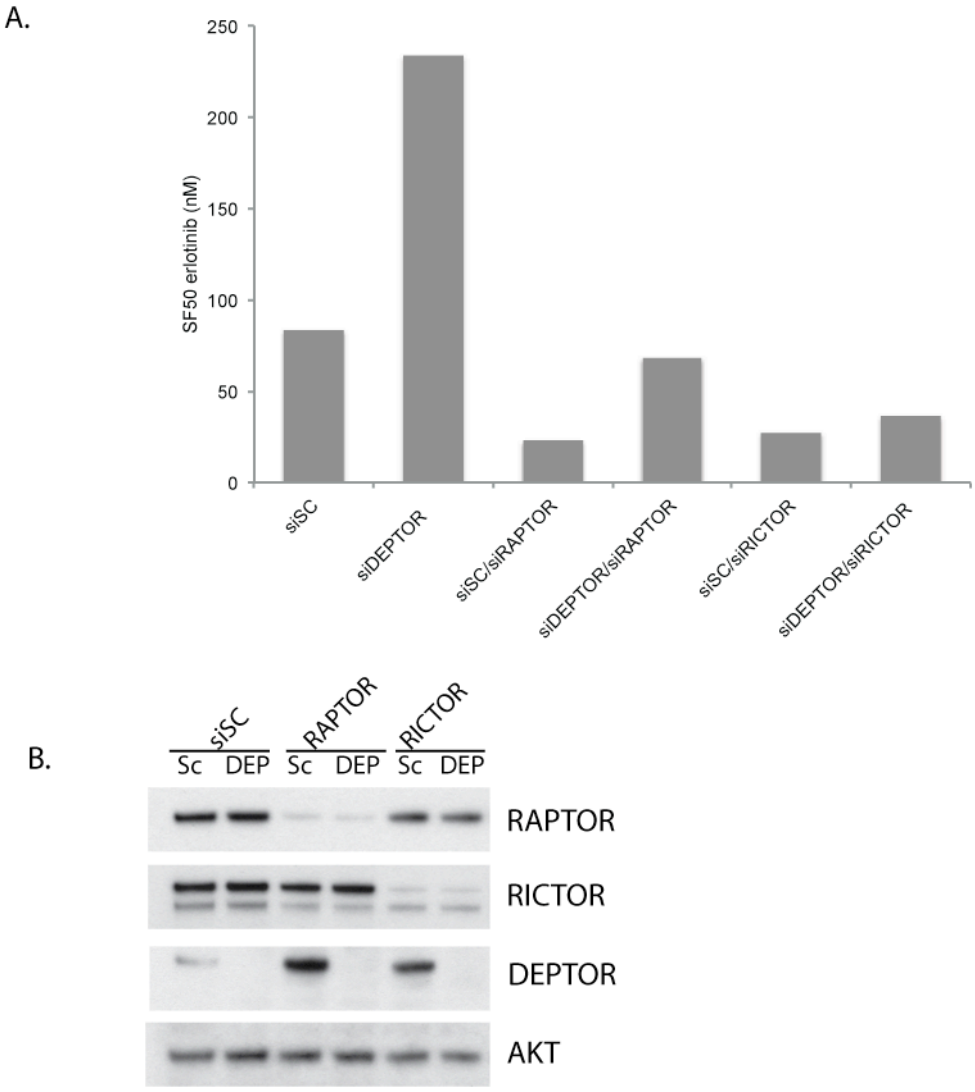

Figure 5.27. RICTOR and RAPTOR are both essential for survival of DEPTOR-depleted cells in the presence of erlotinib.

PC9 cells were transfected with either non-targeting siRNA or siRNA targeting DEPTOR alone or in combination with siRNA targeting RAPTOR or RICTOR. A. Cells were treated with a 0-10 μM dose range of erlotinib for 72 hours and SF50 was determined by CellTiter-Blue. Results shown are from triplicate samples from one representative experiment. Efficiency of silencing was measured at the protein level by immunoblotting.

5.8 Discussion

Here we show that loss of DEPTOR decreases sensitivity of *EGFR*-mutant NSCLC cells to erlotinib treatment. Silencing of DEPTOR resulted in multiple changes in cell signalling. The most prominent changes were modest increases in phosphorylation of EGFR, ERK, AKT and NDRG1 and increased expression of EGFR. As multiple pathways are affected it is a challenge to clearly delineate which of this changes cause the decreased sensitivity of DEPTOR-depleted cells to erlotinib, or how these changes occur. mTOR signalling involves several feedback loops, so perturbation of the pathway can have effects that are not necessarily easy to predict (Efeyan and Sabatini, 2010). The classical example of an mTOR feedback loop is the inhibition of IRS1 and subsequently AKT which occurs downstream of mTORC1 activation via S6K (O'Reilly et al., 2006). This feedback loop has severely limited the effects of mTORC1 allosteric inhibitors, as they block the negative feedback downstream of mTORC1 which leads to increased AKT activation. The same negative regulatory mechanism also leads to upregulation of MAPK signalling, via S6K1/PI3K/RAS, as discovered in the analysis of tumours from patients treated with rapamycin (Carracedo et al., 2008).

Our hypothesis is that DEPTOR-loss upregulates EGFR expression and activation to increase resistance to erlotinib. The mechanism by which DEPTOR loss leads to erlotnib resistance is analogous to the intrinsic resistance to RAF inhibitors seen in BRAF-mutant colon cancer. Recently two studies implicated upregulation of EGFR in resistance to vemurafenib (BRAF inhibitor) (Corcoran et al., 2012a; Prahallad et al., 2012). Both studies showed that feedback to EGFR increased resistance to RAF inhibition by reactivating MAPK signalling. The groups however came up with slightly different mechanisms of action. Prahallad and colleagues postulate that inhibition of ERK signalling by a BRAF inhibitor reduces activity of CDC25C, which in turn leads to de-repression of EGFR phosphorylation (Prahallad et al., 2012). On the other hand, Corcoran et al. did not observe increased phosphorylation of EGFR upon vemurafenib treatment. Instead, they suggest that decreased ERK signalling upon BRAF inhibition decreases expression of Sprouty4, which subsequently increases activation of RAS downstream of RTK activation (Corcoran et al., 2012a).

DEPTOR loss augments levels of EGFR expression and increases erlotinib resistance compared to control cells, similar to the intrinsic resistance to BRAF inhibition of colorectal cancer cells compared to melanoma cells. As will be discussed in greater detail, upregulation of EGFR by DEPTOR seems to be at both the protein and mRNA levels and results in an increase in EGFR and MAPK activation. In contrast, EGFR upregulation in response to BRAF inhibition occurs by inactivation of negative regulators of EGFR signalling as a consequence of drug treatment (Corcoran et al., 2012a)(Prahallad et al., 2012).

In order to ascertain the directionality of signalling we expressed active MEK and AKT proteins in PC9 cells. Expression of an active MEK or AKT construct did not increase EGFR levels, which indicates upregulation of EGFR is not a consequence of the increased AKT and MAPK pathway signalling seen in DEPTOR-depleted cells. The schematic in Figure 5.29 outlines the increases in signalling observed in DEPTOR-depleted cells, and the proposed directionality of signalling. In brief, the hypothesis is that DEPTOR loss activates mTORC1 and mTORC2 to increase EGFR protein synthesis, leading to augmented MAPK signalling. Additionally activation of mTORC2 may contribute to resistance by activating pro-survival signalling downstream of AGC kinases. This is a working hypothesis and more data is needed in order to conclusively state the mechanism by which DEPTOR loss increases resistance to EGFR TKIs. Methods that would allow us to test this proposed mechanism of action will be discussed in the following sections.

Further work is needed to conclusively state that the increase in EGFR protein levels and increased signalling is the cause of resistance in DEPTOR-depleted cells. Possible approaches to address EGFR-dependency include overexpression of EGFR in PC9 cells to confirm increased EGFR expression can mediate erlotinib resistance. Additionally we could test whether combining erlotinib treatment with another EGFR inhibitor such as AG1478 reverses the increased resistance of DEPTOR-depleted cells. DEPTOR loss leads to an upregulation of EGFR mRNA levels, as indicated by Q-RTPCR analysis. However it is not clear whether the upregulation of EGFR occurs solely at the level of transcription or mRNA stability, or whether there is additionally an increase in translation of EGFR transcript. The impact on translation could be assessed by measuring the incorporation of

radiolabelled amino acids such as ^{35}S-Cys/Met into newly synthesised proteins to determine differences in the rate of protein synthesis between control and DEPTOR-depleted cells. Aside from effects on protein synthesis, EGFR protein stability may be increased in DEPTOR-depleted cells. Cycloheximide timecourse experiments could be conducted in order to compare the half-life of EGFR in control and DEPTOR-depleted cells in the absence of new protein synthesis.

Currently it is not possible to decisively conclude that elevated mTOR signalling is responsible for the increase in EGFR protein levels. We think that elevated mTOR signalling is responsible for the upregulation of EGFR as it is well-established that mTOR plays a vital role in the control of transcription and translation (Ma and Blenis, 2009). mTORC1 is thought to regulate gene expression via regulation of transcription factors such as HIF1α (hypoxia-inducible factor 1 alpha), SREBP1 and SREBP2 (sterol regulatory element binding protein 1 and 2) (Magnuson et al., 2012). mTORC1 activates translational initiation and elongation via phosphorylation of S6K which leads to activation of several targets including rpS6 and eukaryotic elongation factor 2 kinase (eEF2K) (Zoncu et al., 2011). Additionally mTORC1 phosphorylates 4EBP1 which causes it to release eIF4E, allowing formation of the translation initiation complex eIF4F and promoting cap-dependent translation (Ma and Blenis, 2009). This year two groups published important studies which elucidate further the role of mTOR signalling in translation (Hsieh et al., 2012) (Thoreen et al., 2012). Both studies identified novel regulatory elements in the 5' UTR of mRNAs specifically regulated by mTOR aside from the previously described 5' terminal oligopyrimidine (TOP) motif. Hsieh et al identified a pyrimidine-rich translational element within the 5'UTRs of 63% of mTOR target mRNAs (Hsieh et al., 2012), whereas Thoreen and colleagues identified previously unrecognised TOP motifs or related TOP-like motifs in mRNAs specifically regulated by mTORC1 (Thoreen et al., 2012). Both studies demonstrate that the translational impact of mTORC1 on specific mRNAs is predominantly mediated by the regulation of 4EBP1 by mTORC1. These new insights are very interesting and prompt us to further examine whether DEPTOR loss may impact EGFR levels by effecting translation via activation of mTORC1.

Aside from the published role of DEPTOR as a negative regulator of mTOR (Peterson et al., 2009), we hypothesise that DEPTOR loss mediates increased erlotinib resistance through augmented mTOR signalling, as immunoblotting of lysates from control and DEPTOR-depleted cells indicates DEPTOR loss increases phosphorylation of downstream targets of mTOR signalling, namely AKT and NDRG1 downstream of mTORC2 (Figure 5.10). Phosphorylation of S6 (Figure 5.20) and 4EBP1 (Figure 5.22) which function downstream of mTORC1 also appear to increased however the effects are more variable between experiments. Experiments using a combination of erlotinib with different targeted drugs revealed an mTOR kinase inhibitor restored the sensitivity of DEPTOR-depleted cells to erlotinib treatment (Figure 5.23) which additionally suggests that the decreased sensitivity of DEPTOR-depleted cells is dependent on augmented mTOR signalling.

mTOR kinase inhibition but not use of a rapamycin analogue (rapalog) could resensitise siDEPTOR cells to erlotinib treatment. This indicates increased activation of both mTOR complexes contributes to a more resistant phenotype, rather than only mTORC1. It is important to note that rapalogs do not inhibit the ability of mTORC1 to phosphorylate all downstream targets equally. In Fig 5.27 phosphorylation of 4EBP1 does not really change in response to treatment with temsirolimus, whereas phosphorylation of ribosomal S6 is completely abolished. This is in keeping with findings by Hsieh et al, who found that the enhanced cytotoxic ability mTOR kinase inhibitor PP242 over rapamycin comes from its inhibition of 4EBP1 phosphorylation, and subsequent cap-dependent translation, rather than inhibition of rpS6 (Hsieh et al., 2010). The mTOR kinase inhibitor AZD8055 used here was more effective at inhibiting phosphorylation of 4EBP1, along with phosphorylation of AKT at Ser473, indicating mTORC2 was also inhibited (Fig 5.24). To examine the function of each mTOR complex more specifically we silenced RAPTOR (mTORC1) or RICTOR (mTORC2), and found both severely affect viability of DEPTOR-depleted cells in the prescence of erlotinib indicating both mTOR complexes still have a role in cell survival (Figure 5.27). Future work could include *in vitro* kinase assays of endogenous mTOR immunoprecipitated by RAPTOR or RICTOR to confirm activity of mTORC1 and mTORC2 in DEPTOR-depleted cells. It is possible DEPTOR loss may increase MAPK and PI3K-AKT signalling independently of mTOR activation, therefore future

experiments will address whether mTOR signalling has a direct role in erlotinib resistance. For example silencing of mTOR in DEPTOR-depleted cells would demonstrate whether mTOR is necessary for the upegulation of EGFR observed upon DEPTOR loss. Additionally we will assess the effect of longer term treatment with the mTOR kinase inhibitor on EGFR levels to determine whether the mTOR kinase inhibitor restores the sensitivity of siDEPTOR cells by reducing EGFR protein abundance. Upon establishing the role of mTOR activation in decreased erlotinib sensitivity upon DEPTOR loss it would be interesting to examine whether activation of mTOR signalling by other means, such as PTEN loss, loss of TSC1/2, or activating mutations in mTOR could also cause increases in EGFR protein abundance. It is possible that loss of PTEN and TSC1/2 that predominantly affect mTORC1 activity would not cause this phenotype. Activating mutations in mTOR, such as those identified by Gerlinger and colleagues (Gerlinger et al., 2012) may result in similar effects as DEPTOR loss, as it affects both complexes.

Apart from upregulation of EGFR through increased transcription and translation via activation of mTORC1, DEPTOR loss may also decrease erlotinib sensitivity via activation of mTORC2. One of the most striking effects of DEPTOR depletion is an increase in phosphorylation of NDRG1 which demonstrates increased mTORC2 activation(Garcia-Martinez and Alessi, 2008). Peterson et al., describe that loss of DEPTOR expression leads to a reduction in apoptosis in response to serum starvation in HeLa cells and HT-29 cells, and suggest that in HeLa cells at least it is an SGK1-dependent mechanism (Peterson et al., 2009). SGK1 in conjunction with AKT can negatively regulate FOXO1/3a to prevent induction of pro-apoptotic factors such as Fas-L and BH3-only BIM_{EL} (Fu and Tindall, 2008; Garcia-Martinez and Alessi, 2008). Additionally AKT and SGK1 can also phosphorylate BAD, which leads to its sequestration by 14-3-3 proteins in the cytoplasm, and blocks its pro-apoptotic function (Datta et al., 1997). Future work could probe the contribution of SGK1 to the increased survival of DEPTOR-depleted cells in response to erlotinib treatment, for example by depletion of SGK1 with RNAi, or inhibition with a specific SGK1 inhibitor (GSK650394). Additionally we would like to assess whether NDRG1 is an essential mediator of the effects of DEPTOR depletion, or whether in this context it purely serves as a read-out of increased mTORC2 activity (Garcia-Martinez and Alessi, 2008).

Aside from the combination treatment of an mTOR kinase inhibitor and erlotinib, the combination of a MEK inhibitor and erlotinib was also effective at resensitising DEPTOR-depleted cells to erlotinib treatment. We hypothesise that this is because DEPTOR loss leads to upregulation of EGFR and subsequent downstream signalling. EGFR mRNA and protein levels are increased in DEPTOR-depleted cells (Figure 5.13 and 5.14), which subsequently leads to increased recruitment of GRB2 (Figure 5.16) and activation of RAS (Figure 5.17) in basal and erlotinib treated conditions. We hypothesise that increased RAS activity drives the higher levels of ERK phosphorylation observed in DEPTOR-depleted cells, and that this increase in ERK activation leads to decreased sensitivity to erlotinib, as we see in NF1-depleted cells. Inhibition of AKT was not as effective as inhibition of MEK at restoring sensitivity of DEPTOR-depleted cells, as we also found be to true with NF1 loss. There are several potential reasons for this. Firstly, as discussed in the previous chapter it seems that oncogenic events that activate RAS, i.e. NF1 loss or RAS activating mutations make cells more reliant on MAPK pathway activation, and therefore more susceptible to MEK inhibition (Misale et al., 2012). Additionally, it has been demonstrated that AKT inhibition can drive increases in RTK expression, for example ERBB3, by activating FOXO-mediated transcription (Chandarlapaty et al., 2011). Therefore such feedback mechanisms may limit the efficacy of AKT inhibition. Also treatment with the combination of erlotinib and an AKT inhibitor (MK2206) resulted in slightly higher levels of phosphorylated ERK compared to erlotinib alone, suggesting there may be some compensatory activation of the MAPK pathway (Figure 5.22). Finally, AKT appears upstream of mTORC1 and downstream of mTORC2, therefore perturbing AKT signalling may have other unforeseen effects on the mTOR signalling network already disturbed by DEPTOR loss.

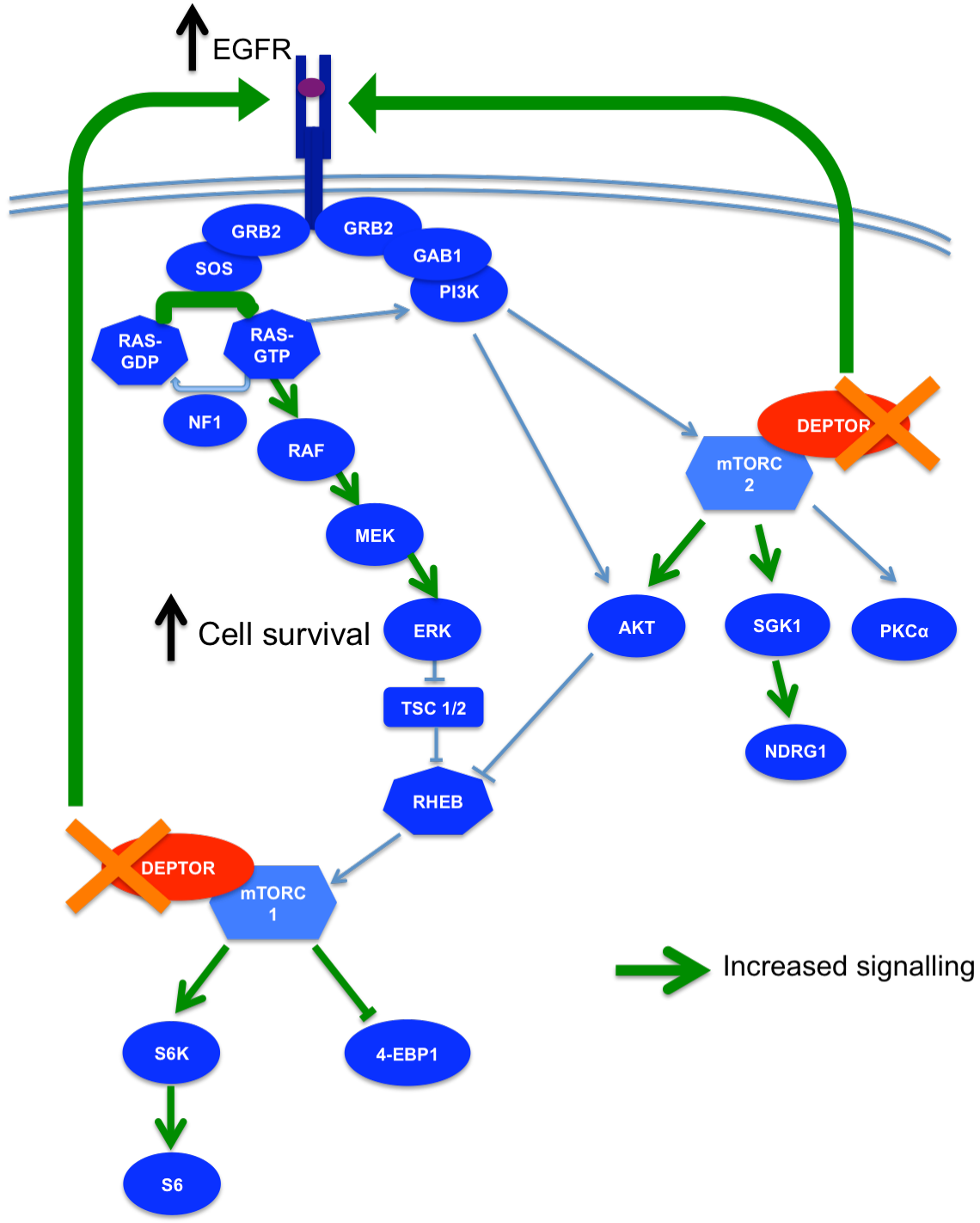

Figure 5.28. Proposed mechanism - DEPTOR loss leads to upregulation of EGFR levels and MAPK pathway signalling.

DEPTOR loss leads to activation of mTOR signalling and increased EGFR abundance. EGFR upregulation results in augmented MAPK signalling, and subsequently enhanced cell survival. mTORC2 activation increases AGC kinase activity to enhance survival. Green arrows represent observed increases in signalling (as assessed by Western blotting).

DEPTOR loss did not appear to increase the abundance of other receptors, namely ERBB2, ERBB3, MET and IGF-R1, however one cannot rule out the possibility that other receptors were also involved. For example Wilson et al recently described activation of FGFR2 in response to exogenous FGF can rescue *EGFR*-mutant NSCLC cell lines from erlotinib treatment, therefore upregulation of FGF2 expression could potentially increase erlotinib resistance (Wilson et al., 2012). Additionally, increased expression of tyrosine kinase receptor AXL has been reported in erlotinib resistant NSCLC xenografts and in patients (Zhang et al., 2012). Further work could more extensively characterise protein levels and activation of these receptors. The decrease in erlotinib sensitivity seen in DEPTOR-depleted cells is an effect one may expect from upregulation of the targeted protein, in that it can still be saturated by higher concentrations of erlotinib. A larger increase in resistance would probably be expected if DEPTOR additionally upregulated alternative receptors not targeted by erlotinib (Engelman et al., 2007; Zhang et al., 2012). It would be interesting to see if DEPTOR-depletion could cause upregulation of EGFR in other cancer cell lines, for example in *HER2*-amplified breast cancer cells, *BRAF*-mutant melanoma and *EML4-ALK*-positive NSCLC since upregulation of signalling through EGFR as an alternative receptor tyrosine kinase is known to be a mechanism of resistance to targeted therapies in these cancer types (Dua et al., 2010) (Corcoran et al., 2012a; Prahallad et al., 2012; Tanizaki et al., 2012). Additionally, it would be intriguing to know whether DEPTOR loss could drive the upregulation of the driving oncogenic receptor in cancer cell lines dependent on other RTKs, rather than EGFR (eg. EML4-ALK fusion protein, or ERBB2). DEPTOR loss therefore could have a wider role in drug resistance in multiple cancer types.

As mTOR signalling is involved in multiple cellular processes (Laplante and Sabatini, 2012), only a small fraction of mTOR signalling has been examined here, and it is likely DEPTOR loss has other effects than considered in this chapter. For example further work could examine the role of PKCα activation downstream of mTORC2, or the effect of DEPTOR loss on autophagy. Inhibitors of growth factor signalling, such as erlotinib, can induce autophagy and autophagic cell death has been proposed to contribute to the anti-cancer activity of some drugs (Cheong et

al., 2012). However it has also been suggested that stress-induced autophagy can drive drug resistance, and that inhibition of autophagy can enhance the growth inhibitory effect of EGFR TKIs in NSCLC (Han et al., 2011). Therefore it would be interesting to examine whether there is a change in the level of autophagy upon depletion of DEPTOR and if this contributes to resistance to erlotinib. Also PKC alpha has been demonstrated to inhibit apoptosis, and may contribute to decreased sensitivity of DEPTOR-depleted cells to erlotinib. For example, increased expression of PKC alpha has been detected in a tamoxifen resistant breast cancer cell line, where PKC alpha downregulates apoptosis by decreasing JNK activity (Wang et al., 2012). Little is known about the effects DEPTOR expression has on these pathways and it would be intriguing to investigate their involvement in drug response in DEPTOR-depleted cells.

Additionally DEPTOR loss may contribute to erlotinib resistance via epithelial-mesenchymal transition (EMT). Earlier this year, Chen and colleagues showed loss of DEPTOR expression occurred as a result of RNAi-mediated silencing of BMK1 (Mitogen Activated Protein Kinase 7) (Chen et al., 2012). They suggest loss of DEPTOR results in activation of PI3K and mTORC2, and subsequent downregulation of GSK3β. GSK3β deactivation increases stability of the transcription factor Snail which in turn downregulates E-cadherin and ZO-1 (Zona Occludens 1), both of which have key functions in maintenance of epithelial morphology (Chen et al., 2012). As EMT is a mechanism of resistance to EGFR TKIs it would be interesting to look for evidence of EMT in NSCLC depleted of DEPTOR (Sequist et al., 2011).

Although NF1 and DEPTOR depletion have some similar effects on signalling, there are subtle but important differences. For example, NF1 loss increases phosphorylation of ERK compared to control cells only in erlotinib-treated conditions while DEPTOR-depleted cells have higher levels of phosphorylated ERK in basal conditions. Sustained activation of MAPK signalling may not be an advantageous situation for cells, due to activation of negative feedback loops, for example upregulation of Sprouty and SPRED (sprout related EVH1 domain) proteins which inhibit RAS/ERK signalling downstream of RTKs (Mason et al., 2006; Meng et al., 2012). Indeed cell growth assays confirmed shDEPTOR cells

grew more slowly than shSC cells which has also been observed in NSCLC cells carrying the *EGFR*^{T790M} mutation (Chmielecki et al., 2011). This means that DEPTOR loss may only be beneficial to cancer cell survival in the event of selection by erlotinib treatment, while NF1 loss potentially could be stably maintained without the negative effects of MAPK hyperactivation.

In conclusion, DEPTOR loss upregulates EGFR expression, MAPK signalling, and mTOR signalling and increases cell survival in the presence of erlotinib. As mTOR signalling is involved in a myriad of cellular processes it is likely DEPTOR loss has other effects than those considered here. Additionally, the mechanism by which DEPTOR functions to inhibit mTOR signalling or what other functions it may have are ill-defined. As described earlier further work is needed to conclusively link the increase in EGFR levels to decreased erlotinib sensitivity, and to determine the mechanism by which EGFR is upregulated. Ongoing work also includes the use of shRNA resistant DEPTOR cDNA to restore sensitivity of DEPTOR-depleted cells erlotinib. As increased resistance to erlotinib and augmented EGFR expression were observed upon the expression of two non-overlapping shRNAs, we are confident it is a real biological effect and not an off-target effect. The upregulation of EGFR in response to DEPTOR loss is an intriguing observation, which may be of relevance in other tumour types where EGFR upregulation can contribute to drug resistance (Corcoran et al., 2012a; Dua et al., 2010; Prahallad et al., 2012). Finally, loss of DEPTOR expression is a novel potential mechanism of resistance to EGFR TKIs. DEPTOR protein expression is negatively regulated by mTOR signalling (Duan et al., 2011; Gao et al., 2011; Zhao et al., 2011), which is upregulated in some NSCLC patients (Liu et al., 2011), therefore it would interesting to see if there was a correlation between low levels of DEPTOR expression and poor response to EGFR TKIs *in vivo*.

Chapter 6. Discussion

6.1 Targeted therapeutics

The aim of developing targeted therapeutic agents in place of treatments that exploit other more general properties of cancer cells, such as sensitivity to DNA damage and hyperproliferation, was to limit the toxic side-effects on healthy cells in the body. The rationale of targeted therapeutics is that cancers have a specific genetic lesion on which they have become dependent, a state commonly referred to as 'oncogene addiction' (Weinstein, 2002). Thus, inhibition of the protein product of this genetic lesion (or signalling pathway in which the protein functions) should cause cancer regression. In contrast, non-cancerous tissues would not be affected by the targeted agent as they do not contain the particular genetic aberration and therefore have not developed dependence on the targeted signalling pathway. Under this premise, an array of targeted therapeutics has been developed, including trastuzumab targeting HER2, imatinib targeting BCR-Abl and erlotinib and gefitinib targeting EGFR (Carter et al., 1992; Druker et al., 1996; Fukuoka et al., 2003).

Beyond directly targeting the mutant oncogene, it is possible for tumours to become dependent on genes that are not oncogenic themselves, but are necessary for the oncogenic state, termed 'non-oncogene addiction' (Solimini et al., 2007). The expression or mutational status of such genes is not altered in cancer, however they have key roles in pathways necessary for tumour cell survival, making them additional potential drug targets. Cancer cells have undergone extensive rewiring in the process of oncogenesis, which makes them more dependent on certain pathways than normal cells. An example of this is the reliance of *BRCA1* and *BRCA2* mutant breast cancers on base-excision repair pathways that sensitises them to Poly (ADP-ribose) Polymerase (PARP) inhibition (Farmer et al., 2005). PARP inhibition prevents the repair of single-strand breaks by base-excising repair, which subsequently progress to double strand breaks. Double-strand breaks are predominantly repaired by homology-directed repair that requires BRCA1/2, therefore in BRCA deficient tumours treated with PARP inhibitors cells are overwhelmed with DNA damage that triggers cell death. Non-

cancerous cells which express wild type BRCA1/2 are still capable of normal DNA repair and are therefore less affected by PARP inhibitors (Annunziata and Bates, 2010). However, whilst therapeutics targeted at oncogene and some non-oncogene addicted cancers have met with initial success in the clinic, resistance is reported eventually for all targeted therapies.

6.2 Resistance – primary or acquired?

Along with effective therapeutic delivery and dose-limiting toxicity, drug resistance is the ultimate problem standing in the way of the success of targeted therapeutics. For example, even with drugs that show remarkable initial responses, such as BRAF inhibitors in *BRAF*-mutant melanoma, the extension of overall patient survival is generally modest as tumours recur as resistance develops. Drug resistance can be divided into two categories: primary (de novo) and acquired resistance. De novo resistance refers to failed response from the start of treatment, while acquired resistance occurs when tumours respond initially to treatment, but later fail to respond and continue to grow. Notably, the distinction between these two categories has increasingly blurred through the years (as discussed below).

An example of primary resistance is the presence of *KRAS* mutations in EGFR-driven colon cancer, which results in insensitivity to the EGFR monoclonal antibodies cetuximab and panitumumab (Amado et al., 2008; Karapetis et al., 2008). An example of acquired resistance is the emergence of the *EGFR* secondary mutation T790M in non-small cell lung cancer (NSCLC), which drives resistance to EGFR tyrosine kinase inhibitors (TKIs) such as erlotinib. However, increasing sensitivity of DNA sequencing has revealed that acquired resistance in many cases is really the emergence of drug resistant clones that are present in the tumour population prior to treatment. This has been shown in several situations of acquired resistance, for example the T790M mutation can be detected in *EGFR*-mutant NSCLC tumours prior to treatment (Maheswaran et al., 2008) (Oh et al., 2011). Additionally, *KRAS* mutations can be detected prior to emergence of panitumumab resistance in colon cancer, which mathematical modelling predicts must be present in subclones before treatment (Diaz et al., 2012). Nevertheless,

there is data suggesting acquired resistance can occur as a result of ongoing somatic mutation, and not only through the selection of pre-existing drug-resistant clones. In another study describing *KRAS* mutations and amplifications in cetuximab resistant colorectal cancer, one *KRAS* mutation found in the Lim1215 cell line after culturing long term in the presence of cetuximab was not found in the parental cell line prior to treatment, even upon high-coverage deep sequencing. This suggests this resistance mutation occurred during drug treatment (Misale et al., 2012). Additionally, a missense S492R mutation in *EGFR* that confers resistance to cetuximab in colorectal cancer could not be detected by deep sequencing of pre-treatment samples although *EGFR* amplification was detected in both pre and post-cetuximab treated samples (Montagut et al., 2012).

6.3 Common themes of resistance mechanisms

When reviewing mechanisms of resistance to different targeted therapies in different cancer types, there is a striking similarity among the common mechanisms and signalling pathways they employ. Broadly, mechanisms can be sub-divided into three modes of action: re-activation of the targeted signalling pathway, activation of a compensatory signalling pathway, or cellular transformation and reprogramming which alters cell phenotype and therefore drug sensitivity.

6.3.1 Reactivation of the targeted pathway

Reactivation of the targeted pathway can occur at multiple stages, either at the point of the targeted protein itself (by amplification or secondary mutations that block drug action), or by activating mutations functioning downstream in the pathway. For example, copy number gain of *ALK* has been detected in NSCLC patients with *ALK* gene rearrangements post-crizotinib treatment; this amplification was associated with acquired resistance to crizotinib (Doebele et al., 2012). Additionally, resistance driven by amplification of the target also occurs in *BRAF*-mutant driven melanoma (Shi et al., 2012). As shown here, loss of DEPTOR functions in an analogous manner to increase resistance to erlotinib in NSCLC by upregulating EGFR expression. In the instance of copy number gain or increased

expression of the targeted gene without additional mutation, the resistance is 'drug-saturable', meaning that tumour cells are still sensitive to the drug at higher concentrations. This is true for both *BRAF* amplification and DEPTOR loss, which shift the response to targeted drugs without making them totally insensitive. Secondary 'gatekeeper' mutations that prevent drug-binding or reduce the affinity of the kinase for the drug have been identified in BCR-ABL, EGFR, and EML4-ALK (Gorre et al., 2001)(Pao et al., 2005a)(Choi et al., 2010). In such cases, tumour cells are rendered unresponsive and higher concentrations of drug are largely ineffective.

One could argue that comparatively small effects on drug sensitivity (drug-saturable) are not clinically relevant as the drug is still effective at a higher concentration. However, the study by Shi and colleagues suggests otherwise. Although *BRAF* amplification caused a level of resistance that was drug-saturable in-vitro, it was found in 20% of patients that experienced disease progression whilst being treated with BRAF inhibitors. No other commonly occurring mechanism was identified in these tumours, suggesting that *BRAF* amplification was enough to drive resistance in patients (Shi et al., 2012). Therefore although the effect of DEPTOR loss on drug sensitivity is relatively modest, it could potentially affect drug response *in vivo*.

Downstream of receptor tyrosine kinases several activating mutations have been identified which reactivate downstream signalling. Prime examples are the amplification and mutation of *KRAS* downstream of EGFR in colorectal cancer (Bonanno et al., 2010) and reactivation of MAPK signalling by COT in RAF inhibitor resistant melanoma (Johannessen et al., 2010). NF1 loss fits with this group of resistance mechanisms to activate RAS downstream of targeted inhibition. Resistance mechanisms resulting from downstream reactivation of signalling are highly potent, as the signalling input of the targeted lesion is now redundant. In patients with such resistance mechanisms, dose escalation of the targeted therapy is not as effective and alternative or additional drugs need to be used. Loss of DEPTOR could potentially also effect erlotinib resistance by activating mTOR signalling separate from its upregulation of EGFR. For example, by activating AKT and SGK1 downstream of mTORC2, DEPTOR loss could inhibit induction of

expression of pro-apoptotic proteins by forkhead transcription factors and downregulate proapoptotic BAD (Datta et al., 1997; Fu and Tindall, 2008; Garcia-Martinez and Alessi, 2008). However, a more substantial resistance to erlotinib might be expected if survival signalling was strongly activated independently of EGFR. NF1 loss results in a much more potent increase in resistance than loss of DEPTOR, indicating mechanisms of resistance activating signalling downstream of the targeted protein are a more effective strategy for cancer cells.

6.3.2 Activation of alternative signalling pathways

Another common finding in acquired resistance is the upregulation of alternative signalling pathways, leading to downstream survival signalling. A key example of this is the amplification of *MET* in erlotinib resistant NSCLC. Amplified *MET* heterodimerises with ERRB3 to activate PI3K-AKT signalling, thereby providing an alternative route to survival (Engelman et al., 2007). One of the most recently identified examples is increased activation of the tyrosine receptor kinase AXL in erlotinib-resistant NSCLC (Zhang et al., 2012). Zhang and colleagues found AXL expression and activation was increased in erlotinib resistant HCC827 cells, which seems to increase resistance at least in part by activating PI3K-AKT and MAPK pathways independently of EGFR. Another example of signalling through alternative receptors can be found in HER2 positive breast cancer, where trastuzumab resistance is associated with overexpression of EGFR and IGFR1 (Gallardo et al., 2012). These findings highlight flexibility and redundancy in the way tumour cells signal through receptor tyrosine kinases, which will be discussed further in later sections. In relation to the role of DEPTOR loss, it would be interesting to see if DEPTOR-depletion could cause upregulation of EGFR in other cancer cell lines, for example in *HER2*-amplified breast cancer cells, *BRAF*-mutant melanoma and *EML4-ALK*-positive NSCLC, where it is associated with drug resistance (Dua et al., 2010) (Corcoran et al., 2012a; Prahallad et al., 2012; Tanizaki et al., 2012). . Potentially DEPTOR loss could increase resistance to targeted therapies in multiple cancer types by upregulating EGFR as an alternative receptor tyrosine kinase

6.3.3 Histological transformation

Arguably, the least well understood class of resistance involves phenotypic transformation. One well-described type of phenotypic change is the epithelial-mesenchymal transition (EMT). EMT is a phenotypic transformation of epithelial cells to a more mesenchymal phenotype, demonstrated by loss of epithelial markers such as E-cadherin and cytokeratins, and gain of mesenchymal markers such as vimentin and N-cadherin. EMT is reported to cause resistance in multiple cancer types to targeted therapeutics, including resistance to EGFR-TKIs in NSCLC (Chung et al., 2010; Sequist et al., 2011). Epithelial-mesenchymal transition is thought to render cells less sensitive to drug treatment, via engagement of cell survival pathways such as signalling through NF-kappaB. Also, as mentioned in the introduction, EMT has been associated with 'kinase switching', therefore therapies targeted at RTKs may fail as the cells have switched dependency to signalling through an alternative receptor (Thomson et al., 2008). Recently activation of an alternative receptor and occurrence of EMT was observed with AXL activation in EGFR-mutant NSCLC which mediates resistance to EGFR TKIs (Zhang et al., 2012). We have found no evidence that NF1 loss causes EMT in NSCLC, therefore it is unlikely that depletion of NF1 contributes to erlotinib resistance via this mechanism. DEPTOR loss has been associated with EMT (Chen et al., 2012), however whether this occurs in NSCLC, or can lead to drug resistance is yet to be elucidated.

More recently histological transformation to small cell lung cancer was observed in patients with non-small cell lung cancer resistant to erlotinib treatment. How this occurs is not known, however it appears to be a bona fide resistance mechanism detected in multiple cases (Arcila et al., 2011; Sequist et al., 2011). Identification of such histological transformation has substantial ramifications for treatment, as transformed tumours behave as SCLC and respond to standard chemotherapy for this class of lung cancer. These observations point out the importance of re-biopsy of patients upon discovery of resistance, in order to successfully adjust therapy to prevent disease progression. Also, it demonstrates that histological analysis is necessary to complement genetic testing for resistance mechanisms. Sequist et al. found tumours demonstrating transformation to small cell lung cancer retained the

EGFR activating mutation and 4 out of 5 tumours showed no evidence of new mutations associated with resistance (Sequist et al., 2011). Therefore from a genetic standpoint these tumours should still be sensitive to erlotinib treatment, however this is clearly not the case.

6.4 Tumour heterogeneity as a challenge to targeted therapeutics.

Aside from the aforementioned issues that generally effect drug resistance on a cell-autonomous level there are many other mechanisms when drug resistance is considered at a tumour or patient level. With increasingly powerful DNA and RNA sequencing techniques it is now possible to probe the heterogeneity that exists within single tumours and between different tumours (primary tumours and metastases) in the same patient. Recently, Gerlinger and colleagues performed exon sequencing on patients with metastatic renal cell carcinoma and identified substantial intratumour heterogeneity, as well as heterogeneity between the primary tumour and different metastatic sites (Gerlinger et al., 2012). They found that only 34% of mutations found by multi-region sequencing of the primary tumour were detected in all regions biopsied. Such findings clearly have significant implications in the administration of targeted therapies, as potentially only a subset of tumour cells would contain the genetic lesion conferring sensitivity to treatment. In such instances only a portion of the tumour would be targeted, and could lead to the outgrowth of the non-targeted population. This work highlights the importance of identifying mutations that occur early in tumour development, and are therefore ubiquitous. Targeting of genetic alterations in the trunk of the phylogenetic tree is more likely to be an effective therapeutic approach, than targeting branch mutations, which only occur in some areas of a tumour or tumours (Gerlinger et al., 2012).

6.4.1 Evolutionary dynamics and implications for therapy

As discussed previously, the emergence of drug resistance is widely accepted to be a Darwinian process, by which tumour cells are a mixed population and the

'fittest' survive and outgrow. Drug treatment acts as a selection pressure, and enriches for tumour cells that have acquired mutations causing resistance to subsequently outgrow the remaining sensitive population. Such a model appears to be supported by studies of patients given 'drug holidays', where resistant tumours can again respond to therapy after a drug-free period, suggesting that without selection pressure the tumour is re-populated by sensitive cells (Becker et al., 2011; Oxnard et al., 2011b). This could be explained by the observation that in the absence of an EGFR TKI NSCLC cells carrying the EGFR T790M mutation proliferate more slowly than their sensitive counterparts, suggesting drug resistant clones may be less 'fit' than the bulk tumour population in untreated conditions (Chmielecki et al., 2011). However, that sensitive cells survive the initial treatment, suggests the possibility of insufficient targeting of the tumour or that these 'sensitive' cells may have some level of resistance, perhaps similar to the drug-tolerant cells seen by Sharma et al (Sharma et al., 2010). One strategy could be to adjust dosing schedules to prevent the selection of drug resistant phenotypes. Chmielecki and colleagues suggest that intermittent high-dose pulses of BIBW-2992 (an irreversible EGFR inhibitor) in conjunction with a continuous low dose of erlotinib treatment would slow the outgrowth of resistant clones (Chmielecki et al., 2011). The idea is that the low dose of erlotinib would kill sensitive cells without creating a high selective pressure which favours the expansion of resistant clones, whilst the intermittent the high dose of BIBW-2992 would kill any emerging T790M-containing cells. They found this regime did not select for T790M mutation, and PC9 cells took twice as long to develop resistance, however eventually an alternative mechanism of resistance did emerge (Chmielecki et al., 2011).

Aside from drug treatment, cancer cells must adapt to other stresses, such as hypoxia or lack of nutrients, which can vary significantly over the area of a tumour. Gillies et al. point out that different areas of a tumour are under different selection pressures, for example some areas will be more hypoxic, due to distance from blood vessels (Gillies et al., 2012). This situation can lead to substantial heterogeneity within a tumour, and can have a significant impact on cell behaviour. Therefore, one suggestion is that instead of targeting specific signalling pathways, general 'hallmarks of cancer' should be targeted instead. An example of this is the targeting of low extracellular pH, a physical characteristic of tumours associated

with drug resistance. Hypoxia and increased glycolysis in tumours creates an acidic extracellular environment, which in turn negatively effects the uptake of weak base chemotherapeutic drugs (Wojtkowiak et al., 2011). However, there are very few hallmarks of cancer that can be targeted and are truly specific to cancer cells. Essentially the same principle of targeting general characteristics underlies chemotherapy, which is aimed at the highly proliferative phenotype of cancer cells, but therefore affects all proliferating cells. This can lead to high levels of toxicity as proliferative cell populations such as lymphocytes and the intestinal epithelium are also affected. Coming full circle, toxicity is one of the reasons why more specifically targeted drugs were developed and could be a problem of more general therapeutic approaches.

6.4.2 Tumour heterogeneity – not so heterogenous after all?

There is one aspect of Gerlinger and colleagues work that does provide hope for the use of targeted agents, which is the suggestion of convergent phenotypic evolution. Distinct mutations of *SETD2*, *PTEN* and *KDM5C* were detected in different regions of the same tumours (Gerlinger et al., 2012). This suggests that mutations in the same genes can arise independently in the same tumour. Therefore, although they are genetically distinct, they rely on the same signalling pathways and potentially could be treated in the same way. This example demonstrates how in natural selection 'nature selects for phenotype, not genotype' (Gillies et al., 2012) and creates some hope that tumour cells in a genetically heterogeneous tumour may not behave so differently after all.

Other suggestions that targeted therapies can be successful in heterogeneous cancers come from ER (estrogen receptor) positive breast cancer. In this subtype of breast cancer only 10% of cells in a tumour need to be assessed as ER positive by immunohistochemistry for the tumour to be classed as ER positive. Most of these tumours respond well to endocrine therapy, which implies the tumour as a whole still depends on estrogens, even if ER expression cannot be found in all cells (Bhatia et al., 2012). This could be due to technical limitations of staining, or because ER expression fluctuates and immunohistochemistry can only provide a

snapshot. Alternatively it could be that signalling is required between different subpopulations and there is a co-dependence between ER positive and ER negative cells.

6.5 Tumour microenvironment in drug resistance

Drug resistance can arise from interactions between tumour cells and the tumour milieu, adding another layer of complexity. It has become clear that the microenvironment has a profound influence on phenotype, and in some instances can override genotype. Recently, Wilson and colleagues performed a matrix analysis where they tested the ability of six different receptor tyrosine kinase ligands to 'rescue' 41 cancer cell lines from RTK-targeted therapies (Wilson et al., 2012). They found in nearly all cell lines that a ligand for an alternative RTK can rescue cells from sensitivity to an RTK-targeted therapy. This suggests a high level of redundancy in RTK signalling, and that growth factors in the extracellular matrix potentially have very broad and potent roles in drug resistance. Some of their key findings were that exogenous HGF rescues *EGFR*-mutant NSCLC cell lines from erlotnib treatment, and also *BRAF*-mutant melanoma cells from RAF inhibition. This work was supported by another study in which expression of HGF by stromal cells is assocated wth innate resistance to RAF inhibitors in *BRAF*-mutant melanoma (Straussman et al., 2012). Mechanisms of resistance arising from the tumour microenvironment would not be identified by sequencing of the tumour cells, but could potentially by identified by immunohistochemistry. This work also relates to the upregulation of alternative receptors in resistant disease. For example, as discussed in the introduction chapter exogenous HGF can lead to resistance by promoting the amplification of *MET*, however there are differences in signalling between the transient resistance mediated by continuous presence of HGF, and permanent resistance mediated via amplified *MET* (Turke et al., 2010).

6.6 The future of targeted therapeutics

6.6.1 Combination therapies

What has become apparent is that resistance arises to all targeted therapeutics and that new approaches are needed to deal with resistance. Recently, it has been suggested that lessons could be learned from the approaches used in treating HIV, where progression is rare with current therapies (Bock and Lengauer, 2012). In contrast to single-agent targeted therapies in cancer, first-line treatment for HIV always uses a combination of drugs with different targets and mechanisms of action. The introduction of combination therapeutics in HIV has had a dramatic impact on patient survival, and one could assume a similar benefit may be seen in cancer patients. Combination therapies could provide a greater barrier to resistance, as they prevent some known feedback loops identified in cancer, and according to evolutionary principles, one would assume more genetic changes would need to be acquired before resistance emerges.

Although combination treatments are not new in cancer treatment, as different chemotherapeutic drugs have been used in combination since the 1960s (Chabner and Roberts, 2005), and targeted therapies are commonly combined with standard-of-care chemotherapy, the combination of targeted therapeutics has only recently emerged. New clinical trials demonstrate an overwhelming shift towards combination treatments has now occurred. It is clear that many drugs are not effective as single agents, most probably due to feedback mechanisms, leading to compensatory cell survival signalling. For example, in the case of rapamycin, and subsequent allosteric mTOR inhibitors, inhibition of mTORC1 results in feedback activation of AKT and MAPK signalling via IRS1/2, rendering them ineffective as single agents in many tumour types ((Carracedo et al., 2008; O'Reilly et al., 2006)). Consequently, IGFR-1 antibodies are now in clinical trials with mTOR inhibitors to prevent this feedback loop (NCT01234857). In our genome-wide screen we identified *NF1* and *DEPTOR* as genes whose loss increased resistance to erlotinib treatment in *EGFR*-mutant NSCLC. In follow-up experiments we used combinations of erlotinib with different drugs to determine combinations that may be effective in resistant patients with reduced expression of these genes. The

combination of erlotinib and a MEK inhibitor was highly effective in both cases, which suggests it may be a therapeutic option for some patients with acquired resistance to erlotinib treatment.

6.6.2 Combinations of targeted therapies – targeting the same pathway or different pathways?

Combinations of targeted therapeutics are most commonly investigated upon development of resistance to a targeted monotherapy, and the strategy of combination varies depending on the mechanisms of resistance they are employed against. Combinations may target the same protein, the same pathway or parallel pathways. For example, resistance to trastuzumab, a Her2 inhibitor is mediated by dimerization of Her2 and Her3 and continued signalling from these dimers. To overcome resistance another Her2 inhibitor, pertuzumab is effective, as it blocks Her2/Her3 dimerization (Nahta et al., 2004). An example of targeting downstream in the same pathway is combined BRAF and MEK inhibition to counteract resistance to BRAF inhibitors in melanoma that can arise through activation of MEK (by COT or CRAF activation) (Al-Lazikani et al., 2012). In this thesis a similar method of combination has been used to counter increased resistance to EGFR-TKIs. Here the EGFR inhibitor erlotinib was combined with a MEK inhibitor, to effectively block downstream activation of RAS by NF1 or DEPTOR loss. Interestingly, combined EGFR and AKT inhibition was not as effective in the mechanisms of resistance found, demonstrating not all downstream signalling pathways contribute equally to resistance.

Additionally, there is evidence to support simultaneous targeting of parallel pathways. Engelman and colleagues have suggested dual inhibition of MAPK and PI3K-mTOR signalling is required for effective treatment of *EGFR*-mutant NSCLC (Faber et al., 2009) as well as KRAS mutant lung cancer (Engelman et al., 2008). Those and similar reports combining MEK and AKT inhibition in NSCLC cell lines (Meng et al., 2010), have led to the phase I clinical trials testing the MEK and AKT inhibitor combination (NCT01021748). The observations described here are supportive of such a combination, as treatment of PC9 cells with a MEK inhibitor leads to increased phosphorylation of AKT, indicating compensatory crosstalk

between MAPK and PI3K-AKT pathways. However, there are several serious issues to consider in the development and administration of combinations of therapeutics. As described above simultaneous targeting of MEK and PI3K pathways is a highly attractive strategy to prevent signalling crosstalk, unfortunately early data from clinical trials suggest toxicity may impose limits on the effectiveness of such a combination. Shimizu and colleagues found 53.9% of patients had grade III or greater adverse effects to the combination of an AKT and MEK inhibitor, or an mTORC1 inhibitor and a MEK inhibitor, 18.4 % of whom exhibited dose-limiting toxicity (Shimizu et al., 2012).

6.6.3 Multi-target therapeutic agents

Aside from combination of (presumably) single-target drugs, drugs that simultaneously target more than one pathway have shown some promise in the clinic. Examples of multi-kinase inhibitors with clinical efficacy are sorafenib (targets PDGFR, VEGFR and Raf kinases) (Escudier et al., 2007) and vandetanib (inhibits EGFR, VEGFR and RET kinases) (Wells et al., 2012). Indeed the 'off-target' effects of drugs often contribute to their overall effectiveness, as was the case with sorafenib which was originally developed as a Raf kinase inhibitor. The use of multi-kinase inhibitors would hopefully combat some of the redundancy seen in Wilson et al. where compensatory signalling via alternative RTKs drive resistance (Wilson et al., 2012)

Other pleiotropic drugs including HSP90 (Heat shock protein 90) inhibitors, neddylation inhibitors and deactylase inhibitors are also coming to the fore. As their actions affect the function or expression of multiple oncogenic proteins simultaneously, it is likely they will provide a greater barrier to resistance than single target therapies, and may be more effective on the heterogenous tumour cell population. For example, HSP90 is a chaperone protein that regulates the folding and stability of multiple 'client' proteins including EGFR, HER2, ALK and BRAF (Neckers and Workman, 2012). Inhibition of HSP90 decreases levels of all of these proteins simultaneously, therefore they can be used in multiple cancers driven by different oncogenes, and also eliminates many potential feedback and crosstalk loops.

The neddylation inhibitor MLN4924 is another drug in phase I clinical trials (NCT00677170, NCT01011530, NCT00911066), which may have relevance to two hits from the genome-wide screen described in this thesis, DEPTOR and NF1. Neddylation is required for the function of the cullin-RING ligases subset of E3 ubiquitin ligases, and controls the targeted degradation of many proteins involved in oncogenesis. For example cullin-RING ligases are involved in the degradation of p53, p27 and IκBα (Nawrocki et al., 2012). It additionally has activity in causing DNA re-replication resulting in cancer cell death. NF1 and DEPTOR are both proteins whose degradation is regulated by cullin-RING E3 ubiquitin ligases (Duan et al., 2011; Gao et al., 2011; Tan et al., 2011; Zhao et al., 2011). Therefore it is possible that in cases where protein degradation is enhanced, such as the loss of NF1 in glioblastoma, use of a neddylation inhibitor could restore NF1 protein levels, and reduce oncogenic signalling through RAS.

However, something to consider when utilising drugs with multiple targets, is that there are also some proteins that you specifically do not want to target as they enhance toxicity and reduce efficacy. Recently Dar and colleagues used a Ret-kinase driven *Drosophila* model of multiple endocrine neoplasia type 2 to identify the compounds with the highest therapeutic index and the molecular mechanism that accounts for this (Dar et al., 2012). They discovered inhibition of Ret in conjunction with Src, Raf and S6K provided the least toxicity and optimal efficacy, whereas drugs that inhibited Ret and Tor where substantially less effective and more toxic. They identify Tor as an 'anti-target', whose inhibition increases activation of Erk signalling via feedback activation of Raf (Dar et al., 2012). This study highlights the importance assessing the toxicity of multi-target therapeutic agents, and demonstrate that multiple rounds of drug development are necessary to produce the most favourable therapeutic index.

6.6.4 Novel approaches to modelling resistance

When resistance to first-line HIV therapies arises computer-assisted resistance prediction is implemented using viral genotyping data to devise patient-specific

combination therapies. Such predictive methods are still some way off for resistance to cancer therapy, however they are certainly an attractive possibility (Bock and Lengauer, 2012). In order to create a modelling system that can predict treatment response in-depth genetic information and drug response data needs to be collected. Recently this has begun with a huge collaborative project called the 'Cancer Cell Line Encyclopedia', which was undertaken to profile the sensitivity of 479 cancer cell lines to 24 anticancer drugs. In parallel with the pharmacological data, detailed gene expression and chromosomal copy number information was obtained, as well as mutational status of more than 1600 genes (Barretina et al., 2012). The aim of the project was to identifiy genetic, gene-expression and lineage-specific determinants of sensitivity to different classes of drugs. Using this approach they confirmed known determinants, such as presence of EGFR mutations conferring erlotinib sensitivity. They also identified unknown determinants of sensitivity, for example high SLFN11 expression confers sensitivity to topoisomerase inhibitors such as Irinotecan (Barretina et al., 2012).

Additionally, screening methodologies, such as the genome-wide siRNA screen used here are useful in providing insight into mechanisms of resistance and have successfully identified clinically relevant causes of resistance. For example RNAi screening identified upregulation of EGFR as a mechanism of resistance to BRAF inhibitors in colorectal cancer (Prahallad et al., 2012). Recently, advances in technology have allowed for the considerable upscaling of RNAi, and cDNA overexpression screening. At the Broad Institute of Harvard and Massachusetts Institute of Technology, they have developed MicroSCALE technology (Microarrays of Spatially Confined Adhesive Lentiviral Features), which is essentially a miniaturised screening platform (Wood et al., 2012). This allows for massive parallel screening of the effect of the expression of lentiviral ORF or shRNA libraries on multiple cell lines, in various drug treated conditions. So far, they have used the technology to identify kinases whose overexpression increases resistance to MAPK inhibition in melanoma, and a potential role for NFκB pathway in MAPK inhibitor resistance (Wood et al., 2012).

Another of the key methodologies coming to the fore is that of 'xenopatient 'models. In such models, pieces of tumour surgical specimems from a patient are

transplanted into nude mice where they can then be treated with various therapeutic regimes in order to identify effective treatments. Bertotti and colleagues used this approach to identify markers of resistance to anti-EGFR therapy in metastatic colorectal cancer (Bertotti et al., 2011). In this study they identified amplification of Her2 as predictive of non-responsiveness to cetuximab. Xenograft experiments are carried out in immunocomprimised mice, therefore ignore any impact of the immune system, so it is necessary to combine these data with studies in good genetically engineered mouse models of resistant disease (such as the EGFR-L858R NSCLC model (Politi et al., 2010)). Such approaches will provide further insight into how tumours respond to drug treatment in the context of the whole organism, more closely mimicking human disease.

One could imagine that by integrating the results from genetically engineered mouse models, xenopatient, and patient cell line assays with detailed genomic characterisation it would be eventually possible to generate predictions of drug response based on genotype, in an approach more similar to that employed in HIV treatment (Bock and Lengauer, 2012). As long as strong biomarkers and fast diagnostic tests, such as analysis of blood biopsies (Diaz et al., 2012) (Misale et al., 2012), could be implemented, this would allow for fast application of highly personalised treatments on the occurrence of drug resistance. However it is important to note that resistance in HIV occurs as a result of mutations in relatively few genes, compared to a much more complex situation in cancer. Several hundred genes have been implicated in tumourigenesis, many of which can contribute to drug resistance, which makes modelling of resistance potentially orders of magnitude more complex.

6.7 Concluding remarks

When the studies described in this dissertation commenced, little was known about mechanisms of resistance to erlotinib in *EGFR*-mutant NSCLC, aside from the *EGFR*^{T790M} mutation and *MET* amplification. The screening approach taken here has yielded two interesting hits that validated in longer term experiments. However, as both NF1 and DEPTOR are negative regulators of downstream EGFR pathway

signalling components, it is likely that these factors could have been identified in a smaller-scale, more-candidate driven approach. Also, although Nf1 mRNA was reduced in resistant tumours in mice, currently we have not identified a mechanism of downregulation, and due to lack of clinical samples we do not have patient data to support the role of either gene in erlotinib resistance *in vivo*. RNAi screening approaches have successfully been employed to identify clinically relevant mechanism of resistance, however they are not sufficient on their own to show the relevance of specific genes *in vivo* (Holzel et al., 2010; Prahallad et al., 2012). Multiple approaches yield the most convincing evidence for mechanisms of acquired resistance, and standard practice now seems to be the combination of *in vitro* cell-based assays, mouse models, and validation in patient samples. Therefore, to confirm the role of NF1 and DEPTOR *in vivo* analysis of patient samples with acquired resistance to erlotinib would be necessary.

Having said that, reduced expression of NF1 and DEPTOR are interesting as they share properties with clinically detectable mechanisms of resistance, in that they reactivate MAPK signalling, either directly, or potentially by feedback to receptor tyrosine kinases. Studying these mechanisms we also came to the same conclusions as others, that the combination of EGFR and MEK inhibition would be effective in some tumours which have acquired resistance to EGFR targeted therapies (Misale et al., 2012). Activation of ERK seems to be a key aspect of many mechanisms of acquired resistance and a large number of clinical trials are exploring the use of MEK inhibitors, either alone or with other drugs. A recent search on the World Health Organisation International Clinical Trials Registry platform (http://apps.who.int/trialsearch) found 67 trials testing MEK inhibitors, 38 of which were testing MEK inhibitors in combination with another drug. These include the combination of erlotinib and a MEK inhibitor (NCT01192165, NCT01229150, NCT01239290), vandetanib (a VEGFR and EGFR inhibitor) and a MEK inhibitor (NCT01586624), and cetuximab and a MEK inhibitor (NCT01217450). The findings of these trials will be interesting, as our data suggests the combination of EGFR and MEK inhibition would be effective in erlotinib resistant, *EGFR*-mutant NSCLC patients who do not have the gatekeeper $EGFR^{T790M}$ mutation, where the combination would be ineffective.

It is unlikely that combination therapeutics such as EGFR-TKI and MEK inhibitor combinations will be totally free from acquired resistance, however they might improve the response rate and duration in patients. Additionally combining oncogene-targeted therapies (such as erlotinib), with more pleiotropic drugs (e.g. HSP90 inhibitors), or those targeting 'non-driver' mutations may also be effective strategies. The biological rationale behind combinations must be strong for each setting in which they are used, and toxicity must be carefully considered. If drug response predictions can be developed, and testing for strong biomarkers of response carried out swiftly, it is possible patients' treatment regimes could be quickly altered upon emergence of resistance. Then, patients may benefit from successive combinatorial treatments to significantly improve their lifespan.

Chapter 7. Appendix

Appendix 1.

Residual Z scores for genome-wide screen 1 and 2. Column A, B and C, provide the plate number, position number and well position for each siRNA pool respectively. Column D states whether the siRNA is a sample siRNA or a control siRNA. Column E shows the ID of the transcript targeted by the siRNA pool according to NCBI RefSeq database. Column F shows the Dharmacon catalog number of the siRNA pool. Column G gives the official gene symbol according to the HUGO Gene Nomenclature Committee. Columns H-P show the residual Z scores calculated by plotting each replicate of the control screen against each replicate of the drug screen. Column Q, highlighted in yellow shows the median residual Z score (median of columns H-P) and is the value we used to rank the siRNA pools. Sheet 1 shows the data for screen 1, sheet 2 shows the data for screen 2.

Appendix 2.

List of siRNA pools which appeared in the top 2.5 % of all pools in screen 1 and the top 5% of screen 2 when ranking by residual Z score. Column A shows the ID of the transcript targeted by the siRNA pool according to NCBI RefSeq database. Column B shows the Dharmacon catalog number of the siRNA pool. Column C gives the official gene symbol according to the HUGO Gene Nomenclature Committee. Column D shows the residual Z score of the siRNA pool in screen 1. Column E shows the residual Z score of the siRNA pool in screen 2. Column F indicates whether the siRNA pool appeared in the top 2.5% of screen 1 only (screen 1), or the top 2.5% of screen 1 and screen 2 (both).

Appendix 3.

Results of the deconvolution screen. Sheet 1. Results of all siRNA pools in the deconvolution screen. Column A shows the ID of the transcript targeted by the siRNA pool according to NCBI RefSeq database. Column B shows the official gene symbol according to the HUGO Gene Nomenclature Committee. Column C gives the Dharmacon ID number for each siRNA oligonucleotide. Columns D-G show the SI (sensitivity index) calculated for each siRNA oligonucleotide of the

SMARTpool. siRNAs are colour-coded as indicated according to the strength of their effect. Sheet 2. siRNA pools regarded as hits for which at least two siRNAs had an SI value of ≥ 0.10 for sensitising siRNAs or ≤ -0.15 for desensitising siRNAs.

Reference List

Al-Lazikani, B., Banerji, U., and Workman, P. (2012). Combinatorial drug therapy for cancer in the post-genomic era. Nat Biotechnol *30*, 679-692.
Amado, R.G., Wolf, M., Peeters, M., Van Cutsem, E., Siena, S., Freeman, D.J., Juan, T., Sikorski, R., Suggs, S., Radinsky, R.*, et al.* (2008). Wild-type KRAS is required for panitumumab efficacy in patients with metastatic colorectal cancer. J Clin Oncol *26*, 1626-1634.
Andersen, L.B., Ballester, R., Marchuk, D.A., Chang, E., Gutmann, D.H., Saulino, A.M., Camonis, J., Wigler, M., and Collins, F.S. (1993). A conserved alternative splice in the von Recklinghausen neurofibromatosis (NF1) gene produces two neurofibromin isoforms, both of which have GTPase-activating protein activity. Mol Cell Biol *13*, 487-495.
Annunziata, C.M., and Bates, S.E. (2010). PARP inhibitors in BRCA1/BRCA2 germline mutation carriers with ovarian and breast cancer. F1000 Biol Rep *2*.
Arcila, M.E., Oxnard, G.R., Nafa, K., Riely, G.J., Solomon, S.B., Zakowski, M.F., Kris, M.G., Pao, W., Miller, V.A., and Ladanyi, M. (2011). Rebiopsy of lung cancer patients with acquired resistance to EGFR inhibitors and enhanced detection of the T790M mutation using a locked nucleic acid-based assay. Clin Cancer Res *17*, 1169-1180.
Arifin, M., Tanimoto, K., Putra, A.C., Hiyama, E., Nishiyama, M., and Hiyama, K. (2010). Carcinogenesis and cellular immortalization without persistent inactivation of p16/Rb pathway in lung cancer. Int J Oncol *36*, 1217-1227.
Arima, Y., Hayashi, H., Kamata, K., Goto, T.M., Sasaki, M., Kuramochi, A., and Saya, H. (2010). Decreased expression of neurofibromin contributes to epithelial-mesenchymal transition in neurofibromatosis type 1. Exp Dermatol *19*, e136-141.
Baek, S.T., and Tallquist, M.D. (2012). Nf1 limits epicardial derivative expansion by regulating epithelial to mesenchymal transition and proliferation. Development *139*, 2040-2049.
Balak, M.N., Gong, Y., Riely, G.J., Somwar, R., Li, A.R., Zakowski, M.F., Chiang, A., Yang, G., Ouerfelli, O., Kris, M.G.*, et al.* (2006). Novel D761Y and common secondary T790M mutations in epidermal growth factor receptor-mutant lung adenocarcinomas with acquired resistance to kinase inhibitors. Clin Cancer Res *12*, 6494-6501.
Balsara, B.R., Sonoda, G., du Manoir, S., Siegfried, J.M., Gabrielson, E., and Testa, J.R. (1997). Comparative genomic hybridization analysis detects frequent, often high-level, overrepresentation of DNA sequences at 3q, 5p, 7p, and 8q in human non-small cell lung carcinomas. Cancer Res *57*, 2116-2120.
Barretina, J., Caponigro, G., Stransky, N., Venkatesan, K., Margolin, A.A., Kim, S., Wilson, C.J., Lehar, J., Kryukov, G.V., Sonkin, D.*, et al.* (2012). The Cancer Cell Line Encyclopedia enables predictive modelling of anticancer drug sensitivity. Nature *483*, 603-607.
Bartel, D.P. (2009). MicroRNAs: target recognition and regulatory functions. Cell *136*, 215-233.
Basu, T.N., Gutmann, D.H., Fletcher, J.A., Glover, T.W., Collins, F.S., and Downward, J. (1992). Aberrant regulation of ras proteins in malignant tumour cells from type 1 neurofibromatosis patients. Nature *356*, 713-715.
Becker, A., Crombag, L., Heideman, D.A., Thunnissen, F.B., van Wijk, A.W., Postmus, P.E., and Smit, E.F. (2011). Retreatment with erlotinib: Regain of TKI sensitivity following a drug holiday for patients with NSCLC who initially responded to EGFR-TKI treatment. Eur J Cancer.
Berger, A.H., Knudson, A.G., and Pandolfi, P.P. (2011). A continuum model for tumour suppression. Nature *476*, 163-169.

Bertotti, A., Migliardi, G., Galimi, F., Sassi, F., Torti, D., Isella, C., Cora, D., Di Nicolantonio, F., Buscarino, M., Petti, C.*, et al.* (2011). A molecularly annotated platform of patient-derived xenografts ("xenopatients") identifies HER2 as an effective therapeutic target in cetuximab-resistant colorectal cancer. Cancer Discov *1*, 508-523.
Bhatia, S., Frangioni, J.V., Hoffman, R.M., Iafrate, A.J., and Polyak, K. (2012). The challenges posed by cancer heterogeneity. Nat Biotechnol *30*, 604-610.
Birge, R.B., Kalodimos, C., Inagaki, F., and Tanaka, S. (2009). Crk and CrkL adaptor proteins: networks for physiological and pathological signaling. Cell Commun Signal *7*, 13.
Bivona, T.G., Hieronymus, H., Parker, J., Chang, K., Taron, M., Rosell, R., Moonsamy, P., Dahlman, K., Miller, V.A., Costa, C.*, et al.* (2011). FAS and NF-kappaB signalling modulate dependence of lung cancers on mutant EGFR. Nature *471*, 523-526.
Bock, C., and Lengauer, T. (2012). Managing drug resistance in cancer: lessons from HIV therapy. Nat Rev Cancer *12*, 494-501.
Bonanno, L., Schiavon, M., Nardo, G., Bertorelle, R., Bonaldi, L., Galligioni, A., Indraccolo, S., Pasello, G., Rea, F., and Favaretto, A. (2010). Prognostic and predictive implications of EGFR mutations, EGFR copy number and KRAS mutations in advanced stage lung adenocarcinoma. Anticancer Res *30*, 5121-5128.
Bonfini, L., Karlovich, C.A., Dasgupta, C., and Banerjee, U. (1992). The Son of sevenless gene product: a putative activator of Ras. Science *255*, 603-606.
Boutros, M., Bras, L.P., and Huber, W. (2006). Analysis of cell-based RNAi screens. Genome Biol *7*, R66.
Bradford, M.M. (1976). A rapid and sensitive method for the quantitation of microgram quantities of protein utilizing the principle of protein-dye binding. Anal Biochem *72*, 248-254.
Brown, M.D., and Sacks, D.B. (2009). Protein scaffolds in MAP kinase signalling. Cell Signal *21*, 462-469.
Buck, E., Eyzaguirre, A., Barr, S., Thompson, S., Sennello, R., Young, D., Iwata, K.K., Gibson, N.W., Cagnoni, P., and Haley, J.D. (2007). Loss of homotypic cell adhesion by epithelial-mesenchymal transition or mutation limits sensitivity to epidermal growth factor receptor inhibition. Mol Cancer Ther *6*, 532-541.
Buday, L., and Downward, J. (1993). Epidermal growth factor regulates p21ras through the formation of a complex of receptor, Grb2 adapter protein, and Sos nucleotide exchange factor. Cell *73*, 611-620.
The Cancer Genome Atlas Research Network (2008). Comprehensive genomic characterization defines human glioblastoma genes and core pathways. Nature *455*, 1061-1068.
The Cancer Genome Atlas Research Network (2011). Integrated genomic analyses of ovarian carcinoma. Nature *474*, 609-615.
Cantley, L.C., and Neel, B.G. (1999). New insights into tumor suppression: PTEN suppresses tumor formation by restraining the phosphoinositide 3-kinase/AKT pathway. Proc Natl Acad Sci U S A *96*, 4240-4245.
Cappione, A.J., French, B.L., and Skuse, G.R. (1997). A potential role for NF1 mRNA editing in the pathogenesis of NF1 tumors. Am J Hum Genet *60*, 305-312.
Cappuzzo, F., Hirsch, F.R., Rossi, E., Bartolini, S., Ceresoli, G.L., Bemis, L., Haney, J., Witta, S., Danenberg, K., Domenichini, I.*, et al.* (2005). Epidermal growth factor receptor gene and protein and gefitinib sensitivity in non-small-cell lung cancer. J Natl Cancer Inst *97*, 643-655.
Carpten, J.D., Faber, A.L., Horn, C., Donoho, G.P., Briggs, S.L., Robbins, C.M., Hostetter, G., Boguslawski, S., Moses, T.Y., Savage, S.*, et al.* (2007). A transforming mutation in the pleckstrin homology domain of AKT1 in cancer. Nature *448*, 439-444.
Carracedo, A., Alimonti, A., and Pandolfi, P.P. (2011). PTEN level in tumor suppression: how much is too little? Cancer Res *71*, 629-633.

Carracedo, A., Ma, L., Teruya-Feldstein, J., Rojo, F., Salmena, L., Alimonti, A., Egia, A., Sasaki, A.T., Thomas, G., Kozma, S.C.*, et al.* (2008). Inhibition of mTORC1 leads to MAPK pathway activation through a PI3K-dependent feedback loop in human cancer. J Clin Invest *118*, 3065-3074.
Carter, P., Presta, L., Gorman, C.M., Ridgway, J.B., Henner, D., Wong, W.L., Rowland, A.M., Kotts, C., Carver, M.E., and Shepard, H.M. (1992). Humanization of an anti-p185HER2 antibody for human cancer therapy. Proc Natl Acad Sci U S A *89*, 4285-4289.
Casar, B., Pinto, A., and Crespo, P. (2008). Essential role of ERK dimers in the activation of cytoplasmic but not nuclear substrates by ERK-scaffold complexes. Mol Cell *31*, 708-721.
Castellano, E., and Downward, J. (2011). RAS Interaction with PI3K: More Than Just Another Effector Pathway. Genes Cancer *2*, 261-274.
Chabner, B.A., and Roberts, T.G., Jr. (2005). Timeline: Chemotherapy and the war on cancer. Nat Rev Cancer *5*, 65-72.
Chai, G., Liu, N., Ma, J., Li, H., Oblinger, J.L., Prahalad, A.K., Gong, M., Chang, L.S., Wallace, M., Muir, D.*, et al.* (2010). MicroRNA-10b regulates tumorigenesis in neurofibromatosis type 1. Cancer Sci *101*, 1997-2004.
Chandarlapaty, S., Sawai, A., Scaltriti, M., Rodrik-Outmezguine, V., Grbovic-Huezo, O., Serra, V., Majumder, P.K., Baselga, J., and Rosen, N. (2011). AKT inhibition relieves feedback suppression of receptor tyrosine kinase expression and activity. Cancer Cell *19*, 58-71.
Chen, R., Yang, Q., and Lee, J.D. (2012). BMK1 kinase suppresses epithelial-mesenchymal transition through the Akt/GSK3beta signaling pathway. Cancer Res *72*, 1579-1587.
Cheong, H., Lu, C., Lindsten, T., and Thompson, C.B. (2012). Therapeutic targets in cancer cell metabolism and autophagy. Nat Biotechnol *30*, 671-678.
Cheung, H.W., Du, J., Boehm, J.S., He, F., Weir, B.A., Wang, X., Butaney, M., Sequist, L.V., Luo, B., Engelman, J.A.*, et al.* (2011a). Amplification of CRKL Induces Transformation and Epidermal Growth Factor Receptor Inhibitor Resistance in Human Non-Small Cell Lung Cancers. Cancer Discov *1*, 608-625.
Cheung, L.W., Hennessy, B.T., Li, J., Yu, S., Myers, A.P., Djordjevic, B., Lu, Y., Stemke-Hale, K., Zhang, F., Ju, Z.*, et al.* (2011b). High Frequency of PIK3R1 and PIK3R2 Mutations in Endometrial Cancer Elucidates a Novel Mechanism for Regulation of PTEN Protein Stability. Cancer Discov *1*, 170-185.
Chmielecki, J., Foo, J., Oxnard, G.R., Hutchinson, K., Ohashi, K., Somwar, R., Wang, L., Amato, K.R., Arcila, M., Sos, M.L.*, et al.* (2011). Optimization of dosing for EGFR-mutant non-small cell lung cancer with evolutionary cancer modeling. Sci Transl Med *3*, 90ra59.
Choi, Y.L., Soda, M., Yamashita, Y., Ueno, T., Takashima, J., Nakajima, T., Yatabe, Y., Takeuchi, K., Hamada, T., Haruta, H.*, et al.* (2010). EML4-ALK mutations in lung cancer that confer resistance to ALK inhibitors. N Engl J Med *363*, 1734-1739.
Chuang, C.F., and Ng, S.Y. (1994). Functional divergence of the MAP kinase pathway. ERK1 and ERK2 activate specific transcription factors. FEBS Lett *346*, 229-234.
Chung, J.H., Rho, J.K., Xu, X., Lee, J.S., Yoon, H.I., Lee, C.T., Choi, Y.J., Kim, H.R., Kim, C.H., and Lee, J.C. (2010). Clinical and molecular evidences of epithelial to mesenchymal transition in acquired resistance to EGFR-TKIs. Lung Cancer.
Cichowski, K., Santiago, S., Jardim, M., Johnson, B.W., and Jacks, T. (2003). Dynamic regulation of the Ras pathway via proteolysis of the NF1 tumor suppressor. Genes Dev *17*, 449-454.
Collinet, C., Stoter, M., Bradshaw, C.R., Samusik, N., Rink, J.C., Kenski, D., Habermann, B., Buchholz, F., Henschel, R., Mueller, M.S.*, et al.* (2010). Systems survey of endocytosis by multiparametric image analysis. Nature *464*, 243-249.

Corcoran, R.B., Ebi, H., Turke, A.B., Coffee, E.M., Nishino, M., Cogdill, A.P., Brown, R.D., Della Pelle, P., Dias-Santagata, D., Hung, K.E.*, et al.* (2012a). EGFR-mediated re-activation of MAPK signaling contributes to insensitivity of BRAF mutant colorectal cancers to RAF inhibition with vemurafenib. Cancer Discov *2*, 227-235.
Corcoran, R.B., Ebi, H., Turke, A.B., Coffee, E.M., Nishino, M., Cogdill, A.P., Brown, R.D., Pelle, P.D., Dias-Santagata, D., Hung, K.E.*, et al.* (2012b). EGFR-mediated re-activation of MAPK signaling contributes to insensitivity of BRAF mutant colorectal cancers to RAF inhibition with vemurafenib. Cancer Discov *2*, 227-235.
Currie, R.A., Walker, K.S., Gray, A., Deak, M., Casamayor, A., Downes, C.P., Cohen, P., Alessi, D.R., and Lucocq, J. (1999). Role of phosphatidylinositol 3,4,5-trisphosphate in regulating the activity and localization of 3-phosphoinositide-dependent protein kinase-1. Biochem J *337 (Pt 3)*, 575-583.
Dar, A.C., Das, T.K., Shokat, K.M., and Cagan, R.L. (2012). Chemical genetic discovery of targets and anti-targets for cancer polypharmacology. Nature *486*, 80-84.
Datta, S.R., Dudek, H., Tao, X., Masters, S., Fu, H., Gotoh, Y., and Greenberg, M.E. (1997). Akt phosphorylation of BAD couples survival signals to the cell-intrinsic death machinery. Cell *91*, 231-241.
DeFeo, D., Gonda, M.A., Young, H.A., Chang, E.H., Lowy, D.R., Scolnick, E.M., and Ellis, R.W. (1981). Analysis of two divergent rat genomic clones homologous to the transforming gene of Harvey murine sarcoma virus. Proc Natl Acad Sci U S A *78*, 3328-3332.
Dempke, W.C., and Heinemann, V. (2010). Ras mutational status is a biomarker for resistance to EGFR inhibitors in colorectal carcinoma. Anticancer Res *30*, 4673-4677.
Dent, P., Haser, W., Haystead, T.A., Vincent, L.A., Roberts, T.M., and Sturgill, T.W. (1992). Activation of mitogen-activated protein kinase kinase by v-Raf in NIH 3T3 cells and in vitro. Science *257*, 1404-1407.
Der, C.J., Krontiris, T.G., and Cooper, G.M. (1982). Transforming genes of human bladder and lung carcinoma cell lines are homologous to the ras genes of Harvey and Kirsten sarcoma viruses. Proc Natl Acad Sci U S A *79*, 3637-3640.
Diaz, L.A., Jr., Williams, R.T., Wu, J., Kinde, I., Hecht, J.R., Berlin, J., Allen, B., Bozic, I., Reiter, J.G., Nowak, M.A.*, et al.* (2012). The molecular evolution of acquired resistance to targeted EGFR blockade in colorectal cancers. Nature *486*, 537-540.
Ding, L., Getz, G., Wheeler, D.A., Mardis, E.R., McLellan, M.D., Cibulskis, K., Sougnez, C., Greulich, H., Muzny, D.M., Morgan, M.B.*, et al.* (2008). Somatic mutations affect key pathways in lung adenocarcinoma. Nature *455*, 1069-1075.
Doebele, R.C., Pilling, A.B., Aisner, D.L., Kutateladze, T.G., Le, A.T., Weickhardt, A.J., Kondo, K.L., Linderman, D.J., Heasley, L.E., Franklin, W.A.*, et al.* (2012). Mechanisms of resistance to crizotinib in patients with ALK gene rearranged non-small cell lung cancer. Clin Cancer Res *18*, 1472-1482.
Dorrello, N.V., Peschiaroli, A., Guardavaccaro, D., Colburn, N.H., Sherman, N.E., and Pagano, M. (2006). S6K1- and betaTRCP-mediated degradation of PDCD4 promotes protein translation and cell growth. Science *314*, 467-471.
Downward, J. (2009). Cancer: A tumour gene's fatal flaws. Nature *462*, 44-45.
Downward, J., Yarden, Y., Mayes, E., Scrace, G., Totty, N., Stockwell, P., Ullrich, A., Schlessinger, J., and Waterfield, M.D. (1984). Close similarity of epidermal growth factor receptor and v-erb-B oncogene protein sequences. Nature *307*, 521-527.
Druker, B.J., Tamura, S., Buchdunger, E., Ohno, S., Segal, G.M., Fanning, S., Zimmermann, J., and Lydon, N.B. (1996). Effects of a selective inhibitor of the Abl tyrosine kinase on the growth of Bcr-Abl positive cells. Nat Med *2*, 561-566.
Dua, R., Zhang, J., Nhonthachit, P., Penuel, E., Petropoulos, C., and Parry, G. (2010). EGFR over-expression and activation in high HER2, ER negative breast cancer cell line induces trastuzumab resistance. Breast Cancer Res Treat *122*, 685-697.

Duan, S., Skaar, J.R., Kuchay, S., Toschi, A., Kanarek, N., Ben-Neriah, Y., and Pagano, M. (2011). mTOR generates an auto-amplification loop by triggering the betaTrCP- and CK1alpha-dependent degradation of DEPTOR. Mol Cell *44*, 317-324.
Ebi, H., Corcoran, R.B., Singh, A., Chen, Z., Song, Y., Lifshits, E., Ryan, D.P., Meyerhardt, J.A., Benes, C., Settleman, J.*, et al.* (2011). Receptor tyrosine kinases exert dominant control over PI3K signaling in human KRAS mutant colorectal cancers. J Clin Invest *121*, 4311-4321.
Echeverri, C.J., Beachy, P.A., Baum, B., Boutros, M., Buchholz, F., Chanda, S.K., Downward, J., Ellenberg, J., Fraser, A.G., Hacohen, N.*, et al.* (2006). Minimizing the risk of reporting false positives in large-scale RNAi screens. Nat Methods *3*, 777-779.
Efeyan, A., and Sabatini, D.M. (2010). mTOR and cancer: many loops in one pathway. Curr Opin Cell Biol *22*, 169-176.
Elbashir, S.M., Harborth, J., Lendeckel, W., Yalcin, A., Weber, K., and Tuschl, T. (2001). Duplexes of 21-nucleotide RNAs mediate RNA interference in cultured mammalian cells. Nature *411*, 494-498.
Engelman, J.A., Chen, L., Tan, X., Crosby, K., Guimaraes, A.R., Upadhyay, R., Maira, M., McNamara, K., Perera, S.A., Song, Y.*, et al.* (2008). Effective use of PI3K and MEK inhibitors to treat mutant Kras G12D and PIK3CA H1047R murine lung cancers. Nat Med *14*, 1351-1356.
Engelman, J.A., Luo, J., and Cantley, L.C. (2006). The evolution of phosphatidylinositol 3-kinases as regulators of growth and metabolism. Nat Rev Genet *7*, 606-619.
Engelman, J.A., Zejnullahu, K., Mitsudomi, T., Song, Y., Hyland, C., Park, J.O., Lindeman, N., Gale, C.M., Zhao, X., Christensen, J.*, et al.* (2007). MET amplification leads to gefitinib resistance in lung cancer by activating ERBB3 signaling. Science *316*, 1039-1043.
Escudier, B., Eisen, T., Stadler, W.M., Szczylik, C., Oudard, S., Siebels, M., Negrier, S., Chevreau, C., Solska, E., Desai, A.A.*, et al.* (2007). Sorafenib in advanced clear-cell renal-cell carcinoma. N Engl J Med *356*, 125-134.
Faber, A.C., Li, D., Song, Y., Liang, M.C., Yeap, B.Y., Bronson, R.T., Lifshits, E., Chen, Z., Maira, S.M., Garcia-Echeverria, C.*, et al.* (2009). Differential induction of apoptosis in HER2 and EGFR addicted cancers following PI3K inhibition. Proc Natl Acad Sci U S A *106*, 19503-19508.
Farmer, H., McCabe, N., Lord, C.J., Tutt, A.N., Johnson, D.A., Richardson, T.B., Santarosa, M., Dillon, K.J., Hickson, I., Knights, C.*, et al.* (2005). Targeting the DNA repair defect in BRCA mutant cells as a therapeutic strategy. Nature *434*, 917-921.
Feller, S.M. (2001). Crk family adaptors-signalling complex formation and biological roles. Oncogene *20*, 6348-6371.
Fire, A., Xu, S., Montgomery, M.K., Kostas, S.A., Driver, S.E., and Mello, C.C. (1998). Potent and specific genetic interference by double-stranded RNA in Caenorhabditis elegans. Nature *391*, 806-811.
Foulds, L. (1954). The experimental study of tumor progression: a review. Cancer Res *14*, 327-339.
Frank, M.J., Dawson, D.W., Bensinger, S.J., Hong, J.S., Knosp, W.M., Xu, L., Balatoni, C.E., Allen, E.L., Shen, R.R., Bar-Sagi, D.*, et al.* (2009). Expression of sprouty2 inhibits B-cell proliferation and is epigenetically silenced in mouse and human B-cell lymphomas. Blood *113*, 2478-2487.
Fu, Z., and Tindall, D.J. (2008). FOXOs, cancer and regulation of apoptosis. Oncogene *27*, 2312-2319.
Fujimoto, N., Wislez, M., Zhang, J., Iwanaga, K., Dackor, J., Hanna, A.E., Kalyankrishna, S., Cody, D.D., Price, R.E., Sato, M.*, et al.* (2005). High expression of ErbB family members and their ligands in lung adenocarcinomas that are sensitive to inhibition of epidermal growth factor receptor. Cancer Res *65*, 11478-11485.

Fujino, S., Enokibori, T., Tezuka, N., Asada, Y., Inoue, S., Kato, H., and Mori, A. (1996). A comparison of epidermal growth factor receptor levels and other prognostic parameters in non-small cell lung cancer. Eur J Cancer *32A*, 2070-2074.
Fukuoka, M., Yano, S., Giaccone, G., Tamura, T., Nakagawa, K., Douillard, J.Y., Nishiwaki, Y., Vansteenkiste, J., Kudoh, S., Rischin, D*., et al.* (2003). Multi-institutional randomized phase II trial of gefitinib for previously treated patients with advanced non-small-cell lung cancer (The IDEAL 1 Trial) [corrected]. J Clin Oncol *21*, 2237-2246.
Gallardo, A., Lerma, E., Escuin, D., Tibau, A., Munoz, J., Ojeda, B., Barnadas, A., Adrover, E., Sanchez-Tejada, L., Giner, D*., et al.* (2012). Increased signalling of EGFR and IGF1R, and deregulation of PTEN/PI3K/Akt pathway are related with trastuzumab resistance in HER2 breast carcinomas. Br J Cancer *106*, 1367-1373.
Galluzzi, L., Vitale, I., Senovilla, L., Olaussen, K.A., Pinna, G., Eisenberg, T., Goubar, A., Martins, I., Michels, J., Kratassiouk, G*., et al.* (2012). Prognostic impact of vitamin b6 metabolism in lung cancer. Cell Rep *2*, 257-269.
Gao, D., Inuzuka, H., Tan, M.K., Fukushima, H., Locasale, J.W., Liu, P., Wan, L., Zhai, B., Chin, Y.R., Shaik, S*., et al.* (2011). mTOR drives its own activation via SCF(betaTrCP)-dependent degradation of the mTOR inhibitor DEPTOR. Mol Cell *44*, 290-303.
Garcia-Martinez, J.M., and Alessi, D.R. (2008). mTOR complex 2 (mTORC2) controls hydrophobic motif phosphorylation and activation of serum- and glucocorticoid-induced protein kinase 1 (SGK1). Biochem J *416*, 375-385.
Gazdar, A.F. (2009). Activating and resistance mutations of EGFR in non-small-cell lung cancer: role in clinical response to EGFR tyrosine kinase inhibitors. Oncogene *28 Suppl 1*, S24-31.
Gerlinger, M., Rowan, A.J., Horswell, S., Larkin, J., Endesfelder, D., Gronroos, E., Martinez, P., Matthews, N., Stewart, A., Tarpey, P*., et al.* (2012). Intratumor heterogeneity and branched evolution revealed by multiregion sequencing. N Engl J Med *366*, 883-892.
Gibbs, J.B., Sigal, I.S., Poe, M., and Scolnick, E.M. (1984). Intrinsic GTPase activity distinguishes normal and oncogenic ras p21 molecules. Proc Natl Acad Sci U S A *81*, 5704-5708.
Gideon, P., John, J., Frech, M., Lautwein, A., Clark, R., Scheffler, J.E., and Wittinghofer, A. (1992). Mutational and kinetic analyses of the GTPase-activating protein (GAP)-p21 interaction: the C-terminal domain of GAP is not sufficient for full activity. Mol Cell Biol *12*, 2050-2056.
Gill, R.K., Yang, S.H., Meerzaman, D., Mechanic, L.E., Bowman, E.D., Jeon, H.S., Roy Chowdhuri, S., Shakoori, A., Dracheva, T., Hong, K.M*., et al.* (2011). Frequent homozygous deletion of the LKB1/STK11 gene in non-small cell lung cancer. Oncogene.
Gillies, R.J., Verduzco, D., and Gatenby, R.A. (2012). Evolutionary dynamics of carcinogenesis and why targeted therapy does not work. Nat Rev Cancer *12*, 487-493.
Godin-Heymann, N., Ulkus, L., Brannigan, B.W., McDermott, U., Lamb, J., Maheswaran, S., Settleman, J., and Haber, D.A. (2008). The T790M "gatekeeper" mutation in EGFR mediates resistance to low concentrations of an irreversible EGFR inhibitor. Mol Cancer Ther *7*, 874-879.
Gorre, M.E., Mohammed, M., Ellwood, K., Hsu, N., Paquette, R., Rao, P.N., and Sawyers, C.L. (2001). Clinical resistance to STI-571 cancer therapy caused by BCR-ABL gene mutation or amplification. Science *293*, 876-880.
Graus-Porta, D., Beerli, R.R., Daly, J.M., and Hynes, N.E. (1997). ErbB-2, the preferred heterodimerization partner of all ErbB receptors, is a mediator of lateral signaling. EMBO J *16*, 1647-1655.

Graus-Porta, D., Beerli, R.R., and Hynes, N.E. (1995). Single-chain antibody-mediated intracellular retention of ErbB-2 impairs Neu differentiation factor and epidermal growth factor signaling. Mol Cell Biol *15*, 1182-1191.
Greulich, H., Chen, T.H., Feng, W., Janne, P.A., Alvarez, J.V., Zappaterra, M., Bulmer, S.E., Frank, D.A., Hahn, W.C., Sellers, W.R.*, et al.* (2005). Oncogenic transformation by inhibitor-sensitive and -resistant EGFR mutants. PLoS Med *2*, e313.
Guix, M., Faber, A.C., Wang, S.E., Olivares, M.G., Song, Y., Qu, S., Rinehart, C., Seidel, B., Yee, D., Arteaga, C.L.*, et al.* (2008). Acquired resistance to EGFR tyrosine kinase inhibitors in cancer cells is mediated by loss of IGF-binding proteins. J Clin Invest *118*, 2609-2619.
Hahn, W.C., Counter, C.M., Lundberg, A.S., Beijersbergen, R.L., Brooks, M.W., and Weinberg, R.A. (1999). Creation of human tumour cells with defined genetic elements. Nature *400*, 464-468.
Hamilton, A.J., and Baulcombe, D.C. (1999). A species of small antisense RNA in posttranscriptional gene silencing in plants. Science *286*, 950-952.
Han, W., Pan, H., Chen, Y., Sun, J., Wang, Y., Li, J., Ge, W., Feng, L., Lin, X., Wang, X.*, et al.* (2011). EGFR tyrosine kinase inhibitors activate autophagy as a cytoprotective response in human lung cancer cells. PLoS One *6*, e18691.
Hanahan, D., and Weinberg, R.A. (2011). Hallmarks of cancer: the next generation. Cell *144*, 646-674.
Harder, A., Rosche, M., Reuss, D.E., Holtkamp, N., Uhlmann, K., Friedrich, R., Mautner, V.F., and von Deimling, A. (2004). Methylation analysis of the neurofibromatosis type 1 (NF1) promoter in peripheral nerve sheath tumours. Eur J Cancer *40*, 2820-2828.
Heist, R.S., and Engelman, J.A. (2012). SnapShot: non-small cell lung cancer. Cancer Cell *21*, 448 e442.
Helfrich, B.A., Raben, D., Varella-Garcia, M., Gustafson, D., Chan, D.C., Bemis, L., Coldren, C., Baron, A., Zeng, C., Franklin, W.A.*, et al.* (2006). Antitumor activity of the epidermal growth factor receptor (EGFR) tyrosine kinase inhibitor gefitinib (ZD1839, Iressa) in non-small cell lung cancer cell lines correlates with gene copy number and EGFR mutations but not EGFR protein levels. Clin Cancer Res *12*, 7117-7125.
Hirsch, F.R., Varella-Garcia, M., Bunn, P.A., Jr., Di Maria, M.V., Veve, R., Bremmes, R.M., Baron, A.E., Zeng, C., and Franklin, W.A. (2003). Epidermal growth factor receptor in non-small-cell lung carcinomas: correlation between gene copy number and protein expression and impact on prognosis. J Clin Oncol *21*, 3798-3807.
Hirsch, F.R., Varella-Garcia, M., and Cappuzzo, F. (2009). Predictive value of EGFR and HER2 overexpression in advanced non-small-cell lung cancer. Oncogene *28 Suppl 1*, S32-37.
Hollander, M.C., Blumenthal, G.M., and Dennis, P.A. (2011). PTEN loss in the continuum of common cancers, rare syndromes and mouse models. Nat Rev Cancer *11*, 289-301.
Holz, M.K., Ballif, B.A., Gygi, S.P., and Blenis, J. (2005). mTOR and S6K1 mediate assembly of the translation preinitiation complex through dynamic protein interchange and ordered phosphorylation events. Cell *123*, 569-580.
Holzel, M., Huang, S., Koster, J., Ora, I., Lakeman, A., Caron, H., Nijkamp, W., Xie, J., Callens, T., Asgharzadeh, S.*, et al.* (2010). NF1 is a tumor suppressor in neuroblastoma that determines retinoic acid response and disease outcome. Cell *142*, 218-229.
Hresko, R.C., and Mueckler, M. (2005). mTOR.RICTOR is the Ser473 kinase for Akt/protein kinase B in 3T3-L1 adipocytes. J Biol Chem *280*, 40406-40416.
Hsieh, A.C., Costa, M., Zollo, O., Davis, C., Feldman, M.E., Testa, J.R., Meyuhas, O., Shokat, K.M., and Ruggero, D. (2010). Genetic dissection of the oncogenic mTOR

pathway reveals druggable addiction to translational control via 4EBP-eIF4E. Cancer Cell *17*, 249-261.
Hsieh, A.C., Liu, Y., Edlind, M.P., Ingolia, N.T., Janes, M.R., Sher, A., Shi, E.Y., Stumpf, C.R., Christensen, C., Bonham, M.J.*, et al.* (2012). The translational landscape of mTOR signalling steers cancer initiation and metastasis. Nature *485*, 55-61.
Inoki, K., and Guan, K.L. (2009). Tuberous sclerosis complex, implication from a rare genetic disease to common cancer treatment. Hum Mol Genet *18*, R94-100.
Inoki, K., Li, Y., Xu, T., and Guan, K.L. (2003a). Rheb GTPase is a direct target of TSC2 GAP activity and regulates mTOR signaling. Genes Dev *17*, 1829-1834.
Inoki, K., Li, Y., Zhu, T., Wu, J., and Guan, K.L. (2002). TSC2 is phosphorylated and inhibited by Akt and suppresses mTOR signalling. Nat Cell Biol *4*, 648-657.
Inoki, K., Zhu, T., and Guan, K.L. (2003b). TSC2 mediates cellular energy response to control cell growth and survival. Cell *115*, 577-590.
Jacinto, E., Loewith, R., Schmidt, A., Lin, S., Ruegg, M.A., Hall, A., and Hall, M.N. (2004). Mammalian TOR complex 2 controls the actin cytoskeleton and is rapamycin insensitive. Nat Cell Biol *6*, 1122-1128.
Jackson, A.L., Bartz, S.R., Schelter, J., Kobayashi, S.V., Burchard, J., Mao, M., Li, B., Cavet, G., and Linsley, P.S. (2003). Expression profiling reveals off-target gene regulation by RNAi. Nat Biotechnol *21*, 635-637.
Ji, D., Deeds, S.L., and Weinstein, E.J. (2007). A screen of shRNAs targeting tumor suppressor genes to identify factors involved in A549 paclitaxel sensitivity. Oncol Rep *18*, 1499-1505.
Johannessen, C.M., Boehm, J.S., Kim, S.Y., Thomas, S.R., Wardwell, L., Johnson, L.A., Emery, C.M., Stransky, N., Cogdill, A.P., Barretina, J.*, et al.* (2010). COT drives resistance to RAF inhibition through MAP kinase pathway reactivation. Nature *468*, 968-972.
Johnson, M.R., DeClue, J.E., Felzmann, S., Vass, W.C., Xu, G., White, R., and Lowy, D.R. (1994). Neurofibromin can inhibit Ras-dependent growth by a mechanism independent of its GTPase-accelerating function. Mol Cell Biol *14*, 641-645.
Kaizuka, T., Hara, T., Oshiro, N., Kikkawa, U., Yonezawa, K., Takehana, K., Iemura, S., Natsume, T., and Mizushima, N. (2010). Tti1 and Tel2 are critical factors in mammalian target of rapamycin complex assembly. J Biol Chem *285*, 20109-20116.
Karapetis, C.S., Khambata-Ford, S., Jonker, D.J., O'Callaghan, C.J., Tu, D., Tebbutt, N.C., Simes, R.J., Chalchal, H., Shapiro, J.D., Robitaille, S.*, et al.* (2008). K-ras mutations and benefit from cetuximab in advanced colorectal cancer. N Engl J Med *359*, 1757-1765.
Karnoub, A.E., and Weinberg, R.A. (2008). Ras oncogenes: split personalities. Nat Rev Mol Cell Biol *9*, 517-531.
Kim, H.H., Vijapurkar, U., Hellyer, N.J., Bravo, D., and Koland, J.G. (1998). Signal transduction by epidermal growth factor and heregulin via the kinase-deficient ErbB3 protein. Biochem J *334 (Pt 1)*, 189-195.
Kim, H.R., Shim, H.S., Chung, J.H., Lee, Y.J., Hong, Y.K., Rha, S.Y., Kim, S.H., Ha, S.J., Kim, S.K., Chung, K.Y.*, et al.* (2011). Distinct clinical features and outcomes in never-smokers with nonsmall cell lung cancer who harbor EGFR or KRAS mutations or ALK rearrangement. Cancer.
Kim, S.M., Kim, J.S., Kim, J.H., Yun, C.O., Kim, E.M., Kim, H.K., Solca, F., Choi, S.Y., and Cho, B.C. (2010a). Acquired resistance to cetuximab is mediated by increased PTEN instability and leads cross-resistance to gefitinib in HCC827 NSCLC cells. Cancer Lett *296*, 150-159.
Kim, Y.H., Kwei, K.A., Girard, L., Salari, K., Kao, J., Pacyna-Gengelbach, M., Wang, P., Hernandez-Boussard, T., Gazdar, A.F., Petersen, I.*, et al.* (2010b). Genomic and functional analysis identifies CRKL as an oncogene amplified in lung cancer. Oncogene *29*, 1421-1430.

King, C.R., Kraus, M.H., and Aaronson, S.A. (1985). Amplification of a novel v-erbB-related gene in a human mammary carcinoma. Science *229*, 974-976.
Klapper, L.N., Glathe, S., Vaisman, N., Hynes, N.E., Andrews, G.C., Sela, M., and Yarden, Y. (1999). The ErbB-2/HER2 oncoprotein of human carcinomas may function solely as a shared coreceptor for multiple stroma-derived growth factors. Proc Natl Acad Sci U S A *96*, 4995-5000.
Knudson, A.G., Jr. (1971). Mutation and cancer: statistical study of retinoblastoma. Proc Natl Acad Sci U S A *68*, 820-823.
Kornfeld, K., Hom, D.B., and Horvitz, H.R. (1995). The ksr-1 gene encodes a novel protein kinase involved in Ras-mediated signaling in C. elegans. Cell *83*, 903-913.
Kraus, M.H., Issing, W., Miki, T., Popescu, N.C., and Aaronson, S.A. (1989). Isolation and characterization of ERBB3, a third member of the ERBB/epidermal growth factor receptor family: evidence for overexpression in a subset of human mammary tumors. Proc Natl Acad Sci U S A *86*, 9193-9197.
Kris, M.G., Natale, R.B., Herbst, R.S., Lynch, T.J., Jr., Prager, D., Belani, C.P., Schiller, J.H., Kelly, K., Spiridonidis, H., Sandler, A.*, et al.* (2003). Efficacy of gefitinib, an inhibitor of the epidermal growth factor receptor tyrosine kinase, in symptomatic patients with non-small cell lung cancer: a randomized trial. JAMA *290*, 2149-2158.
Land, H., Parada, L.F., and Weinberg, R.A. (1983). Tumorigenic conversion of primary embryo fibroblasts requires at least two cooperating oncogenes. Nature *304*, 596-602.
Laplante, M., and Sabatini, D.M. (2012). mTOR signaling in growth control and disease. Cell *149*, 274-293.
Leevers, S.J., and Marshall, C.J. (1992). Activation of extracellular signal-regulated kinase, ERK2, by p21ras oncoprotein. EMBO J *11*, 569-574.
Ley, R., Balmanno, K., Hadfield, K., Weston, C., and Cook, S.J. (2003). Activation of the ERK1/2 signaling pathway promotes phosphorylation and proteasome-dependent degradation of the BH3-only protein, Bim. J Biol Chem *278*, 18811-18816.
Ling, Y.H., Li, T., Yuan, Z., Haigentz, M., Jr., Weber, T.K., and Perez-Soler, R. (2007). Erlotinib, an effective epidermal growth factor receptor tyrosine kinase inhibitor, induces p27KIP1 up-regulation and nuclear translocation in association with cell growth inhibition and G1/S phase arrest in human non-small-cell lung cancer cell lines. Mol Pharmacol *72*, 248-258.
Liu, D., Huang, Y., Chen, B., Zeng, J., Guo, N., Zhang, S., Liu, L., Xu, H., Mo, X., and Li, W. (2011). Activation of mammalian target of rapamycin pathway confers adverse outcome in nonsmall cell lung carcinoma. Cancer *117*, 3763-3773.
Liu, X., and Erikson, R.L. (2003). Polo-like kinase (Plk)1 depletion induces apoptosis in cancer cells. Proc Natl Acad Sci U S A *100*, 5789-5794.
Livak, K.J., and Schmittgen, T.D. (2001). Analysis of relative gene expression data using real-time quantitative PCR and the 2(-Delta Delta C(T)) Method. Methods *25*, 402-408.
Lowenstein, E.J., Daly, R.J., Batzer, A.G., Li, W., Margolis, B., Lammers, R., Ullrich, A., Skolnik, E.Y., Bar-Sagi, D., and Schlessinger, J. (1992). The SH2 and SH3 domain-containing protein GRB2 links receptor tyrosine kinases to ras signaling. Cell *70*, 431-442.
Lu, Y.J., Dong, X.Y., Shipley, J., Zhang, R.G., and Cheng, S.J. (1999). Chromosome 3 imbalances are the most frequent aberration found in non-small cell lung carcinoma. Lung Cancer *23*, 61-66.
Ludovini, V., Bianconi, F., Pistola, L., Chiari, R., Minotti, V., Colella, R., Giuffrida, D., Tofanetti, F.R., Siggillino, A., Flacco, A.*, et al.* (2011). Phosphoinositide-3-kinase catalytic alpha and KRAS mutations are important predictors of resistance to therapy with epidermal growth factor receptor tyrosine kinase inhibitors in patients with advanced non-small cell lung cancer. J Thorac Oncol *6*, 707-715.

Luijten, M., Redeker, S., van Noesel, M.M., Troost, D., Westerveld, A., and Hulsebos, T.J. (2000). Microsatellite instability and promoter methylation as possible causes of NF1 gene inactivation in neurofibromas. Eur J Hum Genet *8*, 939-945.
Lynch, T.J., Bell, D.W., Sordella, R., Gurubhagavatula, S., Okimoto, R.A., Brannigan, B.W., Harris, P.L., Haserlat, S.M., Supko, J.G., Haluska, F.G.*, et al.* (2004). Activating mutations in the epidermal growth factor receptor underlying responsiveness of non-small-cell lung cancer to gefitinib. N Engl J Med *350*, 2129-2139.
Ma, L., Chen, Z., Erdjument-Bromage, H., Tempst, P., and Pandolfi, P.P. (2005). Phosphorylation and functional inactivation of TSC2 by Erk implications for tuberous sclerosis and cancer pathogenesis. Cell *121*, 179-193.
Ma, X.M., and Blenis, J. (2009). Molecular mechanisms of mTOR-mediated translational control. Nat Rev Mol Cell Biol *10*, 307-318.
Madshus, I.H., and Stang, E. (2009). Internalization and intracellular sorting of the EGF receptor: a model for understanding the mechanisms of receptor trafficking. J Cell Sci *122*, 3433-3439.
Maemondo, M., Inoue, A., Kobayashi, K., Sugawara, S., Oizumi, S., Isobe, H., Gemma, A., Harada, M., Yoshizawa, H., Kinoshita, I.*, et al.* (2010). Gefitinib or chemotherapy for non-small-cell lung cancer with mutated EGFR. N Engl J Med *362*, 2380-2388.
Magnuson, B., Ekim, B., and Fingar, D.C. (2012). Regulation and function of ribosomal protein S6 kinase (S6K) within mTOR signalling networks. Biochem J *441*, 1-21.
Maheswaran, S., Sequist, L.V., Nagrath, S., Ulkus, L., Brannigan, B., Collura, C.V., Inserra, E., Diederichs, S., Iafrate, A.J., Bell, D.W.*, et al.* (2008). Detection of mutations in EGFR in circulating lung-cancer cells. N Engl J Med *359*, 366-377.
Mancini, D.N., Singh, S.M., Archer, T.K., and Rodenhiser, D.I. (1999). Site-specific DNA methylation in the neurofibromatosis (NF1) promoter interferes with binding of CREB and SP1 transcription factors. Oncogene *18*, 4108-4119.
Marais, R., Light, Y., Paterson, H.F., and Marshall, C.J. (1995). Ras recruits Raf-1 to the plasma membrane for activation by tyrosine phosphorylation. EMBO J *14*, 3136-3145.
Marais, R., Light, Y., Paterson, H.F., Mason, C.S., and Marshall, C.J. (1997). Differential regulation of Raf-1, A-Raf, and B-Raf by oncogenic ras and tyrosine kinases. J Biol Chem *272*, 4378-4383.
Marmor, M.D., Skaria, K.B., and Yarden, Y. (2004). Signal transduction and oncogenesis by ErbB/HER receptors. Int J Radiat Oncol Biol Phys *58*, 903-913.
Martin, G.A., Viskochil, D., Bollag, G., McCabe, P.C., Crosier, W.J., Haubruck, H., Conroy, L., Clark, R., O'Connell, P., Cawthon, R.M.*, et al.* (1990). The GAP-related domain of the neurofibromatosis type 1 gene product interacts with ras p21. Cell *63*, 843-849.
Mason, J.M., Morrison, D.J., Basson, M.A., and Licht, J.D. (2006). Sprouty proteins: multifaceted negative-feedback regulators of receptor tyrosine kinase signaling. Trends Cell Biol *16*, 45-54.
Masri, J., Bernath, A., Martin, J., Jo, O.D., Vartanian, R., Funk, A., and Gera, J. (2007). mTORC2 activity is elevated in gliomas and promotes growth and cell motility via overexpression of rictor. Cancer Res *67*, 11712-11720.
McDermott, U., Sharma, S.V., Dowell, L., Greninger, P., Montagut, C., Lamb, J., Archibald, H., Raudales, R., Tam, A., Lee, D.*, et al.* (2007). Identification of genotype-correlated sensitivity to selective kinase inhibitors by using high-throughput tumor cell line profiling. Proc Natl Acad Sci U S A *104*, 19936-19941.
McGillicuddy, L.T., Fromm, J.A., Hollstein, P.E., Kubek, S., Beroukhim, R., De Raedt, T., Johnson, B.W., Williams, S.M., Nghiemphu, P., Liau, L.M.*, et al.* (2009). Proteasomal and genetic inactivation of the NF1 tumor suppressor in gliomagenesis. Cancer Cell *16*, 44-54.

McGrath, J.P., Capon, D.J., Goeddel, D.V., and Levinson, A.D. (1984). Comparative biochemical properties of normal and activated human ras p21 protein. Nature *310*, 644-649.
Mendes-Pereira, A.M., Sims, D., Dexter, T., Fenwick, K., Assiotis, I., Kozarewa, I., Mitsopoulos, C., Hakas, J., Zvelebil, M., Lord, C.J.*, et al.* (2011). Breast Cancer Special Feature: Genome-wide functional screen identifies a compendium of genes affecting sensitivity to tamoxifen. Proc Natl Acad Sci U S A.
Meng, J., Dai, B., Fang, B., Bekele, B.N., Bornmann, W.G., Sun, D., Peng, Z., Herbst, R.S., Papadimitrakopoulou, V., Minna, J.D.*, et al.* (2010). Combination treatment with MEK and AKT inhibitors is more effective than each drug alone in human non-small cell lung cancer in vitro and in vivo. PLoS One *5*, e14124.
Meng, S., Zhang, M., Pan, W., Li, Z., Anderson, D.H., Zhang, S., Ge, B., and Wang, C. (2012). Tyrosines 303/343/353 within the Sprouty-related domain of Spred2 are essential for its interaction with p85 and inhibitory effect on Ras/ERK activation. Int J Biochem Cell Biol *44*, 748-758.
Menon, S., and Manning, B.D. (2008). Common corruption of the mTOR signaling network in human tumors. Oncogene *27 Suppl 2*, S43-51.
Misale, S., Yaeger, R., Hobor, S., Scala, E., Janakiraman, M., Liska, D., Valtorta, E., Schiavo, R., Buscarino, M., Siravegna, G.*, et al.* (2012). Emergence of KRAS mutations and acquired resistance to anti-EGFR therapy in colorectal cancer. Nature *486*, 532-536.
Mitsudomi, T., Morita, S., Yatabe, Y., Negoro, S., Okamoto, I., Tsurutani, J., Seto, T., Satouchi, M., Tada, H., Hirashima, T.*, et al.* (2010). Gefitinib versus cisplatin plus docetaxel in patients with non-small-cell lung cancer harbouring mutations of the epidermal growth factor receptor (WJTOG3405): an open label, randomised phase 3 trial. Lancet Oncol *11*, 121-128.
Mok, T.S., Wu, Y.L., Thongprasert, S., Yang, C.H., Chu, D.T., Saijo, N., Sunpaweravong, P., Han, B., Margono, B., Ichinose, Y.*, et al.* (2009). Gefitinib or carboplatin-paclitaxel in pulmonary adenocarcinoma. N Engl J Med *361*, 947-957.
Montagut, C., Dalmases, A., Bellosillo, B., Crespo, M., Pairet, S., Iglesias, M., Salido, M., Gallen, M., Marsters, S., Tsai, S.P.*, et al.* (2012). Identification of a mutation in the extracellular domain of the Epidermal Growth Factor Receptor conferring cetuximab resistance in colorectal cancer. Nat Med *18*, 221-223.
Moodie, S.A., Willumsen, B.M., Weber, M.J., and Wolfman, A. (1993). Complexes of Ras.GTP with Raf-1 and mitogen-activated protein kinase kinase. Science *260*, 1658-1661.
Morrison, D.K. (2001). KSR: a MAPK scaffold of the Ras pathway? J Cell Sci *114*, 1609-1612.
Mukhopadhyay, D., Anant, S., Lee, R.M., Kennedy, S., Viskochil, D., and Davidson, N.O. (2002). C-->U editing of neurofibromatosis 1 mRNA occurs in tumors that express both the type II transcript and apobec-1, the catalytic subunit of the apolipoprotein B mRNA-editing enzyme. Am J Hum Genet *70*, 38-50.
Nahta, R., Hung, M.C., and Esteva, F.J. (2004). The HER-2-targeting antibodies trastuzumab and pertuzumab synergistically inhibit the survival of breast cancer cells. Cancer Res *64*, 2343-2346.
Nawrocki, S.T., Griffin, P., Kelly, K.R., and Carew, J.S. (2012). MLN4924 : a novel first-in-class inhibitor of NEDD8-activating enzyme for cancer therapy. Expert Opin Investig Drugs.
Neckers, L., and Workman, P. (2012). Hsp90 molecular chaperone inhibitors: are we there yet? Clin Cancer Res *18*, 64-76.
Nik-Zainal, S., Alexandrov, L.B., Wedge, D.C., Van Loo, P., Greenman, C.D., Raine, K., Jones, D., Hinton, J., Marshall, J., Stebbings, L.A.*, et al.* (2012). Mutational Processes Molding the Genomes of 21 Breast Cancers. Cell *149*, 979-993.

O'Byrne, K.J., Gatzemeier, U., Bondarenko, I., Barrios, C., Eschbach, C., Martens, U.M., Hotko, Y., Kortsik, C., Paz-Ares, L., Pereira, J.R.*, et al.* (2011). Molecular biomarkers in non-small-cell lung cancer: a retrospective analysis of data from the phase 3 FLEX study. Lancet Oncol *12*, 795-805.
O'Reilly, K.E., Rojo, F., She, Q.B., Solit, D., Mills, G.B., Smith, D., Lane, H., Hofmann, F., Hicklin, D.J., Ludwig, D.L.*, et al.* (2006). mTOR inhibition induces upstream receptor tyrosine kinase signaling and activates Akt. Cancer Res *66*, 1500-1508.
Oh, J.E., An, C.H., Yoo, N.J., and Lee, S.H. (2011). Detection of low-level EGFR T790M mutation in lung cancer tissues. APMIS *119*, 403-411.
Ohashi, K., Sequist, L.V., Arcila, M.E., Moran, T., Chmielecki, J., Lin, Y.L., Pan, Y., Wang, L., de Stanchina, E., Shien, K.*, et al.* (2012). Lung cancers with acquired resistance to EGFR inhibitors occasionally harbor BRAF gene mutations but lack mutations in KRAS, NRAS, or MEK1. Proc Natl Acad Sci U S A.
Olayioye, M.A., Neve, R.M., Lane, H.A., and Hynes, N.E. (2000). The ErbB signaling network: receptor heterodimerization in development and cancer. EMBO J *19*, 3159-3167.
Oxnard, G.R., Arcila, M.E., Chmielecki, J., Ladanyi, M., Miller, V.A., and Pao, W. (2011a). New Strategies in Overcoming Acquired Resistance to Epidermal Growth Factor Receptor Tyrosine Kinase Inhibitors in Lung Cancer. Clin Cancer Res.
Oxnard, G.R., Arcila, M.E., Sima, C.S., Riely, G.J., Chmielecki, J., Kris, M.G., Pao, W., Ladanyi, M., and Miller, V.A. (2011b). Acquired resistance to EGFR tyrosine kinase inhibitors in EGFR-mutant lung cancer: distinct natural history of patients with tumors harboring the T790M mutation. Clin Cancer Res *17*, 1616-1622.
Pacold, M.E., Suire, S., Perisic, O., Lara-Gonzalez, S., Davis, C.T., Walker, E.H., Hawkins, P.T., Stephens, L., Eccleston, J.F., and Williams, R.L. (2000). Crystal structure and functional analysis of Ras binding to its effector phosphoinositide 3-kinase gamma. Cell *103*, 931-943.
Paez, J.G., Janne, P.A., Lee, J.C., Tracy, S., Greulich, H., Gabriel, S., Herman, P., Kaye, F.J., Lindeman, N., Boggon, T.J.*, et al.* (2004). EGFR mutations in lung cancer: correlation with clinical response to gefitinib therapy. Science *304*, 1497-1500.
Pao, W., and Girard, N. (2011). New driver mutations in non-small-cell lung cancer. Lancet Oncol *12*, 175-180.
Pao, W., and Hutchinson, K.E. (2012). Chipping away at the lung cancer genome. Nat Med *18*, 349-351.
Pao, W., Miller, V.A., Politi, K.A., Riely, G.J., Somwar, R., Zakowski, M.F., Kris, M.G., and Varmus, H. (2005a). Acquired resistance of lung adenocarcinomas to gefitinib or erlotinib is associated with a second mutation in the EGFR kinase domain. PLoS Med *2*, e73.
Pao, W., Wang, T.Y., Riely, G.J., Miller, V.A., Pan, Q., Ladanyi, M., Zakowski, M.F., Heelan, R.T., Kris, M.G., and Varmus, H.E. (2005b). KRAS mutations and primary resistance of lung adenocarcinomas to gefitinib or erlotinib. PLoS Med *2*, e17.
Parkin, B., Ouillette, P., Wang, Y., Liu, Y., Wright, W., Roulston, D., Purkayastha, A., Dressel, A., Karp, J., Bockenstedt, P.*, et al.* (2010). NF1 inactivation in adult acute myelogenous leukemia. Clin Cancer Res *16*, 4135-4147.
Pawson, T. (2004). Specificity in signal transduction: from phosphotyrosine-SH2 domain interactions to complex cellular systems. Cell *116*, 191-203.
Pelicci, G., Lanfrancone, L., Grignani, F., McGlade, J., Cavallo, F., Forni, G., Nicoletti, I., Pawson, T., and Pelicci, P.G. (1992). A novel transforming protein (SHC) with an SH2 domain is implicated in mitogenic signal transduction. Cell *70*, 93-104.
Peterson, T.R., Laplante, M., Thoreen, C.C., Sancak, Y., Kang, S.A., Kuehl, W.M., Gray, N.S., and Sabatini, D.M. (2009). DEPTOR is an mTOR inhibitor frequently overexpressed in multiple myeloma cells and required for their survival. Cell *137*, 873-886.

Pircher, A., Ploner, F., Popper, H., and Hilbe, W. (2010). Rationale of a relaunch of gefitinib in Caucasian non-small cell lung cancer patients. Lung Cancer *69*, 265-271.
Plowman, G.D., Culouscou, J.M., Whitney, G.S., Green, J.M., Carlton, G.W., Foy, L., Neubauer, M.G., and Shoyab, M. (1993). Ligand-specific activation of HER4/p180erbB4, a fourth member of the epidermal growth factor receptor family. Proc Natl Acad Sci U S A *90*, 1746-1750.
Plowman, G.D., Whitney, G.S., Neubauer, M.G., Green, J.M., McDonald, V.L., Todaro, G.J., and Shoyab, M. (1990). Molecular cloning and expression of an additional epidermal growth factor receptor-related gene. Proc Natl Acad Sci U S A *87*, 4905-4909.
Politi, K., Fan, P.D., Shen, R., Zakowski, M., and Varmus, H. (2010). Erlotinib resistance in mouse models of epidermal growth factor receptor-induced lung adenocarcinoma. Dis Model Mech *3*, 111-119.
Politi, K., Zakowski, M.F., Fan, P.D., Schonfeld, E.A., Pao, W., and Varmus, H.E. (2006). Lung adenocarcinomas induced in mice by mutant EGF receptors found in human lung cancers respond to a tyrosine kinase inhibitor or to down-regulation of the receptors. Genes Dev *20*, 1496-1510.
Prahallad, A., Sun, C., Huang, S., Di Nicolantonio, F., Salazar, R., Zecchin, D., Beijersbergen, R.L., Bardelli, A., and Bernards, R. (2012). Unresponsiveness of colon cancer to BRAF(V600E) inhibition through feedback activation of EGFR. Nature *483*, 100-103.
Qi, H.H., Sarkissian, M., Hu, G.Q., Wang, Z., Bhattacharjee, A., Gordon, D.B., Gonzales, M., Lan, F., Ongusaha, P.P., Huarte, M*., et al.* (2010). Histone H4K20/H3K9 demethylase PHF8 regulates zebrafish brain and craniofacial development. Nature *466*, 503-507.
Rajalingam, K., Schreck, R., Rapp, U.R., and Albert, S. (2007). Ras oncogenes and their downstream targets. Biochim Biophys Acta *1773*, 1177-1195.
Rosell, R., Carcereny, E., Gervais, R., Vergnenegre, A., Massuti, B., Felip, E., Palmero, R., Garcia-Gomez, R., Pallares, C., Sanchez, J.M*., et al.* (2012). Erlotinib versus standard chemotherapy as first-line treatment for European patients with advanced EGFR mutation-positive non-small-cell lung cancer (EURTAC): a multicentre, open-label, randomised phase 3 trial. Lancet Oncol *13*, 239-246.
Roux, P.P., Ballif, B.A., Anjum, R., Gygi, S.P., and Blenis, J. (2004). Tumor-promoting phorbol esters and activated Ras inactivate the tuberous sclerosis tumor suppressor complex via p90 ribosomal S6 kinase. Proc Natl Acad Sci U S A *101*, 13489-13494.
Rozakis-Adcock, M., Fernley, R., Wade, J., Pawson, T., and Bowtell, D. (1993). The SH2 and SH3 domains of mammalian Grb2 couple the EGF receptor to the Ras activator mSos1. Nature *363*, 83-85.
Salomon, D.S., Brandt, R., Ciardiello, F., and Normanno, N. (1995). Epidermal growth factor-related peptides and their receptors in human malignancies. Crit Rev Oncol Hematol *19*, 183-232.
Salzano, M., Rusciano, M.R., Russo, E., Bifulco, M., Postiglione, L., and Vitale, M. (2012). Calcium/calmodulin-dependent protein kinase II (CaMKII) phosphorylates Raf-1 at serine 338 and mediates Ras-stimulated Raf-1 activation. Cell Cycle *11*.
Sancak, Y., Bar-Peled, L., Zoncu, R., Markhard, A.L., Nada, S., and Sabatini, D.M. (2010). Ragulator-Rag complex targets mTORC1 to the lysosomal surface and is necessary for its activation by amino acids. Cell *141*, 290-303.
Santos, E., Martin-Zanca, D., Reddy, E.P., Pierotti, M.A., Della Porta, G., and Barbacid, M. (1984). Malignant activation of a K-ras oncogene in lung carcinoma but not in normal tissue of the same patient. Science *223*, 661-664.
Sarbassov, D.D., Ali, S.M., Kim, D.H., Guertin, D.A., Latek, R.R., Erdjument-Bromage, H., Tempst, P., and Sabatini, D.M. (2004). Rictor, a novel binding partner of mTOR,

defines a rapamycin-insensitive and raptor-independent pathway that regulates the cytoskeleton. Curr Biol *14*, 1296-1302.
Sarbassov, D.D., Guertin, D.A., Ali, S.M., and Sabatini, D.M. (2005). Phosphorylation and regulation of Akt/PKB by the rictor-mTOR complex. Science *307*, 1098-1101.
Sasaki, H., Yukiue, H., Kobayashi, Y., Moriyama, S., Nakashima, Y., Kaji, M., Fukai, I., Kiriyama, M., Yamakawa, Y., and Fujii, Y. (2001). Expression of the sensitive to apoptosis gene, SAG, as a prognostic marker in nonsmall cell lung cancer. Int J Cancer *95*, 375-377.
Schechter, A.L., Hung, M.C., Vaidyanathan, L., Weinberg, R.A., Yang-Feng, T.L., Francke, U., Ullrich, A., and Coussens, L. (1985). The neu gene: an erbB-homologous gene distinct from and unlinked to the gene encoding the EGF receptor. Science *229*, 976-978.
Schwarz, D.S., Hutvagner, G., Du, T., Xu, Z., Aronin, N., and Zamore, P.D. (2003). Asymmetry in the assembly of the RNAi enzyme complex. Cell *115*, 199-208.
Sequist, L.V., Waltman, B.A., Dias-Santagata, D., Digumarthy, S., Turke, A.B., Fidias, P., Bergethon, K., Shaw, A.T., Gettinger, S., Cosper, A.K.*, et al.* (2011). Genotypic and histological evolution of lung cancers acquiring resistance to EGFR inhibitors. Sci Transl Med *3*, 75ra26.
Shapira, S., Barkan, B., Friedman, E., Kloog, Y., and Stein, R. (2007). The tumor suppressor neurofibromin confers sensitivity to apoptosis by Ras-dependent and Ras-independent pathways. Cell Death Differ *14*, 895-906.
Sharma, S.V., Bell, D.W., Settleman, J., and Haber, D.A. (2007). Epidermal growth factor receptor mutations in lung cancer. Nat Rev Cancer *7*, 169-181.
Sharma, S.V., Lee, D.Y., Li, B., Quinlan, M.P., Takahashi, F., Maheswaran, S., McDermott, U., Azizian, N., Zou, L., Fischbach, M.A.*, et al.* (2010). A chromatin-mediated reversible drug-tolerant state in cancer cell subpopulations. Cell *141*, 69-80.
Shaw, A.T., Yeap, B.Y., Mino-Kenudson, M., Digumarthy, S.R., Costa, D.B., Heist, R.S., Solomon, B., Stubbs, H., Admane, S., McDermott, U.*, et al.* (2009). Clinical features and outcome of patients with non-small-cell lung cancer who harbor EML4-ALK. J Clin Oncol *27*, 4247-4253.
Shepherd, F.A., Rodrigues Pereira, J., Ciuleanu, T., Tan, E.H., Hirsh, V., Thongprasert, S., Campos, D., Maoleekoonpiroj, S., Smylie, M., Martins, R.*, et al.* (2005). Erlotinib in previously treated non-small-cell lung cancer. N Engl J Med *353*, 123-132.
Shi, H., Moriceau, G., Kong, X., Lee, M.K., Lee, H., Koya, R.C., Ng, C., Chodon, T., Scolyer, R.A., Dahlman, K.B.*, et al.* (2012). Melanoma whole-exome sequencing identifies (V600E)B-RAF amplification-mediated acquired B-RAF inhibitor resistance. Nat Commun *3*, 724.
Shimizu, T., Tolcher, A.W., Papadopoulos, K.P., Beeram, M., Rasco, D.W., Smith, L.S., Gunn, S., Smetzer, L., Mays, T.A., Kaiser, B.*, et al.* (2012). The clinical effect of the dual-targeting strategy involving PI3K/AKT/mTOR and RAS/MEK/ERK pathways in patients with advanced cancer. Clin Cancer Res *18*, 2316-2325.
Shoji, K., Oda, K., Nakagawa, S., Hosokawa, S., Nagae, G., Uehara, Y., Sone, K., Miyamoto, Y., Hiraike, H., Hiraike-Wada, O.*, et al.* (2009). The oncogenic mutation in the pleckstrin homology domain of AKT1 in endometrial carcinomas. Br J Cancer *101*, 145-148.
Singh, B., Ittmann, M.M., and Krolewski, J.J. (1998). Sporadic breast cancers exhibit loss of heterozygosity on chromosome segment 10q23 close to the Cowden disease locus. Genes Chromosomes Cancer *21*, 166-171.
Skuse, G.R., Cappione, A.J., Sowden, M., Metheny, L.J., and Smith, H.C. (1996). The neurofibromatosis type I messenger RNA undergoes base-modification RNA editing. Nucleic Acids Res *24*, 478-485.

Snijder, B., Sacher, R., Ramo, P., Damm, E.M., Liberali, P., and Pelkmans, L. (2009). Population context determines cell-to-cell variability in endocytosis and virus infection. Nature *461*, 520-523.
Solimini, N.L., Luo, J., and Elledge, S.J. (2007). Non-oncogene addiction and the stress phenotype of cancer cells. Cell *130*, 986-988.
Sontheimer, E.J. (2005). Assembly and function of RNA silencing complexes. Nat Rev Mol Cell Biol *6*, 127-138.
Sos, M.L., Koker, M., Weir, B.A., Heynck, S., Rabinovsky, R., Zander, T., Seeger, J.M., Weiss, J., Fischer, F., Frommolt, P.*, et al.* (2009). PTEN loss contributes to erlotinib resistance in EGFR-mutant lung cancer by activation of Akt and EGFR. Cancer Res *69*, 3256-3261.
Sousa, L.P., Lax, I., Shen, H., Ferguson, S.M., Camilli, P.D., and Schlessinger, J. (2012). Suppression of EGFR endocytosis by dynamin depletion reveals that EGFR signaling occurs primarily at the plasma membrane. Proc Natl Acad Sci U S A *109*, 4419-4424.
Straussman, R., Morikawa, T., Shee, K., Barzily-Rokni, M., Qian, Z.R., Du, J., Davis, A., Mongare, M.M., Gould, J., Frederick, D.T.*, et al.* (2012). Tumour micro-environment elicits innate resistance to RAF inhibitors through HGF secretion. Nature *487*, 500-504.
Swanton, C., Marani, M., Pardo, O., Warne, P.H., Kelly, G., Sahai, E., Elustondo, F., Chang, J., Temple, J., Ahmed, A.A.*, et al.* (2007). Regulators of mitotic arrest and ceramide metabolism are determinants of sensitivity to paclitaxel and other chemotherapeutic drugs. Cancer Cell *11*, 498-512.
Sweet, R.W., Yokoyama, S., Kamata, T., Feramisco, J.R., Rosenberg, M., and Gross, M. (1984). The product of ras is a GTPase and the T24 oncogenic mutant is deficient in this activity. Nature *311*, 273-275.
Tamm, I., Wang, Y., Sausville, E., Scudiero, D.A., Vigna, N., Oltersdorf, T., and Reed, J.C. (1998). IAP-family protein survivin inhibits caspase activity and apoptosis induced by Fas (CD95), Bax, caspases, and anticancer drugs. Cancer Res *58*, 5315-5320.
Tan, M., Zhao, Y., Kim, S.J., Liu, M., Jia, L., Saunders, T.L., Zhu, Y., and Sun, Y. (2011). SAG/RBX2/ROC2 E3 Ubiquitin Ligase Is Essential for Vascular and Neural Development by Targeting NF1 for Degradation. Dev Cell *21*, 1062-1076.
Tanizaki, J., Okamoto, I., Okabe, T., Sakai, K., Tanaka, K., Hayashi, H., Kaneda, H., Takezawa, K., Kuwata, K., Yamaguchi, H.*, et al.* (2012). Activation of HER family signaling as a mechanism of acquired resistance to ALK inhibitors in EML4-ALK-positive non-small cell lung cancer. Clin Cancer Res.
Therasse, P., Arbuck, S.G., Eisenhauer, E.A., Wanders, J., Kaplan, R.S., Rubinstein, L., Verweij, J., Van Glabbeke, M., van Oosterom, A.T., Christian, M.C.*, et al.* (2000). New guidelines to evaluate the response to treatment in solid tumors. European Organization for Research and Treatment of Cancer, National Cancer Institute of the United States, National Cancer Institute of Canada. J Natl Cancer Inst *92*, 205-216.
Thiery, J.P. (2002). Epithelial-mesenchymal transitions in tumour progression. Nat Rev Cancer *2*, 442-454.
Thomson, S., Buck, E., Petti, F., Griffin, G., Brown, E., Ramnarine, N., Iwata, K.K., Gibson, N., and Haley, J.D. (2005). Epithelial to mesenchymal transition is a determinant of sensitivity of non-small-cell lung carcinoma cell lines and xenografts to epidermal growth factor receptor inhibition. Cancer Res *65*, 9455-9462.
Thomson, S., Petti, F., Sujka-Kwok, I., Epstein, D., and Haley, J.D. (2008). Kinase switching in mesenchymal-like non-small cell lung cancer lines contributes to EGFR inhibitor resistance through pathway redundancy. Clin Exp Metastasis *25*, 843-854.
Thoreen, C.C., Chantranupong, L., Keys, H.R., Wang, T., Gray, N.S., and Sabatini, D.M. (2012). A unifying model for mTORC1-mediated regulation of mRNA translation. Nature *485*, 109-113.

Tokumo, M., Toyooka, S., Ichihara, S., Ohashi, K., Tsukuda, K., Ichimura, K., Tabata, M., Kiura, K., Aoe, M., Sano, Y.*, et al.* (2006). Double mutation and gene copy number of EGFR in gefitinib refractory non-small-cell lung cancer. Lung Cancer *53*, 117-121.
Trahey, M., and McCormick, F. (1987). A cytoplasmic protein stimulates normal N-ras p21 GTPase, but does not affect oncogenic mutants. Science *238*, 542-545.
Turke, A.B., Zejnullahu, K., Wu, Y.L., Song, Y., Dias-Santagata, D., Lifshits, E., Toschi, L., Rogers, A., Mok, T., Sequist, L.*, et al.* (2010). Preexistence and clonal selection of MET amplification in EGFR mutant NSCLC. Cancer Cell *17*, 77-88.
Turner, N., Lambros, M.B., Horlings, H.M., Pearson, A., Sharpe, R., Natrajan, R., Geyer, F.C., van Kouwenhove, M., Kreike, B., Mackay, A.*, et al.* (2010). Integrative molecular profiling of triple negative breast cancers identifies amplicon drivers and potential therapeutic targets. Oncogene *29*, 2013-2023.
Vander Haar, E., Lee, S.I., Bandhakavi, S., Griffin, T.J., and Kim, D.H. (2007). Insulin signalling to mTOR mediated by the Akt/PKB substrate PRAS40. Nat Cell Biol *9*, 316-323.
Vanhaesebroeck, B., Guillermet-Guibert, J., Graupera, M., and Bilanges, B. (2010). The emerging mechanisms of isoform-specific PI3K signalling. Nat Rev Mol Cell Biol *11*, 329-341.
Vichai, V., and Kirtikara, K. (2006). Sulforhodamine B colorimetric assay for cytotoxicity screening. Nat Protoc *1*, 1112-1116.
Vogt, P.K., Kang, S., Elsliger, M.A., and Gymnopoulos, M. (2007). Cancer-specific mutations in phosphatidylinositol 3-kinase. Trends Biochem Sci *32*, 342-349.
Vojtek, A.B., Hollenberg, S.M., and Cooper, J.A. (1993). Mammalian Ras interacts directly with the serine/threonine kinase Raf. Cell *74*, 205-214.
Vousden, K.H., and Lu, X. (2002). Live or let die: the cell's response to p53. Nat Rev Cancer *2*, 594-604.
Wagner, S.A., Beli, P., Weinert, B.T., Nielsen, M.L., Cox, J., Mann, M., and Choudhary, C. (2011). A proteome-wide, quantitative survey of in vivo ubiquitylation sites reveals widespread regulatory roles. Mol Cell Proteomics *10*, M111 013284.
Wang, L., Zhang, Q., Zhang, J., Sun, S., Guo, H., Jia, Z., Wang, B., Shao, Z., Wang, Z., and Hu, X. (2011). PI3K pathway activation results in low efficacy of both trastuzumab and lapatinib. BMC Cancer *11*, 248.
Wang, N., Li, Z., Tian, F., Feng, Y., Huang, J., Li, C., and Xie, F. (2012). PKCalpha inhibited apoptosis by decreasing the activity of JNK in MCF-7/ADR cells. Exp Toxicol Pathol *64*, 459-464.
Warne, P.H., Viciana, P.R., and Downward, J. (1993). Direct interaction of Ras and the amino-terminal region of Raf-1 in vitro. Nature *364*, 352-355.
Weber, J.D., Raben, D.M., Phillips, P.J., and Baldassare, J.J. (1997). Sustained activation of extracellular-signal-regulated kinase 1 (ERK1) is required for the continued expression of cyclin D1 in G1 phase. Biochem J *326 (Pt 1)*, 61-68.
Weinstein, I.B. (2002). Cancer. Addiction to oncogenes--the Achilles heal of cancer. Science *297*, 63-64.
Wellbrock, C., Karasarides, M., and Marais, R. (2004). The RAF proteins take centre stage. Nat Rev Mol Cell Biol *5*, 875-885.
Wells, S.A., Jr., Robinson, B.G., Gagel, R.F., Dralle, H., Fagin, J.A., Santoro, M., Baudin, E., Elisei, R., Jarzab, B., Vasselli, J.R.*, et al.* (2012). Vandetanib in patients with locally advanced or metastatic medullary thyroid cancer: a randomized, double-blind phase III trial. J Clin Oncol *30*, 134-141.
Wennerberg, K., Rossman, K.L., and Der, C.J. (2005). The Ras superfamily at a glance. J Cell Sci *118*, 843-846.
Wilson, T.R., Fridlyand, J., Yan, Y., Penuel, E., Burton, L., Chan, E., Peng, J., Lin, E., Wang, Y., Sosman, J.*, et al.* (2012). Widespread potential for growth-factor-driven resistance to anticancer kinase inhibitors. Nature *487*, 505-509.

Wojtkowiak, J.W., Verduzco, D., Schramm, K.J., and Gillies, R.J. (2011). Drug resistance and cellular adaptation to tumor acidic pH microenvironment. Mol Pharm *8*, 2032-2038.
Wood, K.C., Konieczkowski, D.J., Johannessen, C.M., Boehm, J.S., Tamayo, P., Botvinnik, O.B., Mesirov, J.P., Hahn, W.C., Root, D.E., Garraway, L.A.*, et al.* (2012). MicroSCALE screening reveals genetic modifiers of therapeutic response in melanoma. Sci Signal *5*, rs4.
Yang, J.Y., Zong, C.S., Xia, W., Yamaguchi, H., Ding, Q., Xie, X., Lang, J.Y., Lai, C.C., Chang, C.J., Huang, W.C.*, et al.* (2008). ERK promotes tumorigenesis by inhibiting FOXO3a via MDM2-mediated degradation. Nat Cell Biol *10*, 138-148.
Yano, S., Wang, W., Li, Q., Matsumoto, K., Sakurama, H., Nakamura, T., Ogino, H., Kakiuchi, S., Hanibuchi, M., Nishioka, Y.*, et al.* (2008). Hepatocyte growth factor induces gefitinib resistance of lung adenocarcinoma with epidermal growth factor receptor-activating mutations. Cancer Res *68*, 9479-9487.
Yordy, J.S., and Muise-Helmericks, R.C. (2000). Signal transduction and the Ets family of transcription factors. Oncogene *19*, 6503-6513.
Yuan, T.L., and Cantley, L.C. (2008). PI3K pathway alterations in cancer: variations on a theme. Oncogene *27*, 5497-5510.
Yun, C.H., Mengwasser, K.E., Toms, A.V., Woo, M.S., Greulich, H., Wong, K.K., Meyerson, M., and Eck, M.J. (2008). The T790M mutation in EGFR kinase causes drug resistance by increasing the affinity for ATP. Proc Natl Acad Sci U S A *105*, 2070-2075.
Zakowski, M.F., Ladanyi, M., and Kris, M.G. (2006). EGFR mutations in small-cell lung cancers in patients who have never smoked. N Engl J Med *355*, 213-215.
Zhang, Z., Lee, J.C., Lin, L., Olivas, V., Au, V., Laframboise, T., Abdel-Rahman, M., Wang, X., Levine, A.D., Rho, J.K.*, et al.* (2012). Activation of the AXL kinase causes resistance to EGFR-targeted therapy in lung cancer. Nat Genet *44*, 852-860.
Zhao, L., and Vogt, P.K. (2008). Class I PI3K in oncogenic cellular transformation. Oncogene *27*, 5486-5496.
Zhao, Y., Xiong, X., and Sun, Y. (2011). DEPTOR, an mTOR inhibitor, is a physiological substrate of SCF(betaTrCP) E3 ubiquitin ligase and regulates survival and autophagy. Mol Cell *44*, 304-316.
Zheng, C.F., and Guan, K.L. (1994). Activation of MEK family kinases requires phosphorylation of two conserved Ser/Thr residues. EMBO J *13*, 1123-1131.
Zinzalla, V., Stracka, D., Oppliger, W., and Hall, M.N. (2011). Activation of mTORC2 by association with the ribosome. Cell *144*, 757-768.
Zoncu, R., Efeyan, A., and Sabatini, D.M. (2011). mTOR: from growth signal integration to cancer, diabetes and ageing. Nat Rev Mol Cell Biol *12*, 21-35.